UC Santa Barbara

UC Santa Barbara Electronic Theses and Dissertations

Title

Unity in Split-Brain Patients Behavioral and Neural Evidence from Complete and Partial Callosotomy and New Experimental Paradigms

Permalink

https://escholarship.org/uc/item/96j8g610

ISBN

9798186385660

Author

Bekir, Selin

Publication Date

2026-06-10

Peer reviewed|Thesis/dissertation

eScholarship.org Powered by the California Digital Library
University of California

UNIVERSITY OF CALIFORNIA

Santa Barbara

Unity in Split-Brain Patients

Behavioral and Neural Evidence from Complete and Partial Callosotomy and New Experimental Paradigms

A dissertation submitted in partial satisfaction of the requirements for the degree Doctor of Philosophy in Psychological and Brain Sciences

by

Selin Bekir

Committee in charge:

Professor Michael B. Miller, Chair

Professor Michael S. Gazzaniga

Professor Barry Giesbrecht

Professor Emily G. Jacobs

June 2026

The dissertation of Selin Bekir is approved.

_____

Emily G. Jacobs

_____

Barry Giesbrecht

_____

Michael S. Gazzaniga

_____

Michael B. Miller, Committee Chair

June 2026

Unity in Split-Brain Patients

Behavioral and Neural Evidence from Complete and Partial Callosotomy and New Experimental Paradigms

Copyright © 2026

by

Selin Bekir

To my husband, Gurbuz Demiroglu,

who crossed oceans with me so that I could pursue my passion for studying the human brain. Thank you for being my anchor through every step of this journey, with such love and patience.

I love you.

"Block any way the brain communicates with its modules,

and it will most likely find another strategy to achieve the goal at hand."

—Michael S. Gazzaniga, Tales from Both Sides of the Brain

ACKNOWLEDGEMENTS

First and foremost, I would like to thank my advisor, Dr. Michael Miller, for giving me the freedom to pursue the questions I find fascinating, while also providing the support, guidance, and environment that helped me grow as a scientist. I first met Mike as an undergraduate exchange student in his cognitive neuroscience course, which was one of the best courses I took. Inspired by his class, I approached him about my interest in research, and he welcomed me into his lab that very same day, calling Evan, his former graduate student, and sending me down to the basement where the Miller Lab is. In many ways, my entire research journey began there. Looking back now, I don't think I would be here doing this work, had Mike not opened that door for me so early on. And for that, I am forever grateful to him. Then, during my PhD, Mike has created a space that is very valuable in academia: a true playground for scientific thinking, where I was free to try things, fail, explore, and ultimately learn in a deeper sense. He always led with trust and patience, giving me the space to figure things out while always being there with invaluable guidance when needed, which allowed me to grow so much. What has defined my PhD more than anything else is the deep trust and extraordinary opportunities Mike has provided me with. He gave me opportunities that only a few researchers ever get: the chance to travel across continents, sometimes only for a few days, to work directly with split-brain patients—the very population at the heart of this dissertation. And he did so with a generosity and confidence in me that often exceeded my own. For all of this, I am deeply grateful.

I would also like to express my gratitude to Dr. Michael Gazzaniga, the pioneer of the human split-brain research. His foundational work with split-brain patients gave us not only an entire field, but also a standard to live up to as scientists—from building a mobile testing van to reach and test split-brain patients, to designing creative and critical experiments that revealed the drastic effects of hemispheric severance, even at a time when many thought that severing the hemispheres had little to no effect on cognition in humans. It is these principles of dedication, persistence, creativity, and open-mindedness that I strive to carry forward in my own work as a scientist. It was Mike's foundational discoveries that first made me fascinated by the human brain. I was a high school student in Turkey when I first encountered his work on split-brain patients, and the deep fascination and curiosity it sparked in me led me to pursue a life dedicated to understanding the human brain. Now, years later, having the opportunity to do this very work alongside Mike still feels surreal in a way I can hardly describe. I am deeply grateful to Mike—for the field he built, for the many hours he so generously and humbly spent meeting with me to share his wisdom and guidance, and for always encouraging me to think about the big picture. Thank you. I would also like to thank his beloved wife, Charlotte Gazzaniga, who also worked directly with split-brain patients and generously shared her firsthand experiences with me.

I am also very thankful to my committee members, Dr. Barry Giesbrecht and Dr. Emily Jacobs. Barry is one of the best mentors and cognitive experimentalists I have ever known. His care for his students is extraordinary, and I aspire to one day be even half the mentor he is. I have learned a lot from him about how to think carefully and rigorously when designing

behavioral experiments. His feedback was always exceptionally insightful, and on point. A single meeting with Barry would make both my experiments and my own thinking substantially clearer and better. And Emily. As a young woman in science, I am so grateful to have a role model like you to aspire to. Emily's fierce advocacy for women's health research and the waves she creates around her are truly inspiring. Every conversation with Emily would leave you inspired and fueled. The impact she has, both scientifically and personally, is immense, and I can only hope to one day become even a fraction of the powerhouse she is.

I am grateful to the members of the Miller lab: Tyler Santander, for teaching me so much throughout my PhD, including how to scan people and how to analyze fMRI data and being such a helpful resource and a great friend ever since; Evan Layher, for bringing so much joy, humor, and life into the lab; Sara Leslie, for her friendship and for being such an inspiring researcher who cares deeply about her work; Luna Li and Henri Skinner, for being my lab-mates from the very beginning and great companions through our conference journeys, Julie Eitzen for being such a wonderful addition to the lab, and the dearest Courtney Durdle, for creating such a welcoming environment where everyone felt they truly belonged. I miss you deeply.

I also thank my amazing undergraduate research mentees: Leila Loose, Emily Yi, Emma Kates-Harbeck, Esther Blanco Hermoso, Jacqueline McGuinness, Joe Gibbons, Ayra Bandali, Maya Ayres, Cary Higgins, Neda Riaziat and Jasmine Diaz.

This work would not have been possible without the exceptional collaborators abroad. I am particularly grateful to Prof. Dr. Christian Bien for making this research possible, and to Prof. Dr. Lukas J. Volz, Dr. Julia Siemann, Dr. Anna Rada, Dr. Friedrich Wörmann, Dr. Thilo Kalbhenn, Lena Hopf, and many others who facilitated access to patients, provided invaluable clinical expertise, and generously supported this work. Thank you very much.

And most essentially, I want to thank the split-brain patients. Every encounter was something I will carry with me for the rest of my life. To BT—the very first split-brain patient I have ever met. You arrived behaving so much like a neurotypical individual that I nearly walked away disappointed, only to reveal some of the most unexpected findings of my entire PhD. You reminded me, in the most vivid way possible, of why unexpected cases are at the heart of science. To HY—the very first (complete) split-patient I met—who showed me, beyond any doubt, what hemispheric disconnection looks like in the flesh. I will never forget the goosebumps I felt after witnessing it in person for the very first time. To TJ—you blew my mind. Watching the left-hemisphere interpreter at work, in real time, made me appreciate the workings of the human brain even further. To WU—for your warmth and kindness throughout. And to LJ, NR, NE, NO, EM, and DD—you are the stars of this work. My deepest hope is that this surgery makes your lives easier, and that your remarkable contributions to science are recognized and honored. I cannot thank you enough.

I would also like to thank the Summer Seminars in Neuroscience and Philosophy (SSNAP) community. To Walter Sinnott-Armstrong and Felipe De Brigard, for creating such a remarkable intellectual space. To Anya Ivanova, Jake Gavenas, Eric Hochstein, Corey Allen, Akila Kadambi, Laura Kaltwasser and many others—I learned so much from you all, and I am grateful that many of those conversations also grew into collaborations and friendships.

I want to acknowledge my beloved home institution, Boğaziçi University, which shaped me profoundly. To the Department of Psychology—Esra Mungan, Ayşecan Boduroğlu, Ali Tekcan, Nur Yeniceri, Falih Köksal, and many others—thank you for teaching me the beauty of cognitive and psychological research. And to the Department of Philosophy, particularly Berna Kılınç and Yıldız Silier, who taught me so much about Philosophy of Science and formal and informal logic, laying the foundation for my critical thinking and showing me that science without philosophy risks losing sight of its own assumptions.

I thank my cohort and friends, with whom I got to share this PhD journey. To Elle Murata—thank you for your friendship and for the countless lavender lattes and our writing sessions together. Without you, this journey wouldn't be the same. And to Carly Chak, Hannah Grotzinger, Madhuri Kashyap, Ava Ma de Sousa, Lexie Topete, Guillem Fernández Villà, Dylan Benkley, and many others—thank you for making this journey so much richer.

I also want to thank my dearest friends who made a place so far from home feel like home: Beyza Arican Dinc, Fatih Dinc, Oya Serbest, Anil Simsek, Zeki Duman, and Baris Kurtkaya. You became family to me here. And to Sedef Akay, Sinem Yalniz, and Su Uyanik—thank you for being my sisters through every part of my life. Even from thousands of miles away, you were always only a phone call away. I love you so much.

Most of all, I want to thank my parents, Hüseyin and Özgül Bekir. My dad, an orthopedic surgeon, was my first window into the world of science and medicine. Some of my earliest memories are of tagging along to orthopedic congresses in Greece and being around people who cared deeply about understanding and healing the human body. They were one of my favorite parts of summers growing up. Thank you for showing me the value of science, education, and dedication through your example. And my mom, my rock. You are the strongest person I know. Your love and endless support have carried me through every stage of my life. You are my superhero. As long as I have you, I know I will be okay. Thank you for always being there. Without you, none of this would have been possible. And my brother, Serkan Bekir, my favorite person on earth. One of the greatest gifts in my life is that I was born with a best friend already by my side. From when I was a kid to now, you are always the first person I call. Your mind is one of the most remarkable I know, and I have been lucky enough to have it on my side always. I am forever grateful for you.

I would also like to thank my mother and father-in-law, Neriman and Muşti Demiroğlu, for welcoming me so fully into family, for your constant love and support, and for raising one of the kindest and best human beings I have ever known.

And finally, to the person who shared every part of this journey with me, my husband, Gürbüz Demiroğlu. I don't even know where to begin. You left everything behind and moved across the world with me so that I could pursue my passion. Through every high and low, you held me steady. You are my anchor, my grounding. You always remind me what truly matters whenever I lose sight of it. Thank you for carrying me through everything, both technically and emotionally. Your technical support became an essential part of my work. Thank you for helping me with my code and for teaching me Python along the way. But more importantly, I learned a lot from your emotional depth and your calmness. You are the most accepting,

grounded, and compassionate person I know. You always seem to have the right perspective, the right advice, and a way of making everything feel manageable. I don't know how I got this lucky, but I am grateful for you every single day. You are my home. No words could ever feel enough, but with all my love and gratitude, I dedicate this thesis to you.

VITA OF SELIN BEKIR

June 2026

sbekir@ucsb.edu | selinbekir.com

Education

University of California Santa Barbara — Santa Barbara, CA
Ph.D. in Cognitive Neuroscience — *2020 – 2026*
Advisor: Michael B. Miller
Committee: Michael S. Gazzaniga, Emily G. Jacobs, Barry Giesbrecht

Boğaziçi University — Istanbul, Turkey
BAs. in Psychology and Philosophy — *2014 – 2020*

Research

Graduate Student Researcher — *2020 - 2026*
Behavioral and Neural Consequences of Callosotomy
UC Santa Barbara, Miller Memory Lab.
Advisor: Michael B. Miller

Research Assistant — *2019 - 2020*
Relationship between Sleep, Affect, and Emotion Regulation
Stanford University, Psychophysiology Lab.
Advisor: James Gross

Research Assistant — *2019*
Tactile Sensitivity of Pacinian and Non-Pacinian I tactile channels
Boğaziçi University, Biomedical Engineering Tactile Research Lab.
Advisor: Burak Guclu

Research Assistant — *2018 – 2019*
Neural correlates of Criterion Shifting in Recognition Memory using tDCS
UC Santa Barbara, Miller Memory Lab.
Advisor: Michael B. Miller

Undergraduate Research Project — *2017*
Cognitive Processes Behind Backward Speech
Boğaziçi University.
Supervision from: Esra Mungan

Publications

Journal Papers

2025. No Disconnection Syndrome after Near-Complete Callosotomy.
Bekir, S., Hopf, J. L., Paul, T., Wiemer, V. M., Santander, T., Skinner, H. E., Rada, A., Woermann, F. G., Kalbhenn, T., Giesbrecht, B., Bien, C. G., Sporns, O., Gazzaniga, M. S., Volz, L. J., & Miller, M. B.
Communications Psychology
https://www.nature.com/articles/s44271-025-00377-5

2025. Full inter-hemispheric integration sustained by a fraction of posterior callosal fibers

Santander, T., **Bekir, S**., Paul, T., Simonson, J. M., Wiemer, V. M., Skinner, H. E., Rada, A., Woermann, F. G., Kalbhenn, T., Giesbrecht, B., Bien, C. G., Sporns, O., Gazzaniga, M. S., Volz, L. J., & Miller, M. B.
Proceedings of the National Academy of Sciences
https://www.pnas.org/doi/10.1073/pnas.2520190122

Manuscripts In Preparation

Split-Brain: Divided Perception and Divided Motor Control.
Distinguishing cortical integration from subcortical facilitation and cross-cueing
Bekir, S., Siemann, J., Rada, A., Woermann, F. G., Kalbhenn, T., Bien, C. G., Santander, T., Sporns, O.,Gazzaniga, M. S.,Volz, L. J. & Miller, M. B.

Willful Modulation of Brain Activity in Disconnected Hemispheres: A Divided Visual Field Mental Imagery fMRI Paradigm for future Split-Brain Application
Bekir, S., Santander, T., Kates-Harbeck, E., Volz, L. J., & Miller, M. B.

Measuring the Sense of Agency Across Hemispheres: Lateralized Adaptations of the Intentional Binding and Cognitive Control Paradigms
Bekir, S., Gavenas, J., Allen, C., McGuinness, J., Hochstein, E., Kaltwasser, L., De Brigard, F., Sinnott-Armstrong, W., & Miller, M. B.

Cognitive Mechanisms Underlying the Right Visual Field Advantage and Bilateral Redundancy Gain in Visual Word Recognition: Evidence from Hierarchical Drift Diffusion Modeling
Bekir, S., Loose, L., Blanco Hermoso, E., Dundon, N., & Miller, M. B.

Book Chapters

2026. What Split-Brain Cases Can Teach Us about Human Agency.
Bekir, S., Gavenas, J., & Hochstein, E.
In De Brigard & Sinnott-Armstrong (Eds.),
Neuroscience and Philosophy II (forthcoming)
MIT Press, Cambridge MA

2025. Hemispheric Specialization (reviewed)
In Gazzaniga, Phelps, Bassett, Mangun, Ivry (Eds.),
Cognitive Neuroscience: The Biology of the Mind (6th edition)
W. W. Norton & Company, New York NY

Presentations Conferences

2026. Cognitive Neuroscience Society, Vancouver, Canada.
Data Blitz Talk: Splitting Mental Imagery: A Divided Visual Field Adaptation of the Mental Imagery fMRI Paradigm for future Split-Brain Application

2025. Cognitive Neuroscience Society, Boston, MA.
Poster Presentation: Structure-function dependencies in large-scale networks: Novel insights from the split-brain.

2024. Psychonomic Society, New York City, NY.
Poster Presentation: Disconnection syndrome in split-brain patients: Splenium's unexpected role in integrating interhemispheric information beyond just visual.

2024. Cognitive Neuroscience Society, Toronto, Canada.
Poster Presentation: Disconnection Syndrome in Split-Brain Patients: Impact of Callosotomy on Cognition and Behavior.

2023. Cognitive Neuroscience Society, San Francisco, CA.
Poster Presentation: Progesterone differentially modulates inter- and intra-hemispheric functional connectivity of the inferior frontal gyrus.

2022. Cognitive Neuroscience Society, San Francisco, CA.
Poster Presentation: Progesterone-Mediated Interhemispheric Decoupling Hypothesis Revisited using Dense Sampling and Intrinsic Functional Connectivity

Awards

2026. UC Santa Barbara Academic Senate Doctoral Student Travel Grant

2023. Summer Seminars in Neuroscience and Philosophy
Research Grant, awarded as a subaward through the John Templeton Foundation. Is Sense of Agency Computed Differently Across the Hemispheres? $25,750

2020. Valedictorian, Boğaziçi University, Istanbul, Turkey.
Awarded for highest academic achievement in the graduating class.

2020. High Honors, BA, Boğaziçi University, Istanbul, Turkey.
Recognizing outstanding academic performance.

2019. Kesişen Yollar Derneği International Internship Grant.
Awarded to support the research internship at Stanford University.

2012. Biology Award, Bornova Anadolu Liseli (High School),
Recognized for an essay on the human brain, exploring key questions in cognitive neuroscience.

Mentorship

Undergraduate Research Assistants Supervised

Emma Kates-Harbeck. Honors thesis; incoming PhD student in Cognitive Neuroscience at University of Miami

Emily Yi. Honors thesis (joint with the Jacobs Lab); currently PhD student Neuroscience at University of California, Irvine

Leila Loose. Incoming MD student at Yale School of Medicine

Esther Blanco Hermoso. Incoming MSc student in Neuroscience at University of Geneva

Jacqueline McGuinness. Currently Lab Manager at the META Lab, University of California Santa Barbara

Joe Gibbons. Currently MSc Student in Kinesiology and Exercise Science at Michigan State University

Cary Higgins
Maya Ayres
Ayra Bandeli
Neda Riaziat
Jasmine Diaz

Teaching **PSY131, Perception: Audition**

Guest Lecturer Fall 2022 –Topics Covered: auditory nerve function, place coding, phase locking,
UC Santa Barbara ascending and descending auditory pathways, and cortical processing of sound.

Teaching **PSY1, Introduction to Psychology**
Assistant Winter 2021, Instructor: Shelly Gable, Ph.D.
UC Santa Barbara Summer 2021, Instructor: Elliott Ihm, Ph.D

PSY10A, Introduction to Research Methods in Psychology
Spring 2021, Instructor: Vanessa Woods, Ph.D.

PSY10B, Statistical Methods in Psychological and Brain Sciences
Spring 2022, Instructor: Elliott Ihm, Ph.D.
Fall 2024, Instructor: Melinda Baham, Ph.D.
Spring 2025, Instructor: Sierra Feasel.

PSY131, Perception: Audition
Fall 2021 – Instructor: John Hajda, Ph.D.

PSY120L, Lab in Advanced Research Methods
Spring 2024, Instructor: Katerina Ford, Ph.D.

PSY113L, Complex Systems
Winter 2023, Instructor: Skirmantas Janusonis, Ph.D.
Winter 2024, Instructor: Skirmantas Janusonis, Ph.D.
Winter 2025, Instructor: Skirmantas Janusonis, Ph.D.
Winter, 2026, Instructor: Skirmantas Janusonis, Ph.D.

Professional Development **2023.** Summer Seminars in Neuroscience and Philosophy (SSNAP), Duke University.
Two-week program exploring interdisciplinary topics at the intersection of neuroscience and philosophy

Skills
Programming Python, R, JavaScript, HTML, Bash, MATLAB.
Languages English, French (Delf B2), Greek, Turkish.
Experimental & Neuroimaging JsPsych, PsychoPy, PsychToolbox, EyeLink & Tobii eye-tracking, fMRI (resting state and event-related)

Other Experiences
ESTIEM Co-founder and First Leader of the Analysis Committee 2017
ESTIEM consists of 60,000+ European Industrial Engineering Students. The aim of this committee was to provide data analyses and data visualizations to support the strategic decision-making of this network.

Snowboard Bogazici University Snowboarding Team

Sailing Sailing Certificate from Fenerbahce Sports Committee

ABSTRACT

Unity in Split-Brain Patients

Behavioral and Neural Evidence from Complete and Partial Callosotomy and New Experimental Paradigms

By

Selin Bekir

What are the neural and behavioral consequences of severing the cerebral hemispheres in humans? Split-brain patients are individuals whose corpus callosum is surgically severed to treat intractable epilepsy. Their unique condition has attracted neuroscientists, psychologists, and philosophers, raising fundamental questions about the nature of human consciousness, selfhood, and agency. In this thesis, I use behavioral and functional neuroimaging approaches, and develop new experimental tools, to examine what remains integrated versus disconnected after hemispheric severance. In Chapter 1, I review different conceptualizations of "unity" in split-brain patients. In Chapter 2, I investigate the behavioral effects of hemispheric severance using both bedside and computerized testing. First, I develop a bedside assessment battery that can be used clinically to characterize disconnection effects across various sensory-motor and cognitive domains, and a novel "disconnection score" that quantifies these effects. This work provides standardized baseline assessments that enable systematic longitudinal testing across pre- and post-surgical timepoints—an approach not previously implemented in this

population. I then use gaze-contingent computerized experiments to test which types of visual information and judgments—from simple presence/absence detection to object identification—remain integrated versus become disrupted under different response conditions. Both bedside and computerized testing provide converging behavioral evidence for disconnection effects: following complete hemispheric severance, each hemisphere can perceive, process, and respond to stimuli without the awareness of the other hemisphere. Critically, a partial patient with only the splenium intact showed no signs of disconnections in these experiments. Chapter 3 investigates the neural correlates of callosotomy using resting-state fMRI and network-based measures. Complete hemispheric severance was associated with marked reductions in interhemispheric functional connectivity and a substantially more lateralized network organization, whereas our partial patient retaining only the splenium showed functional network organization comparable to healthy controls. These neural findings closely mirror the behavioral results observed in Chapter 2. In Chapter 4, I develop and validate new experimental paradigms to more directly probe the unity of sense of agency and conscious awareness across disconnected hemispheres: a lateralized implicit (intentional binding) and explicit (cognitive control) sense of agency paradigms, and a lateralized fMRI mental imagery paradigm. Finally, in Chapter 5, I discuss the implications of these findings for theories of consciousness, and their neural correlates, arguing that not only complete split-brain patients, but sometimes even more critically partial cases, can provide unique insights. Based on the findings from our unique splenium patient, I conclude by entertaining the idea that conscious unity may, in some cases, be hanging by a thread.

TABLE OF CONTENTS

CHAPTER 1. INTRODUCTION 1

A. BACKGROUND 1

1. Split brain Patients and the Disconnection Syndrome 1
2. Debates on Unity in Split-Brain 2

B. OVERVIEW OF THIS WORK 5

1. Primary Aims and Rationale 5
2. Approach and Predictions 8

CHAPTER 2. BEHAVIORAL EFFECTS OF CALLOSOTOMY 11

A. BEDSIDE TESTING OF THE DISCONNECTION SYNDROME AND DISCONNECTION SCORE. 11

1. Abstract 11
2. Introduction 12
3. Methods 15
4. Results 23
   Comprehensive Disconnection Score 27
5. Discussion 28

B. COMPUTERIZED TESTING OF THE DISCONNECTION SYNDROME 35

1. Abstract 35
2. Introduction 36
3. Methods 41
4. Results 48
5. Discussion 64

CHAPTER 3. NEURAL CORRELATES OF CALLOSOTOMY 69

1. Abstract 69
2. Introduction 70
3. Methods 71
5. Results 79
6. Discussion 85

CHAPTER 4. NEW PARADIGMS TO TEST THE UNITY IN SPLIT-BRAIN PATIENTS 89

A. LATERALIZED ADAPTATIONS OF THE SENSE OF AGENCY PARADIGMS 89

1. Abstract 89
2. Introduction 90
3. Methods 93
4. Results 101
5. Discussion 112

B. A DIVIDED VISUAL FIELD ADAPTATION OF THE MENTAL IMAGERY FMRI PARADIGM 119

1. Abstract 119
2. Introduction 120
3. Methods 124
4. Results 132
5. Discussion 140

CHAPTER 5. CONCLUSION 143

1. Thesis Summary 143
2. Implications 143
3. Conscious Unity Hanging by a Thread? 145

REFERENCES 148

APPENDIX 170

CHAPTER 1.
INTRODUCTION

A. BACKGROUND

1. Split brain Patients and the Disconnection Syndrome

Split-brain patients are people whose cerebral hemispheres have been surgically severed to treat intractable epilepsy (Vaddiparti et al., 2021). This surgery, callosotomy, severs the corpus callosum, the major white matter tract connecting the two hemispheres. The introduction of callosotomy in the 1940s emerged from the observation that tumors in the corpus callosum could alleviate epilepsy seizures (Van Waganen & Herren, 1940). Contrary to the initial expectation that severing the right and left hemispheres would significantly impact personality, consciousness, and behavior, most patients showed little change when tested with standardized neuropsychological assessments (Akelaitis, 1945). Although some initial abnormalities like alien hand syndrome (referred to as diagnostic dyspraxia) were observed following surgery, Akelaitis attributed most of these symptoms to factors other than the transection of the corpus callosum. Consequently, the initial clinical assessments concluded that severing the hemispheres had minimal to no cognitive alterations, suggesting that the patient's conscious experience and mental life remained unified and unaltered.

The initial clinical assessments contrasted sharply with subsequent cognitive experiments that utilized *lateralized* testing methods, revealing *the* ***limited sensitivity*** *of early clinical assessments* to callosotomy's cognitive effects. By the time, Sperry and colleagues pioneered innovative testing paradigms in non-human animals, revealing significant cognitive impacts of hemispheric severance (Glickstein & Sperry, 1960; Myers & Sperry, 1958). Gazzaniga later employed similar lateralized procedures on human split-brain patients, demonstrating that each hemisphere could independently perceive, process, and respond to stimuli without the awareness of the other (Gazzaniga et al., 1962), which later led to the awarding of the Nobel Prize in Physiology or Medicine in 1981 to Roger Sperry. These disconnection effects, also referred to as the *'disconnection syndrome'*, not only advanced our understanding of hemispheric information processing and functional specialization but also

prompted profound questions about the unity of consciousness, self, and agency (Bayne, 2008; Schechter, 2012).

2. Debates on Unity in Split-Brain

Split-brain patients' unique condition has long captured the attention of neuroscientists, psychologists, and philosophers, raising a fundamental questions: what happens to a person's consciousness when the brain is split in two? Does severing the corpus callosum create two minds, two independent streams of consciousness in one skull, or does some form of unified consciousness remain intact?

Consciousness is a multifaceted phenomenon (Hansen, 2024), and it is difficult to define, operationalize, and measure. Consequently, the concept of the "unity of consciousness" is difficult to define and test (Bayne & Chalmers, 2003; Dennet, 1992; Nagel, 1971). Nevertheless, several useful criteria have been proposed for what might reflect aspects of conscious unity and the conditions under which it may be disrupted (Schechter & Bayne, 2021). One common way in split brain work is the division between *(i)* perceptual (or experiential-based) unity and *(ii)* motor (or behavioral or agential based) unity:

> *(i)* **Perceptual unity** (Pinto et al., 2017)—or **representational** (Bayne, 2008) or **experience-based conception of conscious unity** (Schecter & Bayne, 2021)—refers to the ability to *integrate* perceptual information across the two hemispheres into a single, unified experience. Disruptions to this form of unity are observed when split-brain patients have difficulty comparing or combining information presented simultaneously to opposite hemispheres. For example, when two images are presented at the same time—one to each visual field—patients are typically unable to determine whether the images are the same or different (Corballis, 1995). Similarly, if the two halves of a compound word are presented separately to each hemisphere (e.g., "hot" to one hemisphere and "dog" to the other), patients can typically respond accurately to each individual word yet fail to integrate them into the unified concept of "*hotdog*" (Kingstone & Gazzaniga, 1995; Miller & Kingstone, 2005). These findings suggest that perceptual information presented to the hemispheres are not readily shared or integrated following complete severance of the corpus callosum.

(ii) **Motor unity** (Pinto et al., 2017)—or **behavioral** (Bayne, 2008) or **action-based agential unity** (Schecter & Bayne, 2021)—refers to the ability of one hemisphere to *respond* to the information presented to the other hemisphere. Disruptions to this form of unity are typically examined through crossed-uncrossed differences in lateralized tasks. Uncrossed trials are those in which the input and output hemisphere are the same (e.g., right visual field input requiring a right-hand or verbal response, both perceived and controlled by the left hemisphere). In contrast, crossed trials are those in which the input and output hemisphere differ (e.g., left visual field input, received by the right hemisphere, requiring a verbal or right-hand response controlled by the left hemisphere). If a patient can accurately respond to stimuli presented to either hemisphere using any response modality, they are considered to exhibit motor unity. However, if performance shows a crossed-uncrossed difference, a double dissociation, where each hemisphere can only respond to information presented to it, this suggests a disruption of motor unity.

The classical view of split-brain syndrome suggests that complete severance of the corpus callosum produces both perceptual and motor disunity, such that perceptual information and behavioral control become separated across the two hemispheres (Gazzaniga, 2000). In contrast, some researchers have argued that split-brain patients continue to exhibit substantial degrees of behavioral or motor unity (Pinto, Neville, et al., 2017; Sergent, 1983). However, we argue that much of this apparent unity can be more illusory than real, arising from methodological artifacts. Indeed, outside tightly controlled lateralized paradigms, split-brain patients often appear behaviorally unified in everyday life. Yet much of this apparent unity may arise from intact subcortical pathways and clever behavioral strategies that preserve the appearance of a unified system without requiring direct cortical integration across the hemispheres (Volz et al., 2018; Volz & Gazzaniga, 2017). These include:

1) *cross-cueing*, where subtle bodily cues compensate for the lack of direct hemispheric communication, akin to the communication seen in close pairs like conjoined twins or friends who can anticipate each other's intentions and actions through subtle bodily cues. In experimental contexts, cross-cueing should be especially considered when the task involves only a few response options, such as binary choices or three-, four- choice options. Decades of split-brain research offer

many compelling examples of this phenomenon: a task initially appears to show no disconnection, yet a small methodological manipulation designed to minimize cooperation outside of the skull—cross-cueing—is all it takes for the disconnection to emerge. For example, Ramachandran et al. reported that split-brain patients could judge apparent motion across visual fields (Ramachandran et al., 1986) . However, Gazzaniga later argued that this did not reflect true cortical integration between the hemispheres, but rather a clever strategy occurring "outside the skull" (Gazzaniga, 1987) . In the original study, every trial contained two flashes—one in each visual field—meaning that each hemisphere "knew" that the other hemisphere had also received a stimulus. Thus, once one hemisphere detected its own flash, subtle behavioral cues could be used to signal which hemisphere had received the flash first, allowing the patient to correctly infer the direction of apparent motion without integrating that information cortically. Critically, when Gazzaniga (1987) introduced proper control trials in which not every trial had two flashes, this strategy collapsed: the hemispheres could no longer assume—or "know"—that the other hemisphere had also been stimulated, and the apparently "unified" behavior disappeared. There are many examples like this in the split-brain literature: whenever a task has a binary or limited possible options to pick from, cueing must always be considered as an alternative explanation, before concluding that a patient shows no disconnections.

2) *intact subcortical structures* that can enable the transfer of some type of simple information to guide the patient's behavior in a seemingly coordinated manner. In the experimental contexts, these typically include simple and coarse visual judgements like presence/absence detection or localization, which may be supported by superior colliculus, a subcortical structure involved in directing reflexive eye movements toward a stimulus (Basso et al., 2021). These eye movements can then convey coarse visual and spatial information that may guide behavior. Indeed, the split-brain literature has long documented that patients can respond in a seemingly unified manner to simple visual and spatial information, which Roger Sperry and Colwyn Trevarthen referred to as the "ambient visual system" (Trevarthen & Sperry, 1973).

3) *the Left Hemisphere Interpreter hypothesis,* which proposes that the left hemisphere readily generates post hoc explanations for behaviors initiated by the right hemisphere,

often misattributing intentions, actions, and outcomes (Gazzaniga, 2000). Especially in everyday life, this interpretive tendency may mask the effects of hemispheric disconnection and create the illusory appearance of an intact, unified intentional and agential system.

Without carefully controlling or considering these factors, apparent behavioral "unity" should not be taken at face value. And critically, even a single clear demonstration that each hemisphere can only respond to information presented to it remains theoretically significant.

Overall, while distinctions between perceptual and motor unity do not fully capture the complexity of the "unity of consciousness," and while many other forms of unity have also been discussed—including "attentional unity," which is typically discussed in terms of both resource allocation and spatial attention (Holtzman et al., 1981; Holtzman & Gazzaniga, 1982; Luck et al., 1989)—we argue that the distinction between perceptual and motor unity remains an experimentally useful first step for examining under what conditions, and for what types of information, perceptual and motor unity remain intact versus become disrupted. And by doing so, it provides a tractable means of experimentally distinguishing complete callosotomy patients from neurotypical individuals with an intact corpus callosum.

B. OVERVIEW OF THIS WORK

1. Primary Aims and Rationale

The aim of this dissertation is to investigate the behavioral and neural consequences of callosotomy, specifically investigating what remains integrated versus disconnected after hemispheric severance; and to develop and validate new experimental paradigms in healthy controls that can later be used to probe unity of consciousness and sense of agency more directly in split-brain patients. Together, these findings can inform current theories of consciousness, sense of agency, and their neural correlates in the intact human brain.

Across four chapters, I aim to approach the question of split-brain "unity" from different angles. Chapter 2A aims to bridge the gap between clinical neuropsychology and experimental cognitive neuroscience by developing a standardized bedside assessment battery for characterizing hemispheric disconnection in split-brain patients that can be easily implemented in clinical settings. This work was motivated by the lack of routine lateralized assessment protocols in clinical practice. Standard neuropsychological assessments used by

clinicians are often insensitive to the effects of callosotomy because they primarily rely on centralized, non-lateralized testing approaches. As a result, clinical evaluations often miss the effects of callosotomy, whereas experimental approaches reveal profound disconnection effects. To address this, Chapter 2A introduces a comprehensive and easy-to-administer bedside battery, along with a novel "***disconnection score***" that systematically quantifies hemispheric disconnection across sensory-motor and cognitive domains. This metric provides a reliable baseline for interpreting performance of each patient in more sophisticated behavioral and neuroimaging experiments and, importantly, enables systematic longitudinal tracking across pre- and multiple post-surgical timepoints—an approach not previously implemented in this population.

Chapter 2B aims to investigate what types of information (from simple presence/absence detection to more complex object identification) can and cannot be integrated across hemispheres, and under what response conditions apparent "unity" versus disconnection emerges. Specifically, investigating whether performance differs between pointing responses, which may allow ipsilateral control of proximal muscles, and button-press responses, which are more cleanly controlled contralaterally. This work was motivated by a study showing that a split-brain could accurate respond to stimuli across visual fields regardless of response modality, arguing that the classic picture of split-brain syndrome are not universally true (Pinto, Neville, et al., 2017). We argue that the apparent unity reported in that study could be due to methodological artifacts rather than a direct cortical integration. To address those methodological artifacts, Chapter 2B introduces carefully controlled lateralized computerized paradigms to investigate under what conditions the classic split-brain disconnection syndrome emerges.

Chapter 3 aims to investigate the neural correlates of hemispheric severance by examining large-scale functional brain organization in split-brain patients compared to healthy controls. Despite decades of behavioral work with split-brain patients, neural consequences of severing the largest white matter tract in the human brain is unknown. This was because callosotomy was largely discontinued around the turn of the 21st century, coinciding with the emergence of modern network neuroscience. As a result, only a few neuroimaging studies in split-brain patients exist and they are very limited in their scope and methods: many were conducted in anesthetized pediatric patients (Hung et al., 2019; Johnston et al., 2008; Pizoli

et al., 2011; Roland et al., 2017), or decades after surgery in aging patients with possible extra-callosal damage (Uddin et al., 2008). Thus, we still do not know how severing the largest white matter pathway in the human brain affects the topological organization and intrinsic dynamics of large-scale functional networks. Chapter 3 aims to address this gap by investigating the neural consequences of hemispheric severance in large scale resting state functional networks measured by fMRI, and to investigate whether neural correlates of callosotomy parallel the behavioral disconnection effects described in Chapter 2.

Chapter 4 aims to develop and validate novel experimental paradigms in healthy controls that could later be used to more directly assess the unity of the sense of agency and conscious awareness across the disconnected hemispheres in split-brain patients. Chapter 4A aims to bridge two largely separate literatures—split-brain research and Sense of Agency research (Haggard, 2017)—by developing lateralized versions of established implicit and explicit Sense of Agency paradigms. Much of the discussion of unity of agency in split-brain patients has relied on simple sensorimotor demonstrations of disconnections (Schecter & Bayne, 2021), while concurrently a large and growing body of Sense of Agency work has introduced principled cognitive experiments to investigate how humans form a Sense of Agency. The novel paradigms introduced in Chapter 4A could provide data that can more directly inform the debates on unity of the sense of agency in split-brain patients.

Similarly, Chapter 4B aims to develop and validate a novel lateralized fMRI mental imagery paradigm for assessing conscious awareness through the willful modulation of brain activation patterns during motor versus spatial mental imagery within each hemisphere. Specifically, this work builds on the seminal work by Owen et al., (2006), who showed that when behaviorally unresponsive patients were asked to imagine playing tennis or walking through their homes in the scanner, they showed activation patterns similar to those of healthy controls: supplementary motor area for tennis and parahippocampal place area for house imagery. Extending this approach, Chapter 4B introduces a lateralized version of the task that can later be applied to split-brain patients to investigate whether unilateral visual cues can engage the imagery-related activation patterns in the contralateral hemisphere, and whether the behavioral reportability from each hemisphere is dissociable from the fMRI activation patterns. Together, these new paradigms aim to provide an experimental tool to directly

investigate the unity of conscious awareness and sense of agency across disconnected hemispheres.

Finally, Chapter 5 synthesizes the behavioral and neuroimaging findings presented in the dissertation and discusses what the outcomes of complete—and, most critically, partial—split-brain patients can reveal about broader debates and theories of consciousness, sense of agency, and their neural correlates.

2. Approach and Predictions

To address these aims, I use behavioral and neuroimaging experiments to test complete and partial callosotomy patients, as well as healthy controls. Chapter 2A uses bedside testing to assess a range of sensorimotor and cognitive domains across anterior-to-posterior functions, including visual, tactile, language and visuospatial processing. I predict that complete callosotomy patients will show clear disconnection effects: impaired performance in crossed conditions (when the input and output hemisphere is different), but intact performance in uncrossed conditions (the input and output hemisphere is the same)—which demonstrates that the task itself can still be performed when inter-hemispheric integration is not required. For the partial callosotomy case with only ~1 cm of his splenium intact, I predict selective disconnections in line with the hypothesized topographic organization of the corpus callosum (Hofer & Frahm, 2006).

Chapter 2B uses a series of well-controlled gaze-contingent computerized tasks to investigate disconnection effects across different types of judgements (from simple presence/absence to more complex identity), different types of stimuli (from simple shapes to everyday objects), and different types of response modalities (from gross-arm movement like pointing, to more fine-motor control like button-presses). I predict that simple judgments such as presence/absence and localization can remain intact in complete split-brain patients, as these judgments may be facilitated by subcortical pathways and gaze cues, whereas identity judgments, which rely more heavily on cortical processing, would reveal clearer disconnection effects. However, even for identity judgments, these disconnections can still be masked if patients use pointing responses, which may be ipsilaterally controlled through proximal muscles, and/or if the response option space is too small, such as binary or three-choice responses, which could facilitate cross-cueing. In contrast, button-press responses and

larger response option sets should reduce these strategies and better reveal disconnection effects in complete split-brain patients. For the partial patient, because the splenium primarily supports visual integration across the hemispheres, I predict no disconnection effects.

Chapter 3 uses resting-state fMRI to investigate the neural correlates of complete and partial callosotomy on large-scale functional brain network organization. Interhemispheric functional connectivity and large-scale functional network organization is characterized in complete and partial split-brain patients relative to healthy controls, using whole-brain functional connectivity matrices, laterality indices across canonical resting-state networks, and data-driven community detection techniques. A foundational assumption of modern cognitive neuroscience is that structural connectivity constrains functional connectivity: although this structure-function relationship is not one-to-one, functional networks are thought to be shaped by the underlying structural connectivity, such that if two brain regions are connected by a direct structural pathway, they are more likely to be functionally coupled (Bassett & Sporns, 2017; Honey et al., 2009; Wang et al., 2013). If structural connectivity indeed constrains functional connectivity, given that the corpus callosum is the primary structural pathway connecting the two hemispheres, I predict that the complete split-brain patients would show marked reductions in inter-hemispheric functional connectivity. For the partial patient with only ~1 cm of the splenium, based on the topographic organization of the corpus callosum, I predict selective disruptions in inter-hemispheric functional connectivity along the anterior–posterior axis, with relatively preserved connectivity in posterior networks but greater disruption in anterior functional networks.

Chapter 4A uses novel lateralized behavioral paradigms based on established implicit and explicit Sense of Agency tasks: intentional binding and cognitive control paradigms. These paradigms adapt classic Sense of Agency experiments into divided visual field designs to investigate hemispheric differences and the role of inter-hemispheric interaction in Sense of Agency formation to develop tasks suitable for future split-brain testing. As a validation step, we tested healthy controls and predicted that the modified paradigms would replicate canonical Sense of Agency effects, including greater intentional binding for self-initiated compared to externally generated actions, stronger binding for expected compared to unexpected outcomes, and reduced perceived control during incongruent compared to congruent cognitive control conditions.

Finally, Chapter 4B uses a novel lateralized fMRI mental imagery paradigm adapted from Owen et al. (2006), in which tennis or house cues are briefly flashed to the left or right visual field to probe the content of the mental imagery. The original paradigm uses auditory cues; here we introduce a divided visual field version so that inputs can be given to each hemisphere in isolation in split-brain patients. We also replaced rest blocks with explicit "nothing" trials as a baseline, which was a practical modification to make the paradigm more suitable for split-brain testing. Given these modifications to the original paradigm, we scanned healthy controls as a validation step and predicted that this modified version of the task would successfully replicate the original findings, showing imagery-related activation in the expected regions of interest: supplementary motor area for tennis imagery and parahippocampal place area for house imagery.

CHAPTER 2.
BEHAVIORAL EFFECTS OF CALLOSOTOMY

A. BEDSIDE TESTING OF THE DISCONNECTION SYNDROME and DISCONNECTION SCORE

This part of the chapter has been published as a journal article in *Communications Psychology*:

Bekir, S., Hopf, J. L., Paul, T., Wiemer, V. M., Santander, T., Skinner, H. E., Rada, A., Woermann, F. G., Kalbhenn, T., Giesbrecht, B., Bien, C. G., Sporns, O., Gazzaniga, M. S., Volz, L. J., & Miller, M. B. (2025). No disconnection syndrome after near-complete callosotomy. *Communications psychology*, *4*(1), 9. https://doi.org/10.1038/s44271-025-00377-5

It is reproduced here with slight alterations.

1. Abstract

Sensorimotor processing in the human brain is largely lateralized, with the corpus callosum integrating these processes into a unified experience. Following complete callosotomy, this integration breaks down, resulting in disconnection syndromes. We asked how much of the corpus callosum is sufficient to support functional unity—the absence of disconnection syndrome—by comparing three complete callosotomy patients with one retaining only the splenium. Using lateralized tasks across visual, tactile, visuospatial, and language domains, we predicted domain-specific deficits in the splenium-only patient based on established anatomical models of callosal topography. Strikingly, while complete callosotomy patients exhibited disconnection syndromes, the splenium patient demonstrated functional unity across all domains—as if his entire corpus callosum were intact. Our findings highlight the brain's remarkable capacity to maintain behavioral integration through minimal preserved pathways, highlighting how the structure-dependent reorganizational capacity of the human brain may allow to preserve functional unity.

2. Introduction

When we began testing a new cohort of callosotomy patients, one patient, BT, stood out with unexpected behavioral outcomes during our initial bedside tasks. On tasks that typically reveal inter-hemispheric disconnections, he showed no signs of impairment, performing comparably to neurotypical individuals with an intact corpus callosum. A closer look at his structural MRI scan and the neurosurgeon's report revealed the source of this surprising observation: a small portion of BT's posterior corpus callosum (part of the splenium) was left intact to prevent surgical complications. This seemingly minor detail would go on to challenge our assumptions about the corpus callosum's functional organization and its mechanistic role in integrating information across the human cerebral hemispheres.

The corpus callosum (CC) is the largest white matter tract connecting the left and right cerebral hemispheres (Aboitiz & Montiel, 2003). Evidence from callosotomy patients—in whom the CC is surgically severed—shows that the CC plays a crucial role in integrating sensorimotor events across the hemispheres. In lateralized tasks that isolate sensory input and motor output to a single hemisphere, these patients show a profound disruption in inter-hemispheric information flow, known as the disconnection syndrome. Although other commissural pathways—such as the anterior, posterior, and hippocampal commissures—typically remain intact and may provide limited residual inter-hemispheric integration (Risse et al., 1978), they cannot fully compensate for the loss of the corpus callosum, as patients still typically exhibit disconnection syndromes (Gazzaniga et al., 1985). For example, consider a callosotomy patient whose speech areas are located in the left hemisphere. When the word "hot" is presented in their left visual field (processed by the right hemisphere) and the word "dog" in their right visual field (processed by the left hemisphere), they verbally report seeing only the word "dog". However, when asked to draw what they saw using their left hand (controlled by the right hemisphere), they draw a fire. Crucially, the emergent concept of a hotdog is never reported, even though each hemisphere accurately processes its respective input (Kingstone & Gazzaniga, 1995; Miller & Kingstone, 2005). This demonstrates the lack of integration and awareness of sensorimotor events in the opposite hemisphere when the CC is fully severed. By contrast, neurotypical individuals with an intact CC do not show such disconnection effects, exhibiting what we refer to as 'functional unity'. We define functional

unity as the absence of a disconnection syndrome—where lateralized inputs and outputs are readily shared and integrated across hemispheres, enabling unified perception and behavior.

The CC is thought to be topographically organized, where anterior callosal fibers project to anterior cortical regions like the prefrontal cortex, and posterior fibers project to posterior regions like the occipital lobe (Hofer & Frahm, 2006). As a result, the CC is argued to have a modality-specific organization with different subsections—from anterior to posterior: rostrum, genu, body, isthmus, and splenium—facilitating information integration in distinct cognitive and sensorimotor domains (Fabri & Polonara, 2023; Liu et al., 2021). The splenium, the most posterior section of the CC, is typically implicated in visual integration, while the posterior midbody is thought to be involved in tactile integration (Caillé et al., 2005; Fabri et al., 2001; Saenz & Fine, 2010). Evidence from partial callosotomy cases sparing these posterior subregions supports this notion (Fabri et al., 1999, 2005; Fabri & Polonara, 2013, 2023; Polonara et al., 2015). However, in most previous partial callosotomy patients, both the splenium and posterior midbody remain intact, rendering a precise functional distinction impossible. The question thus arises: which kinds of information can the splenium alone integrate across hemispheres?

Cases in which only the splenium is left intact are incredibly scarce. Most callosotomy procedures are either completed in a single stage (severing the entire CC) or performed in two stages, with the first stage preserving more than just the splenium (Vaddiparti et al., 2021). Only a few splenium-only cases exist in the literature, and their findings are mixed: some suggest the splenium supports broad inter-hemispheric integration (Gordon et al., 1971), while others indicate it is insufficient beyond visual information (Risse et al., 1989). However, these studies have limitations—some lack MRI confirmation of exact preserved structures (Gordon et al., 1971), while others conducted testing very soon after surgery (within 6 months), making it unclear whether any reorganization had occurred over time (Risse et al., 1989). As a result, the specific contribution of the splenium to inter-hemispheric integration remains unclear.

The current study addresses this gap by reporting on a rare, splenium-only callosotomy case, compared against three complete callosotomy patients. We used an array of lateralized bedside tasks to sample performance across the anteroposterior axis of the CC to identify disconnection syndromes in visual, tactile, and higher-order cognitive functions to determine where performance breakdowns occur after complete versus partial callosotomy, (see **Fig. 2A-**

1A). Based on the framework of the CC's topographic and modality-specific organization, we predicted that complete callosotomy would result in a full disconnection syndrome. Conversely, the partial callosotomy patient with only ~1 cm of splenium intact was expected to show disconnection effects in all tasks except the visual modality, reflecting restricted inter-hemispheric integration along splenial fibers connecting the bilateral visual cortex (see **Fig. 2A-1B**).

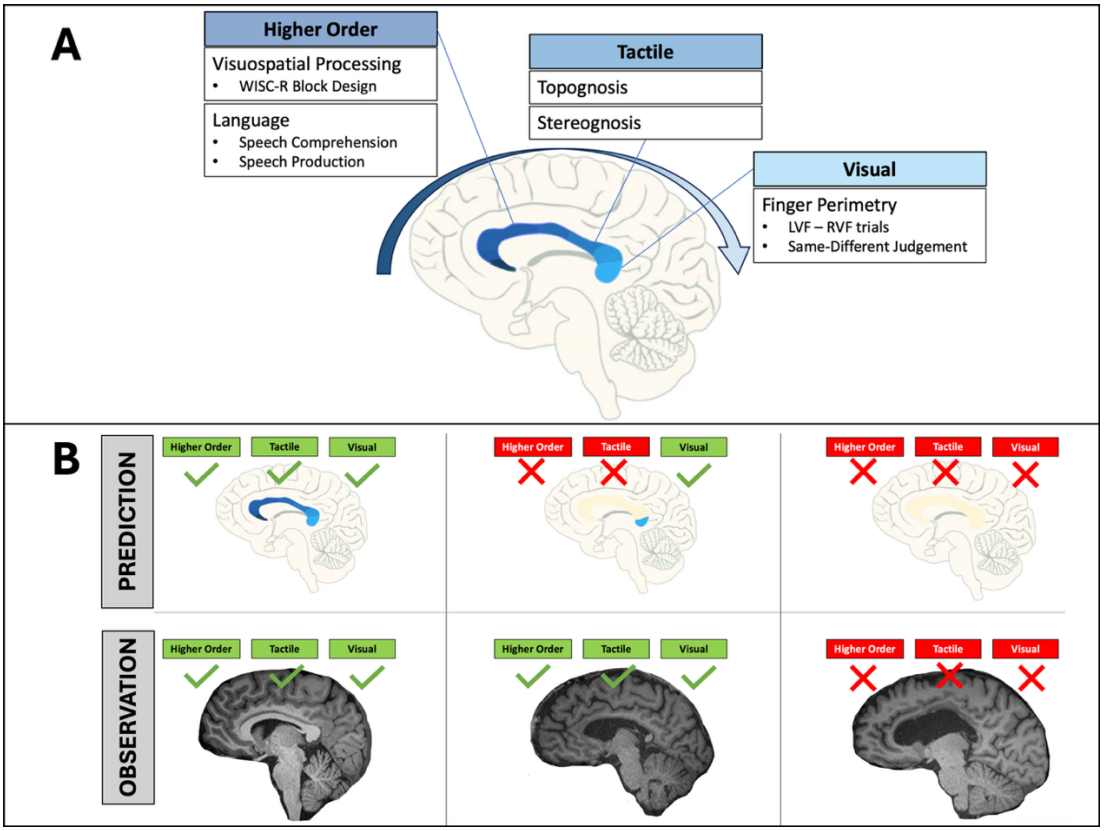


Figure 2A-1 Overview of bedside tests, hypothesized corpus callosum (CC) topography, predicted outcomes, and observed results. (A) Assumed topographic and modality-specific organization of the CC and our bedside tests. The splenium (the most posterior part of the CC) is typically associated with visual integration, while the posterior body is associated with tactile transfer. We used simple bedside tests to assess each domain: finger perimetry for visual integration; topognosis and stereognosis for tactile; and additional tasks probing higher-order functions (visuospatial and language) to test the impact of hemispheric disconnection. LVF = left visual field; RVF = right visual field. **(B)** Predicted (top) vs. observed (bottom) disconnections across three schematic cases: a neurotypical brain (intact CC, shown for reference only), BT* (with only the splenium intact), and a complete callosotomy (patient TJ). Green checks indicate preserved integration; red crosses indicate disconnection. Based on CC topography, we predicted that BT* would show visual integration only. However, BT* exhibited intact integration across all domains, suggesting preserved inter-hemispheric integration despite very limited callosal connectivity.

3. Methods

Participants

We tested four patients (BT, NR, TJ, LJ) who underwent callosotomy to alleviate epileptic seizures. Three patients (NR, TJ, LJ) had complete callosotomy, which fully sectioned the corpus callosum. In BT only posterior fibers were left intact due to technical surgical reasons. All patients were tested post-operatively (see **Table 2A-1** and **Fig. 2A-2**). The surgeries effectively reduced drop seizures in most patients. TJ and NR were entirely drop seizure-free post-surgery (100% reduction), BT experienced a near-complete reduction (98%), and LJ showed moderate improvement with a 20% decrease in drop seizures. No sedation was administered during behavioral testing or MRI scanning procedures. All reported patients here are right-handed (Salmaso & Longoni, 1985), and have language areas in the left hemisphere, confirmed by pre-operative bilateral Wada tests (Wada & Rasmussen, 2007). All patients completed secondary school degrees (10-13 years of education). Post-operative general neuropsychological testing indicated performance ranging from below average to average on working memory and executive function tasks (WAIS-IV Digit Span, forward and backward) (Wechsler, 2012),with BT and NR performing in the below-average range and TJ and LJ falling in the low-average to average range. Dominant-hand praxis was intact in all patients, as assessed by the Apraxia Screen of Tulia (AST) (Vanbellingen et al., 2011). For ease of comprehension, BT is referred to as BT* to denote his status as a partial callosotomy patient. Finally, the anterior, posterior and hippocampal commissures remained intact in all patients. The study was approved by the Ethics committee Westphalia-Lippe (2021-523-f-S). Each patient or the legal representative consented to participate in the study as approved by the Ethics committee. Patients received €100 for attending the examination program at the Bethel Epilepsy Center. Travel, accommodation, and meal expenses were reimbursed with an average of €250 per person. Partial compensation was provided to those who missed some examinations.

Table 2A-1 Clinical Profiles of Callosotomy Patients

Patient	Age at surgery	Age at testing	Time from surgery in months	Sex	Handedness	Intelligence	Extent of Callosotomy	Education (years)
BT*	22	28	70^{+}	M	Right	Low average	Partial	10 years

TJ	49	52	34	F	Right	Average	Complete	13 years
LJ	57	60	26	M	Right	Low average	Complete	10 years
NR	18	18	6	M	Right	Moderately impaired	Complete	12 years

Table 2A-1. Patients Overview. [+]Patient BT was first assessed 70 months after surgery, showing no disconnections; a full battery was conducted later (~87 months post-surgery), yielding the same results. Patient Intelligence classifications are based on the Stanford–Binet Fifth Edition (SB5) classification (Kaufman, 2009; Sattler, 2008). Sex refers to biological sex and was determined from participants' medical records.

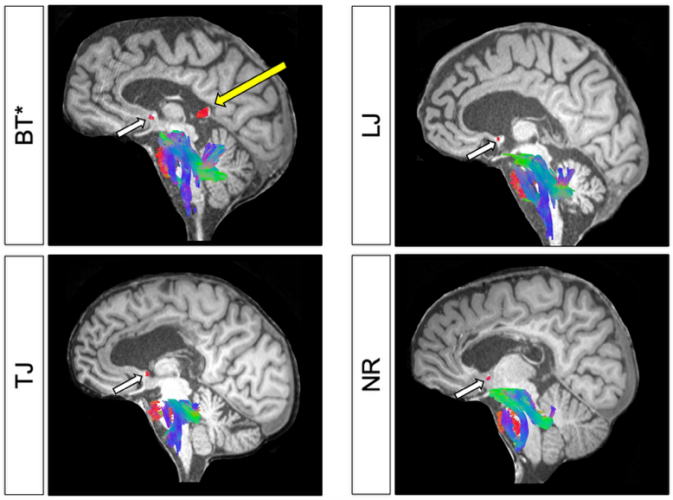
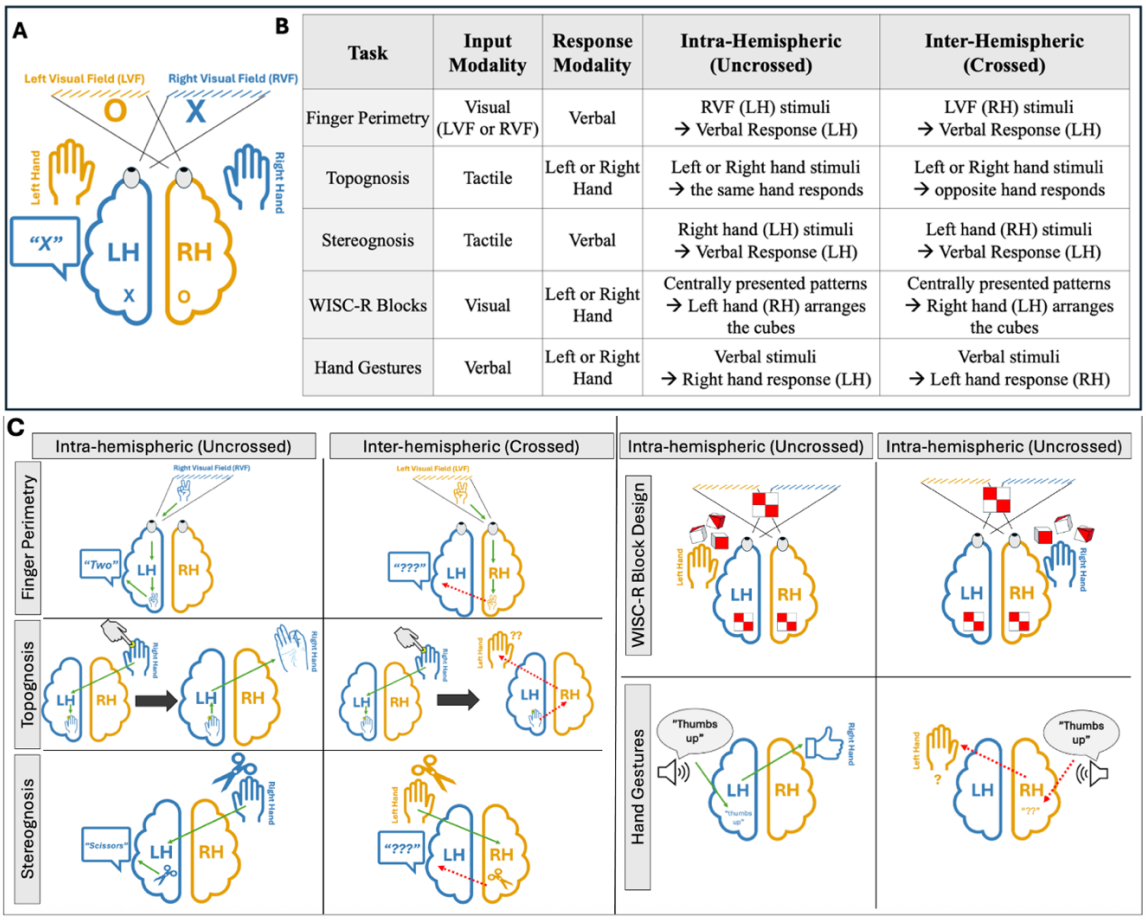


Figure 2A-2 Anatomical Scans of the Patients. Midsagittal T1-weighted MRI images with overlaid DTI-based fiber tractography are shown for each patient. Only select commissural fibers—the anterior commissure and corpus callosum –as well as some cerebellar and brainstem fibers, are displayed. Tractography parameters were adjusted for each patient to provide the clearest midsagittal depiction. The fiber orientations are color-coded: red for left-right, green for anterior-posterior, and blue for superior-inferior directions. All patients exhibit an intact anterior commissure (white arrow), but only patient BT* retains a preserved splenium (yellow arrow), in contrast to the complete sectioning of the corpus callosum in the remaining three patients.

Bedside testing of the Disconnection Syndrome

We conducted a total of five bedside tests to sample performance along the anteroposterior axis of the corpus callosum (see **Fig. 2A-1**). The tasks included visual, tactile, language, and visuospatial tasks, described in detail below. Critically, the tasks comprised an *'intra-hemispheric'* (uncrossed) condition, where the input and output hemispheres were the same, and an '*inter-hemispheric'* (crossed) condition, where the input and output hemispheres differed. We operationalized the presence of a disconnection syndrome as *(i)* above chance

performance in *intra-hemispheric* conditions with concurrent *(ii)* chance-level performance in *inter-hemispheric* conditions for a given task. This contrast establishes that the patient can understand and perform a given task when it is confined to a single hemisphere (*intra-hemispheric* uncrossed trials) and *only* fails to do so if it requires inter-hemispheric integration (*inter-hemispheric* crossed trials). Please see **Fig. 2A-3** for the details of the tasks and conditions. There was no preregistration of this study.



Task	Input Modality	Response Modality	Intra-Hemispheric (Uncrossed)	Inter-Hemispheric (Crossed)
Finger Perimetry	Visual (LVF or RVF)	Verbal	RVF (LH) stimuli → Verbal Response (LH)	LVF (RH) stimuli → Verbal Response (LH)
Topognosis	Tactile	Left or Right Hand	Left or Right hand stimuli → the same hand responds	Left or Right hand stimuli → opposite hand responds
Stereognosis	Tactile	Verbal	Right hand (LH) stimuli → Verbal Response (LH)	Left hand (RH) stimuli → Verbal Response (LH)
WISC-R Blocks	Visual	Left or Right Hand	Centrally presented patterns → Left hand (RH) arranges the cubes	Centrally presented patterns → Right hand (LH) arranges the cubes
Hand Gestures	Verbal	Left or Right Hand	Verbal stimuli → Right hand response (LH)	Verbal stimuli → Left hand response (RH)

Figure 2A-3 Classic split-brain framework and task descriptions. **A**. Hemispheric organization of inputs and outputs. Stimuli in the left visual field (LVF) projects to the right hemisphere (RH), while stimuli in the right visual field (RVF) projects to the left hemisphere (LH). Motor outputs are also lateralized: the LH controls speech and the right hand, while the RH controls the left hand. **B**. Task summary table showing, for each task, the input and the response modality, and examples of uncrossed and crossed trial types. **C.** Examples illustrating uncrossed and crossed trials for each task.

1. Visual Tasks

Finger Perimetry. The experimenter showed varying numbers of fingers in the patient's peripheral vision (in the left or right visual field; LVF or RVF) while the patient fixated

on the experimenter's nose. Then the patient verbally reported the number of fingers while keeping their gaze fixated at the experimenter (i.e., center of the visual field). A same/different version of the task was also conducted: The experimenter showed fingers on both sides simultaneously while the patient maintained central fixation and reported whether the numbers were the same or different.

Inter- and intra-hemispheric trials: Since all patients have speech areas in the left hemisphere and this task required verbal responses, RVF trials (processed by the left hemisphere) were intra-hemispheric trials, and LVF trials were inter-hemispheric trials. In the same/different task, all trials were inter-hemispheric in nature.

Chance-level performance was 20%, as patients could guess any number from one to five in each trial. In the same/different version of the task, chance level was 50% when guessing "same" or "different".

Due to LJ's difficulties with maintaining fixation and/or motivation to perform the task, finger perimetry was successfully conducted for BT*, TJ, and NR only.

2. **Tactile Tasks**

Topognosis—intra- and inter-manual touch localization. The experimenter lightly touched specific points on the fingers of the blindfolded patient's right or left hand. In the intra-manual (i.e., *intra-hemispheric*) condition, the patient used their thumb of the same hand to indicate the stimulated spot; in the inter-manual (i.e., *inter-hemispheric*) condition, the patient used their thumb of the opposite hand to show the corresponding spot on the opposite hand. For example, if the tip of the right index finger was touched, the patient pointed to the tip of the left index finger with their left thumb. Alternatively, in some cases, the patient rested their hands on the table. After the experimenter lightly touched distal segments of the fingers, they indicated its location by raising the corresponding finger. Both versions measure the same underlying ability—tactile localization in intra- and inter-manual conditions. Moreover, the tasks were always compared within subjects—contrasting intra-manual and inter-manual conditions for the same patient—and the task procedure remained consistent across both intra- and inter-manual conditions within each subject. Thus, the findings remained comparable across conditions, and the chance levels were adjusted according to the specific procedure used for each patient.

Inter- and intra-hemispheric trials: *Intra-hemispheric* trials were the summed intra-manual trials from the left and right hands separately; *inter-hemispheric* trials were inter-manual trials summed across both directions (left-hand stimulated, right-hand responds, and vice-versa).

Chance-level performance: For patients NR and TJ, who completed the task using their thumb (indicating tactile stimulation across four fingers), the chance level was 25%. For patients BT and LJ, who completed the task by raising one of their five fingers to indicate the location, chance level was 20%.

Stereognosis—naming objects held in hand. Blindfolded patients were given common objects (e.g., scissor, spoon, fork, ball) to identify using tactile exploration with one hand at a time, alternating between the left and right hand on separate trials. Then, they were asked to name the presented objects. A towel was used to prevent any auditory cues.

Inter- and intra-hemispheric trials: Since all patients have speech areas in the left hemisphere and this task required verbal responses, right hand trials (processed by the left hemisphere) were *intra-hemispheric*, and left-hand trials were the *inter-hemispheric*.

Chance-level performance was 20% as there were five trials (five objects) per hand.

3. **Hemispheric Lateralization of Visuo-Spatial Processing**

WISC-R Block Design. The patient was given colored cubes with surfaces that were solid red, solid white, or half red and half white bisected across the diagonal and were shown pictures of patterns. Patients were then asked to replicate these patterns using the cubes (Wechsler, 2012). A total of 16 trials were conducted, with eight trials using the right hand and eight using the left hand. The first two trials involved creating simpler patterns using two cubes, while the remaining six trials involved arranging four cubes into 2x2 square patterns.

Inter- and intra-hemispheric trials: Previous studies suggest a left hand (right hemisphere) dominance over the right-hand trials (LeDoux et al., 1977). Thus, left hand (right hemisphere) trials were considered *intra-* and the right hand (left hemisphere) trials were considered *inter-hemispheric* trials.

Chance-level performance was not clearly defined for this task. Thus, the left hand (intra-hemispheric) and the right hand (inter-hemispheric) trials were contrasted to assess the disconnection syndrome.

4. Hemispheric Lateralization of Language

Language is a classic example of a lateralized cognitive function (Bishop, 2013; Güntürkün et al., 2020). In most people, the language network is mainly located in the left hemisphere (Lipkin et al., 2022; Szaflarski et al., 2006). Thus, for all language tasks, *intra-hemispheric* corresponded to right hand response trials (controlled by the left hemisphere) trials and *inter-hemispheric* corresponded to left hand response trials (controlled by the right hemisphere).

Language Comprehension in the form of Speech: Hand Gestures Task. The patient performed hand gestures with either the left or right hand, following verbal instructions, with their eyes closed. The gestures included thumbs up, thumbs down, an okay sign, a fist, and two or four fingers up.

Chance-level performance was not clearly defined for this task. Right-hand trials (*intra-hemispheric*) and the left-hand trials (*inter-hemispheric*) were contrasted to assess the disconnection syndrome.

Control—mimicking task. We included a control task to rule out the possibility of general motor impairments, motivational issues, or a broader inability of the right hemisphere to perform a given task using the left hand—independent of its language processing capabilities. In this task, patients, with their eyes open, were asked to mimic hand gestures demonstrated by the experimenter using their left hand. The ability to successfully mimic the gestures in this control condition but not when following verbal instructions suggested that the deficit was not due to motor impairments, lack of motivation, or general performance difficulties, but rather a difficulty to understand the verbal command. Therefore, performance on this control task was more relevant for the cases where one or both hands failed to perform the main task (i.e., executing hand gestures following verbal commands). In such cases, good performance in this control task could serve to rule out general motor deficits or motivational issues as potential explanations for poor performance in the main task.

Language Production in the form of Speech. Tasks that require a verbal response to lateralized stimuli (e.g., finger perimetry, and stereognosis) were used to assess speech production from left hemisphere and right hemisphere. While we previously noted that all patients were left hemisphere dominant for speech production, as determined by the Wada

protocol prior to surgery, there are reports in the literature suggesting that sometimes the non-dominant right hemisphere can develop the capacity to generate speech years after surgery (Gazzaniga et al., 1987). Thus, assessing and reporting speech production from both hemispheres is important during periodic post-operative assessments.

Statistical Analyses

We conducted binomial tests (two-tailed) to determine whether the patient's performance differed from chance-level performance for *inter*- and *intra-hemispheric* trials. The disconnection syndrome was operationalized as (*i*) above-chance performance on *intra-hemispheric* trials and (*ii*) chance-level performance on *inter-hemispheric* trials for the same task. Significance ($p < 0.05$) indicated that the observed performance was statistically different from chance-level; non-significance ($p \geq 0.05$) indicated that the observed performance did not differ from chance. To account for the fact that all tests were conducted in a clinical setting with a limited number of trials, we also performed Monte Carlo simulations with 10,000 iterations to ensure the robustness of our findings. We generated new data under the null hypothesis (chance-level performance) via simulations to estimate the distribution of outcomes and determine the significance of the observed empirical results. For all tasks, the Monte Carlo simulations produced results consistent with the binomial tests.

For tasks where chance performance was not well-defined (WISC-R Block Design and hand gestures), we used permutation tests to compare performance between the right and left hands. To assess this, we used the absolute difference between the hands' proportion correct scores as our test statistic. The permutation test was implemented with 10,000 iterations. For each iteration, we first created binary arrays representing correct (1) and incorrect (0) trials for each hand. We then pooled all these trials from both hands and randomly reassigned them to either hand while maintaining the original number of trials per hand. For each such permutation, we calculated the absolute difference in proportion correct between hands. The *p*-value was computed as the proportion of permuted differences that were equal to or greater than the observed difference. This approach allowed us to estimate how likely it would be to observe a difference as large as the one we found if there were no differences between the hands (statistical significance was set at $p < 0.05$).

Lastly, despite the limited trial numbers and small sample size, our statistical inferences were based on within-subject comparisons of *intra*- versus *inter-hemispheric* trials

within each task. This approach allowed each patient to serve as their own control. In other words, we used each patient's intra-hemispheric trials as a baseline to compare their inter-hemispheric performance and characterize the disconnection syndrome.

Disconnection Score

This *Disconnection Score* was calculated as the proportion-correct in the *intra-hemispheric* condition (ranging from 0 to 1) minus the proportion-correct in the *inter-hemispheric* condition. We computed the proportion-correct scores from the number of correct trials out of the total trials for each condition (**Table 2A-2**). For example, if a patient has a proportion correct of 0.9 in the *intra-hemispheric* condition and 0.1 in the *inter-hemispheric* condition, their disconnection score for that task would be 0.8 (calculated as 0.9 - 0.1). Below is a detailed explanation of the methods used to create the Disconnection Score for each cognitive domain and sensory modality.

Visual. The proportion of correct trials in intra-hemispheric (right visual field) trials minus inter-hemispheric (left visual field) trials from Finger Perimetry was used for the visual disconnection score.

Tactile. Topognosis (intra-manual minus inter-manual trials) was used to calculate the tactile disconnection score, which is considered one of the most sensitive tests for assessing tactile disconnections (Geffen et al., 1985).

Speech Production. For BT*, NR, and TJ, we used Finger Perimetry (RVF minus LVF trials) and Stereognosis (right-hand minus left-hand trials). Difference scores were calculated and averaged for each task. For LJ, only Stereognosis data was available, so the difference score was based solely on this task.

We only included disconnection scores for tasks with clearly defined chance levels and binomial test outcomes. WISC-R spatial block design and hand gestures tasks were not included here because the combination of limited trial numbers and undefined chance levels significantly reduced our statistical power, making the statistical detection of disconnection syndrome challenging in these tasks, even though qualitative evidence supports their presence (see **Results**).

Diffusion MRI Acquisition and Fiber Tractography

To generate tractography images for illustration purposes (**Figure 2A-2**), diffusion-weighted images were acquired on a 3 T Siemens Vida at the Bethel Epilepsy Center using a

32-channel head coil. A single-shot echo-planar imaging sequence was used with one $b = 0$ volume, and diffusion-encoding gradients applied along 30 directions at $b = 1000$ s/mm² (TR = 13.2 s, TE = 83 ms, flip angle = 90°, slice thickness = 2 mm, voxel size = 2 × 2 × 2 mm³, FOV = 256 mm). Parallel imaging was applied using GRAPPA (acceleration factor = 2).

Tractography was performed in DSI Studio (Yeh, 2025). Diffusion data were reconstructed using generalized q-sampling imaging (GQI) (Yeh et al., 2010), and deterministic streamline tracking was applied (Yeh et al., 2013). The anisotropy threshold was randomly selected. The step size was set to voxel spacing. Parameters such as the angular threshold (35-90° range), and the total number of seeds were placed (around 50000 seeds) were individually adjusted across patients to achieve optimal anatomical visualization. Tracks shorter than 40 mm or longer than 200 mm were excluded. Tractography was used solely for illustrative purposes in Figure 2 and was not analyzed quantitatively. Only select commissural, cerebellar, and brainstem fibers were retained for display after manual pruning to enhance clarity. Each tractography rendering was overlaid on the patient's own T1-weighted structural image to highlight the anatomical landmarks relevant to surgical outcomes.

4. Results

As predicted, all complete callosotomy patients exhibited signs of a disconnection syndrome. However, contrary to our expectations, the partial callosotomy patient, BT*, who underwent a near-complete resection, only sparing his splenium, showed no behavioral disconnection effects in any of the tested domains (see **Table 2A-2**). Across all intra-hemispheric (uncrossed) conditions, patients performed significantly above chance (overall $p < 0.05$; individual p-values per task are reported below). These results indicate intact sensory and motor integrity when tasks did not require inter-hemispheric information integration, whereas performance typically broke down once such integration was necessary.

The number of trials varied across patients and tasks because of practical bedside constraints, including fatigue, limited testing time, and stopping some inter-hemispheric trials early to avoid frustration when patients struggled with task performance. For some tasks, when testing time was limited, we prioritized inter-hemispheric trials, once intra-hemispheric ones were performed easily, which led to uneven trial numbers. These case-specific reasons are detailed below; nevertheless, the overall pattern of intact intra-hemispheric and impaired inter-hemispheric performance was generally consistent across patients.

Visual Integration is preserved with splenial sparing

As predicted, BT* with his intact splenium showed no disconnections in visual tasks. He performed significantly above chance in both RVF and LVF trials (4/4 correct, $p = 0.002$ for both) and accurately identified whether numbers in his periphery were the same or different (9/10 correct, $p = 0.021$). The complete callosotomy cases, NR and TJ, on the other hand, showed expected disconnections. They could correctly report the numbers shown in RVF trials (4/5 and 3/3 respectively $p < 0.05$ for both), but not in LVF trials (2/5 and 0/3, $p > 0.05$ for both). NR was also unable to report whether the numbers simultaneously presented in the LVF and RFV were the same or different. (4/10, $p = 0.754$).

Tactile Integration is preserved with splenial sparing

In Topognosis (touch localization) task, BT*, despite only having a small portion of the splenium intact, correctly located tactile stimulation in inter- and intra-manual trials (10/10, $p < 0.001$ for both). In contrast to BT*, all complete callosotomy patients (NR, TJ and LJ) exhibited clear signs of disconnection syndrome. They all failed to cross-locate touch in inter-manual trials (3/8, 4/30, and 0/3 respectively, all $p > 0.05$) but they correctly did so in intra-manual trials (7/8, 26/26, and 3/4, all $p < 0.05$).

In stereognosis task, where we asked patients to name common objects placed in their left or right hand, to test whether tactile information could be transferred to the speaking left hemisphere, contrary to our prediction, patient BT* correctly named the objects handed to his left hand (4/5) and right hand (5/5, $p < 0.05$ for both), showing no signs of disconnection. In contrast to BT*, all complete callosotomy patients (NR, TJ and LJ) failed to name the objects placed in their left hands (3/5, 0/1, and 1/5, all $p > 0.05$), but were able to correctly name them in their right hands (5/5, 6/6, and 4/5, all $p < 0.05$), showing the expected disconnection syndrome.

Note that with TJ, only one left hand trial could be conducted in this task because she verbally reported feeling nothing on the left hand. Thus, the remaining trials were abandoned to prevent further frustration. While this limited the statistical analysis, it is, in-and-of-itself, an excellent demonstration of the disconnection syndrome: When an object was placed in her left hand—processed by the mute right hemisphere—her disconnected speaking left hemisphere repeatedly insisted she felt nothing. However, note that, during the tactile localization task reported above, she performed perfectly fine with her left hand—accurately

locating touch stimuli within her left hand in the intra-manual trials. We administered a higher number of trials in the tactile localization (Topognosis) task for TJ compared to the other patients, specifically to confirm that she was able to perceive and localize the tactile input on the left hand—which she did. This indicates that she did not have any actual sensory loss in her left hand. Instead, it highlights the disconnection between the hemispheres: her right hemisphere could perceive and process tactile input, but her speaking left hemisphere could not access or verbalize that information.

Right hemisphere dominance in visuospatial processing after complete callosotomy

To assess the visuospatial disconnection, we used the WISC-R Block design task (Wechsler, 2012). BT* showed no disconnection in this task. He correctly completed all patterns with his left and right hands (observed difference in proportion correct = 0).

TJ showed clear disruption when using her dominant right hand but not her left hand, consistent with previous reports (LeDoux et al., 1977). Although only two trials were attempted with her right hand—limiting statistical analysis—anecdotal evidence highlights her disconnection, and potentially the involvement of the left hemisphere interpreter (Gazzaniga, 2000). TJ visibly struggled with her right hand. She was incapable of arranging the cubes into a simple 2x2 square, instead repeatedly forming a 3x1 shape, let alone creating the correct patterns. After some effort, she claimed there was something wrong with her vision. However, when switched to her left hand, TJ quickly and accurately created most of the patterns without difficulty (she completed one as a mirror image, resulting in a score of 5/6). Although this is an anecdotal observation and lacks quantification, it is compelling: her left hemisphere verbally rationalized her right-hand struggles, incorrectly attributing them to vision problems, only for her left hand (mute right hemisphere) to perform the task perfectly. Despite this observation, permutation test showed no statistically significant difference between the hands (observed difference in proportion correct = 0.83, $p = 0.1$), potentially due to the limited trial numbers with the right hand (0/2).

NR, being a complete callosotomy patient, successfully completed this task with both hands. There were no significant differences between hands (observed difference in proportion correct = 0). His family reported regular rehabilitation exercises involving similar tasks, which may explain his unexpected right-hand performance compared to other complete

callosotomy patients in this study and in the literature (LeDoux et al., 1977). Alternatively, it is also plausible that he possesses bilateral representations for visuospatial processing.

Speech comprehension and production from the disconnected hemispheres

Speech Comprehension –Hand Gestures Task. BT* successfully carried out hand gestures following verbal commands with his right hand (6/6) and left hand (6/6), showing no difference between the two hands (observed difference in proportion correct = 0).

In contrast, TJ showed difficulty performing hand gestures with her left hand (4/12) when instructed verbally. Remarkably, she easily and accurately performed all gestures when mimicking the experimenter's hand movements with her left hand (9/9), showing no signs of motor or motivational deficits. The difference between her left-hand performance following verbal commands (4/12) and when simply mimicking the experimenter's hand gestures (9/9) was significant (observed difference in proportion correct = 0.66, $p = 0.004$). This suggests that her right hemisphere may be limited in its ability to comprehend speech. There was, however, no significant difference between her left-hand trials (4/12) and right-hand trials (3/3) following verbal commands (observed difference in proportion correct = 0.66, $p = 0.07$). This is likely due to the small and unmatched number of trials despite the observation that her right hand performed the task without difficulty (3/3), while the left hand struggled (4/12). Similarly, even though LJ performed the task well with his right hand (3/4) and struggled with his left hand (0/3), there was no statical difference between the hands (observed difference in proportion correct = 0.75, $p = 0.15$). NR, in contrast, had no difficulty performing hand gestures with his left and right hand following verbal instructions (4/5 and 5/5, observed difference in proportion correct = 0.16, $p = 1$), suggesting that he might have bilateral representations for speech comprehension.

Speech Production. BT* was able to verbally respond to all inputs, whether presented to the left or right hemisphere. In contrast, all complete callosotomy cases demonstrated a clear disconnection syndrome, suggesting that the speech production is still exclusively controlled by the left hemisphere. They could verbally respond only to inputs presented to their left hemisphere (e.g., RVF trials in visual task and right-hand trials in tactile task that requires naming the objects), but not to their right hemisphere (e.g., LVF trials in the visual task and left-hand trials in tactile naming task).

Table 2A-2 Individual Performance on Disconnection Assessments

			Patients			
Domain	Task	Condition	BT*	NR	TJ	LJ
Visual	*Finger Perimetry*	*Intra (RVF)*	**4/4** *P* = .002	**4/5** *P* = .007	**3/3** *P* = .008	NA
		Inter (LVF)	**4/4** *P* = .002	2/5 *P* = .263	0/3 *P* = 1	NA
	Same-Diff.	*Inter-*	**9/10** *P* = .021	4/10 *P* = .754	NA	2/4 *P* = 1
Tactile	*Topognosis*	*Intra-manual*	**10/10** *P* < .001	**7/8** *P* < .001	**26/26** *P* < .001	**3/4** *P* = .027
		Inter-manual	**10/10** *P* < .001	3/8 *P* = .422	4/30 *P* = .204	0/3 *P* = 1
	Stereognosis	*Intra (right hand)*	**5/5** *P* < .001	**5/5** *P* < .001	**6/6** *P* < .001	**4/5** *P* = .007
		Inter (left hand)	**4/5** *P* = .007	3/5 *P* = .058	0/1	1/5 *P* = 1
Visuo-spatial	Block Design	Intra (left hand)	8/8	8/8	5/6	NA
		Inter (right hand)	8/8 *P* =1	8/8 *P* =1	0/2 *P* = 0.105	NA
Language	Hand Gestures	Intra (right hand)	6/6	6/6	3/3	3/4
		Inter (left hand)	6/6 *P* =1	5/6 *P* =1	4/12 *P* = 0.076	0/3 *P* = 0.14

Table 2A-2. Performance of each patient across tasks and conditions. The table presents the number of correct trials for each patient. Tasks in *italic* (e.g., Visual and Tactile tasks) were analyzed using binomial tests to assess whether performance exceeded chance-level. **Bold** scores indicate above-chance performance ($p < 0.05$), while non-bold scores reflect chance-level performance. Notably, BT* consistently performed at ceiling levels in both *inter-* and *intra-hemispheric* conditions. In contrast, complete callosotomy patients generally struggled with *inter-hemispheric* tasks but performed well on *intra-hemispheric* trials. Block Design and Hand Gesture tasks were analyzed using permutation tests to compare the left- and right-hand performances, with a single *p*-value reported for each comparison. While BT* and NR showed no differences between hands, TJ and LJ exhibited trends suggestive of differences. However, due to limited and unmatched trial numbers (e.g., 5/6 vs. 0/2 for TJ), none of the comparisons were statistically significant (all $p > 0.05$). Some tasks were aborted early (e.g., 0/2) when patients showed visible struggles, to prevent further frustration. These methodological limitations are discussed in the Results and Discussion sections.

Comprehensive Disconnection Score

To summarize the disconnection syndrome across different domains for each patient, a difference score was calculated between intra- and inter-hemispheric conditions, providing a measure of the degree of disconnection (see **Figure 2A-4**). This *Disconnection Score* was calculated as the proportion-correct trials in the *intra-hemispheric* condition (ranging from 0 to 1) minus the proportion-correct trials in the *inter-hemispheric* condition. A Disconnection Score close to 0 indicated no disconnection (i.e., equal performance in intra- and inter-hemispheric conditions); and a Disconnection Score close to 1 indicated full disconnection. Complete callosotomy cases showed varying degrees or severity of the disconnection

syndrome across domains, but all exhibited clear signs highlighting a disruption of inter-hemispheric information integration. In contrast, BT* consistently had scores near 0, suggesting no difference between intra- and inter-hemispheric performance—indicating no disconnection syndrome.

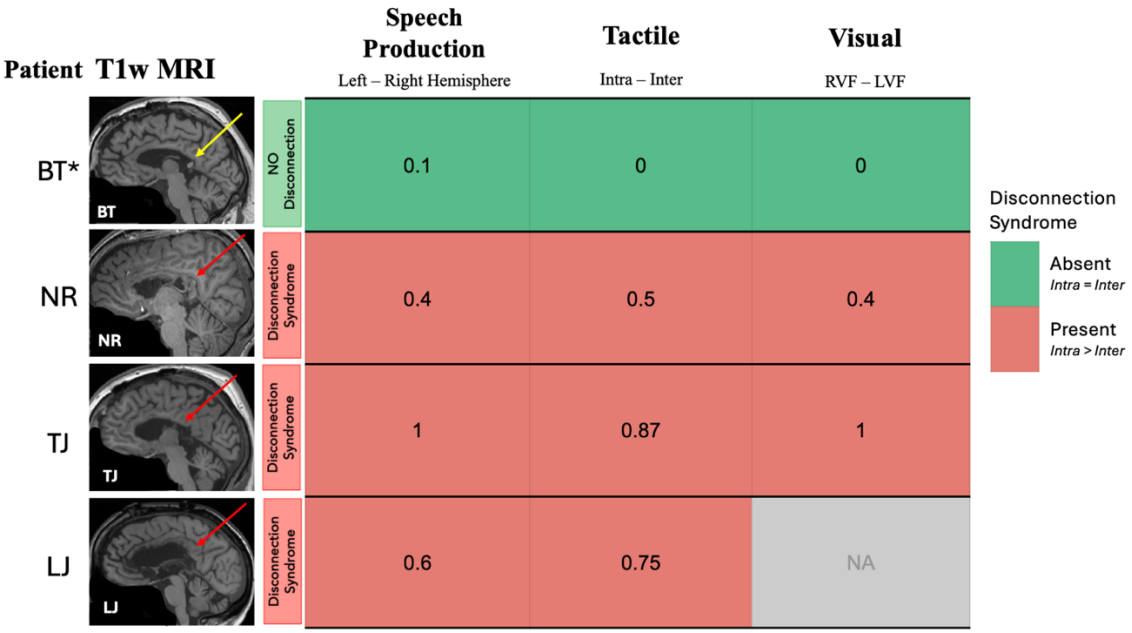


Figure 2A-4 Disconnection Scores. Binary color-coded representation of the disconnection syndrome. *Red* indicates the presence of the disconnection syndrome, defined by above-chance performance in intra-hemispheric trials ($p < 0.05$), and chance-level performance in inter-hemispheric trials. *Green* indicates no disconnection, with above-chance performance in both inter- and intra-hemispheric conditions. *Gray* indicates no available data. Disconnection Scores range from 0 (equal performance in inter- and intra-hemispheric conditions) to 1 (perfect intra-hemispheric performance with chance-level inter-hemispheric accuracy). Structural MRIs with red arrows indicate complete callosotomies, while the yellow arrow indicates partial callosotomy. Patient BT*, while structurally more similar to complete callosotomy cases with the majority of the CC severed, exhibited no disconnection syndrome, performing equally well in inter- and intra-hemispheric conditions.

5. Discussion

This study presents the first behavioral findings from a new cohort of adult callosotomy patients tested between 1 and 6 years post-surgery. We found that the complete callosotomy patients exhibited disconnection syndromes across multiple sensory and cognitive domains. In contrast, the patient with a partial callosotomy, sparing only the

splenium, showed no evidence of disconnection syndrome. These results offer two key contributions to our understanding of the cognitive and behavioral effects of hemispheric severance.

First, our current results provide new evidence for the ongoing debate regarding the extent of disconnection syndromes in callosotomy patients (de Haan et al., 2020; Pinto, De Haan, et al., 2017; Pinto, Neville, et al., 2017; Schechter & Bayne, 2021; Volz et al., 2018; Volz & Gazzaniga, 2017). This recent debate concerns whether the traditional characterization of the 'split-brain phenomenon'—marked by performance disruptions when input and output hemispheres differ during inter-hemispheric trials—is as robust or widespread as traditionally reported. It was sparked by a report of complete callosotomy patients who could respond to lateralized inputs with either hand, leading the authors to argue that "motor unity" persists despite the complete severance of the CC (Pinto, Neville, et al., 2017). In contrast, our findings with this new cohort replicate the classical findings: all complete callosotomy patients exhibited clear disconnection syndromes—performing well on intra-hemispheric trials but poorly on inter-hemispheric ones. Hence, there was no behavioral evidence of motor unity. Our results suggest that alternative explanations, such as the cross-cueing (Volz et al., 2018; Volz & Gazzaniga, 2017), may account for the apparent unity reported in Pinto and colleagues (Pinto, De Haan, et al., 2017; Pinto, Neville, et al., 2017).

Second, our study presents a unique and exceptionally rare splenium case whose performance challenges the assumptions of the current anatomical models of callosal topography. Given that BT* retained only the posterior portion of the splenium, we expected to observe a partial disconnection syndrome, such that visual information integration would remain intact, facilitated by the splenium, while more anterior functions such as tactile integration or higher order functions would be disrupted (see **Fig. 2A-1B**). However, BT* showed no disconnections at all, leading to the question how functional unity can be achieved in light of the minimal structural integrity of the corpus callosum.

One critical factor can be the *timing of the testing since surgery*. There are reports of splenium-only patients who demonstrated selective disconnections when tested shortly after surgery (within 2–6 months (Risse et al., 1989); see **Fig. 2A-5** for case comparisons). In contrast, we tested BT* six years after his surgery. These six years may have allowed enough time for the brain to undergo profound reorganization, with the splenium serving as the critical

anatomical substrate enabling the inter-hemispheric transfer of information for various functional networks (Santander et al., 2025). While subcortical structures have also been proposed as alternative routes for such reorganization (Pinto, Neville, et al., 2017; Uddin et al., 2008), all patients in our cohort featured intact subcortical pathways. Yet only BT* showed functional unity across all tested domains. This suggests that it is the presence of the splenium—rather than intact subcortical pathways alone— may enable functional unity across hemispheres.

Further support for this notion stems from resting-state functional connectivity analyses which revealed that BT*'s inter-hemispheric connectivity was largely sustained; various measures of functional network integration resembled that of healthy controls with an intact corpus callosum, in stark contrast to complete callosotomy patients (Santander et al., 2025). These observations show that even small posterior callosal remnants can sustain widespread inter-hemispheric functional coupling, consistent with his intact behavioral performance.

Additionally, BT*'s unexpected behavioral results, compared to the other splenium-only cases, may be explained by *the extent of CC preservation*, in line with a *threshold effect*. For instance, patient JKN(**Fig. 2A-5D**) (Gazzaniga, 1988) may have had a smaller intact portion of the splenium than BT*, which could explain the selective disconnections observed in him but not in BT*. In other words, JKN's smaller intact portion of the CC may have fallen below the critical threshold needed for reorganization, leading to persistent disconnection symptoms. Of note, threshold effects are common in complex systems, where gradual changes often produce no noticeable impact until a critical point is reached, leading to a sudden state shift (Mitchell, 2011).

The direction of the callosal resection—anterior-to-posterior versus posterior-to-anterior—might also be an important factor (Funnell et al., 2000). One of the proposed evolutionary origins of the CC is argued to be midline fusion for the sensory cortices (Aboitiz & Montiel, 2003), with humans heavily relying on sensorimotor processes to interact with the world. Thus, posterior inter-hemispheric integration might better preserve the system's integrity and may allow for more effective compensation than vice versa. What, then, is the role of the anterior CC? Our tasks may have been insensitive to effectively probe this question. While we cannot definitively rule out the absence of *any* disconnection syndromes in BT*, he

showed no such signs on our battery of bedside assessments**.** Moving forward, more rigorous and targeted testing with BT* is needed to better probe the anterior CC's role in cognition.

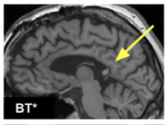
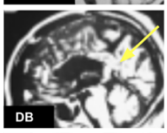
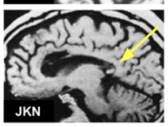
		Patient	Testing Time Post-Surgery	Disconnections	Factors That May Explain Discrepancies	MRI Reference Sources
A		BT*	6 years	Visual. **NO** Topog. **NO** Stereog. **NO**	-	The Current Study
B		Case 9	2-6 months	Visual. **NO** Topog. **YES** Stereog. **YES**	Timing of Post-Surgery Testing	Risse et al., 1989
C		DB	12 years	Visual. **NO** Topog. **NA** Stereog. **YES****	**Unclear behavioral reports	Fabri et al., 1999
D		JKN	Probably < 1 year†	Visual. **NO** Topog. **NA** Stereog. **YES**	Timing of Post-Surgery Testing and/or Extent of Preserved CC fibers	Gazzaniga, 1988

Figure 2A-5 Case Comparisons: Splenium Patients. Overview of previous partial callosotomy cases similar to BT*, with testing times since surgery, observed selective disconnections, and potential factors explaining differences in disconnection profiles. **A.** Patient BT* (current study). **B.** Case 9. **C.** Patient DB. **D.** Patient JKN. "Topog." refers to topognosis, "Stereog." to stereognosis. "No" indicates the absence of disconnection syndrome. For case JKN, the testing time is probably within the first year (†Prof. Gazzaniga, personal communication). **For case DB, stereognosis performance is unclear. DB was described as showing disconnection syndrome in stereognosis, however, the report states that she successfully named objects with her left hand 75% of the time (Fabri et al., 1999). This relatively high success rate suggests that her tactile processing may be more similar to BT*'s preserved abilities than to the clear deficits typically seen in complete callosotomy patients.

A further relevant comparison can be made with patients who suffer from non-surgical lesions affecting the CC. Such partial lesions to the CC typically result in selective functional impairments that align with the CC's topographic organization (Caillé et al., 2005)—unlike what we observed in BT*. Previous research has highlighted that behavioral outcomes tend to differ between surgical and non-surgical CC disruptions (Gordon et al., 1971), partly because non-surgical lesions may involve more diffuse, extra-callosal damage, whereas callosotomy targets the CC more precisely. Another key difference could be the temporal progression of these lesions: callosotomy involves a sudden severance of the CC, whereas non-surgical lesions may develop more gradually. Initially, sudden disruption may lead to clearer disconnections compared to gradual lesions where compensatory mechanisms might develop simultaneously with the lesion. However, over time, the non-progressive nature of

callosotomy can offer a stable foundation for network reorganization, potentially resulting in the preserved functional unity we observed in BT* six years after his surgery. A similar distinction can be seen in agenesis of the corpus callosum (Paul et al., 2007), a non-progressive, congenital absence of the CC. Despite the total lack of inter-hemispheric callosal fibers, individuals with callosal agenesis often do not show the disconnection syndromes observed in complete callosotomy patients—likely due to developmental plasticity that reorganizes function from birth.

Methodologically, our study introduces a key contribution: the Disconnection Score. Split-brain research has long lacked standardized tools and metrics, making it difficult to compare cases across studies. While in-depth domain-specific investigations have provided valuable insights into specific aspects of callosal function, we lack a standardized disconnection profile metric that could be reported for each patient regardless of the study's primary focus. Our multi-domain assessment provides a standardized framework for quantifying disconnection severity. By assessing performances across visual, tactile, and higher-order cognitive domains using simple bedside tests, this method aims to provide an initial “disconnection profile” for each patient. Moreover, the tasks are simple enough for patients with intermediate cognitive impairment to perform.

Limitations

There are four main limitations of our study. First, the *lack of longitudinal* data prevents us from determining whether BT*'s intact performance reflects an absence of disconnection syndrome all along or their resolution through network reorganization over the years post-surgery. While network reorganization remains the most plausible explanation given the existing reports of selective impairments in other splenium cases (Risse et al., 1989), we cannot definitively establish BT*'s symptom trajectory. Similarly, we cannot fully rule out alternative factors such as rehabilitation-induced plasticity or premorbid bilateral representations. However, such explanations are highly unlikely to account for all task domains. For example, while premorbid bilateral organization may support functions with hemispheric dominance (e.g., speech comprehension or visuospatial processing), they are insufficient to explain preserved performance on tasks such as topognosis that strongly rely on inter-hemispheric transfer. Second, while BT* showed no disconnection syndrome on our battery of bedside assessments, our current methodology does not allow us to pinpoint the

underlying mechanisms for this functional unity. In other words, the precise nature of what is being integrated remains unclear. While the splenium is traditionally associated with visual information integration, recent evidence suggests its fibers also project to temporal cortices (Friedrich et al., 2020). It is possible that what is transferred may not be the sensory input, but more abstract, conceptual representations. More rigorous behavioral testing, alongside event-related functional neuroimaging and high-resolution diffusion MRI—including tractography analyses to identify cortical termination points—will be necessary to further delineate these mechanisms and clarify the functional contributions of preserved splenial pathways. Third, with respect to our language tasks, we make inferences about speech comprehension and production, but more rigorous testing is needed to evaluate these processes in more detail. Our "speech comprehension" task likely engaged a multi-step process: (1) auditory speech perception, (2) semantic comprehension, and (3) motor planning/execution. The control gesture imitation task rules out step 3—praxis or motor deficits—if the patient was able to accurately mimic gestures on sight. Thus, failure to perform gestures on verbal command, despite intact imitation, points to a disruption in the auditory-to-semantic pathway (steps 1 and/or 2), which our current design cannot further dissociate. Future studies using refined controls, such as more rigorous testing of meaningless gesture imitation or lateralized auditory tasks, may help to further delineate why patients were not able to successfully perform the task (e.g., whether it is related to phonological input vs semantics). Similarly, our speech production tasks would benefit from the addition of a systematic non-verbal response condition (e.g., left-hand responses during finger perimetry) to ensure that observed deficits indeed reflected impaired verbalization rather than failures in visual or sensory processing. Finally, our findings are limited in *generalizability* due to the single-subject nature of BT*'s case and the *limited number of trials* due to clinical testing constraints—which significantly reduced statistical power. Then again, several aspects of our study design strengthen the validity of these findings. The within-subject design offers robust control over individual variability, and the selective disruption observed in complete callosotomy cases—only in inter- but not intra-hemispheric conditions—suggests a targeted impairment in tasks requiring inter-hemispheric transfer or integration, rather than a general deficit. This pattern of selective disruption stands in stark contrast to BT*'s intact performance across similar tasks

In conclusion, our study suggests that even a small, intact posterior callosal remnant can sustain remarkable functional capabilities years after surgery. While BT* is a single case, and the absence of longitudinal data prevents us from determining whether this integration was preserved immediately post-surgery or emerged through network reorganization over time, this observation nevertheless highlights the splenium's remarkable role in such integration. Our current findings support the notion that inter-hemispheric structure-function relationships in the human brain do not follow a linear pattern where behavioral disruptions scale with the extent of structural (callosal) resection. Instead, minimal preserved structural connectivity may maintain broad integration beyond what our classical anatomical models predict.

Data availability

The data supporting the findings of this study are available on GitHub at https://github.com/selinbekir/splitbrain-disconnection-analysis. The structural MRI scans were not quantitatively analyzed and were included only to illustrate the extent of callosal resection (Figure 2). Due to existing data-sharing agreements with the clinical site, the full MRI datasets cannot be made publicly available at this stage. However, access can be granted upon request following the establishment of an appropriate data-sharing agreement.

Code availability

Analysis code is openly available on GitHub at https://github.com/selinbekir/splitbrain-disconnection-analysis.

B. COMPUTERIZED TESTING OF THE DISCONNECTION SYNDROME

Collaborators:

Julia Siemann, Anna Rada, Friedrich G. Woermann, Thilo Kalbhenn, Christian G. Bien, Barry Giesbrecht, Tyler Santander, Olaf Sporns, Michael S. Gazzaniga, Lukas J. Volz, & Michael B. Miller

1. Abstract

Does severing the corpus callosum create two independent conscious perceivers within one brain? The canonical split-brain literature suggests it does: patients can only respond to stimuli presented in the left visual field with the left hand, and to stimuli in the right visual field with the right hand and verbally. Recently, this view has been challenged by a study showing that a split-brain patient could accurately detect, localize, and identify stimuli throughout the entire visual field regardless of response modality—leading to the conclusion that "consciousness is undivided" despite callosal disconnection. We argue that this apparent unity is better described as "motor unity"—unified responding irrespective of which hemisphere receives the input—and that it likely reflects methodological artifacts rather than genuine interhemispheric integration or "conscious unity". Using a series of experiments in six split-brain patients (five complete, one partial), we show that three factors can mask the classic disconnection syndrome: (1) simple detection and localization judgments can be facilitated by subcortical pathways and stimulus-driven eye movements, making unified responding on such tasks neither novel nor evidence of preserved cortical integration; (2) pointing responses involve gross arm movements that, via ipsilateral control of proximal muscles, can be guided by either hemisphere—making it unclear which hemisphere is guiding the response and thus, rendering the results uninformative—whereas fine finger movements involving distal muscles are more cleanly contralaterally controlled; and (3) small response sets (e.g., binary or three-choice options) enable cross-cueing, allowing one hemisphere to infer what the other hemisphere saw without actually perceiving it. We show that when these confounds are controlled, the classic disconnection emerges in complete split-brain patients: each hemisphere responds only to stimuli presented to it. These findings reinstate the canonical view: severing the corpus callosum creates independent conscious perceivers within one brain.

2. Introduction

The corpus callosum is the largest white-matter tract connecting the two cerebral hemispheres of the human brain (Aboitiz & Montiel, 2003). Research with split-brain patients–whose corpus callosum is surgically severed to alleviate intractable epilepsy (Vaddiparti et al., 2021)–established the corpus callosum as essential for integrating lateralized sensory inputs and motor outputs into coherent perception and behavior (Bekir et al., 2025; Gazzaniga et al., 1962). When the corpus callosum is fully severed, sensory input given to one hemisphere can no longer be reported by the contralateral hemisphere, leading to the *disconnection syndrome*.

Pinto et al. (2017), however, reported findings that challenge this canonical view. They report that a split-brain patient could accurately **detect** whether a stimulus was present, **localize** where it appeared, and even **identify** what it was across both visual fields using any response modality—left hand, right hand, or verbal. Based on these findings, Pinto and colleagues concluded that the canonical textbook claims about the split-brain patients are not universally true and that severing the cortical connections between hemispheres does not create two independent conscious perceivers within one brain (Pinto, De Haan, et al., 2017; Pinto, Neville, et al., 2017). Yet the same patient could not tell if the two images simultaneously presented to opposite visual fields were the same or different. This failure led Pinto et al. conclude that callosal disconnection splits visual perception (termed "divided perception") even though the ability to respond to stimuli in either field appears intact (from this observation, they inferred "undivided consciousness") (Pinto, De Haan, et al., 2017; Pinto et al., 2023; Pinto, Neville, et al., 2017).

How do we reconcile this "divided perception" with the seemingly intact ability to respond to stimuli in either visual field using any response modality ("undivided consciousness")? We argue that this apparent unity in responding better described as "motor unity"—unified responding irrespective of which hemisphere receives the input—and that it likely reflects methodological artifacts rather than genuine interhemispheric integration or "undivided consciousness".

Specifically, we argue that whether the disconnection is behaviorally observable depends on three factors: (1) **the judgment type** (simple detection/localization versus complex identity discrimination), (2) **the response type** (gross motor movements like pointing versus fine motor movements like button-presses), and (3) **number of response**

options (small sets, such as binary or three-choice options—enabling cross-cueing—versus larger response options where guessing or cross-cueing between hemispheres is minimized) (see **Fig. 2B-1**).

First, the **type of perceptual judgment** is critical when drawing conclusions about apparent "motor unity" in split-brain patients. Simple detection and localization can be supported through subcortical pathways, such as the superior colliculus, which can direct reflexive eye movements toward a stimulus (Basso et al., 2021). When an image appears in one visual field, the hemisphere that saw it can shift the gaze toward it. This eye movement itself can signal, to both hemispheres, that something appeared (facilitating presence/absence detection), and the direction of gaze can signal where it appeared (facilitating localization, as the patient can simply point to where they are looking). In contrast, identifying what a stimulus is (e.g., determining its color, shape, object identity etc.) require cortical processing, and therefore, are more likely to reveal disconnections. Yet Pinto et al. reported accurate performance on identity judgments as well, including reporting the shape or category of an image (e.g., a fox or a tank) (Pinto, Neville, et al., 2017). We argue that this apparent unity on identity tasks can be attributed to the remaining two methodological factors:

Second, the **type of motor response** can determine whether disconnections are observable or not. Pointing involves proximal muscles (shoulder, upper arm) that can be controlled ipsilaterally (Gazzaniga, 2000; Miller & Kingstone, 2005; Tazoe & Perez, 2014). This means that when the patient points to a response option, either hemisphere can guide that movement. As a result, hemisphere-specific responding is no longer isolated, making the task uninformative for detecting disconnection effects. In contrast, fine-motor responses like button-presses involve distal muscles that are more cleanly controlled contralaterally, which can better preserve hemisphere-specific responding, making it more likely to detect the disconnection effects. Thus, the unified pointing responses reported in Pinto et al., (2017) may simply reflect the ipsilateral control aspect of pointing responses rather than providing evidence for undivided consciousness.

Third, **number of response options** can contribute whether cross-cueing is possible or not. Whenever response options are binary or limited to a small set, cross-cueing should be considered (Volz et al., 2018; Volz & Gazzaniga, 2017). Even tasks involving identity judgments and fine motor or verbal responses can therefore fail to reveal the disconnection if

the answer space is too small. In such situations, one hemisphere can use subtle behavioral cues to signal the other hemisphere so that it can get the correct answer from a short list of possibilities. Decades of split-brain research offer many compelling examples of this phenomenon: whenever a task has a binary or limited possible options to pick from—and especially if the patients fail at cross-integration tasks like the same/different judgments—cross-cueing must always be considered as an alternative explanation, before concluding that a patient shows no disconnections.

Because there can be *many subtle ways* in which the cross-cueing can take place, Pinto et al. criticized it to be too vague and difficult to falsify (Pinto, Lamme, et al., 2017), arguing that it can easily become a post hoc explanation invoked to explain away any anomalous result. That is a fair methodological concern. But we are not arguing for some abstract, all-purpose notion of "cross-cueing" that can explain any unified behavior. Rather, we argue that researchers should make an educated guess about the specific compensatory strategy a patient might be using, design a control condition that directly removes that strategy, and then test whether unified behavior still persists. In the present context, we argue that tasks with small response spaces—such as three-choice shape discrimination or binary fox-versus-tank judgments used in Pinto et al., study (2017)—can permit accurate performance through cross-cueing. To test this, we asked a simple question: what happens when the patient no longer knows the set of possible answers? Rather than repeatedly selecting among a small number of predictable alternatives (e.g., triangle/square/circle or fox/tank), what happens when patients were required to identify everyday object drawings that were—critically—presented only once and therefore could not be inferred through elimination, guessing, or indirect hemispheric cooperation?

Finally, an important but rarely discussed methodological concern in split-brain research involves the **practical challenge of reliably testing each disconnected hemisphere**. Even when potential confounds are controlled through careful experimental design (some mentioned above), misleading results can still arise if one hemisphere does not understand or engage with the task. In such cases, poor performance in one visual field may falsely appear as a "hemispheric difference," when in reality the underperforming hemisphere may simply not understand or engage with the task. Researchers who have worked with split-brain patients for many years have long recognized this issue. Both Michael Gazzaniga and Michael Miller

emphasized that effectively testing each of the disconnected hemispheres can be far from straightforward. Standard training and practice procedures that work well with non-split people can fall short, especially for the disconnected right hemisphere. Moreover, verbal reports from the speaking left hemisphere can misleadingly give a naïve experimenter the impression that the patient (i.e. both hemispheres) understood the task. Michael Gazzaniga once noted that testing the right hemisphere can be as if testing a chimpanzee: one should never assume it understood something simply because it was told (M. Gazzaniga, personal communication). Instead, proper testing requires gradual and extensive training through demonstration and repetition. Training should begin with very simple actions—e.g., flashing a stimulus at the center of the screen and asking for a button press—and only gradually build toward the actual task demands and response mappings. Critically, the practice phase should continue, without any time constraints, until it is unambiguously clear from the right hemisphere's behavior that it can reliably follow the task rules. Only then should the actual divided visual field experimental trials begin. Michael Miller echoed this further, recalling from his own experience testing patient V.P., that it could sometimes take half a day or more to "wake" the right hemisphere to a level of engagement where meaningful data could be collected (M. Miller, personal communication).

To sum, in this study, we addressed these factors by systematically manipulating (1) judgment type—from simple presence/absence and location to identity discrimination, (2) response modality—button-press versus pointing; and when patients showed no disconnection on identity tasks with button-press or verbal responses, we further (3) repeated the task with a larger stimulus set to minimize cross-cueing. For systematic comparison with prior work, we also included a cross-integration same/different judgment task.

We predicted that there won't be any disconnections for the partial case, BT, as his intact splenium should transfer any visual information across the hemisphere, for the complete split-brain patients, we hypothesized that: (1) for presence/absence and location judgments, some split-brain patients can perform well across visual fields with either response modality, as these judgements can be facilitated by subcortical pathways and gaze cues; (2) for identity judgments, performance would fail on crossed trials when using button presses—revealing the disconnection—whereas pointing responses might show better performance due to ipsilateral motor control; (3) patients who appear intact on identity judgments with a small

stimulus set would show disconnection once the stimulus set is expanded; and (4) cross-integration same/different judgments would fail, confirming that the two hemispheres cannot integrate visual information.

Proposed Framework

Judgement Type	Needs Corpus Callosum? (for crossed trials)	Response Type matters?	"Unified" behavioral Prediction
Presence/Absence	NO - Subcortical + Gaze can reveal presence/absence	NO - All response types work	✓ Intact across all VF
Location	NO - Subcortical + Gaze direction can reveal location	NO - All response types work	✓ Intact across all VF
Identity	YES - Higher level cortical processing needed	YES - CRITICAL! Pointing vs Button-press can have different results	✗ Disconnection with button-press*, Maybe OK with pointing

Response Type	Motor Control	Predicted Effect	Cross-Cueing?
Pointing (proximal)	Can be ipsilateral	Can create "apparent" unity—either hemisphere can guide gross arm movement	**Possible** with small sets or binary choices*
Button-press (distal)	Contralateral	Reveals disconnections (correct only when the responding hemisphere sees stimulus)	**Possible** with small sets or binary choices*
Verbal	Speaking hemisphere only	Reveals disconnections (correct only when the speaking hemisphere sees stimulus)	**Possible** with small sets or binary choices*

* Whenever the task involves a **binary choice** or a **very limited set of alternatives**, **cross-cueing must be considered and ruled out** (via replication of the task with a larger stimulus set, when possible)

Figure 2B-1. Proposed Framework for the Apparent "Motor Unity" in Split-Brain Patients. We propose that whether a split-brain patient can accurately respond to stimuli across visual fields with any response modality, depends on the type of the visual judgement (Presence/Absence, Location, Identity). Simple judgements like presence/absence and localization are predicted to appear unified because subcortical pathways and gaze cues can convey sufficient information for those judgements. Identity judgements, by contrast, require higher-level cortical processing that are better suited to test disconnection effects. For the Identity judgements, the response modality and whether the task permits cross-cueing can also influence whether motor unity will be observed or not. The lower table elaborates that, for the Identity Judgments, pointing responses (which involves proximal muscles) can be guided ipsilaterally by either hemisphere, potentially creating an appearance of unity. In contrast, button-press responses (which involves distal muscles) and verbal responses can be more cleanly controlled

contralaterally. Lastly, even when the judgement type and response type are controlled, a patient can still appear unified if the task relies on binary or small-set response options. In such cases, cross-cueing—the use of indirect cues that one hemisphere can give to the other to infer the correct response option—remains possible; and should be ruled out through replication with larger stimulus sets, if possible.

3. Methods

Participants

We tested six patients (BT, TJ, WU, NR, NE, NO) who underwent callosotomy to alleviate epileptic seizures (**Table 2B-1, Fig. 2B-2**). Four patients (TJ, WU, NR, NE) underwent a complete single-staged callosotomy, fully sectioning the corpus callosum in one operation. Patient NO underwent a two-staged callosotomy, with the anterior portion of his corpus callosum sectioned first followed by the posterior. And in patient BT, posterior fibers were left intact due to surgical reasons. All patients are right-handed (Salmaso & Longoni, 1985) and have language areas in the left hemisphere as confirmed by pre-operative bilateral Wada testing (Wada & Rasmussen, 2007). The anterior, posterior, and hippocampal commissures remain intact in all patients. Patients BT, TJ, WU, and NR have no extra-callosal damage and are considered "clean" callosotomy cases. Patients NE, and NO have some extra-callosal damage (NE: extensive atrophy throughout the left insular cortex as well as in right somatomotor cortex, both laterally and throughout the midsagittal section; NO: bilateral parietal atrophy, with concomitant enlargement of the posterior horns of the lateral ventricle, see **Fig. 2B-2**). We include all patients for completeness and transparency; however, findings from BT, TJ, WU, and NR afford the clearest inferences about callosotomy-specific effects, and results from NE, and NO should be interpreted with caution. The study was approved by the Ethics committee Westphalia-Lippe (2021-523-f-S). Each patient or the legal representative consented to participate in the study as approved by the Ethics committee. Finally, due to differences in patient availability and testing feasibility, not all patients completed every experiment. In all result figures, patients are shown in fixed panel positions for consistency; empty panels indicate tasks or conditions that were not completed for that patient.

Table 2B-1 Clinical Profiles of Callosotomy Patients

Patient	Age at surgery	Age at testing	Sex	Handedness	Extent of Callosotomy	Extra-callosal Damage?

BT	**22**	**31**	**M**	**Right**	**Partial**	**No**
TJ	**49**	**55**	**F**	**Right**	**Complete**	**No**
NR	**18**	**20**	**M**	**Right**	**Complete**	**No**
WU	**41**	**42**	**F**	**Right**	**Complete**	**No**
NE	19	20	M	Right	Complete	Yes
NO	13 & 17	37	M	Right	Complete	Yes

Table 2B-1. Patients Overview. Patient BT is a partial callosotomy case with his splenium intact, whereas the other patients are complete callosotomy patients with their entire corpus callosum severed. Bolded patients (BT, TJ, WU, NR) have no extra-callosal damage and therefore are considered the "clean" callosotomy cases who afford the clearest inferences about callosotomy-specific effects; whereas patients NE and NO have some extra-callosal damage. Hence their results should be interpreted with caution.

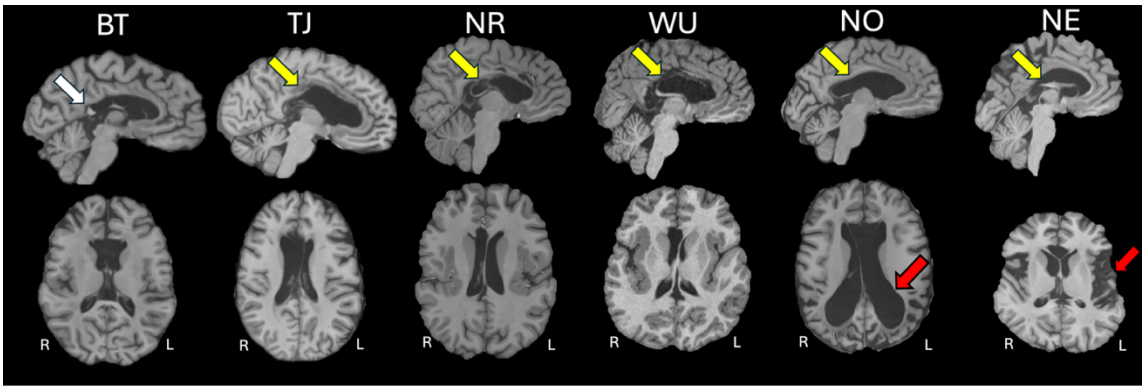


Figure 2B-2. Anatomical Images of the Patients. Midsagittal (top row) and axial (bottom row) T1-weighted MRI images are shown for each patient. BT is a partial callosotomy patient with his splenium intact (white arrow). The remaining patients are complete callosotomy patients with their entire corpus callosum severed (yellow arrows). Patients BT, TJ, NR, and WU show no extra-callosal damage, whereas patients NO and NE exhibit some extra-callosal damage (red arrows). R: Right, L: Left.

Materials and General Procedure

All experiments were programmed using PsychoPy (version 2023.2.3) (Peirce et al., 2019). Patients were seated 56 cm from the monitor, with their heads stabilized by a chinrest. Visual stimuli were presented on a Dell XPS 17 laptop, 17-inch display (1920x1200) with a refresh rate of 60 Hz. Eye movements were recorded with a Tobii Pro Fusion eye tracker (screen-based) with a sampling rate of 60 Hz (Tobii AB, n.d.). For the button-press responses, a MiliKey 5 (MH-5) button box was used. Stimulus details for each task are described below. For divided visual field (DVF) conditions, stimuli were presented either to the left visual field (LVF) or right visual field (RVF), between 2.5 and 5.6 visual angle degrees from central

fixation depending on the task. The exact eccentricity used in each experiment is specified in their corresponding sections below. The central fixation cross subtended 1 visual angle degree.

Procedure

Each experiment followed the same general procedure. Responses were collected in separate blocks using the right hand, left hand, or verbal; response modality remained constant within a block. For each response modality, patients first completed an extensive training phase followed by the experimental trials.

Training blocks. Training was designed to gradually familiarize patients with the task demands and DVF presentation procedure. Each training block began with a centralized, full-field stimulus presentation with no time constraints, allowing participants to learn the stimuli and what response to make (e.g., which button, pointing or verbal response corresponded to that stimulus) without time pressure. Once the patients achieved consecutive correct responses on these "central slow" trials, "central fast" training blocks began where the stimulus is flashed for 120 ms at the center of the screen, so that participants could get familiar to the brief stimulus presentations they would encounter in the experimental trials. After consecutive successful responses, patients were introduced to divided visual field (DVF) presentations: stimuli appeared in the LVF or RVF without a flash and remained on screen until a response was made. After the successful completion of this training block, the actual experimental block started. Notably, this training structure was refined over the course of data collection. Initially, we used fixed training and practice blocks, and some patients showed poorer performance on left visual field trials—when stimuli were directed to the nondominant right hemisphere—compared to right visual field trials—when stimuli were directed to the dominant left hemisphere. As noted in the Introduction, effectively engaging and testing the disconnected right hemisphere can be nontrivial, often requiring extensive repetition and practice before reliable task performance can be collected. Once we switched to unlimited practice phases that continued until reliable performance was clearly demonstrated for the training trials, classic patterns of disconnections emerged during the subsequent divided visual field trials (e.g., see **Fig. 2B-6B** and **2B-6C** for patient W.U's left hand performance for

LVF trials). Thus, apparent hemispheric differences may sometimes reflect insufficient training or engagement of one hemisphere.

Experimental blocks. Each experimental trial began with a fixation period consisting of a fixed 1 sec interval followed by a randomly jittered gaze-contingent interval (100-150 ms). Stimulus presentation was triggered only if fixation was continuously maintained on the central cross throughout the gaze-contingent interval; if a saccade occurred, the gaze-contingent interval was reset—this was to ensure proper lateralized stimulus presentation. Stimuli were then presented for 120 ms to the LVF, RVF, or bilaterally (BVF only in Experiment 4 same/different task), after which participants provided a response according to the response modality assigned to that block (see **Fig. 2B-3F**).

Experiment 1: Detecting a stimulus (presence/absence)

A red filled circle (2.5 visual angle degree) was presented for 120 ms either to the LVF or RVF at an eccentricity of 5.6 visual angle degree from central fixation. The stimulus appeared on 50% of trials; on trials in which a stimulus was presented, it could appear in the upper, middle, or lower position along the vertical axis. Patients were instructed to indicate whether a stimulus had appeared or not (yes/no, binary response, see **Fig 2B-3A**). The task comprised three blocks per response mode, one per response hand/modality, each consisting of 60 trials: 15 trials per visual field (LVF, RVF) and 30 stimulus-absent trials.

Experiment 2: Localizing a stimulus (location)

The stimulus and display parameters were identical to Experiment 1, a red filled circle (2.5 visual angle degree) presented for 120 ms to either the LVF or RVF at 5.6 visual angle degree eccentricity. On each trial, the stimulus appeared in the upper, middle, or lower position, either on the LVF or RVF. Patients were instructed to indicate where the stimulus had appeared via one of three response modes: verbal, button-press (pressing one of three vertically arranged buttons corresponding to the three positions), or pointing (see **Fig 2B-3B**). Each block comprised 18 trials per visual field, with a total of 36 trials per response block.

Experiment 3A: Identifying a shape (filled, square, circle or triangle)

A red filled circle, square or triangle (3 visual angle degree) was presented for 120 ms either to the LVF or RVF at an eccentricity of 3.5 visual angle degree from central fixation. Patients were instructed to indicate what shape they saw either saying (verbal), pressing one of the 3 keys dedicated for each shape (button-press) or pointing to one of the 3 shape options presented on the screen after each trial (pointing, see **Fig 2B-3C**). Each block comprised 15 trials per visual field, with a total of 30 trials per response block.

Experiment 3B: Identifying a shape (unfilled, square, circle or triangle)

This task was identical to Experiment 3A except that the shapes were presented as contoured, unfilled outlines rather than filled stimuli (see **Fig 2B-3F**), minimizing potential differences in low-level visual features, such as luminance, which could arise due to subtle surface-area differences between shapes. This control experiment was administered only to patient NO following his unexpectedly preserved performance in Experiment 3A (**Fig. 2B-7A**). Because NO's performance did not differ between filled (Experiment 3A) and unfilled stimuli (Experiment 3B), the task was not administered to the remaining patients.

Experiment 3C: Identifying everyday objects (black and white drawings of objects)

Black-and-white line drawings of everyday objects (see **Fig. 2B-3F**) were presented for 120 ms either to the LVF or RVF at an eccentricity of 3.5 visual angle degree from central fixation. Patients were instructed to identify the object either by naming them (verbal response) or by pointing to the matching image from a set of four alternatives shown after each trial (pointing), with the four options varying on every trial. Each object was presented only once per session. This experiment was administered after NO's unexpectedly intact performance across both Experiment 3A and 3B, to investigate whether his intact shape identification reflected cross-cueing because of there were only three-shape options to pick from. Especially the verbal blocks of this task (picture naming), effectively minimizes guessing. Each block comprised 22 trials per visual field, with a total of 44 trials per response block.

Experiment 4A: Comparing stimuli across visual fields (shapes, filled)

Two red filled shapes (either circle, square, or triangle, 2.5 visual angle degree) were presented simultaneously for 120 ms, either bilaterally (BVF, one shape to the LVF

and one to the RVF, with an eccentricity of 2.5 visual angle degree from central fixation) or unilaterally (both shapes presented to either the LVF, uni-LVF, or RVF, uni-RVF). For unilateral presentations, the two shapes were separated by 1 visual angle degree and extended up to 8.5 visual angle degree at the farthest point from central fixation. Patients were instructed to indicate whether the two shapes were the same or different (binary response, see **Fig. 2B-3D**). Each block comprised 18 trials per condition (18 BVF, 18 uni-LVF, and 18 uni-RVF), with a total of 54 trials per response block.

Experiment 4B: Comparing stimuli across visual fields (shapes, contoured)

This experiment was identical to Experiment 4A, except that the shapes were presented as contoured, unfilled outlines rather than filled stimuli, minimizing potential differences in low-level visual features such as luminance that could arise from surface-area differences between shapes (see **Fig. 2B-3F**).

Experiment 4C: Comparing stimuli across visual fields (black and white drawings of objects)

Similarly, this experiment was identical to Experiment 4A, except that the stimuli consisted of black-and-white line drawings of everyday objects rather than geometric shapes (see **Fig. 2B-3F**). On each trial, two object drawings were presented simultaneously, and patients were instructed to indicate whether the two objects were the same or different (binary response).

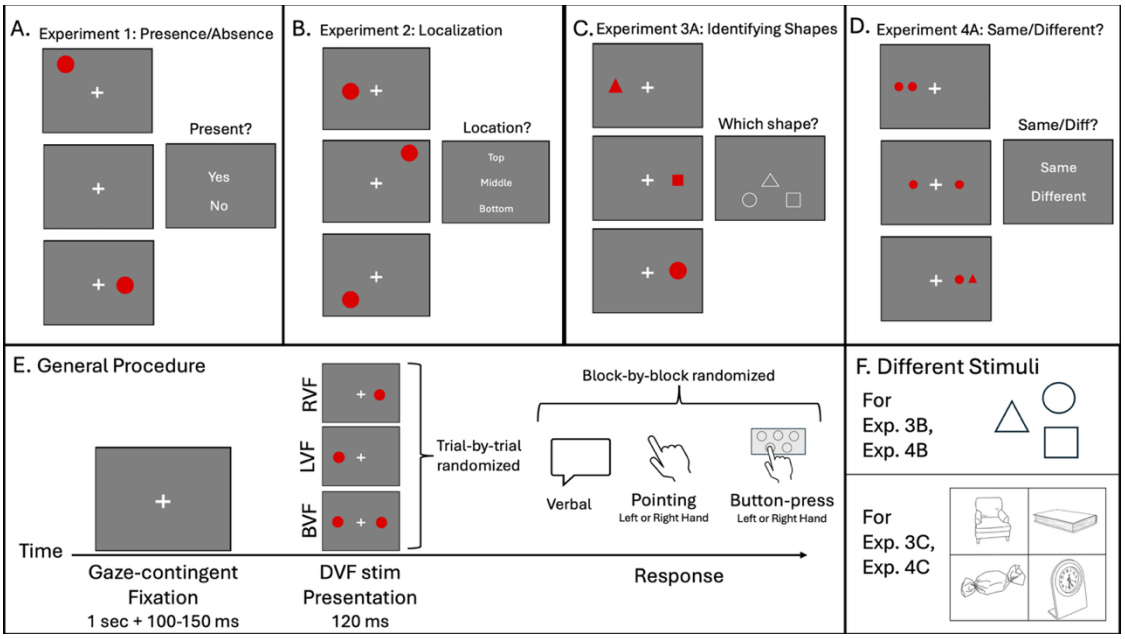


Figure 2B-3. Experiments. ***(A)*** Experiment 1 (Presence/Absence): a filled circle was presented to either the left visual field (LVF) or right visual field (RVF), and patients indicated whether a stimulus had appeared (Yes/No). ***(B)*** Experiment 2 (Localization): a filled circle was presented at one of three vertical positions (Top, Middle, or Bottom) in either the LVF or RVF, and patients indicated its location. ***(C)*** Experiment 3A (Shape Identification): a filled shape (circle, square, or triangle) was presented to either the LVF or RVF, and patients indicated which shape they saw, selecting from three options. ***(D)*** Experiment 4A (Same/Different): two shapes were presented simultaneously either bilaterally (one per visual field) or unilaterally (both to the same visual field), and patients indicated whether the two shapes were the same or different. ***(E)*** General procedure: each trial began with a gaze-contingent fixation period, followed by a 120 ms stimulus presentation to the RVF, LVF, or bilaterally (BVF, for Experiment 4 only). Patients responded via verbal report, pointing (left or right hand), or button-press (left or right hand) on separate blocks. ***(F)*** Stimulus sets used for B and C versions of the experiments: contoured unfilled shapes (triangle, circle, square) were used in Experiments 3B and 4B; black-and-white line drawings of everyday objects were used in Experiments 3C and 4C.

Statistical Analysis

For all experiments, trials were classified as either *uncrossed* or *crossed*. *Uncrossed* trials were those in which the input and output hemispheres were the same (e.g., left-hand responses for LVF trials; both involving the right hemisphere), whereas crossed trials were those in which the input and output hemispheres differed (e.g., left-hand responses for RVF trials; left hemisphere input but right hemisphere motor output). For verbal responses, RVF trials were considered uncrossed (input to the speaking left hemisphere) and LVF trials crossed (input to the non-dominant right hemisphere), except for patient DD, who showed atypical right-

hemisphere language dominance, for whom these assignments were reversed (LVF uncrossed; RVF crossed).

We conducted binomial tests (two-tailed) to determine whether the patient's performance differed from chance-level performance for *crossed* and *uncrossed* trials. Significance ($p < 0.05$) indicated that the observed performance was statistically different from chance-level; non-significance ($p \geq 0.05$) indicated that the observed performance did not differ from chance. The disconnection syndrome (whether there are crossed-uncrossed differences) was operationalized as (*i*) above-chance performance on *uncrossed* trials and (*ii*) chance-level or significantly different form chance but worse than chance performance on *crossed* trials for the same task.

For tasks where chance performance was not well-defined (verbal responses for Experiment 3C), we used permutation tests to compare performance between the left visual field (LVF) and right visual field (RVF). To assess this, we used the absolute difference between RVF and LVF proportion correct scores as our test statistic. The permutation test was implemented with 10,000 iterations. For each iteration, we first created binary arrays representing correct (1) and incorrect (0) trials for each VF. We then pooled all these trials from both VFs and randomly reassigned them to either VF while maintaining the original number of trials per VF. For each such permutation, we calculated the absolute difference in proportion correct between VFs. The *p*-value was computed as the proportion of permuted differences that were equal to or greater than the observed difference. This approach allowed us to estimate how likely it would be to observe a difference as large as the one we found if there were no differences between the VFs (statistical significance was set at $p < 0.05$).

4. Results

For all experiments, performance on *crossed* trials (when input and output hemispheres are different) was compared with the *uncrossed* trials (when input and output hemispheres are the same). Not all patients were tested across all experiments due to patient availability. In all figures, each patient is shown in a fixed panel position for consistency, with empty panels indicating experiments that were not tested with that patient.

Experiment 1: Can Split-Brain Patients Detect Presence/Absence of a Stimulus Across Visual Fields?

We predicted that detecting presence/absence would be preserved both in partial and complete split-brain patients. Nevertheless, several complete callosotomy patients still showed classic disconnection patterns, with above-chance performance on uncrossed trials but chance or below-chance performance on crossed trials. Detailed results are in **Table 2B-2** and **Figure 2B-4**.

Verbal Responses. As predicted, partial patients BT showed no evidence of disconnection, performing significantly above chance for LVF, RVF and absent trials (all *p*s < .001). Similarly, patient NE performed above chance across all visual field conditions, although performance was somewhat lower for LVF (crossed) than RVF (uncrossed) trials. In contrast, complete callosotomy patients NO, TJ, and WU exhibited classic disconnection syndrome: all three performed significantly above chance on uncrossed trials—where the speaking left hemisphere received input—but performance fell to chance (NO) or significantly below chance (TJ and WU) on crossed LVF trials, indicating a marked breakdown in verbally reporting stimuli presented to the nondominant right hemisphere.

Hand Responses. Consistent with the verbal findings, partial patient BT showed no disconnections, performing above chance in all conditions (all *p*s < .05). Complete patient TJ showed the clearest evidence of disconnection syndrome. Performance was above chance on uncrossed trials (left-hand responses to LVF stimuli and right-hand responses to RVF stimuli) but below chance on crossed trials, indicating that each hemisphere could successfully respond only to stimuli presented to it, while failing to respond to the stimulus presented to the other hemisphere. Patients NO and WU showed above-chance performance for all RVF trials, but chance-level or below-chance performance for all LVF trials regardless of response hand, suggesting that task performance was reduced whenever the non-dominant right hemisphere received the visual input. This pattern may partly reflect reduced engagement or incomplete task comprehension by the non-dominant right hemisphere. Finally patient NE performed above chance across all visual field and response conditions regardless of whether button-presses or pointing responses were used (all *p*s < .05).

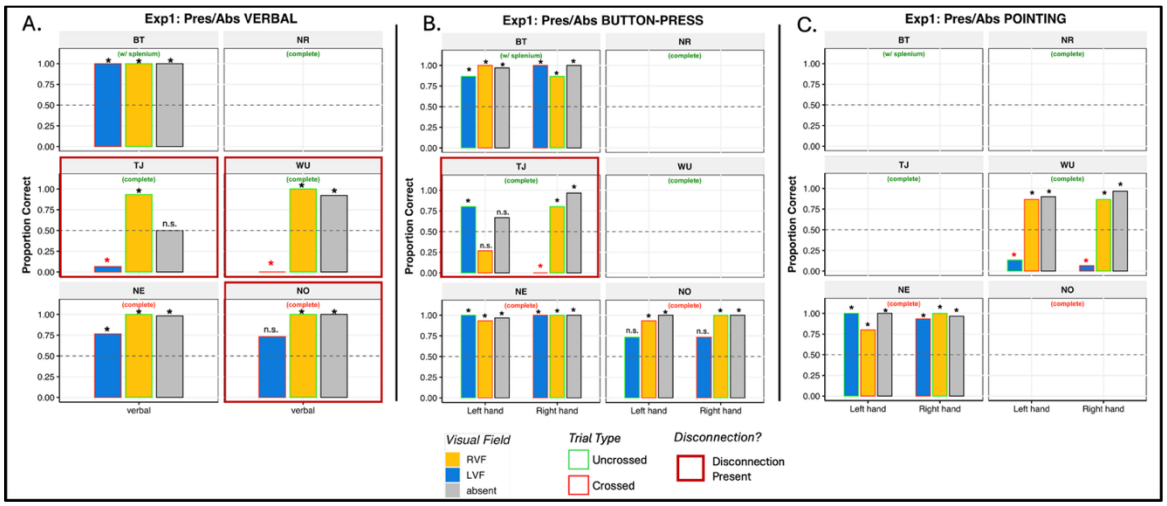


Figure 2B-4. Experiment 1: Presence/Absence Performance. Proportion correct for each patient across ***(A)*** verbal, ***(B)*** button-press, and ***(C)*** pointing response modalities. Bars represent performance for left visual field (LVF; blue, input to right hemisphere), right visual field (RVF; yellow, input to left hemisphere), and absent trials (gray). Bar borders indicate trial type: green borders denote uncrossed trials (input and output hemispheres are the same) and red borders denote crossed trials (input to one hemisphere, output from the other). The dashed horizontal line indicates chance-level performance (0.5). * Performance significantly different from chance (binomial test, $p < .05$): black * indicate above-chance performance, red * indicate below-chance performance, and "n.s." indicates chance-level performance ($p \geq .05$). Red boxes denote patients exhibiting clear disconnection syndrome. Patients BT was a partial callosotomy case with his splenium spared (w/ splenium), whereas the remaining patients were complete callosotomy cases (complete). Green labels (on "complete" or "w/ splenium") indicate no extra-callosal damage—hence "cleaner" split-brain patients, whereas patients with red labels (NE and NO) show some extra-callosal damage. Thus, their results should be interpreted with caution.

Table 2B-2. Experiment 1: Presence/Absence Detection

			Visual Field		
Patient	**Response Mode**	**Hand**	**RVF**	**LVF**	**Absent**
BT	Verbal	—	15/15 (p < .001)	15/15 (p < .001)	30/30 (p < .001)
	Button-press	Right	13/15 (p = .007)	15/15 (p < .001)	30/30 (p < .001)
		Left	15/15 (p < .001)	13/15 (p = .007)	29/30 (p < .001)
TJ	Verbal	—	14/15 (p < .001)	**1/15 (p < .001)[b]**	**15/30 (p = 1.000)[a]**
	Button-press	Right	12/15 (p = .035)	**0/15 (p < .001)**	29/30 (p < .001)
		Left	**4/15 (p = .118)[a]**	12/15 (p = .035)	**20/30 (p = .099)[a]**
WU	Verbal	—	15/15 (p < .001)	**0/15 (p < .001)[b]**	27/30 (p < .001)
	Pointing	Right	13/15 (p = .007)	**1/15 (p < .001)[b]**	29/30 (p < .001)

		Left	13/15 (p = .007)	**2/15 (p = .007)[b]**	27/30 (p < .001)
NE[c]	Verbal	—	30/30 (p < .001)	23/30 (p = .005)	59/60 (p < .001)
	Button-press	Right	15/15 (p < .001)	15/15 (p < .001)	30/30 (p < .001)
		Left	14/15 (p < .001)	15/15 (p < .001)	29/30 (p < .001)
	Pointing	Right	15/15 (p < .001)	14/15 (p < .001)	29/30 (p < .001)
		Left	12/15 (p = .035)	15/15 (p < .001)	30/30 (p < .001)
NO	Verbal	—	15/15 (p < .001)	**11/15 (p = .118)[a]**	30/30 (p < .001)
	Button-press	Right	15/15 (p < .001)	**11/15 (p = .118)[a]**	30/30 (p < .001)
		Left	14/15 (p < .001)	**11/15 (p = .118)[a]**	30/30 (p < .001)

Table 2B-2. Values represent the number of correct responses out of total trials in detection task (present/absent binary judgement; chance = 0.5). All p-values are two-tailed binomial tests against chance (0.5). RVF = right visual field; LVF = left visual field. Because the majority of trials showed performance significantly above chance, **bold values** indicate exceptions: either **[a] performance not significantly different from chance**, or **[b] performance significantly below chance.** [c] NE was tested across two sessions, one for button-press and one for pointing responses; verbal trials from those two sessions are combined.

Experiment 2: Can Split-Brain Patients Localize a Stimulus Across Visual Fields?

We predicted that simple stimulus localization performance would be preserved both in partial and complete split-brain patients. The results were mixed.

Verbal Responses. As predicted, partial patient BT showed no evidence of disconnection, performing significantly above chance for LVF and RVF trials (all *p*s < .05, see **Table 2B-3** and **Figure 2B-5** for detailed results). In contrast, patient TJ exhibited classic disconnection syndrome: she performed above chance when the speaking left hemisphere received the input (RVF trials, $p < .001$), but at chance when the mute right hemisphere received the input (LVF trials, $p = .62$). Patient NE performed above chance across all visual field conditions (all *p*s < .05), showing no evidence of disconnection.

Hand Responses. Partial patient BT again showed no disconnections, performing above chance in all conditions (all *p*s < .05). Patient TJ showed a disconnection pattern for right-hand responses, with above-chance performance on uncrossed RVF trials ($p < .001$) but chance-level performance on crossed LVF trials ($p = .62$). For left-hand responses, performance was at chance across both uncrossed LVF and crossed RVF trials (*p*s > .05). Patient NE performed above chance across all VF and hand condition, for both button-press

and pointing responses (all *p*s < .05), suggesting no disconnection effects when localizing stimuli.

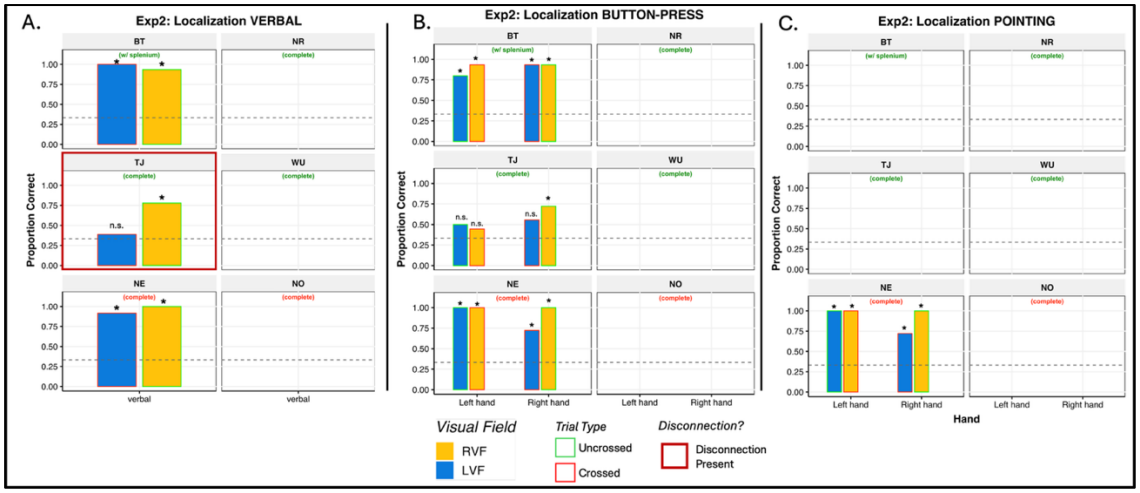


Figure 2B-5. Experiment 2: Localization Performance. Proportion correct for each patient across ***(A)*** verbal, ***(B)*** button-press, and ***(C)*** pointing response modalities. Blue bars represent left visual field (LVF; input to right hemisphere) trials, and yellow bars represent right visual field (RVF; input to left hemisphere) trials. Bar borders indicate trial type: green borders denote uncrossed trials (input and output hemispheres are the same) and red borders denote crossed trials (input to one hemisphere, output from the other). The dashed horizontal line indicates chance-level performance (0.33). * Performance significantly different from chance (binomial test, $p < .05$): black * indicate above-chance performance, red * indicate below-chance performance, and "n.s." indicates chance-level performance ($p \geq .05$). Red boxes denote patients exhibiting clear disconnection syndrome. BT was a partial callosotomy case with his splenium spared (w/ splenium), whereas the remaining patients were complete callosotomy cases (complete). Green labels (on "complete" or "w/ splenium") indicate no extra-callosal damage—hence "cleaner" split-brain patients, whereas patients with red labels (NE and NO) show some extra-callosal damage. Thus, their results should be interpreted with caution.

Table 2B-3. Experiment 2: Localization

			Visual Field	
Patient	**Response Mode**	**Hand**	**RVF**	**LVF**
BT	Verbal	—	14/15 (p < .001)	15/15 (p < .001)
	Button-press	Right	14/15 (p < .001)	14/15 (p < .001)
		Left	14/15 (p < .001)	12/15 (p < .001)
TJ	Verbal	—	14/18 (p < .001)	**7/18 (p = .623)[a]**
	Button-press	Right	13/18 (p = .002)	**10/18 (p = .076)[a]**
		Left	**8/18 (p = .325)[a]**	**9/18 (p = .140)[a]**
NE[c]	Verbal	—	36/36 (p < .001)	33/36 (p < .001)

Button-press	Right	18/18 (p < .001)	13/18 (p = .002)
	Left	18/18 (p < .001)	18/18 (p < .001)
Pointing	Right	18/18 (p < .001)	13/18 (p = .002)
	Left	18/18 (p < .001)	18/18 (p < .001)

Table 2B-3. Values represent the number of correct responses out of total trials in localization task (top/middle/bottom; chance = 0.33). All p-values are two-tailed binomial tests against chance (0.33). RVF = right visual field; LVF = left visual field. Because the majority of trials showed performance significantly above chance, **bold values** indicate [a] **performance not different from chance.** [c] NE was tested across two sessions, one for button-press and one for pointing responses; verbal trials from those two sessions are combined.

Experiment 3: Can Split-Brain Patients Identify What a Stimulus Is Across Visual Fields?

We predicted that identifying stimulus identity (e.g., shape, color, or object category) would depend on cortical processing and therefore reveal classic disconnection effects in complete callosotomy patients. At the same time, we predicted that methodological and procedural factors, such as limited response options that could permit cross-cueing, and the use of pointing responses which would permit ipsilateral proximal motor control, could mask these effects.

Experiment 3A: Identifying Shapes.

Verbal Responses. As predicted, partial patient BT named shapes accurately across VFs (all *p*s < .001). In contrast, a clear disconnection pattern emerged for all but one complete callosotomy patients (see **Table 2B-4** and **Fig. 2B-6** for full results). They could all name shapes correctly when the shapes are presented to the speaking left hemisphere (RVF trials) (all *p*s < .001) but not when presented to the mute right hemisphere (LVF trials) (NE and NR's performance were at chance, *p*s > .05; TJ and WU's were below chance, *p*s < .05). The only exception was patient NO, who could name shapes correct across both RVF and LVF (all *p*s <.001). This result motivated the follow-up investigations in Experiments 3B and 3C.

Hand Responses. Partial patients BT again showed no disconnection syndrome, performing well across visual fields and hands when pointing (all *p*s < .05, see **Table 2B-4** and **Fig. 2B-6** for full results). Patients TJ and WU showed clear disconnections; when using button-press responses, both patients performed above chance only on uncrossed trials (all *p*s < .05), but not on crossed trials (all *p*s > .05). We then investigated whether pointing responses—which could permit greater ipsilateral motor control—would mask these disconnection effects. For the dominant right hand responses, it didn't. Both patients could

point correctly only when the dominant left hemisphere received the input (RVF trials) and remained at chance when the non-dominant right hemisphere received the input (LVF trials). This could suggest that the non-dominant right hemisphere may have limited ability to exert ipsilateral control over the dominant right hand. For TJ's left hand, however, pointing responses eliminated the disconnection effects: performance was above chance not only on uncrossed trials, but also on crossed trials: suggesting that even when the dominant left hemisphere received the input (RVF trials), the non-dominant left hand could still respond accurately, possibly reflecting ipsilateral motor control.

The remaining three participants (NE, NO, and NR) did not show the predicted pattern of disconnection. NE performed above chance across nearly all visual field and hand combinations for both pointing and button-press responses (all *p*s < .05), with the only exception of left-hand pointing responses to RVF inputs ($p = .10$). NR, who completed the button-press task only, performed above chance on all RVF trials regardless of response hand (*p*s < .05), while all LVF trials were at chance (*p*s > .05). NO performed above chance across all conditions even with button-press responses (all *p*s < .05), the response modality in which disconnection effects were predicted. And notably, he was also the only patient who did not show the expected disconnection effects in the verbal responses. As the results for NE, NO, and NR diverged from our predictions, their split-brain profiles in general are discussed more thoroughly and holistically in the Discussion, where performance across all tasks is considered together.

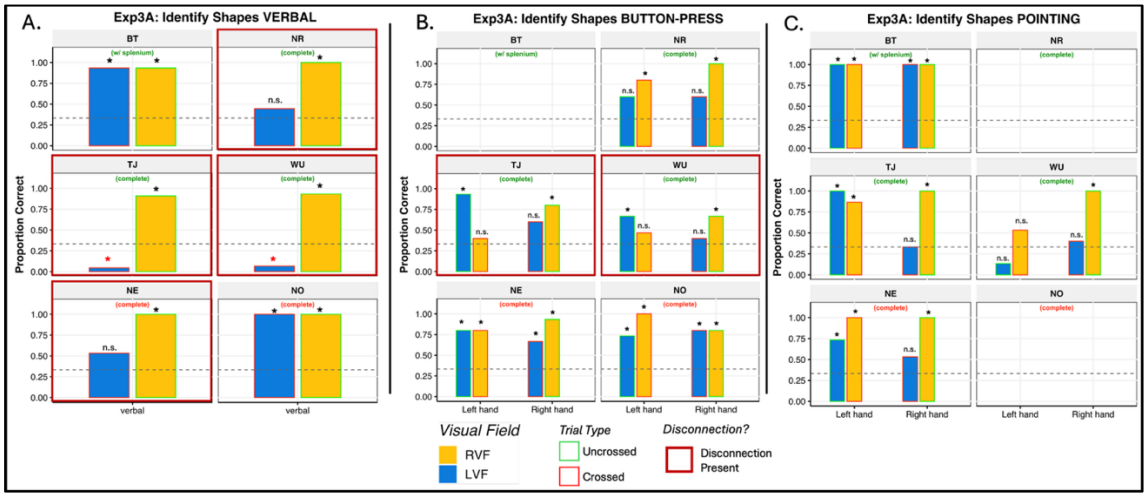


Figure 2B-6 Experiment 3A: Identifying Shapes. Proportion correct for each patient across ***(A)*** verbal, ***(B)*** button-press, and ***(C)*** pointing response modalities. Blue bars represent left visual field (LVF; input to right hemisphere) trials, and yellow bars represent right visual field (RVF; input to left

hemisphere) trials. Bar borders indicate trial type: green borders denote uncrossed trials (input and output hemispheres are the same) and red borders denote crossed trials (input to one hemisphere, output from the other). The dashed horizontal line indicates chance-level performance (0.33). * Performance significantly different from chance (binomial test, $p < .05$): black * indicate above-chance performance, red * indicate below-chance performance, and "n.s." indicates chance-level performance ($p \geq .05$). Red boxes denote patients exhibiting clear disconnection syndrome. BT was a partial callosotomy case with his splenium spared (w/ splenium), whereas the remaining patients were complete callosotomy cases (complete). Green labels (on "complete" or "w/ splenium") indicate no extra-callosal damage—hence "cleaner" split-brain patients, whereas patients with red labels (NE and NO) show some extra-callosal damage. Thus, their results should be interpreted with caution.

Table 2B-4. Experiment 3A: Identify Shapes

			Visual field	
Patient	**Response Mode**	**Hand**	**RVF**	**LVF**
BT	Verbal	—	14/15 (p < .001)	14/15 (p < .001)
	Pointing	Right	15/15 (p < .001)	15/15 (p < .001)
		Left	15/15 (p < .001)	15/15 (p < .001)
NE	Verbal	—	15/15 (p < .001)	**8/15 (p = .108)[a]**
	Pointing	Right	15/15 (p < .001)	**8/15 (p = .108)[a]**
		Left	15/15 (p < .001)	11/15 (p = .002)
	Button-press	Right	14/15 (p < .001)	10/15 (p = .011)
		Left	12/15 (p < .001)	12/15 (p < .001)
NO	Verbal	—	15/15 (p < .001)	15/15 (p < .001)
	Button-press	Right	12/15 (p < .001)	12/15 (p < .001)
		Left	15/15 (p < .001)	11/15 (p = .002)
NR	Verbal	—	9/9 (p < .001)	**4/9 (p = .493)[a]**
	Button-press	Right	15/15 (p < .001)	**9/15 (p = .050)[a]**
		Left	12/15 (p < .001)	**9/15 (p = .050)[a]**
TJ	Verbal	—	20/22 (p < .001)	**1/22 (p = .002)[b]**
	Pointing	Right	15/15 (p < .001)	**5/15 (p = 1.000)[a]**
		Left	13/15 (p < .001)	15/15 (p < .001)
	Button-press	Right	12/15 (p < .001)	**9/15 (p = .050)[a]**
		Left	**6/15 (p = .591)[a]**	14/15 (p < .001)
WU	Verbal	—	14/15 (p < .001)	**1/15 (p = .028)[b]**
	Pointing	Right	15/15 (p < .001)	**6/15 (p = .591)[a]**
		Left	**8/15 (p = .108)[a]**	**2/15 (p = .168)[a]**
	Button-press	Right	10/15 (p = .011)	**6/15 (p = .591)[a]**
		Left	**7/15 (p = .282)[a]**	10/15 (p = .011)

Table 2B-4. Values represent the number of correct responses out of total trials in the shape identification task (circle/square/triangle responses; chance = 0.33). All p-values are two-tailed binomial tests against chance (0.33). RVF = right visual field; LVF = left visual field. Because the majority of trials showed performance significantly above chance, **bold values** indicate exceptions: either [a] **performance not significantly different from chance**, or [b] **performance significantly below chance.**

Experiment 3B: Identifying Shapes (Contoured, Unfilled)

In Experiment 3A, patient NO was able to name shapes accurately across both visual fields, including LVF trials in which stimuli were presented to the mute right hemisphere (**Fig. 2B-6A**). What could explain this unexpected preservation of performance? One potential explanation was that the filled shapes used in Experiment 3A may have introduced subtle luminance differences across stimuli: because the shapes varied in surface area (e.g., a square having a larger illuminated surface area than a triangle), this could have introduced systematic differences in low-level visual features, such as luminance, that facilitated accurate performance without relying on cortical processing or callosal transfer, thereby masking the predicted disconnection effects.

To test this possibility, NO completed a modified version of the task in which the same shapes were presented as contoured, unfilled outlines rather than solid filled stimuli, thereby minimizing potential surface-area and luminance differences between shapes. NO's performance with the unfilled shapes were very similar to his performance in Experiment 3A: performing above-chance across all visual field and hand conditions (see **Table 2B-5** and **Fig. 2B-7** for detailed results). This suggests that whether the shapes were filled or unfilled did not affect performance. Thus, Experiment 3B was not administered to the remaining patients.

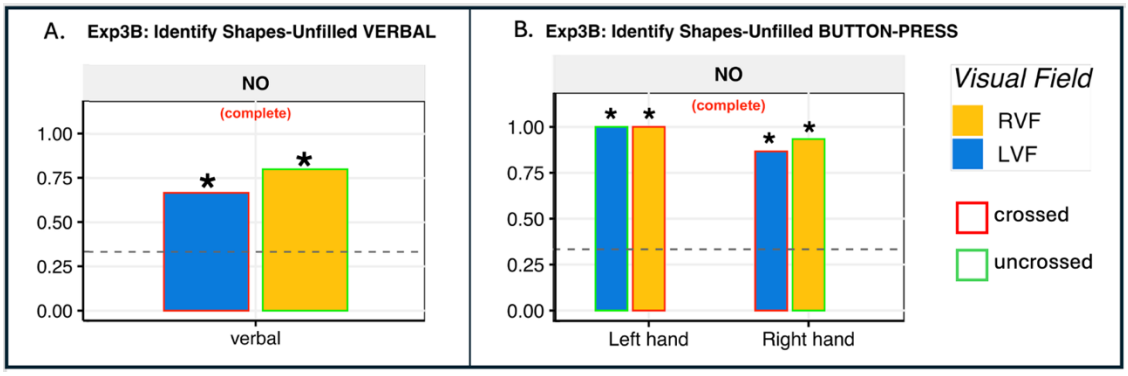


Figure 2B-7. Experiment 3B: Identifying Shapes (Contoured, Unfilled). This experiment was only administered to patient NO, following his unexpected above-chance performance in Experiment 3A (**Fig. 2B-7A**). Proportion correct is shown for NO's ***(A)*** verbal and ***(B)*** button-press responses. Blue bars represent left visual field (LVF; input to right hemisphere) trials, and yellow bars represent right

visual field (RVF; input to left hemisphere) trials. Green bar borders denote uncrossed trials (input and output hemispheres are the same) and red borders denote crossed trials (input to one hemisphere, output from the other). The dashed horizontal line indicates chance-level performance (0.33). * Performance significantly different from chance (binomial test, $p < .05$). . Patient NO was as a complete callosotomy case with potential extra-callosal damage (indicated by red "complete" labeling).

Table 2B-5. Experiment 3B: Identify Shapes (Contoured, Unfilled)

			Visual field	
Patient	**Response Mode**	**Hand**	**RVF**	**LVF**
NO	Verbal	—	12/15 (p = .0002)	10/15 (p = 0.01)
	Pointing	Right	14/15 (p < .001)	13/15 (p < .001)
		Left	15/15 (p < .001)	15/15 (p < .001)

Table 2B-5. Values represent the number of correct responses out of total trials in identifying (unfilled, only contoured) shapes task (circle/square/triangle responses; chance = 0.33). All p-values are two-tailed binomial tests against chance (0.33). RVF = right visual field; LVF = left visual field.

Experiment 3C: Identifying Objects (black and white drawings of everyday objects)

This experiment was motivated by patient NO's unexpected performance in Experiment 3A (**Fig. 2B-6A**). Curiously, NO accurately named shapes presented to both visual fields. Experiment 3B ruled out stimulus-level confounds such as luminance differences as an explanation. A remaining possibility was that NO's intact performance in Experiment 3A could be due to cross-cueing: with only three possible shapes, patients could use subtle behavioral cues to pick the correct response out of those three options. To test this, we administered an object identification task using black-and-white drawings of everyday objects. Because each object presented only once, guessing was effectively minimized. We also included a hand-response version of the task in which each object was presented only once, and patients selected the target from a set of four options presented after each trial. The four options were different at each trial. We predicted that verbal responses would reveal the clearest disconnection effects, given that freely naming objects has no defined chance level, making any correct response to LVF stimuli particularly telling. For hand responses, we predicted that the disconnection effects could be weaker because the task still involved selecting among four alternatives (chance = 0.25) using pointing responses (potentially allowing for ipsilateral control). Nevertheless, the greater stimulus complexity and

continuously changing response options each trial could yield a clearer disconnection profile than the simpler shape-pointing task used in Experiment 3A.

Verbal Responses. As predicted, all complete callosotomy patients—including patient NO—showed clear disconnection effects in this task. Permutation tests showed significant differences between RVF and LVF performance (all *p*s < .05, see **Table 2B-6** and Fig. **2B-8A**): patients could name objects accurately when stimuli were presented to the speaking left hemisphere (RVF trials), but failed when stimuli were presented to the mute right hemisphere (LVF trials).

Hand Responses. All complete patients showed the expected disconnection pattern for right-hand responses, performing above chance on uncrossed RVF trials (all *p*s < .001) and at chance on crossed LVF trials (all *p*s > .05; see **Table 2B-7** and Fig. **2B-8B**). Left-hand response patterns, however, varied across patients. TJ performed better on uncrossed LVF trials than crossed RVF trials, consistent with a disconnection pattern, but both conditions were above chance. Patients NE and WU performed above chance for both RVF and LVF trials and even showed slightly better performance on crossed RVF trials, when the input was received by the dominant left hemisphere.

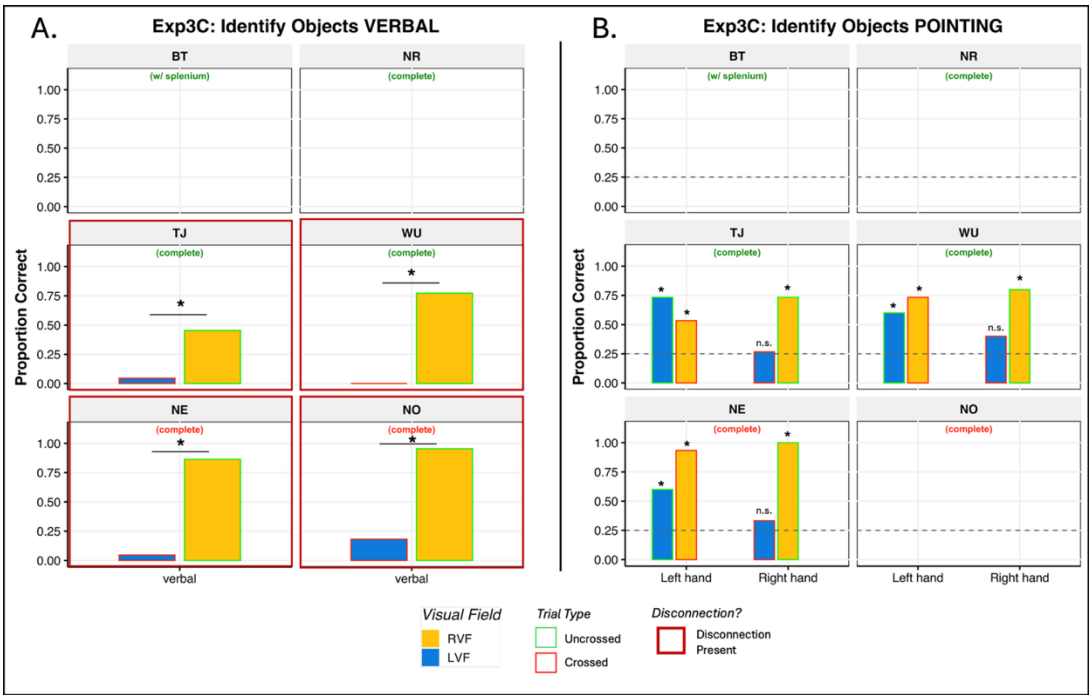


Figure 2B-8. Experiment 3C: Identifying Everyday Objects (Black-and-White Drawings). Proportion correct for each patient across ***(A)*** verbal, and ***(B)*** pointing responses. Blue bars represent left visual field (LVF; input to right hemisphere) trials, and yellow bars represent right visual field

(RVF; input to left hemisphere) trials. Bar borders indicate trial type: green borders denote uncrossed trials (input and output hemispheres are the same) and red borders denote crossed trials (input to one hemisphere, output from the other). For *(B)* pointing responses, four response options were presented on each trial, and the dashed horizontal line indicates chance-level performance (chance = 0.25). Asterisk * for pointing responses indicates performance significantly different from chance (binomial test, $p < .05$): and "n.s." indicates chance-level performance ($p \geq .05$). For *(A)* verbal responses, no chance level was defined because each object is only presented once and patients were asked to name it freely; therefore, no dashed chance line is shown. Asterisk * for verbal responses indicate a significant difference between LVF and RVF performance (permutation test, $p < .05$). Red boxes denote patients exhibiting clear disconnection syndrome. BT was a partial callosotomy case with his splenium spared (w/ splenium), whereas the remaining patients were complete callosotomy cases (complete). Green labels (on "complete" or "w/ splenium") indicate no extra-callosal damage—hence "cleaner" split-brain patients, whereas patients with red labels (NE and NO) show some extra-callosal damage. Thus, their results should be interpreted with caution.

Table 2B-6. Experiment 3C: Identify Everyday Objects (Black-and-White Drawings)

Patient	Response Mode	Hand	RVF	LVF
TJ	Verbal	—	*10/22 (diff: 0.409)*	*1/22 (p = .0028)*
	Pointing	Right	11/15 (p < .001)	**4/15 (p = 1.000)**
		Left	8/15 (p = .017)	11/15 (p < .001)
WU	Verbal	—	*17/22 (diff: 0.77)*	*0/22 (p < .001)*
	Pointing	Right	12/15 (p < .001)	**6/15 (p = .229)**
		Left	11/15 (p < .001)	9/15 (p = .004)
NE	Verbal	—	*19/22 (diff: 0.82)*	*1/22 (p < .001)*
	Pointing	Right	15/15 (p < .001)	**5/15 (p = .550)**
		Left	14/15 (p < .001)	9/15 (p = .004)
NO	Verbal	—	*21/22 (diff 0.772)*	*4/22 (p < .001)*

Table 2B-6. Values represent the number of correct responses out of total trials. For verbal responses, a defined chance level does not exist as each object was presented once and patients were asked to name it freely; RVF and LVF performance were therefore compared using permutation testing (10000 iterations), with the observed difference in proportion correct between visual fields as the test statistic. The "diff" value reflects this observed difference, and the associated *p*-value indicates the proportion of permuted differences equal to or exceeding the observed difference. A *p*-value < .05 for the permutation test indicates a *statistically significant difference between LVF and RVF* performance and is *italicized*. For pointing responses, four response options were presented on each trial (chance = 0.25); *p*-values are two-tailed binomial tests against chance. Bold values indicate **performance not significantly different from chance** ($p \geq .05$). RVF = right visual field; LVF = left visual field.

Experiment 4: Can Split-Brain Patients Determine Whether Two Stimuli Are the Same Across Visual Fields?

Next, we examined whether split-brain patients could compare two stimuli presented either bilaterally (one to each visual field; BVF) or unilaterally (both to the same visual field; LVF or RVF). We predicted that complete patients would fail to compare stimuli presented across visual fields (BVF trials), as this would require integration of information across the two disconnected hemispheres. For unilateral trials, we predicted that crossed and uncrossed differences could arise for some patients but were predicted to be less pronounced or less consistent across patients, given the binary nature of the task (same/different judgement), potentially enabling cross-cueing.

Experiment 4A: Comparing Shapes

Verbal responses. As predicted, splenium patient BT showed no disconnection, performing above chance for all VF conditions, including BVF (all *p*s < .001, see Table **2B-7** and **Fig. 2B-9A**). Patients NE and TJ showed the expected disconnection patterns where their performance was at chance in BVF condition and crossed uni-LVF condition (all *p*s > .05); but above chance for in uncrossed uni-RVF condition (all *p*s < .05). Patient WU also showed the disconnection pattern where she was at chance for the BVF condition but above chance for the central test trails, confirming that she was able to do this task fine when both stimuli are presented at the midline. Patient NO's performance at chance for all VF conditions, suggesting poor comprehension and/or engagement with this task.

Hand responses. As predicted, splenium patient BT showed no disconnection, performing above chance in all VF conditions with both hands (all *p*s < .001, see Table **2B-7** and **Fig. 2B-9C**). All complete patients were unable to compare shapes when they were presented bilaterally (BVF), irrespective of which hand they were using or whether they were pointing or using button-presses (all *p*s > .05). Patient TJ showed clear disconnection patterns when pointing, performing above chance for only uncrossed unilateral trials but at chance for crossed unilateral trials. When using button-presses, her performance was at chance for all conditions, similar to patient NO, which could suggest poor comprehension and/or engagement with this task in general. Patient NR showed predicted disconnection pattern for his right hand responses, performing above chance on the uncrossed unilateral-RVF trials but at chance for the crossed unilateral-LVF trials, but his left-hand performance was at

chance for all VF conditions. Finally, despite his poor performance for BVF trials, patient NE was able to determine if the shapes are the same or different for all unilateral trials, irrespective of which hand and what response modality he was using.

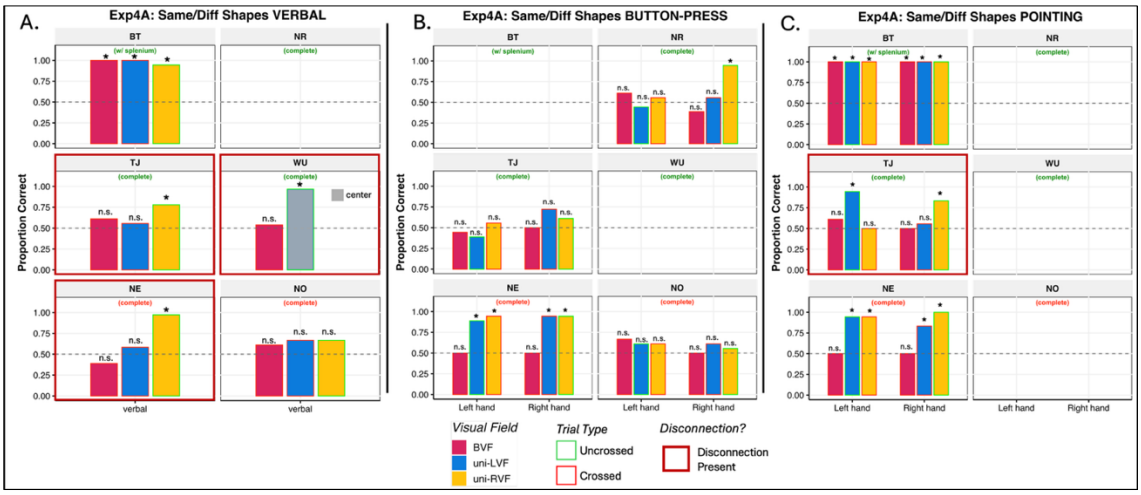


Figure 2B-9. Experiment 4A: Compare Shapes Across and Within Visual Fields. Proportion correct for each patient across ***(A)*** verbal, ***(B)*** button-press, and ***(C)*** pointing response modalities. Pink bars represent bilateral visual field (BVF; one stimulus presented in each visual field, each hemisphere, simultaneously), blue bars represent unilateral left visual field (uni-LVF; both stimuli to right hemisphere) trials, and yellow bars represent unilateral right visual field (uni-RVF; both stimuli to left hemisphere) trials, gray bars (only for patient WU's verbal responses) represent central trials (both stimuli presented at the midline). Bar borders indicate trial type: green borders denote uncrossed trials (input and output hemispheres are the same) and red borders denote crossed trials (input to one hemisphere, output from the other; or simultaneous inputs to both hemispheres). The dashed horizontal line indicates chance-level performance (0.5). * Performance significantly different from chance (binomial test, $p < .05$), and "n.s." indicates chance-level performance ($p \geq .05$). Red boxes denote patients exhibiting clear disconnection syndrome. BT was a partial callosotomy case with his splenium spared (w/ splenium), whereas the remaining patients were complete callosotomy cases (complete). Green labels (on "complete" or "w/ splenium") indicate no extra-callosal damage—hence "cleaner" split-brain patients, whereas patients with red labels (NE and NO) show some extra-callosal damage. Thus, their results should be interpreted with caution.

Table 2B-7. Experiment 4A: Comparing Shapes Across and Within Visual Fields

Patient	Response Mode	Hand	Visual field		
			BVF	**uni-RVF**	**uni-LVF**
BT	Verbal	—	18/18 (p < .001)	17/18 (p < .001)	18/18 (p < .001)
	Pointing	Right	18/18 (p < .001)	18/18 (p < .001)	18/18 (p < .001)
		Left	18/18 (p < .001)	18/18 (p < .001)	18/18 (p < .001)
TJ	Verbal	—	**11/18 (p = .481)**	14/18 (p = .031)	**10/18 (p = .815)**
	Pointing	Right	**9/18 (p = 1.000)**	15/18 (p = .008)	**10/18 (p = .815)**
		Left	**11/18 (p = .481)**	**9/18 (p = 1.000)**	17/18 (p < .001)
	Button-press	Right	**9/18 (p = 1.000)**	**11/18 (p = .481)**	**13/18 (p = .096)**

		Left	**8/18 (p = .815)**	**10/18 (p = .815)**	**7/18 (p = .481)**
WU	Verbal[+]	—	**28/52 (p = .678)** Central[+]: 30/31 (p < .001)	—	—
NR	Button-press	Right	**7/18 (p = .481)**	17/18 (p < .001)	**10/18 (p = .815)**
		Left	**11/18 (p = .481)**	**10/18 (p = .815)**	**8/18 (p = .815)**
NE	Verbal	—	**14/36 (p = .243)**	35/36 (p < .001)	**21/36 (p = .405)**
	Pointing	Right	**9/18 (p = 1.000)**	18/18 (p < .001)	15/18 (p = .008)
		Left	**9/18 (p = 1.000)**	17/18 (p < .001)	17/18 (p < .001)
	Button-press	Right	**9/18 (p = 1.000)**	17/18 (p < .001)	17/18 (p < .001)
		Left	**9/18 (p = 1.000)**	17/18 (p < .001)	16/18 (p = .001)
NO	Verbal	—	**11/18 (p = .481)**	**12/18 (p = .238)**	**12/18 (p = .238)**
	Button-press	Right	**9/18 (p = 1.000)**	**10/18 (p = .815)**	**11/18 (p = .481)**
		Left	**12/18 (p = .238)**	**11/18 (p = .481)**	**11/18 (p = .481)**

Table 2B-7. Values represent the number of correct responses out of total trials on the same/different judgement task (Chance = 0.5). All p-values are two-tailed binomial tests against chance (0.5). **Bold** values indicate **performance not significantly different from chance** ($p > .05$). BVF = bilateral visual field, one stimulus presented in each visual field simultaneously; uni-RVF = unilateral right visual field, both stimuli presented in the right visual field; uni-LVF = unilateral left visual field, both stimuli presented in the left visual field. [+]WU completed a color version of the task (same/different judgments for equiluminant colors) rather than the shape version, and did not complete unilateral trials; instead, she completed a central test block, in which both stimuli were presented at the midline, in addition to the standard BVF condition

Experiment 4B: Comparing Shapes (Contoured, Unfilled)

This experiment was only run for patient NO. In experiment 4A, his performance was at chance for all conditions, suggesting poor comprehension and/or engagement. For this task, his engagement was somewhat better. Even though he was at chance for all BVF trials, he was able to perform above chance for most of the unilateral trials, except the unilateral RVF trials when responding with his right hand (see **Fig. 2B-11** and **Table 2B-8**)

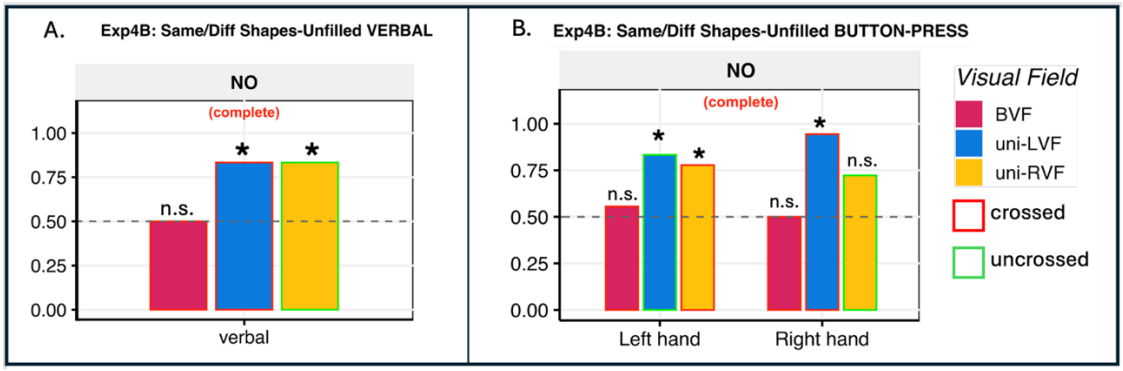


Figure 2B-10. Experiment 4B: Compare (Unfilled) Shapes Across and Within Visual Fields. This experiment was only administered to patient NO. Proportion correct is shown for NO's ***(A)*** verbal and ***(B)*** button-press responses. Pink bars represent bilateral visual field (BVF; one stimulus presented in each visual field, each hemisphere, simultaneously), blue bars represent unilateral left visual field (uni-LVF; both stimuli to right hemisphere) trials, and yellow bars represent unilateral right visual field (uni-RVF; both stimuli to left hemisphere) trials. Green bar borders denote uncrossed trials (input and output hemispheres are the same) and red borders denote crossed trials (either input to one hemisphere, output from the other; or simultaneous inputs to both hemispheres). The dashed horizontal line indicates chance-level performance (0.5). * Performance significantly different from chance (binomial test, $p < .05$), and "n.s." indicates chance-level performance ($p \geq .05$). Patient NO was as a complete callosotomy case with potential extra-callosal damage (indicated by red "complete" labeling).

Table 2B-8. Experiment 4B: Comparing (Unfilled) Shapes Across and Within Visual Fields

Patient	Response Mode	Hand	Visual field		
			BVF	**uni-RVF**	**uni-LVF**
NO	Verbal	—	**9/18 (p = 1.000)**	15/18 (p = .007)	15/18 (p = .007)
	Button-press	Right	**9/18 (p = 1.000)**	**13/18 (p = .096)**	17/18 (p < .001)
		Left	**10/18 (p = .815)**	14/18 (p = .030)	15/18 (p = .007)

Table 2B-8. Values represent the number of correct responses out of total trials on the same/different judgement task (Chance = 0.5). All p-values are two-tailed binomial tests against chance (0.5). **Bold** values indicate **performance not significantly different from chance** ($p > .05$). BVF = bilateral visual field, one stimulus presented in each visual field simultaneously; uni-RVF = unilateral right visual field, both stimuli presented in the right visual field; uni-LVF = unilateral left visual field, both stimuli presented in the left visual field

Experiment 4C Comparing Objects (black and white drawings of everyday objects)

Verbal responses. NE's performance was at-chance on BVF trials and crossed unilateral trials, but above chance for the uncrossed unilateral trials (see **Fig. 2B-11** and **Table 2B-9**).

Hand Responses. NE's performance was at-chance on BVF trials. All unilateral VF conditions and hand responses were above chance.

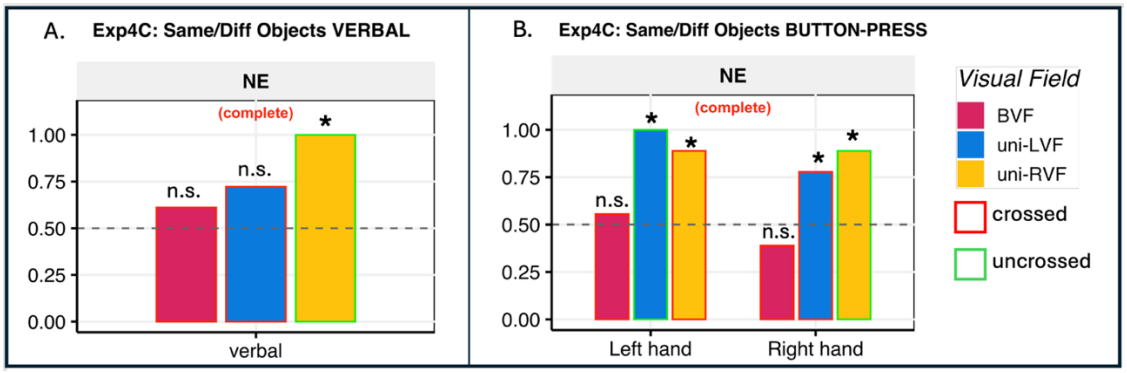


Figure 2B-11. Experiment 4C: Compare Objects Across and Within Visual Fields. Proportion correct for patients NE and DD across ***(A)*** verbal, and ***(B)*** button-press. Pink bars represent bilateral visual field (BVF; one stimulus presented in each visual field, each hemisphere, simultaneously), blue bars represent unilateral left visual field (uni-LVF; both stimuli to right hemisphere) trials, and yellow bars represent unilateral right visual field (uni-RVF; both stimuli to left hemisphere) trials. Bar borders indicate trial type: green borders denote uncrossed trials (input and output hemispheres are the same) and red borders denote crossed trials (input to one hemisphere, output from the other; or simultaneous inputs to both hemispheres). The dashed horizontal line indicates chance-level performance (0.5). * Performance significantly different from chance (binomial test, $p < .05$), and "n.s." indicates chance-level performance ($p \geq .05$). Red stars denote patients exhibiting clear disconnection syndrome.

Table 2B-9. Experiment 4C: Comparing Objects Across and Within Visual Fields

			Visual field		
Patient	**Response Mode**	**Hand**	**BVF**	**uni-RVF**	**uni-LVF**
NE	Verbal	—	**11/18 (p = .481)**	18/18 (p < .001)	**13/18 (p = .096)**
	Button-press	Right	**7/18 (p = .481)**	16/18 (p = .001)	14/18 (p = .031)
		Left	**10/18 (p = .815)**	16/18 (p = .001)	18/18 (p < .001)

Table 2B-9. Values represent the number of correct responses out of total trials on the same/different judgement task (Chance = 0.5). All p-values are two-tailed binomial tests against chance (0.5). **Bold** values indicate **performance not significantly different from chance** ($p > .05$). BVF = bilateral visual field, one stimulus presented in each visual field simultaneously; uni-RVF = unilateral right visual field, both stimuli presented in the right visual field; uni-LVF = unilateral left visual field, both stimuli presented in the left visual field.

5. Discussion

Over a series of experiments, we tested six split-brain patients (one partial, five complete) to investigate under what judgement type (from simple detection to more complex object identification), and what response modality conditions (from verbal and pointing—which may involve ipsilateral control via proximal arm muscles, to button-press responses—which can be more cleanly controlled more contralaterally) the disconnections emerge, if any. We

predicted that simple detection and localization judgements can be intact in complete split-brain patients as those judgements can be facilitated by subcortical pathways and gaze-cues, whereas identity judgement would better reveal disconnection effects. We further predicted that even for identity judgements, if the task relies on only binary or limited response options set and/or conducted with pointing responses; cross-cueing and ipsilateral motor control can mask the disconnection effects. And finally for our partial case BT, we predicted no disconnections as his splenium would transfer visual information across hemispheres.

Overall, three broad conclusions emerged: *First*, as predicted, the partial patient BT showed no evidence of disconnection across tasks. He performed well across visual field and response modality conditions. This is consistent with the role of the splenium in transferring visual information across hemispheres. *Second,* complete split-brain patients TJ and WU clearly replicated the classic split-brain disconnection pattern, particularly in the shape identification task (Experiment 3A) using button-press and verbal responses. They performed well when the hemisphere receiving the input was also making the response, but failed on crossed conditions, when the input is given to one hemisphere, but the response was required from the other. *Third,* the amount of variability observed both between patients (e.g., TJ vs. NO) and within the same patient across different tasks and conditions (e.g., NO in shape naming (Exp. 3A) vs. object naming (Exp.3C)) further underscore how nontrivial testing split-brain patients is.

Clear Replication of Classic Split-Brain Effects

In this study, we present a clear replication of the classic split-brain syndrome with a new cohort of split-brain patients, particularly in patients TJ and WU. Split-brain patients already appear largely unified in everyday life, due to many factors such as subcortical pathways, cross-cueing, left-hemisphere interpreter etc. The role of researchers, therefore, is not merely to show that these patients can behave coherently under some conditions, but to critically probe and test under what conditions that unity might break down. It is precisely those conditions that would critically inform our understanding of human consciousness, agency, self and their neural correlates. Relatedly, even a single robust case is theoretically significant. Patient TJ showed disconnection effects not only on identity judgments, but also on simple presence/absence judgments. The variability across patients—i.e., some patients behaving in a unified manner even on identity judgements, while TJ showing disconnections even on

simple presence/absence task—may reflect individual differences in how patients adapt to their condition. One contributing factor could be age at surgery. TJ was the oldest patient at the time of surgery (49 years old), and similarly WU was 41 years old, whereas the other patients underwent surgery in their teenage years or early twenties. Younger patients may adapt better by developing or using compensatory strategies more effectively.

Experimental and Procedural Confounds Can Produce Apparent Unity

Cross-Cueing.

Patient NO, who underwent a two-stage callosotomy at relatively young ages (13 and 17 years old), was the only complete patient who didn't show disconnections in his verbal responses during shape naming (Experiment 3A, **Fig. 2B-6**). We wondered whether selecting among three options was an easy enough task to permit effective cross-cueing. We therefore replicated the task using black-and-white drawings of everyday objects, critically presenting each object only once and effectively minimizing guessing. Under these conditions, NO showed a clear disconnection pattern (**Fig. 2B-8**). This dramatic difference in NO's performance between shape naming (Exp. 3A) and object naming (Exp. 3C) shows very clearly that under some conditions these patients can appear perfectly unified, yet a simple change in task demands can immediately reveal the underlying disconnection. In Pinto et al. study (2017), the identity judgments relied on either simple shape identification or binary fox-vs-tank choices. We therefore wonder whether patient DDC would still show unified behavior when asked to name everyday objects (especially presented to the LVF), without any predefined response choices. That would be fruitful to test.

Ipsilateral Control (Asymmetric?)

Ipsilateral motor control of proximal muscles, especially when pointing, can be another source of apparent behavioral unity. TJ's identity judgements in Exp. 3A (**Fig. 2B-6**) could demonstrate this. When pointing, the left hand performed well even on crossed RVF trials, but performance declined with button-press responses. This suggests that the dominant hemisphere can guide both hands when pointing. The same did not appear to hold for the non-dominant hemisphere. In other words, ipsilateral motor control may be asymmetric, favoring the dominant hemisphere. A clear example

of this could the hand-responses in Exp. 3C (**Fig. 2B-8**). Disconnection effects were evident for right-hand responses: performance was poor when stimuli were presented to the LVF, where the non-dominant hemisphere received the input but could not effectively control the dominant right hand. In contrast, left-hand responses showed no disconnections, likely because either hemisphere could control the left hand. Previous studies reported similar asymmetries in ipsilateral motor control, showing that the dominant hemisphere could use either hand to draw what it saw, whereas the non-dominant hemisphere could guide only the left hand (Miller & Kingstone, 2005).

Verbal responses provided a clearer picture of disconnections

Because hand responses can be influenced by ipsilateral motor control, verbal responses may provide cleaner lateralized outputs and therefore reveal disconnection effects more clearly. Consistent with this, verbal responses revealed disconnection effects in nearly all complete split-brain patients (e.g., Exp 3A, **Fig 2B-6A**). Even patient NO, who initially appeared relatively intact on the shape naming task (**Fig 2B-6A**), later demonstrated clear disconnections during object naming (**Fig. 2B-8A**).

At the same time, verbal responses have an important limitation: they only provide output from the speaking hemisphere. Unlike hand-responses, verbal tasks cannot establish the clear "double dissociation" where each hemisphere can independently demonstrate successful performance for information presented only to it. As a result, poor verbal performance for LVF stimuli could, in principle, reflect factors other than disconnection, such as hemineglect or other attentional or cognitive issues. Patient NR illustrates this problem directly. His verbal performance on LVF trials was poor, but he never showed above-chance performance in LVF trials across any task or response modality, including in the uncrossed left-hand trials. Thus, as is, it is difficult to rule out alternative explanations. We suspect that NR's non-dominant hemisphere was never engaged in any task, which is plausible given that he was also the patient with whom we had the most limited testing time with the most limited training and practice trials.

In contrast, for the other patients, this is less of an issue. Their above-chance performance on LVF trials in other response modalities rules out more general deficit

explanations and therefore makes it more likely that their poor performance on LVF trials during verbal responses was likely due to the disconnection effects.

Limitations

The main limitation of this study is the lack of complete and extensive testing of every patient across all tasks and conditions. Due to patient availability, extensive behavioral testing was not always feasible, which limited our ability to draw more comprehensive conclusions.

Conclusion

Taken together, testing split-brain patients is far from trivial. Valid conclusions require careful experimentation and attention to what exactly is being tested, and how. In fact, some of the earliest split-brain work concluded that severing the corpus callosum had no effect on cognition (Akelaitis, 1945), a finding that later proved to be an artifact of using non-lateralized testing procedures that were simply *insensitive* to the drastic disconnection effects (Gazzaniga et al., 1962).

There are many reasons why a split-brain patient may appear behaviorally unified, including subcortical facilitation, cross-cueing, ipsilateral motor control, and methodological insensitivity. Without carefully controlling or considering these factors, apparent "unity" should not be taken at face value. And critically, even a single clear demonstration that each hemisphere can only respond to information presented to it is theoretically significant. For such clear double dissociations, the most parsimonious explanation is that severing the corpus callosum creates two independent conscious perceivers within one brain.

Data availability

The data supporting the findings of this study are provided within this chapter (**Tables 2B-2 to 9**).

Code availability

Analysis code for this study is identical to that used in the previous study (Chapter 2A) and is openly available on GitHub at https://github.com/selinbekir/splitbrain-disconnection-analysis.

CHAPTER 3.
NEURAL CORRELATES OF CALLOSOTOMY

This chapter is based on work published as a journal article in *Proceedings of the National Academy of Science:*

Santander, T., **Bekir, S.,** Paul, T., Simonson, J. M., Wiemer, V. M., Skinner, H. E., Hopf, J. L., Rada, A., Woermann, F. G., Kalbhenn, T., Giesbrecht, B., Bien, C. G., Sporns, O., Gazzaniga, M. S., Volz, L. J., & Miller, M. B. (2025). Full interhemispheric integration sustained by a fraction of posterior callosal fibers. *Proceedings of the National Academy of Sciences of the United States of America*, *122*(43), e2520190122. https://doi.org/10.1073/pnas.2520190122.

It has been adapted for inclusion in this dissertation, with revisions to the text, structure, and analyses.

1. Abstract

The corpus callosum is the largest white matter tract connecting the two cerebral hemispheres and is thought to play a central role in inter-hemispheric communication. Behavioral research, including the findings presented in Chapter 2, shows that severing this major pathway produces profound behavioral effects: split-brain patients are markedly impaired on tasks requiring inter-hemispheric information integration. Yet the neural consequences of severing the brain's primary inter-hemispheric pathway remain poorly understood. Are these behavioral disconnections also reflected in the brain's functional organization? Using resting-state fMRI, we characterized whole-brain functional connectivity (FC) and assessed large-scale functional network organization in complete and partial callosotomy patients relative to neurotypical healthy controls. We examined the balance of inter- and intra-hemispheric functional organization and the degree of lateralization across functional networks. Complete callosotomy was associated with marked reductions in inter-hemispheric FC and a substantially more lateralized functional network organization. In contrast, partial callosotomy patients—including one who retains only ~1 cm of splenium—showed inter-hemispheric FC patterns broadly comparable to healthy controls. These neural findings closely parallel the behavioral results described in Chapter 2, providing converging evidence that the neural consequences of callosotomy track the presence or absence of behavioral disconnection. These results demonstrate that the corpus callosum is important for

maintaining large-scale inter-hemispheric functional coupling, while also revealing that even a minimal posterior callosal remnant may be sufficient to preserve surprisingly extensive inter-hemispheric network organization.

2. Introduction

The corpus callosum is the largest white matter tract, consisting of approximately 200-250 million axons that connect the two cerebral hemispheres, and is thought to play a central role in inter-hemispheric communication (Aboitiz & Montiel, 2003). In split-brain patients, the corpus callosum is surgically severed to treat intractable epilepsy. Decades of behavioral research with these patients have documented striking behavioral disconnection effects: when a task requires information to be shared across hemispheres, split-brain patients fail, revealing that information presented to one hemisphere often fails to reach the other following complete callosotomy (Gazzaniga et al., 1962). In this thesis, we replicated these behavioral disconnection effects in a new split-brain cohort, confirming robust behavioral consequences of complete callosal severance (Bekir et al., 2025). But what are the neural consequences of callosotomy? How do functional brain networks react to the severance of the brain's largest white matter pathway? To what extent are the behavioral disconnection effects observed in split-brain patients reflected in the brain's intrinsic functional network architecture?

Surprisingly, these questions remain unclear because neural data from split-brain patients remain very scarce. Callosotomy was largely discontinued around the turn of the 21st century, coinciding with the emergence of modern network neuroscience. As a result, only a few neuroimaging studies in split-brain patients exist, but each with limitations that complicate straightforward interpretation of the findings. Most of them were conducted in anesthetized pediatric patients (Hung et al., 2019; Johnston et al., 2008; Pizoli et al., 2011; Roland et al., 2017), raising two important concerns: anesthesia can alter functional network organization relative to the awake state (Boveroux et al., 2010), and pediatric split-brain patients often do not show the classic disconnection syndrome (Ferrand-Sorbets et al., 2022), as their developing brains adapt differently than adult brains. Other studies were conducted decades after surgery in aging patients with possible extra-callosal damage (Uddin et al., 2008). Thus, it remains largely unknown how severing the largest white matter pathway in the

human brain affects the topological organization and intrinsic dynamics of large-scale functional networks.

Here, we used resting-state fMRI to characterize whole-brain functional connectivity in complete and partial callosotomy patients relative to neurotypical healthy controls. We combined whole-brain functional connectivity matrices, laterality indices across canonical resting-state networks, and data-driven community detection approaches to examine how hemispheric severance alters large-scale functional organization in adult human brain.

Resting-state fMRI measures spontaneous, low-frequency fluctuations in the BOLD signal while a person simply rests in the scanner without performing any task. It became a widely used tool for mapping the brain's intrinsic functional network architecture (Bassett & Sporns, 2017). A foundational assumption of modern cognitive neuroscience is that structural connectivity constrains functional connectivity: although this structure-function relationship is not one-to-one, intrinsic functional networks are shaped by the underlying structural connectivity, such that if two brain regions are connected by a direct structural pathway, they are more likely to be functionally coupled (Bassett & Sporns, 2017; Honey et al., 2009; Wang et al., 2013). If structural connectivity constrains functional connectivity, then, given that the corpus callosum is the primary structural pathway connecting the two hemispheres, complete callosotomy should lead to marked reductions in inter-hemispheric functional connectivity.

Finally, we asked whether patterns of functional organization would parallel behavioral disconnection profiles across patients. In particular, one patient in our cohort (BT), who retained only a small splenial remnant, showed no evidence of classic behavioral disconnection effects (Bekir et al., 2025), We therefore examined whether his surprisingly preserved behavioral integration would also be reflected in his whole-brain functional connectivity patterns.

3. Methods

Participants

Patients. Six adult callosotomy patients (5 men, 1 woman; aged 19 to 60; all right-handed; **Fig. 3-1** and **Table 3-1**) were recruited during routine postoperative follow-up visits to the Bethel Epilepsy Center (Bielefeld, Germany). In two patients (EM and BT), surgery did not result in a complete callosal transection; they are hereafter referred to as “partial patients”.

In patient EM, the surgery was stopped after sectioning the anterior CC (roughly, ~38% of the CC's cross-sectional area in the mid-sagittal plane); patient BT was spared approximately 1 cm of splenium (losing ~90% of the CC's cross-sectional area). The remaining four patients (HY, DT, TJ, and LJ) were completely sectioned. All patients have intact anterior and posterior commissures regardless of the extent of the callosal section; and all patients underwent resting-state functional MRI without sedation. The study was approved by the Ethics Committee of the University of Münster,Germany (2021-523-f-S). The patients or their legal representatives provided written informed consent.

Healthy Adult Controls. We used open-access data from the Human Connectome Project 100 Unrelated Subjects (HCP100) cohort (46 men, 54 women; M_{Age} = 29.11, *SD* = 3.68) as a robust benchmark for various network features estimated in callosotomy patients. Participant recruitment and imaging procedures have previously been detailed elsewhere (62, 63).In brief, data were collected over two sessions on a custom 3T Siemens Kyra with a 32-channel head coil. T1-weighted structural scans were acquired using a 3D magnetization prepared rapid gradient echo (MPRAGE) sequence(TR = 2,400 ms, TE = 2.14 ms, TI = 1,000 ms, flip angle = 8◦, voxel size =0.7 mm3). Resting-state fMRI was collected with eyes open over four 14.5-minscans, using a multiband echo-planar imaging (EPI) sequence sensitive to the blood-oxygen-level-dependent (BOLD) contrast (TR = 720 ms, TE = 33.1 ms, flip angle = 52◦, voxel size = 2 mm3, multiband factor = 8). All participants gave written informed consent for a protocol approved by the Washington University Institutional Review Board. All imaging data were downloaded in their raw (unprocessed) state.

Table 3-1 Overview of Callosotomy Patients

Patient	Age at surgery	Age at testing	Sex	Handedness	Extent of Callosotomy
EM	17	19	M	Right	Partial
BT	22	28	M	Right	Partial
HY	21	22	M	Right	Complete
DT	15	20	M	Right	Complete
TJ	49	52	F	Right	Complete
LJ	57	60	M	Right	Complete

Table 3-1. Patients Overview. All patients were right handed. Sex refers to biological sex and was determined from participants' medical records.

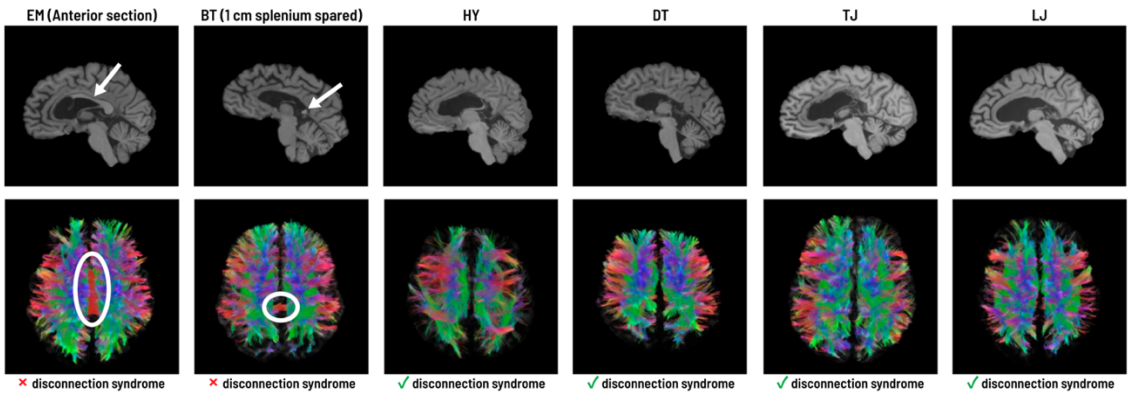


Figure 3-1. Patient anatomical scans. Postoperative T1w and diffusion-weighted MRI scans collected for all six patients at time of testing. White arrows/ellipses for patients EM and BT highlight intact corpus callosum (i.e., partial callosotomy patients). The remaining four patients' corpus callosum was fully sectioned. Note that a series of clinical observations suggested behavioral disconnection syndromes (described in Chapter 2 of this thesis) in all complete callosotomy patients, but not in partial patience.

Callosotomy Procedure

Callosotomies were performed with the assistance of intraoperative neuronavigation, with patients in a supine position and the head inclined by roughly 30 degrees (fixed in the Mayfield clamp). A straight skin incision was made running slightly next to the midline on the nonlanguage dominant hemisphere. Craniotomy was then performed by making one drill hole in the midline at approximately the level of the precentral sulcus. A bone flap was sawn out with an outline of 3x5 cm. The dura was incised longitudinally and then opened with two wings under microneurosurgical conditions—access to the interhemispheric fissure was successively created while preserving the cortical bridging veins. Next, using a self-retaining retractor to carefully shift the frontal lobe, the level of the corpus callosum was gradually exposed under sharp dissection with microscissors.

Dissection is often made considerably more difficult by the course of the pericallosal arteries, which run parallel to the corpus callosum but are often tightly intertwined and twisted in the interhemispheric fissure. In cases where the risk of vascular damage is too great, the surgery may be halted short of a full disconnection (resulting in partial splits). However, under most conditions, the interhemispheric fissure may be opened along the entire length of the knee of the corpus callosum. The corpus callosum was then perforated into the lateral ventricle

of the ipsilateral hemisphere. Next, following the pericallosal artery and the anterior cerebral artery down to the frontal base, the knee of the callosum was split in the midline, continuing backward to about the level of the foramen of Monroi. From this point, it is critical to protect the fornix of the language-dominant hemisphere: To mitigate the risk of postoperative functional impairment, we carefully ensure that the self-retaining retractor is not placed on the precentral gyrus within the interhemispheric fissure. The disconnection can now be carried out completely into the splenium—the severing of the splenium was performed subpially to protect all the cisternal vessels. Extensive hemostasis is not usually necessary, and thus, a ventricular drainage is not used. To conclude, the dura mater was closed and the bone flap reinserted and fixed with titanium plates and screws. Finally, a subgaleal drainage was inserted and the skin closed in two layers.

MRI Acquisition

Patient data were collected on a 3T Siemens Vida at the Bethel Epilepsy Center using a 32-channel head coil. T1-weighted structural scans were acquired using a 3D MPRAGE sequence (TR = 1900 ms, TE = 2.47 ms, TI = 900 ms, flip angle = 8 , voxel size = 0.8 mm^3). Resting-state fMRI was collected with eyes open using a single-shot EPI sequence sensitive to the BOLD contrast (TR = 2000 ms, TE = 30 ms, flip angle = 75 , voxel size = 3x3x3.30 mm, iPAT/GRAPPA factor = 2). We note that each patient varied somewhat in the amount of resting-state data obtained (from 8 to 20 min total) due to differences in clinical scheduling and other imaging protocols not relevant to the current analysis. This information is detailed in **Appendix Table S3-1.**

Functional Data Preprocessing.

All data (from both patients and healthy controls) were run through a unified preprocessing pipeline. Initial preprocessing relied on functions from the Statistical Parametric Mapping 12 software (SPM12, Wellcome Trust Centre for Neuroimaging, London) in MATLAB and Advanced Normalization Tools (ANTs) (Tustison et al., 2021). Resting-state fMRI data were realigned and unwarped to correct for head motion and motion x susceptibility artifact as well as slice-time corrected. Anatomical images were denoised (ANTs' DenoiseImage with a spatially adaptive Gaussian filter) and submitted to ANTs' cortical thickness pipeline, which includes N4 bias field correction and high-quality image segmentation and brain extraction

(Tustison et al., 2014). For some patients, the brain extraction mask included extracerebral components: This was corrected by manually eroding the extraction mask and reapplying it to the anatomical scan when necessary. Image coregistration parameters were subsequently estimated between an N3 bias-corrected mean BOLD reference and the skull-stripped image via antsRegistration (including both linear and nonlinear transformations to minimize residual signal deformations, cf. "SyN distortion correction" as implemented by the widely used fMRIPrep and QSIPrep pipelines).

Subsequent spatial normalization to a standard stereotaxic space presented a nontrivial problem for patient data. In the absence of a corpus callosum, generic registration routines (with both linear and nonlinear stages) will frequently pull structures such as the cingulate gyrus into the space occupied by the corpus callosum in the MNI template image, which misaligns brain regions relative to their location in our functional parcellation. We mitigated this problem in two ways. First, we implemented cost-function masking during the nonlinear step to minimize the influence of callosal regions that were transected by the surgery: These masks were specified in the fixed image space (i.e., the MNI152NLin6Asym template, as provided by the FMRIB Software Library, FSL) (Evans et al., 2012; Jenkinson et al., 2012) because we lacked preoperative data for patients, and corpus callosum segments were defined by the JHU-DTI white matter atlas (Hua et al., 2008; Wakana et al., 2007) (also provided in FSL). For patient EM, the genu was masked out; for patient BT, all but the splenium was masked out; and for all full splits, the entire cross-section of the callosum was masked out. Second, in addition to these masks, we specified a series of registration metric objectives at the nonlinear step. As is typical for antsRegistration, we estimated similarity between the MNI template and images using both ANTs' neighborhood cross-correlation and Mattes mutual information similarity metrics. We also provided smoothed segmentation posteriors derived from the ANTs cortical thickness pipeline (six in total: white matter, cortical gray matter, CSF, deep/subcortical gray matter, brainstem, and cerebellum) and estimated similarity between the MNI template segments and patient segments using a mean-squares objective, with cortical white matter and CSF segments down weighted in importance relative to the other four segments (by a factor of one third). Thus, the nonlinear step was composed of eight similarity metrics. The transformation was estimated using BsplineSyN to allow for smoother deformations without sacrificing accuracy. Ultimately, we concatenated and applied the

estimated coregistration and spatial normalization parameters to all fMRI data in a single interpolation via antsApplyTransforms, resampled into 2 mm^3 isotropic voxels. Registration quality was visually assessed to ensure appropriate mapping to MNI space.

Functional images were then smoothed using a 3D Gaussian kernel with FWHM = 5 mm^3. Prior to functional connectivity estimation, several additional preprocessing steps were performed using custom MATLAB code: This included global signal scaling (median = 1000), linear detrending, and nuisance regression. The nuisance regression model followed a "36-parameter" (36P) approach including the six motion regressors from realignment, the first eigenvariate of white matter signal, the first eigenvariate of CSF signal, and mean global signal—along with their squares, their first derivatives (via backward differentiation), and the squares of the derivatives. All nuisance regressors were detrended to match the BOLD data. We further augmented the design matrix of the nuisance model with a series of binary spike regressors: one for each image volume where the relative framewise displacement in head motion (accounting for both translation and rotation) was ≥0.50 mm. This "36P + spike regression" model has importantly been shown to outperform alternative confound regression strategies (e.g., motion scrubbing and ICA-based methods) and provide the best control for motion artifact in functional connectivity analyses (Ciric et al., 2022; Parkes et al., 2018). Patients generally showed no more head motion than HCP subjects; for reference, we provide a summary of head motion parameters and the frequency of motion spikes for each patient in **Appendix Table S3-1**.

Functional Connectivity Estimation

Functional network nodes were defined by parcellating the brain into 400 cortical regions and 32 subcortical regions, according to the Schaefer and Tian atlases, respectively (Schaefer et al., 2018; Tian et al., 2020). We extracted a summary time course from each parcel by taking the first eigenvariate over time. These regional time series were bandpass filtered to the range of 0.01 to 0.08 Hz. We then constructed 432 x 432 FC matrices by estimating the zero-order Pearson correlation between all pairs of regional time series. For both HCP100 subjects and callosotomy patients with more than one resting-state scan, runs were concatenated prior to FC estimation.

Laterality Indices Across Canonical Resting-State Networks

We sought to quantify differences in interhemispheric functional connectivity (IFC) between callosotomy patients and healthy controls from a number of network neuroscience perspectives. To do this, we began with an initial, breadth-first assessment of inter-hemispheric functional connectivity (IFC) within each of the seven canonical resting-state networks (Yeo et al., 2011) defined by our cortical parcellation, as well as regions spanning the subcortex. Similarly to studies of functional lateralization in task-based fMRI, we derived a network laterality index as a simple means of summarizing and quantifying the relative magnitude of IFC as compared to the magnitude of intra-hemispheric FC. Each FC matrix was first thresholded at an uncorrected level of $p < 0.001$ to avoid overly conservative and highly nonlinear effects of multiple comparisons correction on the distribution of edge weights, while simultaneously minimizing the influence of weak (potentially spurious) connections. We then Fisher-z transformed the thresholded FC matrices and, for each individual and for each network, estimated a laterality index, LI, as:

$$LI = \frac{(\sum zFC_{IntraLH} + \sum zFC_{IntraRH}) - \sum zFC_{Inter}}{\sum zFC_{IntraLH} + \sum zFC_{IntraRH} + \sum zFC_{Inter}}$$

Intra-hemispheric connections within the left and right hemispheres are necessarily summed in the numerator given that there are, by definition, twice as many inter-hemispheric connections as each hemisphere alone. The result is a ratio on the interval of [-1, +1] that captures the extent to which each canonical resting-state network is predominantly connected intra- or inter-hemispherically: In the limit, a value of -1 would suggest that there is no intra-hemispheric FC and the network is solely composed of inter-hemispheric connections, while a value of +1 would indicate the reverse. A value of 0 therefore represents a network that is perfectly balanced in the magnitude of intra- versus interhemispheric connections. Here, we focus on positively correlated edges, where higher values would reflect greater functional coupling between regions (**Fig. 3-3)**.

Data-driven Community Detection and Modularity

Next, while the above approach is useful for considering differences among canonical functional networks, these networks are defined in healthy adult brains. And it is unclear whether these networks follow a similar spatial organization in callosotomy patients. Data-

driven community detection techniques can, therefore, provide a better assessment of functional network topologies, without any prior assumptions about specific brain regions and their canonical network memberships (Sporns & Betzel, 2016; Zamani Esfahlani et al., 2021). This is achieved via decomposition of FC matrices using modularity maximization algorithms, which group regions into functional modules: These represent regions that are generally more functionally coupled to each other than they are connected to other regions. The optimization objective is subject to a quality metric, Q—unlike our previous laterality analysis (which required separating out positive and negative edges), this can be estimated over FC matrices composed of both positive and negative correlations (Rubinov & Sporns, 2011). We performed this decomposition using the community_louvain function from the Brain Connectivity Toolbox (https://sites.google.com/site/bctnet/) with asymmetric treatment of negative edge weights (Rubinov & Sporns, 2011). Importantly, modularity maximization is sensitive to spatial scale, subject to a resolution parameter, γ (Fortunato & Barthélemy, 2007). Small values of γ typically yield coarse partitions with a small number of large communities; larger values of γ, by contrast, afford more fine-grained partitions. Because the solution of this decomposition is dependent upon one's choice for the resolution parameter, we tested a range of values from (in steps of 0.10). To further account for variability in community assignments (e.g., due to algorithmic stochasticity arising from random initializations), we estimated modularity 1000 times for each value of γ—optimal consensus partitions were obtained using the consensus_similarity function from the Network Community Toolbox (https://commdetect.weebly.com/). In similar fashion to the network laterality indices described above, we derived a modular laterality index for the resulting partitions according to prior work (K. W. Doron et al., 2012). This metric is limited to the interval, where a value of 0, for example, indicates that all functional communities are perfectly bilateral (i.e., the number of brain regions constituting each community are equally balanced between the left and right hemispheres), and values closer to 1 indicate progressively more lateralized topologies. We note that in this case, more fine-grained partitions may be beneficial for assessing modular laterality. Nevertheless, the results shown in **Fig. 3-4** and **Fig. 3-5** reflect a "default" ($\gamma = 1$) and we further illustrate in **Appendix Fig. S3-1** that complete callosotomy patients rapidly diverge from controls even at smaller values of γ (while partial patients and healthy controls remain relatively consistent, regardless of γ).

5. Results

To characterize how large-scale functional networks react to hemispheric severance, we assessed resting-state FC, with three complementary approaches: First, we present whole-brain FC matrices (carpet plots) to provide a broad overview of intra- and inter-hemispheric connectivity patterns in split-brain patients and in healthy controls. Second, we quantify the relative balance of intra- versus inter-hemispheric connectivity within each of the seven canonical resting-state networks using a laterality index. Finally, because these seven canonical resting-state networks are defined from healthy brains and may not accurately capture network organization in split-brain patients, we used a data-driven community detection approach to identify functional modules (regions more connected with each other and less with others) without imposing predefined parcellations or network boundaries. We then quantified a laterality index for these modules to assess how symmetric versus asymmetric these functional modules are across the hemispheres.

Whole-Brain Functional Connectivity (FC)

All complete callosotomy patients showed markedly reduced inter-hemispheric FC compared to both neurotypical controls and partial callosotomy patients (**Fig. 3-2B, 3-2C**), with one notable exception: the visual network. Inter-hemispheric FC within the visual network appeared relatively preserved across most complete callosotomy patients. What might be underlying this preserved synchrony is unclear. One possibility is shared perceptual input, as scans were acquired with eyes open, both hemispheres received similar visual information from the same environment. Alternatively, intact subcortical pathways may also contribute; the superior colliculus, which plays a role in directing gaze, could mediate some degree of bilateral visual coordination. In contrast to the marked reductions in inter-hemispheric FC, intra-hemispheric FC patterns in complete callosotomy patients appeared more similar to those observed in healthy controls, suggesting that hemispheric severance has a greater impact on inter-hemispheric than intra-hemispheric functional organization. Both partial callosotomy patients, including the one with approximately 1 cm of splenium remaining, showed inter-hemispheric FC patterns that were more similar to healthy controls than to complete callosotomy patients.

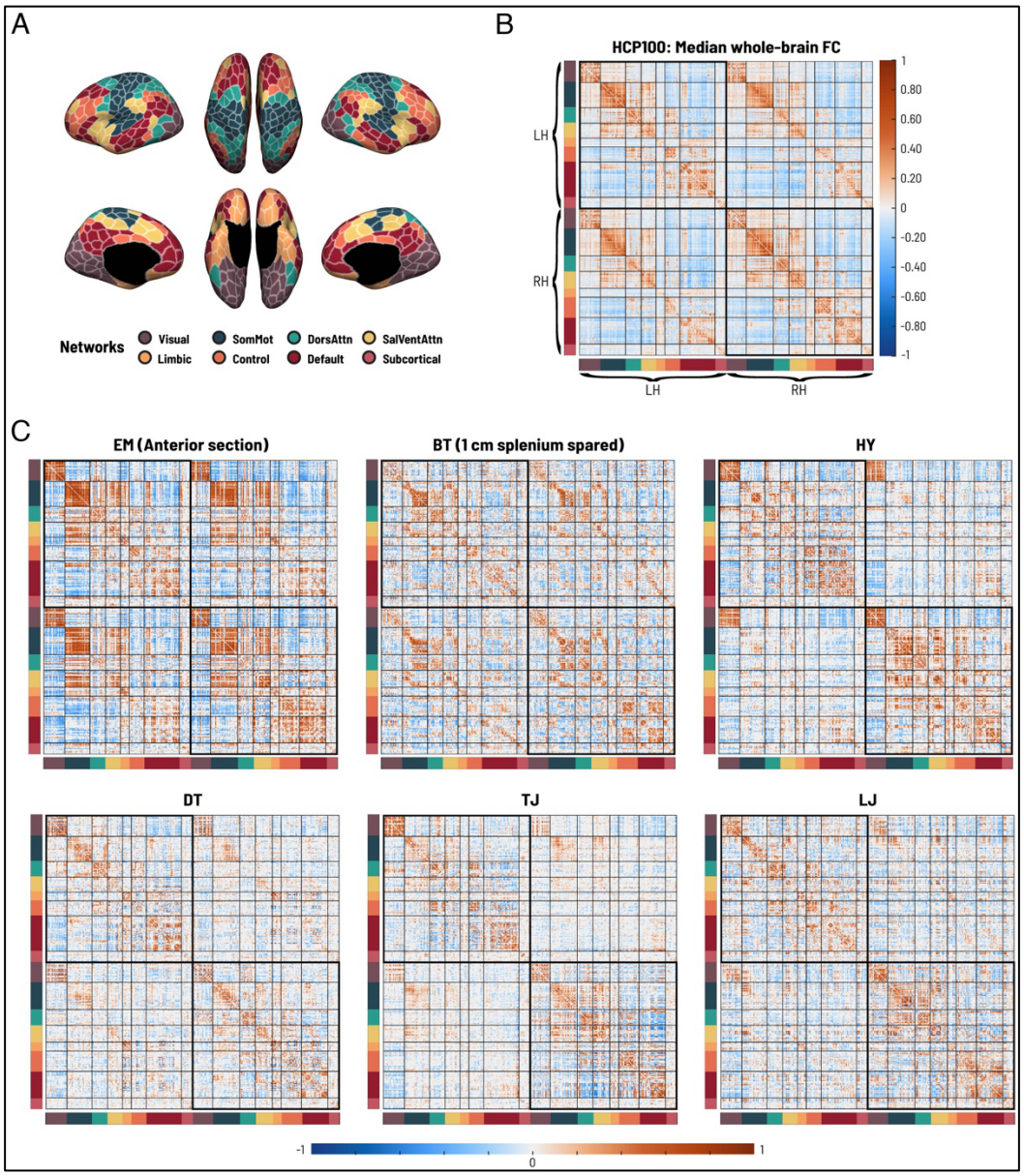


Figure 3-2. Whole-brain Functional Connectivity Matrices for Patients and for Healthy Controls. ***(A)*** Whole-brain functional parcellation composed of seven canonical resting-state networks (Schaefer et al., 2018; Yeo et al., 2011) and subcortical nodes (Tian et al., 2020). SomMot: SomatoMotor Network; DorsAttn: Dorsal Attention Network; SalVentAttn: Salience/Ventral Attention Network; LH: Left Hemisphere; and RH: Right Hemisphere. ***(B)*** A standard reference for neurotypical whole-brain functional connectivity (FC), given as the median over HCP100 subjects. FC was estimated by correlating low-frequency brain activity (0.01 to 0.08 Hz) between all pairs of regions (parcels) shown in in panel A. The large boxes outlining the Upper Left and Lower Right quadrants denote intra-hemispheric FC; the Upper Right and Lower Left quadrants thus capture inter-hemispheric FC. The main diagonal (representing self-connections) was blanked as these are irrelevant for subsequent analyses. ***(C)*** Whole-brain FC estimates for each callosotomy patient, thresholded at $p < 0.001$ (uncorrected for multiple comparisons). Typical patterns of IFC were largely abolished in

complete callosotomy patients (HY, DT, TJ, LJ), while partial patients (EM, BT) were more similar to healthy controls.

Laterality Indices of Canonical Resting-State Networks

To measure how much each network connects within versus across hemispheres, we calculated a laterality index for each of the seven canonical networks. The laterality index ranged from -1 (all inter-hemispheric FC) to +1 (all intra-hemispheric FC), with 0 indicating a balanced distribution of inter- and intra-hemispheric connectivity. All complete callosotomy patients showed more lateralized FC patterns than healthy controls and partial callosotomy patients, whose values generally fell within the control distribution (**Fig. 3-3**). This pattern of greater lateralization was observed in both higher-order transmodal networks, such as the default mode and dorsal attention networks, and in somatomotor networks (with the exception of patient TJ, who fell within the upper tail of the control distribution in the somatomotor network). Patient EM was more lateralized across frontoparietal control nodes, which include a number of regions likely to be structurally disconnected given the extent of their callosotomy; however, BT generally showed degrees of network bilaterality equivalent to healthy adults, despite having a mere fraction of splenium intact. Finally, complete callosotomy patients appeared to show conserved bilateral FC across limbic regions like the orbitofrontal cortex and temporal poles, which are known to be structurally coupled through the preserved anterior commissure as well as the corpus callosum (Catani & Schotten, 2012; Di Virgilio et al., 1999; Zamani Esfahlani et al., 2021). In sum, these results highlight the dependence of inter-hemispheric networks on corpus callosum connectivity—yet neurotypical levels of functional integration were possible even when only the splenium was left intact.

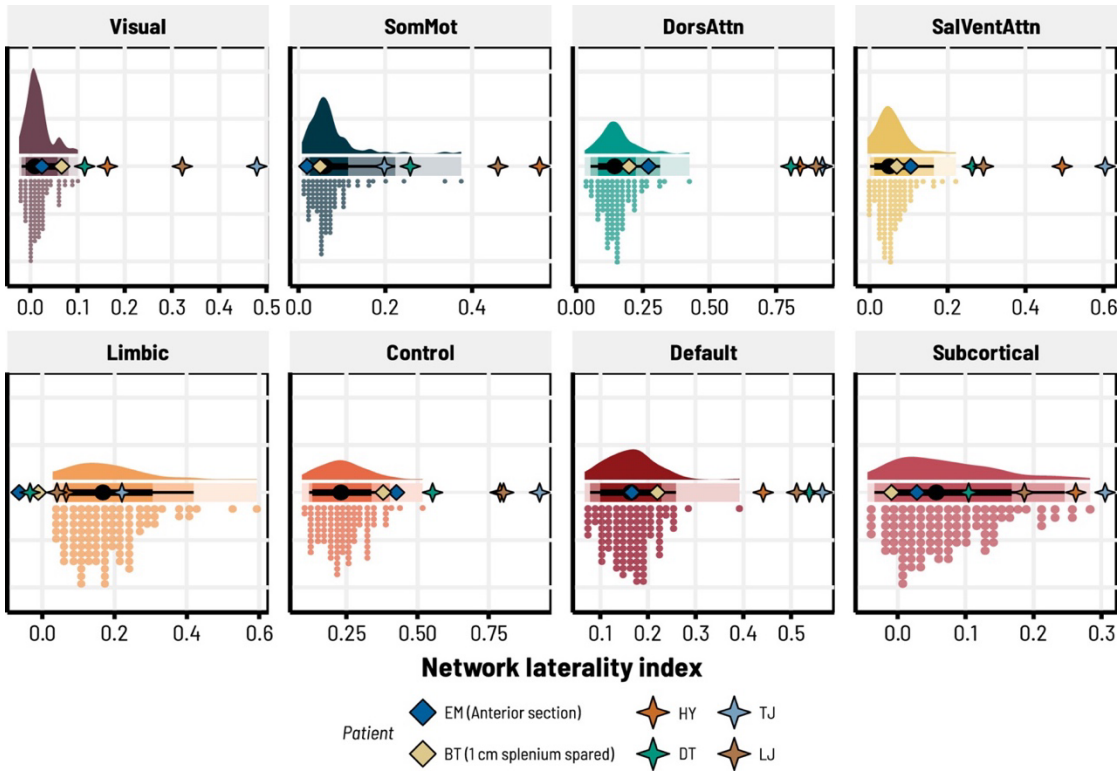


Figure 3-3. Laterality Indices for the Canonical resting-state functional networks. Network laterality indices are shown across seven canonical resting-state systems and subcortical regions (SomMot: SomatoMotor Network, DorsAttn: Dorsal Attention Networkm, SalVentAttn: Salience/Ventral Attention Network). Values closer to zero indicate an equal balance between intra- and inter-hemispheric FC, while values closer to one indicate more intra-hemispheric FC relative to inter-hemispheric FC. Note that each subplot captures a unique range of values, given differences in variability observed across neurotypical adults (colored distributions), patients, and networks. Complete callosotomy patients generally demonstrated more strongly lateralized FC compared to partials, who fell within the control distributions. Point intervals for each control distribution give the HCP100 median (black dot) and the 80 to 95% quantiles around the median (thick black lines and thin black lines, respectively).

Data-Driven Communities and Modular Laterality

To further investigate whole-brain differences in functional network topology (agnostic to any a priori assignment of the brain regions to canonical functional networks) we employed data-driven community detection techniques to cluster whole-brain patterns of FC into functional modules (**Fig. 3-4**). We then computed a laterality index (K. W. Doron et al., 2012) for these modules. A value of 0 indicated perfectly bilateral functional modules, i.e., the number of brain regions constituting each community are equally balanced between the left and right hemispheres, whereas values closer to 1 reflected increasingly lateralized network topologies. Importantly, we note that modularity maximization is sensitive to spatial scale, subject to a

resolution parameter, γ (Fortunato & Barthélemy, 2007). Here, we describe results using a γ = 1 "default". Complete callosotomy patients had greater degrees of modular laterality, suggesting that functional networks became increasingly confined within the hemispheres following hemispheric disconnection. (**Fig. 3-5**). Partial callosotomy patient EM, who retained the majority of his corpus callosum, showed bilateral patterns of network organization similar to those observed in neurotypical controls. Patient BT, who retained only the splenium, also fell within the control distribution of modular laterality but exhibited a markedly different modular topology (**Fig. 3-4**). In BT, functional communities appeared to segregate along the Sylvian fissure, with dorsal and ventral modules extending across the anterior–posterior axis of the brain. Thus, although BT's modules were relatively symmetric across the two hemispheres—as reflected by his low modular laterality index, comparable to healthy controls—the spatial organization of these modules differed substantially from the canonical network structure observed in controls. In neurotypical participants, communities seemed to be organized around well-known functional systems, such as somatomotor and visual networks, spanning both hemispheres (e.g., the green, and blue modules in the HCP data shown in **Fig. 3-4**). In BT, however, this network-based organization was replaced by a dorsal-ventral partitioning of functional modules (e.g., the green and blue modules shown for BT in **Fig. 3-4**), which, though bilaterally symmetric, reflects a very different functional architecture compared to healthy controls. Together, these findings suggest that complete callosotomy was associated with markedly greater modular laterality, reflecting pronounced hemispheric segregation; preservation of the posterior two-thirds of the corpus callosum was associated with bilateral modular organization very similar to that of healthy controls; and retention of ~1 cm of the splenium alone was associated with a similarly symmetric modularity (**Fig. 3-5**), yet with a fundamentally different underlying functional topology (**Fig 3-4**).

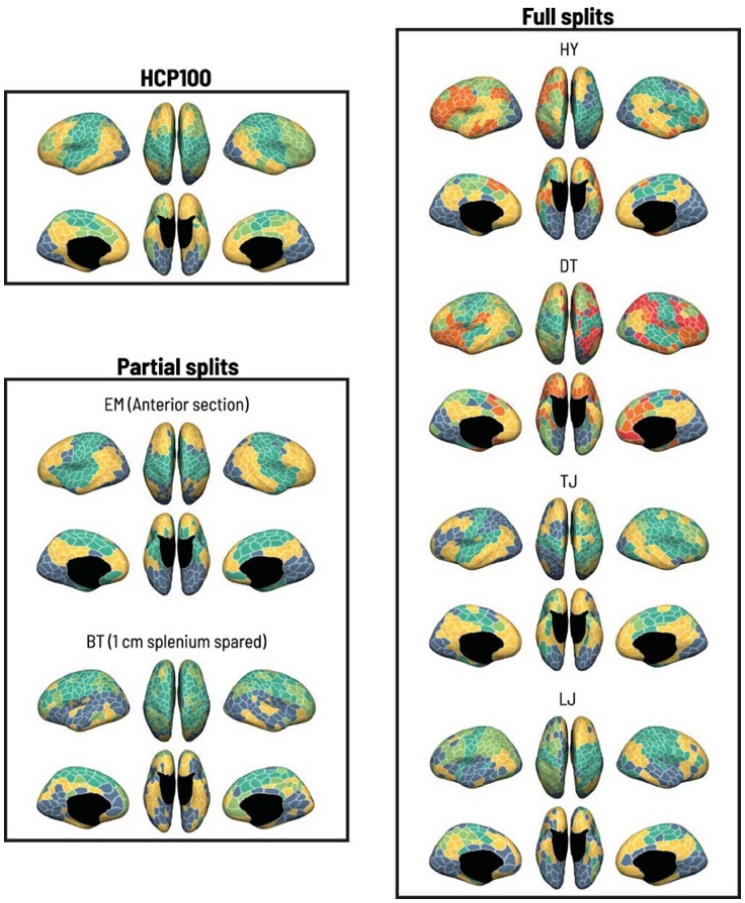


Figure 3-4. Modular decomposition of whole-brain functional connectivity. Spatial maps of consensus community assignments derived via data-driven modularity maximization are shown at a default level of resolution, $\gamma = 1$. Regional coloring indicates the assignment to a given functional module (unrelated to the "canonical" coloring of regions/networks in **Fig. 3-2A**). Because this decomposition is dependent upon individual-specific patterns of FC, individual patients may exhibit different numbers/organizations of modules, and therefore not all colors appear for all patients. Complete callosotomy patients (Full splits) generally exhibited more lateralized clustering of regions into modules relative to partial splits and healthy adult controls.

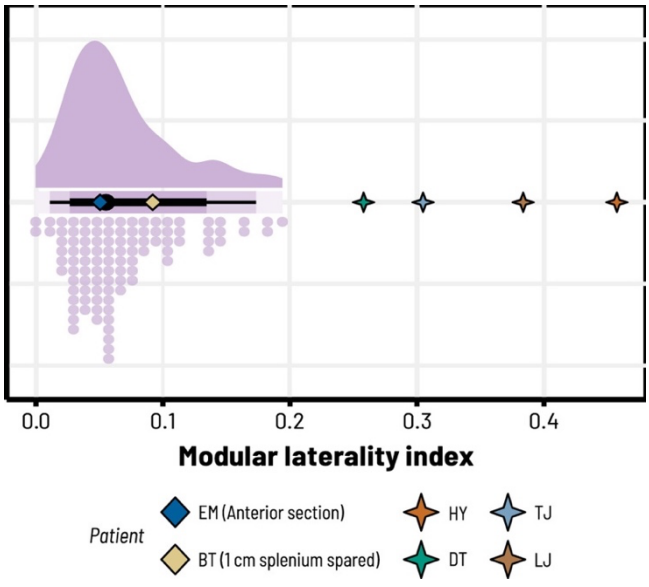


Figure 3-5. Modular Laterality Index for healthy controls and patients. The modular laterality index quantifies the extent to which functional communities exhibit inter-hemispheric representations (values closer to zero) or are restricted to one hemisphere or the other (values closer to one). Point intervals under the control distribution give the HCP100 median (black dot) and the 80 to 95% quantiles around the median (thick black lines and thin black lines, respectively). Functional modules are more strongly lateralized in complete callosotomy patients.

6. Discussion

In this study, we characterized whole-brain functional network organization in complete and partial split-brain patients, compared to neurotypical healthy controls (HCP data), using whole-brain functional connectivity matrices and laterality indices across canonical resting-state networks, as well as data-driven community detection and the laterality of those communities. Together, these findings converge on a consistent picture: complete callosotomy was associated with profound disruption of inter-hemispheric functional connectivity across cortical networks, while subcortical networks appeared relatively preserved, consistent with the fact that subcortical structures and non-callosal commissural pathways such as the anterior commissure remain intact in all patients, just as in healthy controls. In contrast, both partial callosotomy patients—including patient BT, who retained only the splenium—showed functional connectivity and laterality measures that were more similar to healthy controls. These neural findings closely parallel the behavioral effects described in Chapter 2 of this thesis. Complete callosotomy patients exhibited marked behavioral impairments on tasks requiring inter-hemispheric integration, whereas BT showed no evidence of classical behavioral disconnection (Bekir et al., 2025). Observing similarly preserved large-scale inter-hemispheric functional organization in BT therefore provides converging neural evidence for his intact behavioral performance.

Complete Callosotomy and Structure-Function Relationships in the Human Brain

These findings are theoretically important because split-brain patients provide a rare opportunity to directly test the assumptions about structure-function relationships in the human brain. Structure-function relationship refers to the assumption that the structural connectivity constrains functional connectivity (Honey et al., 2009; Wang et al., 2013). In other words, when two regions are connected by a direct structural pathway, they are more likely to be functionally coupled. Although the relationship between structural and functional connectivity is not strictly one-to-one, this principle remains one of the central assumptions in modern cognitive neuroscience (Bassett & Sporns, 2017). In complete callosotomy, the largest white matter tract connecting the two cerebral hemispheres is severed. If structural connectivity constrains functional connectivity (Honey et al., 2009), then the loss of this major structural pathway would disrupt inter-hemispheric functional connectivity. Consistent with

this prediction, we observed a marked reduction in inter-hemispheric functional connectivity in complete callosotomy patients, suggesting that widespread functional synchrony between the hemispheres depends on intact callosal pathways. This was evident across both canonical resting-state networks and data-driven functional communities, where network organization became markedly more lateralized following complete hemispheric severance. At the same time, the relative preservation of subcortical connectivity suggests that some bilateral coordination can persist through intact subcortical structures, or intact non-callosal commissures, such as the anterior commissure. Overall, these findings support the view that the corpus callosum plays an important role in coordinating large-scale inter-hemispheric functional dynamics in the adult human brain, providing converging neural evidence for the behavioral findings reported in Chapter 2.

Preserved Inter-hemispheric Integration in Partial Split-Brain Patients

In contrast to the complete callosotomy patients, the partial callosotomy patients showed functional connectivity patterns and laterality metrics that were similar to those observed in healthy controls. For patient EM, who retained the posterior two-thirds of his corpus callosum, this finding is perhaps expected: The corpus callosum is argued to have evolved to facilitate midline fusion of sensorimotor processes, with posterior callosal fibers considered critical for this function; the role of the anterior corpus callosum, by contrast, remains less clear as anterior callosal fibers have not been reliably linked to a specific functional role (Aboitiz & Montiel, 2003). Consistent with this, prior partial callosotomy studies have found that resections confined to the anterior callosum do not typically produce the hallmark behavioral disconnections observed following complete or posterior callosal section (Funnell et al., 2000), suggesting that the anterior callosum is not critical for the inter-hemispheric integration probed by standard disconnection paradigms. Thus, largely preserved inter-hemispheric functional network organization in EM was expected.

The most striking finding, however, was observed in BT, who retains only a small splenial remnant of approximately 1 cm. Based on established anatomical models of callosal topography (Hofer & Frahm, 2006), the splenium is thought to be the primary conduit for visual information transfer between hemispheres. We therefore predicted that BT might show relatively preserved inter-hemispheric coupling specifically within posterior networks, particularly the visual network, while exhibiting functional disruption in more anterior

systems. Contrary to this prediction, BT demonstrated inter-hemispheric functional connectivity patterns that were remarkably similar to those of healthy controls across canonical networks and exhibited a similarly bilateral pattern of large-scale functional community organization. These neural findings closely parallel the equally surprising behavioral findings described in Chapter 2: a mere remnant of splenium appears sufficient to support large-scale inter-hemispheric functional coupling, both behaviorally and neurally.

How might such extensive bilateral coordination be maintained through so little residual callosal segment? Intact subcortical pathways and non-callosal commissures have been proposed to contribute to maintaining coordinated activity between the hemispheres (Uddin et al., 2008). However, this account alone appears insufficient, because these same subcortical pathways remained intact in the complete callosotomy patients, who nevertheless showed profound disruptions in cortical—but not subcortical—inter-hemispheric functional organization. Another possibility is that the brain can leverage both existing intra-hemispheric pathways along with polysynaptic connectivity through the remaining posterior callosal fibers to maintain functional integration across hemispheres. In other words, rather than crossing directly through anterior callosal regions, information may be rerouted posteriorly within each hemisphere via long-range association tracts—such as the superior and inferior longitudinal fasciculi—which could act as intra-hemispheric "freeways" directing information toward the preserved splenial remnant. This bottleneck then may serve as a critical bridge for inter-hemispheric communication, allowing information to ultimately reach the other hemisphere. The ventral-dorsal organization observed in the data-driven functional communities in BT (**Fig. 3-4**) may reflect this reorganization and hence may be consistent with this possibility. Importantly, the posterior location of the spared callosal fibers may be critical for enabling such reorganization, particularly given the role of posterior and parietal regions in sensorimotor and multisensory integration across hemispheres; these regions may serve as "inter-hemispheric hubs" (van den Heuvel & Sporns, 2011), potentially allowing information from distributed cortical regions to be integrated and exchanged across hemispheres.

Limitations

Several limitations should be considered when interpreting these findings. The most important limitation concerns the inferences drawn from BT. Although the preserved inter-hemispheric functional organization observed in BT is striking given the minimal spared splenial tissue,

our interpretations regarding compensatory reorganization remain necessarily speculative because pre-operative imaging data are unavailable. Consequently, it cannot be definitively ruled out that some aspects of BT's functional organization—such as the unusual ventral–dorsal topology observed in the data-driven functional communities—may have predated the surgery rather than emerged as a consequence of callosal section and subsequent reorganization. While this possibility appears unlikely, it nevertheless remains an important limitation. Second, the small sample size limits the generalizability of the findings. Split-brain studies are necessarily constrained by the rarity of these cases. Although single-case and small-sample patient studies have historically provided critical insights in cognitive neuroscience, these findings should nevertheless be interpreted in the context of the limited sample size. Finally, longer resting-state scan durations may provide more stable estimates of functional connectivity and could help better characterize more subtle patterns of network organization, particularly in partial callosotomy patients.

Conclusion

These findings demonstrate that complete callosotomy markedly disrupts inter-hemispheric functional organization, while even a minimal posterior callosal remnant may be sufficient to preserve surprisingly extensive bilateral functional coupling. The close correspondence between the behavioral findings of Chapter 2 and the neural findings presented here further suggests that the neural consequences of callosotomy closely parallel the presence or absence of behavioral disconnection. Together, these findings contribute to ongoing debates regarding unity in split-brain patients by showing that the behavioral disconnection effects observed following complete callosotomy are also reflected in disrupted inter-hemispheric resting-state functional connectivity, providing converging neural evidence for large-scale hemispheric disconnection following complete severing of the corpus callosum. At the same time, these findings also demonstrate that substantial inter-hemispheric integration may nevertheless persist through even a small splenial remnant.

CHAPTER 4.
NEW PARADIGMS TO TEST THE UNITY IN SPLIT-BRAIN PATIENTS

A. LATERALIZED ADAPTATIONS OF THE SENSE OF AGENCY PARADIGMS

Collaborators:

Jake Gavenas, Corey H. Allen, Jacqueline McGuinness, Eric Hochstein, Laura Kaltwasser, Felipe De Brigard, Walter Sinnott-Armstrong, Michael B. Miller

1. Abstract

The sense of agency (SoA) is the feeling of control over actions and their consequences, and it is thought to arise from the integration of prospective (pre-action) and retrospective (post-action) signals. Evidence from split-brain patients suggests that these signals can be lateralized across hemispheres, raising the possibility that SoA may be computed independently within each hemisphere. To investigate hemispheric contributions to SoA, we developed lateralized versions of two established paradigms: an implicit measure (intentional binding; IB) and an explicit measure (cognitive control; CC), with the goal of applying them in split-brain patients in the future. Healthy participants completed both tasks across two sessions separated by one week. We tested whether these paradigms (1) replicate canonical SoA effects, (2) show stable individual differences over time, and (3) correlate across implicit and explicit measures. Intentional binding replicated canonical effects in session 1 but markedly attenuated in session 2. The cognitive control task showed weak sensitivity to prospective (congruency) manipulations. And outcome predictability did not reliably modulate either measure. In contrast, both tasks showed hand-related effects: binding was stronger for left-hand actions, whereas the control ratings were higher for right-hand actions. Individual differences in binding were moderately stable across sessions, whereas explicit control ratings were not. No correlations were observed between implicit and explicit measures. This work provides a methodological foundation for studying hemispheric contributions to SoA, particularly in populations with disrupted interhemispheric communication, such as split-brain patients, whose condition continues to inform debates about the nature of human agency.

Keywords: sense of agency, intentional binding, cognitive control, split-brain, lateralization

2. Introduction

The Sense of Agency (SoA) is our feeling of control over our actions and their consequences (Haggard, 2017). Current models propose that SoA emerges from the integration of prospective signals (such as intentions, predictions occurring before the action) and retrospective signals (such as motor feedback and outcome observations occurring after the action) (Frith et al., 2000; Haggard, 2017). When these temporally distinct signals align (i.e. when predicted and actual movements and outcomes match), we experience the subjective feeling of "I did that." (see **Fig. 4A-1A**).

Each of these components can be lateralized in the brain. Split-brain patients, whose cerebral hemispheres have been surgically disconnected to treat intractable epilepsy, provide a particularly informative window into this lateralization (Gazzaniga, 2000). Classic divided visual field paradigms show that each hemisphere can guide behavior based on information unavailable to the other. For example, when a split-brain patient is shown a snow scene in the left visual field (processed by the right hemisphere) and a chicken foot in the right visual field (processed by the left hemisphere), each hand selects corresponding objects: the left hand (controlled by the right hemisphere) picks a shovel picture, while the right hand (controlled by the left hemisphere) picks a chicken picture. When the patient is asked to explain their choice of the shovel, the speaking left hemisphere—unaware of the snow scene—confabulates: "*You need the shovel to clean the chicken shed*" (Gazzaniga & LeDoux, 1978) (see **Fig. 4A-1B**). This example illustrates how action selection (i.e. which object to pick), motor execution (independent hand movements to pick up different objects), and retrospective signals (the left hemisphere's post-hoc interpretation) may remain largely confined to one hemisphere when the hemispheres are disconnected. Moreover, the left hemisphere's post-hoc rationalization in the absence of reliable prospective signals suggests that it could overweight retrospective signals when constructing SoA. Wegner proposed that the SoA is essentially all a retrospective inference (Wegner, 2003). The behavior of the left hemisphere in split-brain patients appears to be consistent with this account—it seems to construct a SoA relying on retrospective signals, while lacking the prospective ones. This raises the possibility of hemispheric asymmetries in how prospective and retrospective signals are weighted. For instance, can the left hemisphere rely more heavily on retrospective signals than the right

hemisphere? Investigating these hemispheric asymmetries could inform both how SoA emerges in the intact brain and how it breaks down in clinical populations.

SoA is typically measured either implicitly or explicitly. Intentional binding paradigms provide an implicit measure of SoA, operationalized as the perceived temporal compression between a voluntary action and its outcome (Haggard et al., 2002). Voluntarily generated actions and their outcomes are perceived as closer together in time compared to externally generated or passively observed action-outcome pairs; this relative temporal compression in agentive compared to non-agentive conditions is referred to as "binding". Explicit SoA measures, by contrast, ask people to directly rate their sense of control over actions and their outcomes. In these paradigms, prospective signals can be manipulated using cognitive control tasks. A common approach employs the flanker task, in which congruency manipulations is used to disrupt the action selection fluency (a prospective signal) by introducing response conflict during action selection (i.e., which button to press in congruent vs. incongruent trials). This manipulation has been shown to reduce explicit SoA judgments, with participants reporting greater control on congruent relative to incongruent trials (Chambon & Haggard, 2012; Wenke et al., 2010). In addition to prospective signal manipulations, retrospective signals can be manipulated by varying outcome properties such as its valence (positive vs. negative) or predictability (expected vs. unexpected). Positive or expected outcomes generally enhance SoA relative to negative or unexpected ones, in both explicit and implicit SoA measures (Barlas & Kopp, 2018; Oishi et al., 2018; Pryke et al., 2025). Importantly, prospective and retrospective signals appear to be dissociable: individuals with schizophrenia, for instance, tend to underweight prospective signals while overweighting retrospective ones (Voss et al., 2010), suggesting that a balanced integration is critical for a coherent SoA. Understanding how these signals are weighted is therefore both theoretically and clinically important. Whether the two cerebral hemispheres differ in this weighting remains an open question.

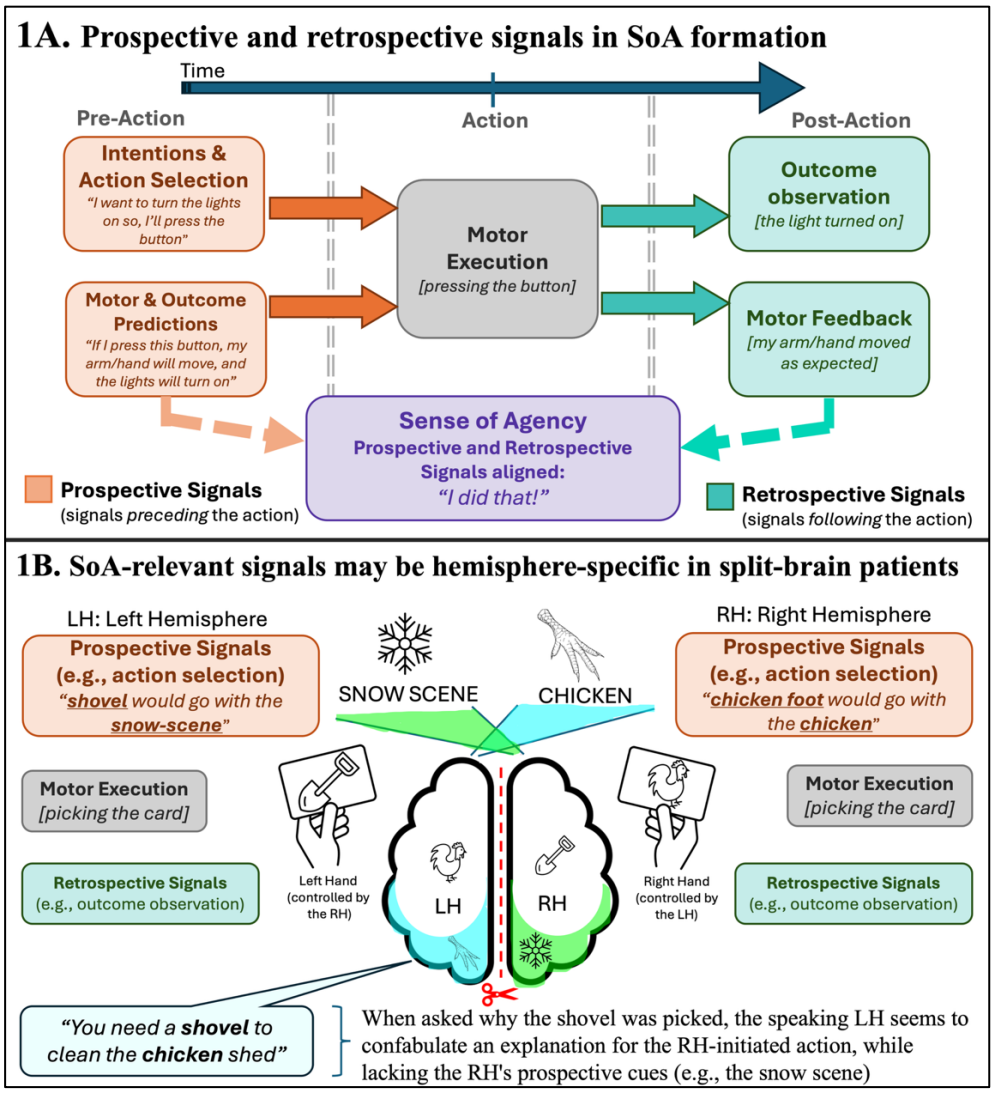


Figure 4A-1. Motivation for the Current Study ***(A)*** The sense of agency (SoA) is thought to emerge from prospective signals occurring before the action (such as intentions and motor predictions) and retrospective signals occurring after the action (such as sensory feedback and outcome observation). When these signals align, we experience the feeling of "I did that." ***(B)*** Split-brain patients illustrate that key components of SoA can be lateralized across hemispheres. Prospective signals, motor execution, and retrospective signals may operate largely within each hemisphere and may not be readily shared across the disconnected hemispheres. Furthermore, the two hemispheres may differ in how they weight prospective versus retrospective signals when forming SoA. The speaking left hemisphere often confabulates explanations for actions initiated by the right hemisphere, suggesting it relies heavily on retrospective cues to construct SoA, when lacking prospective signals. With lateralized SoA paradigms, one can probe hemispheric contributions to SoA formation.

Here, we introduce lateralized versions of both implicit and explicit SoA paradigms designed for eventual use with split-brain patients. Our lateralization manipulation independently varies which hand generates the action and which hand provides the subsequent

SoA judgment. Because each hand is primarily controlled by the contralateral hemisphere, the hemisphere generating the action and the hemisphere making the SoA judgment can either be the same (uncrossed) or different (crossed). In healthy participants—where interhemispheric communication is intact—lateralization effects can be negligible. We therefore predict no effect of hand-use or no crossed-uncrossed difference in this study. This design is motivated by its future application to split-brain patients, allowing direct investigation of whether SoA can be formed under crossed conditions compared to uncrossed ones and whether the hemispheres differ in how they weight prospective versus retrospective cues.

Both tasks were completed twice, one week apart. To our knowledge, the test-retest reliability of SoA paradigms has not been systematically assessed, and this longitudinal design allowed us to evaluate the temporal stability of SoA measures within individuals, which is an important practical consideration for future patient testing, where data collection often spans multiple sessions to achieve adequate statistical power at the individual level. In this study we asked: (1) whether these lateralized paradigms reproduce expected SoA effects, (2) whether individual differences in SoA are stable over time, and (3) whether implicit and explicit SoA measures are correlated at the individual level. Establishing lateralized SoA paradigms can lay the groundwork for applying them to split-brain patients and other clinical populations with disrupted interhemispheric communication, ultimately informing our understanding of hemispheric contributions to SoA formation in the intact brains.

3. Methods

Participants

31 people (22 females, *M*age = 20.61, *SD*age = 2.64; 29 right-handed, 2 left-handed) from the University of California, Santa Barbara participated in this study. There were four sessions over two weeks, each lasting one hour (see **Fig 4A-2A**). Participants were recruited through UCSB's Paid SONA system and compensated $10 for each of the first two sessions and $20 for each of the final two, totaling $60 for their participation. All participants provided informed consent before taking part. The experiment was approved by the Human Subjects Committee at the University of California, Santa Barbara. One participant was excluded for completing fewer than half of the total trials. This left us with a final sample of 30 participants. Trials with reaction times (RTs) < 100 ms were considered as anticipatory and excluded,

comprising less than 1% of all trials. Incorrect trials were also excluded, comprising less than 3% of all trials.

Apparatus and stimuli

All experiments were programmed using PsychoPy (version 2022.2.5, Pierce et al., 2019). Participants were seated 93 cm from the monitor, with their heads stabilized by a chinrest. Visual stimuli were presented on a Mac Mini HP 22uh 22.5" (1920x1080) monitor with a refresh rate of 60 Hz and WLED backlight (HP Inc., 2015) and auditory stimuli were delivered through OneOdio® Pro-10 Over Ear wired noise-canceling headphones. Eye movements were recorded with an EyeLink Plus 1000 Desktop eye tracker (SR Research, Ltd.). Participants used two lower buttons on the MiliKey 5 (MH-5) button box, left index finger on the left button and right index finger on the right button to respond and used a mouse to move the slider. A 4x9x7.87in no-peek keyboard cover (Plastic Perfection, n.d.) was placed over the button box and participants' hands to prevent them from viewing their hands while pressing the buttons (see **Fig. 4A-2B**). After each button press, participants heard either an expected (high-probability) or unexpected (low-probability) tone, these tones were either high-pitched (1900 Hz) or low-pitched (880 Hz). Which tone (high or low pitch) is the low vs high probability tone counterbalanced across participants.

Procedure

Participants completed four sessions across two consecutive weeks. In Week 1, they completed one session of the lateralized Intentional Binding (IB) paradigm and one session of the lateralized Cognitive Control (CC) paradigm, separated by one day. In Week 2, they repeated each paradigm following the same schedule. The order of paradigms (IB-first vs. CC-first) was counterbalanced across participants, and all sessions were held at the same time of day for each participant (**Fig. 4A-2A**). For both paradigms, participants responded using the two-buttons of a response box, with their hands occluded by a no-peek keyboard cover to prevent visual feedback of their hand movements (**Fig. 4A-2B**). This occlusion was implemented to ensure compatibility with future testing in split-brain patients to limit cross-cuing (Volz et al., 2018). For example, seeing which hand pressed the button could inform the patient which hemisphere initiated the response, providing indirect information that might otherwise not be readily available to the other hemisphere.

Lateralized Intentional Binding Paradigm (IB)

Each trial began with a gaze-contingent fixation period (200, 400, or 600 ms) during which participants maintained fixation on a central crosshair. A lateralized cue was then flashed for 100 ms: a right visual field (RVF) cue (“>”) indicated that participants should press the right button with their right index finger; a left visual field (LVF) cue (“<”) indicated a left button press with the left index finger. On no-cue trials, participants were instructed to wait passively while the computer generated the button press. On RVF or LVF cued trials, participants were instructed not to respond immediately but to wait briefly and press whenever they wanted; this was intended to promote a sense of agency over the action rather than mere stimulus-response behavior. The computer’s reaction time (RT) was randomly sampled on each trial from a normal distribution based on pilot data (M = 650 ms, SD = 490 ms). Every button press—regardless of source (right hand, left hand, or computer)—produced an audible mechanical click sound. Following the click sound, a tone (high or low pitch; 50 ms) was presented after one of three base intervals (200, 400, or 800 ms), jittered ±100 ms.

Participants then used a mouse to move a slider—ranged between 100-1000 ms, in 100 ms increments—to estimate the duration of the interval between the click and the tone (**Fig. 4A-2C**). The same hand was used to control the slider within each block, alternating every three blocks across the 12 blocks per session (e.g., RRRLLLRRRLLL or LLLRRRLLLRRR, counterbalanced across participants). Before the main task, participants completed a practice phase in which they were familiarized with the three base intervals (four trials each at 200, 400, and 800 ms), followed by additional practice trials with jittered intervals. Participants were told that the interval could range anywhere from 100 ms to 1000 ms.

The task comprised 12 blocks of 30 trials (360 trials per session; 720 across two sessions). The three response conditions (left hand, right hand, computer) were evenly distributed (60 trials each per session). Within each response condition, 70% of trials led to the high-probability tone and 30% to the low-probability tone.

Lateralized Cognitive Control Paradigm (CC)

Each trial began with the same gaze-contingent fixation period as the IB task. A five-arrow array was then presented for 100 ms. Participants were instructed to respond to the direction

of the central arrow while ignoring the surrounding arrows: a central arrow pointing right (“>”) required a right-hand press; a central arrow pointing left (“<”) required a left-hand press (**Fig. 4A-2D**). The surrounding arrows could be congruent (all pointing in the same direction as the central arrow), incongruent (all in the opposite direction), or semi-congruent (arrows in one visual field congruent, arrows in the opposite visual field incongruent). Semi-congruent trials were included to dissociate the influence of ipsilateral and contralateral flanker information on control judgments—a distinction that becomes critical in split-brain patients, who receive visual input exclusively from the contralateral hemifield.

After each button press, a tone (high or low pitch) was presented. Tone probabilities were contingent on which button was pressed (i.e., which hand—left or right—pressed the button). For each button, one tone occurred on 70% of trials and the other tone on 30% of trials, whereas the opposite mapping applied to the other button. This means that which tone was “expected” (high probability) depended on which hand/button was used, not on the tone itself. For example, a right-hand (right-button) press might produce the high-pitched tone 70% of the time and the low-pitched tone 30% of the time, while the left hand (left button) would be the reversed. The assignment of pitch (high vs. low) to probability (70% vs. 30%) for each hand was counterbalanced across participants.

Following the tone, participants rated their perceived control on a 1-9 scale (1 = no control; 9 = full control) using a mouse-controlled slider. To ensure consistency with prior work, we adopted the instructions from Sidarus and Haggard (2016) and Imaizumi and Tanno (2019)

which were as follows: “*In each trial, a tone will be presented. Please pay close attention to the relation between your action and the tone. You will judge this relation. Specifically, you will judge how much you feel that your action caused the tone*.” The same hand was used to move the slider within each block, switching every three blocks across the 18 blocks total. Which hand they started with (right or left) was counterbalanced across participants (**Fig. 4A-2D**) .

The task comprised 18 blocks of 24 trials (432 trials per session; 864 across two sessions). Eight flanker configurations were presented (two congruent, two incongruent, four semi-congruent; see **Fig. 4A-2E**), each appearing equally often (54 trials per session per configuration).

Study Design and Measures

For the IB paradigm, the primary dependent variable was temporal judgment error (in ms), defined as the participant's estimated interval minus the actual interval between the action-tone. Negative values indicate underestimation. Within-subjects factors were responding hand (which hand is pressing the button; right, left, or computer), tone outcome probability (30% vs. 70%), session (1 vs. 2), reporting hand (which hand is used to make the temporal judgement; left vs. right), and base interval (200, 400, 800 ms; **Fig. 4A-2F**). Intentional binding was operationalized as the difference in judgment error between self-generated (left- or right-hand) and computer-generated responses.

For the CC paradigm, the primary dependent variable was the control rating (1-9). Within-subjects factors were flanker congruency (congruent, semi-congruent, incongruent), outcome probability (30% vs. 70%), session (1 vs. 2), responding hand (which hand is pressing the button; right vs. left—defined by the direction of the central arrow), reporting hand (which hand is rating the control; right vs. left), and base interval (200, 400, 800 ms; **Fig. 4A-2E**).

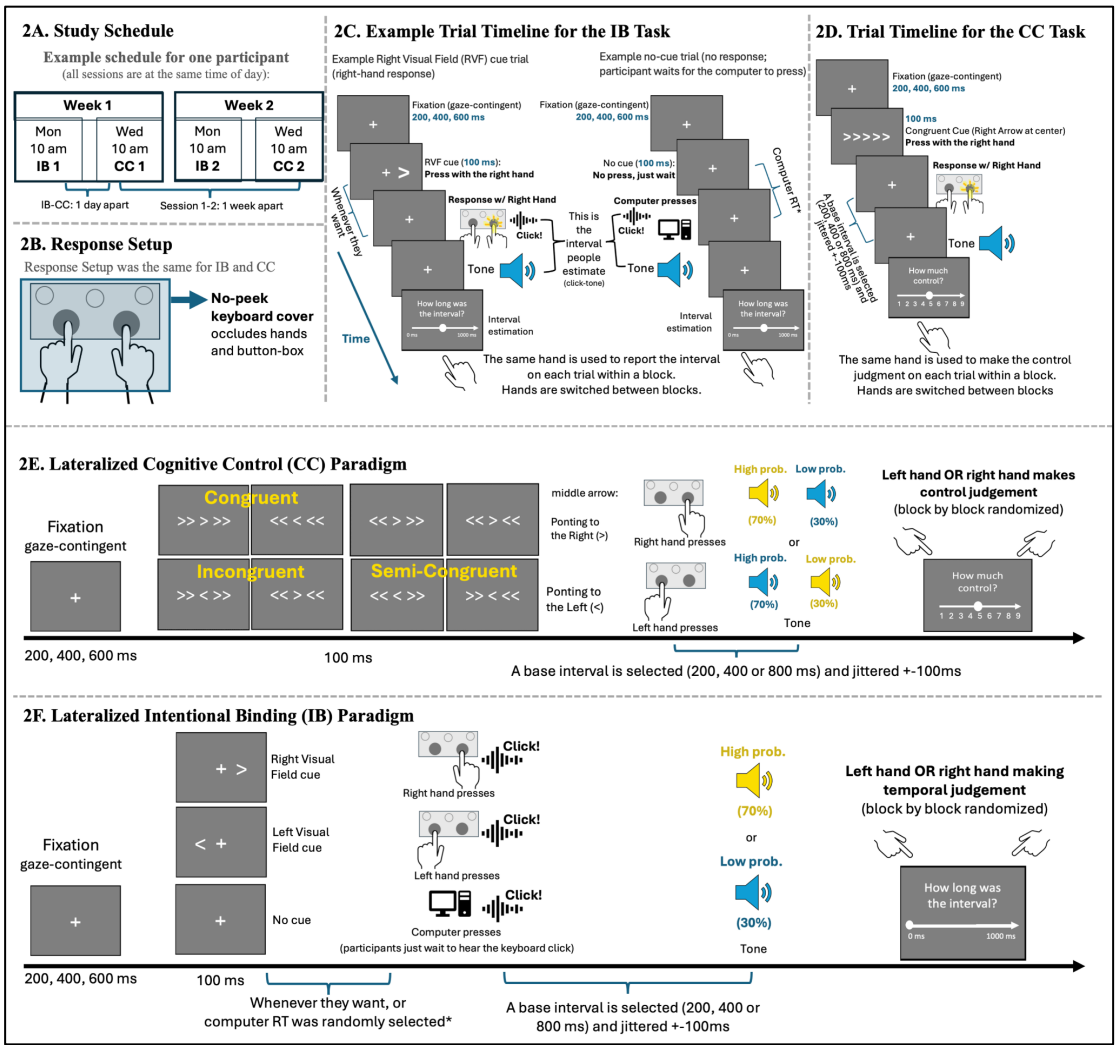


Figure 4A-2. Study design and task paradigms. ***(A)*** **Study schedule.** Participants completed four sessions over two weeks. Within each week, Intentional Binding (IB) and Cognitive Control (CC) sessions were separated by one day; second sessions were separated by a week. Session order (IB-first vs. CC-first) was counterbalanced across participants, and all sessions occurred at the same time of day. ***(B)*** **Response setup.** Both paradigms used the same two-button response box. Participants had their right index finger on the right button and left index finger on the left button. A no-peek keyboard cover occluded participant's hands and the button box throughout all button-press responses. ***(C)*** **IB paradigm trial timeline**. Trials began with a gaze-contingent fixation (200, 400, or 600 ms), followed by a 100 ms cue: a right visual field (RVF) cue prompting a right-hand press, a left visual field (LVF) cue prompting a left-hand press, or no cue (computer-generated press). Every key press, regardless of source, produced a click sound, after which a tone followed at a base interval of 200, 400, or 800 ms (jittered +-100 ms). Participants estimated the click-to-tone interval using a slider (100-1000 ms). The reporting hand (that uses the slider) was the same within blocks and alternated between blocks. ***(D)*** **CC paradigm trial timeline**. After gaze-contingent fixation, a five-arrow array was displayed for 100 ms. Participants responded to the central arrow direction (right hand for ">", left hand for "<") while ignoring surrounding arrows. A tone followed the button press (70% expected / 30% unexpected pitch per hand), after which participants rated their perceived control over the tone using a 1-9 slider. This

reporting hand (that uses the slider) was the same within blocks and alternated between blocks. ***(E)* CC paradigm design.** Flanker arrays varied in congruency (congruent, incongruent, semi-congruent) across eight configurations. A base interval of 200, 400, or 800 ms (jittered ±100 ms) preceded the tone, which could either be high probability (70%) or low probability tone (30%). ***(F)* IB paradigm design.** Responding hand (right, left, computer), tone probability (high/low, 70%/30%), and base interval (200, 400, or 800 ms, jittered ±100 ms) were fully crossed within participants.

Statistical Analyses and Predictions

1. Manipulation and Confound Checks

Prior to testing the primary hypotheses, we conducted manipulation and confound checks for each paradigm using repeated-measures analyses of variance (ANOVA) in R (version 4.0.3) using aov_ez function from afex package (Singmann et al., 2015). Significant effects were followed up with post hoc pairwise comparisons using estimated marginal means (EMMs) using emmeans package (Lenth, 2023), with *p*-values adjusted using Tukey's HSD.

For the IB paradigm, we conducted a one-way repeated measures ANOVA on mean RT with three levels of response hand (computer, left hand, right hand), to verify that computer-generated RTs were comparable to participants' voluntary right and left-hand RTs. This was to ensure that any differences in judgement errors (binding) across response conditions could not be attributed to systematic timing differences between self-generated actions and computer-generated actions. We predicted no RT differences across response conditions.

For the CC paradigm, we conducted a one-way repeated-measures ANOVA on mean RTs with three levels of flanker congruency (congruent, semi-congruent, incongruent) as a manipulation check. If the flanker manipulation successfully induced response conflict (thereby disrupting action selection fluency as intended), RTs should be slowest for incongruent and fastest for congruent trials (RT_incongruent > RT_semi-congruent > RT_congruent).

2. Group-level SoA effects: IB and CC Linear Mixed-Effects Models

Linear mixed-effects models were fitted using the lme4 package (Bates et al., 2015), and p-values were obtained using lmerTest. Significant interactions were followed up with pairwise post hoc comparisons based on estimated marginal means (EMMs) using the emmeans package (Lenth, 2023), with Tukey-adjusted p values for multiple comparisons. For pairwise contrasts, we report adjusted p-value, and standardized effect size (Cohen's d). All

categorical predictors were coded using deviation coding (sum-to-zero) to allow for ANOVA-like interpretation of main effects and interactions.

2.A. Intentional binding (IB).

The dependent variable was temporal judgment error (ms). Fixed effects included response hand (computer, left, right), outcome probability (low, high), session (1, 2), reporting hand (left, right), and base interval (200, 400, 800 ms), with all interactions and a random intercept for participant:

Judgment Error ~ Response Hand x Outcome x Session x Reporting Hand x Base Interval + (1 | Participant)

We predicted: (1) Canonical binding: self-generated actions (left and right hand) should produce greater temporal underestimation than computer-generated actions; expected outcomes should produce stronger binding than unexpected outcomes. (2) Session stability: no response hand x session interaction if binding is stable over time. (3) No lateralization effects: binding should not differ between left- and right-hand actions, and reporting hand should not influence judgment errors or interact with response hand. (4) Longer base intervals should produce greater binding, consistent with prior work.

2.B. Cognitive Control (CC).

The dependent variable was the control rating (1-9). Fixed effects included flanker congruency (congruent, semi-congruent, incongruent), outcome probability (low, high), session (1, 2), responding hand (left, right), reporting hand (left, right), and base interval (200, 400, 800 ms), with all interactions and a random intercept for participant:

Control Rating ~ Congruency x Outcome x Session x Response Hand x Reporting Hand x Base Interval + (1 | Participant)

We predicted: (1) Canonical SoA effects: congruent trials should yield the highest control ratings, followed by semi-congruent, then incongruent; expected outcomes should yield higher ratings than unexpected outcomes. (2) Session stability: If the explicit SoA measures are stable over time, we predict no session x congruency or session x outcome interactions. (3) No lateralization effects: control ratings should not differ between hands, and no interactions with congruency or outcome are expected. (4) Shorter base intervals should yield higher control ratings, consistent with prior work.

3. Individual Differences in IB and CC effects and their stability over time

To assess within-person stability of SoA effects, we examined whether individual differences in task-related effects were consistent between sessions. For each paradigm, separate linear mixed-effects models were fitted to Sessions 1 and 2 using the same fixed-effects structure as the primary models (excluding session). Participant-specific random slopes were extracted from each model (using ranef function from lme4 package in R) and correlated across sessions using Pearson correlations. Three participants who did not complete both sessions were excluded from this analysis. For IB, we extracted random slopes for response hand; for CC, we extracted random slopes for congruency. Random-effects structures were specified as (Response Hand | Participant) for IB and (Congruency | Participant) for CC. If SoA-related effects are stable within individuals, we predicted significant positive cross-session correlations.

4. Cross-Task Correlations Between IB and CC

We examined whether individual differences in SoA-related effects were correlated across paradigms. Using the model specifications described above, participant-specific slopes were obtained separately for each task and session. These slopes were then correlated across tasks using Pearson correlations, conducted separately for each session as SoA-related effects may vary across sessions. We predicted significant positive correlations if both paradigms index a common underlying SoA-related individual difference.

4. Results

1. Manipulation and Confound checks

For the IB paradigm, the repeated-measures ANOVA revealed no significant difference in RTs across response conditions, $F(2, 58) = 0.98$, $p = .381$. Computer-generated RTs (M = 744 ms, SD = 27 ms), left-hand RTs (M = 854 ms, SD = 536 ms), and right-hand RTs (M = 815 ms, SD = 528 ms) were comparable, confirming that there are no systematic differences in button-press timing between self-generated and computer-generated actions.

For the CC paradigm, the repeated-measures ANOVA revealed a significant main effect of congruency on RTs, $F(2, 58) = 8.73$, $p < .001$. Post hoc pairwise comparisons showed that RTs differed significantly between all pairs of conditions. RTs were significantly slower in the incongruent condition (M = 514 ms, SD = 183 ms) than both the congruent condition

(M = 444 ms, SD = 144 ms, p = .008) and the semi-congruent condition (M = 464 ms, SD = 127 ms, p = .038). RTs in the congruent condition were also significantly faster than in the semi-congruent condition (p = .02).This graded RT pattern confirms that the flanker manipulation successfully induced graduated levels of response conflict.

2. Group-Level SoA Effects

2A. Intentional Binding (IB)

A linear mixed-effects model examined judgment error (the difference between the estimated time interval vs actual interval between the action and the tone) by response hand, outcome, session, reporting hand, and base interval, with a random intercept for participants. Because our hypotheses and predictions concerned a limited set of effects and their interactions, we focused our reporting on those predicted effects (see **Table 4A-1**).

Canonical Effects of Intentional Binding

There was a significant main effect of response hand (F(2,17923 = 23.6, p < .001). Participants showed greater time underestimation for the left hand button presses (M= -66 ms, SD = 187 ms) compared to computer-generated presses (M = -45 ms, SD = 187 ms, Mdiff (binding) = 21 ms, p < .001, d = 0.13), in line with the expected intentional binding effect. However, the right-hand button-presses (M = -53 ms, SD = 191 ms) didn't differ from computer-generated ones (Mdiff (binding) = 8 ms, p = .14). Left-hand button presses also led to greater time interval underestimation compared to right hand button-presses (Mdiff = 13 ms, p < .001, d = 0.09), suggesting that the observed binding effect was primarily driven by left-hand responses. There was no main effect of outcome probability, F(1,17923) = 1.48, p = .22, and no interaction between outcome and response hand, F(2,17923) = 0.8, p = .44 suggesting that outcome predictability did not modulate binding (**Fig 4A-3B**).

Session Effects

There was a significant main effect of Session, F(1,17952) = 118.9, p < .001. Judgement error in Session 1 (M = -69.5 ms, SD = 193.5 ms) was larger than Session 2 (M = -39.7 ms, SD = 182.8 ms, d = 0.18) suggesting that people got better in their time estimation over time. Critically, there was a session x response hand interaction, F(2, 17923) = 5.6, p = .0037, indicating that the binding effect differed across sessions (**Fig. 4A-3A**).

In Session 1, the canonical binding pattern was replicated for both hands: Computer-generated presses showed the least underestimation (M = -53.8 ms, SD = 195 ms), followed

by right-hand presses (M = -68.9 ms, SD = 194 ms) and left-hand presses (M = -84.8 ms, SD = 190 ms). All pairwise differences were significant: (computer vs. right hand: Mdiff (binding) = 15 ms, p = .005, d = 0.09; computer vs. left hand: Mdiff (binding) = 31 ms, p < .001, d = 0.2).

In Session 2, binding was substantially attenuated. The difference between computer-generated (M = -36.1 ms, SD = 179 ms) and right-hand presses (M = -37.2 ms, SD = 186 ms) was negligible and non-significant (Mdiff (binding) = 1.2 ms, p = .90), indicating that binding for right-hand actions had disappeared entirely. Left-hand presses (M = -45.9 ms, SD = 182 ms) continued to show greater underestimation than computer-generated (Mdiff (binding) = 9.8 ms, p = .046, d = 0.07), though the effect was markedly reduced relative to Session 1.

Session also interacted with outcome probability, F(1, 17923) = 3.8, p = .049, and reporting hand, F(1, 17925) = 7.2, p = .007. However, because response hand did not interact with these factors (i.e., no session x outcome x response hand interaction: F(2, 17923) = 0.04, p = .96), these additional interactions reflect general time estimation changes rather than modulations of intentional binding. In Session 1, people underestimated the interval more when they heard the low-probability tone (M = -75.3 ms, SD = 196 ms) compared to the high-probability tone (M = -67 ms, SD = 192 ms; p = .02, d = 0.05). In Session 2, this difference was gone (p = 0.6).

Lateralization Effects

Consistent with predictions in healthy controls, there was no interaction between response hand and reporting hand, F(2, 17923) = 0.60, p = .54, indicating that the judgment error by response hand—and thus binding—did not depend on which hand was used to report the interval (i.e. no crossed-uncrossed differences, **Fig 4A-3C**). However, contrary to predictions, left-hand actions produced reliably stronger binding than right-hand actions. This hand asymmetry is discussed in the Discussion section.

Base Interval Effects

Following recent intentional binding literature (Suzuki et al., 2019) we also included three base intervals between the action and tone (200, 400 and 800 ms) to investigate effects of binding across different intervals. Base interval had a significant main effect, F(2, 17924) = 4287, p < .001. Trials with 200 ms base interval were overestimated (M = 56 ms, SD = 122 ms), whereas 400 ms (M= -17 ms, SD = 140 ms) and 800 ms intervals (M = -204 ms, SD =

190 ms) were underestimated (**Fig 4A-3D**), with all pairwise comparisons significant (all ps < 0.001), the 200 vs. 400 ms comparison showed a medium effect size (d = 0.53); and the 200 vs. 800 ms (d = 1.81), and 400 vs. 800 ms comparisons had large effects (d = 1.28). Critically, there was no interaction between base interval and response hand, F(4, 17924) = 1.7, p = .15, indicating that binding did not vary as a function of interval duration.

Table 4A-1. Fixed Effects of the Linear Mixed Model for Interval Judgement Errors (ms)

Effect	**Contrast**	***b***	***95% CI***	***p***
Intercept		-55.83	[-73.91, -37.76]	**<.001**
Response hand	Left hand vs. Computer	-19.34	[-25.06, -13.63]	**<.001**
	Right hand vs. Computer	-5.46	[-11.17, 0.25]	.061
Outcome	High vs. Low	2.89	[-1.75, 7.53]	.222
Session	1 vs. 2	-26.63	[-31.42, -21.85]	**<.001**
Report hand	Left vs. Right	0.34	[-4.32, 4.99]	.887
Base interval	400 vs. 200	-76.24	[-81.93, -70.55]	**<.001**
	800 vs. 200	-261.85	[-267.57, -256.14]	**<.001**
Response hand x Outcome	Left hand vs. Computer x High vs. Low	2.15	[-9.29, 13.58]	.713
	Right hand vs. Computer x High vs. Low	-4.95	[-16.37, 6.46]	.395
Session x Response hand	1 vs. 2 x Left hand vs. Computer	-18.79	[-30.22, -7.35]	**.001**
	1 vs. 2 x Right hand vs. Computer	-14.26	[-25.68, -2.85]	**.014**
Session x Outcome	1 vs. 2 x High vs. Low	9.28	[0.00, 18.56]	**.050**
Base interval x Response hand	400 vs. 200 x Left hand vs. Computer	-4.15	[-18.17, 9.87]	.562
	400 vs. 200 x Right hand vs. Computer	-5.24	[-19.25, 8.76]	.463
	800 vs. 200 x Left hand vs. Computer	-16.26	[-30.33, -2.18]	**.024**
	800 vs. 200 x Right hand vs. Computer	-15.13	[-29.16, -1.10]	**.035**

Session x Response hand x	1 vs. 2 x Left hand vs. Computer x High vs. Low	3.29	[-19.58, 26.15]	.778
Outcome	1 vs. 2 x Right hand vs. Computer x High vs. Low	1.39	[-21.44, 24.22]	.905

Note. *b* = regression coefficient (estimate), *CI* = confidence interval.

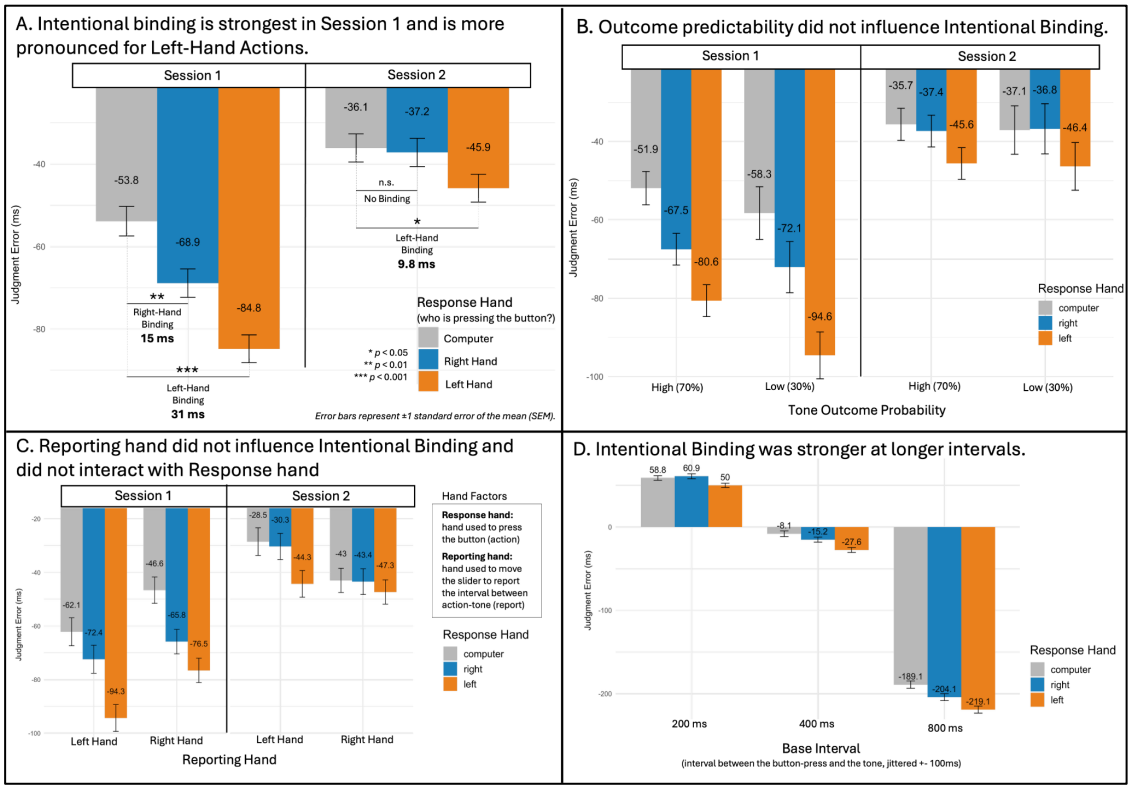


Figure 4A-3. Intentional binding effects. ***(A)*** Mean judgment error (ms) as a function of response hand (left, right, computer) in Sessions 1 and 2. Negative values indicate temporal underestimation; greater underestimation for self-generated relative to computer-generated actions reflects intentional binding. Error bars represent +-1 standard error of the mean. In Session 1, binding was evident for both hands (computer > right hand > left hand); in Session 2, binding was absent for right-hand actions and markedly attenuated for left-hand actions. ***(B)*** Mean judgment error (ms) across levels of tone outcome probability (30% vs 70%) in Sessions 1 and 2, by response hand (computer, right hand, left hand). Binding magnitude was comparable within each session, indicating that outcome predictability did not modulate intentional binding. ***(C)*** The hand used to report the action-tone interval did not systematically influence judgement errors, nor did it interact with the response hand. ***(D)*** Mean judgment error (ms) as a function of base interval (200, 400, and 800 ms) and response hand (computer, right hand, left hand). Intentional binding increases with longer action-outcome intervals.

2B. Cognitive Control (CC)

A linear mixed-effects model examined control ratings as a function of congruency, outcome probability, session, responding hand, reporting hand, and base interval (with a random intercept for participant). Key predicted effects are summarized in **Table 4A-2**.

Canonical SoA Effects

There was a main effect of congruency, $F(2, 21976) = 3.45$, $p = .03$. Control ratings were numerically highest for congruent trials ($M = 5.9$, $SD = 2.26$), followed by semi-congruent ($M = 5.85$, $SD = 2.25$), and incongruent trials ($M = 5.84$, $SD = 2.25$). Pairwise comparisons, however, revealed that only the congruent vs. semi-congruent contrast was statistically significant ($p = 0.03$, $d = 0.043$), and this was a very small effect. Incongruent trials did not differ from semi-congruent trials ($p = .98$) or from congruent trials ($p = .1$). Thus, the flanker manipulation did not robustly modulate explicit control ratings (**Fig. 4A-4A**), despite successfully inducing graded response conflict as indexed by RTs.

There was no significant main effect of outcome probability, $F(1, 21976) = 0.03$, $p = .85$ (**Fig. 4A-4B**). Control ratings did not differ between expected ($M = 5.79$, $SD = 2.24$) and unexpected outcomes ($M = 5.95$, $SD = 2.26$). There was also no interaction between congruency and outcome, $F(2,21976) = 1.9$, $p = .14$. Together, these findings suggest that the canonical prospective (congruency) and retrospective (outcome) signals of SoA were not robustly reflected in explicit control judgements in this task.

Session Effects

There was a small but significant main effect of session, $F(1, 21982) = 42.47$, $p < .001$. People reported a slightly higher sense of control in Session 1 ($M = 5.86$, $SD = 2.3$) than in Session 2 ($M = 5.85$, $SD = 2.1$; $d = 0.10$). There was no interaction between session and congruency, $F(2,21976) = 1.17$, $p = .3$, or between session and outcome, $F(1,21979) = 1.42$, $p = 0.23$.

Lateralization Effects

Contrary to our predictions, both response hand, $F(1,21976) = 79.2$, $p < .001$, and report hand, $F(1,21976) = 61.6$, $p < .001$, had significant main effects. Participants reported higher control ratings when pressing the button with their right hand ($M = 5.99$, $SD = 2.20$) than their left hand ($M = 5.72$, $SD = 2.20$; $d = 0.13$; **Fig. 4A-4A**), and when using their right hand to move the slider ($M = 5.96$, $SD = 2.26$) compared to their left hand ($M = 5.75$, $SD = 2.23$; $d = 0.12$; **Fig. 4A-4C**). Response hand did not interact with congruency, $F(2,21976) =$

0.6, p = .53, suggesting that irrespective of whether it was congruent, semi-congruent or incongruent, people reported higher sense of control when they used their right hand (**Fig. 4A-4A**); but it did interact with outcome, F(1,21976) = 4.6, p = .03. The difference between response hand (i.e., control ratings following right hand button press being greater than the left hand) was larger for expected outcomes (right: M = 5.95, left: M = 5.63, p < .001, d = 0.16) and reduced for unexpected outcomes (right: M = 6.05, left: M = 5.86, p < .001, d = 0.10).

Base Interval Effects

Base interval had a large significant main effect, F(2,21976 = 2078, p < .001. People reported a higher sense of control when the tone followed their action after a short delay compared to longer delays (**Fig. 4A-4D**). Control ratings were the highest for the 200 ms base interval (M = 6.72, SD = 1.98), followed by the 400 ms (M = 5.99, SD = 2.00) and 800 ms base interval (M = 4.86, SD = 2.30). All pairwise comparisons were significant (all ps < .001), with a moderate difference between 200 and 400 ms (d = 0.45), a large difference between 200 and 800 ms (d = 1.17), and a moderate-to-large difference between 400 and 800 ms (d = 0.72). Base interval interacted with response hand, F(2, 21976) = 6.2, p = .002. The difference between right- and left-hand responses increased as the action-outcome delay lengthened, with higher control ratings for right-hand responses at all intervals. This difference was small at 200 ms (M right hand = 6.82, SD = 1.93; M left hand = 6.63, SD = 2.04; d = 0.07, p = .009), larger at 400 ms (M right hand = 6.11, SD = 2.00; M left hand = 5.88, SD = 2.06; d = 0.14, p < .001), and largest at 800 ms (M right hand = 5.04, SD = 2.32; M left hand = 4.70, SD = 2.30; d = 0.20, p < .001).

Table 4A-2. Fixed Effects of the Linear Mixed Model for Control Ratings

Effect	**Contrast**	***b***	***95% CI***	***p***
Intercept		5.95	[5.45- 6.46]	**<.001**
Congruency	Incongruent vs. Congruent	-0.07	[-0.13, -0.00]	**.043**
	Semi-congruent vs. Congruent	-0.07	[-0.12, -0.02]	**.011**
Outcome	High vs. Low	-0.00	[-0.05, 0.04]	.853
Session	1 vs. 2	-0.16	[-0.21, -0.11]	**<.001**
Response hand	Left vs. Right	-0.21	[-0.26, -0.17]	**<.001**
Report hand	Left vs. Right	-0.19	[-0.24, -0.14]	**<.001**
Base interval	400 vs. 200	-0.72	[-0.78, -0.67]	**<.001**
	800 vs. 200	-1.88	[-1.94, -1.83]	**<.001**
Outcome x Congruency	High vs. Low x Incongruent vs. Congruent	0.02	[-0.11, 0.14]	.785
	High vs. Low x Semi-congruent vs. Congruent	0.10	[-0.01, 0.20]	.082
Session x Congruency	1 vs. 2 x Incongruent vs. Congruent	-0.02	[-0.14, 0.11]	.804
	1 vs. 2 x Semi-congruent vs. Congruent	0.06	[-0.05, 0.17]	.271
Session x Outcome	1 vs. 2 x High vs. Low	0.06	[-0.04, 0.15]	.232
Response hand x Report hand	Left vs. Right x Left vs. Right	0.01	[-0.09, 0.10]	.880
Response hand x	Left vs. Right x Incongruent vs. Congruent	-0.04	[-0.16, 0.09]	.581
Congruency	Left vs. Right x Semi-congruent vs. Congruent	0.03	[-0.08, 0.13]	.633
Response hand x Outcome	Left vs. Right x High vs. Low	-0.10	[-0.20, -0.01]	**.032**
Report hand x	Left vs. Right x Incongruent vs. Congruent	-0.05	[-0.17, 0.08]	.464
Congruency	Left vs. Right x Semi-congruent vs. Congruent	0.03	[-0.08, 0.14]	.554
Report hand x Outcome	Left vs. Right x High vs. Low	0.03	[-0.06, 0.13]	.506
Response hand x	Left vs. Right x 400 vs. 200	-0.11	[-0.22, 0.01]	.064

Base interval	Left vs. Right x 800 vs. 200	-0.21	[-0.32, -0.09]	**<.001**

Note. b = regression coefficient (estimate), *CI* = confidence interval

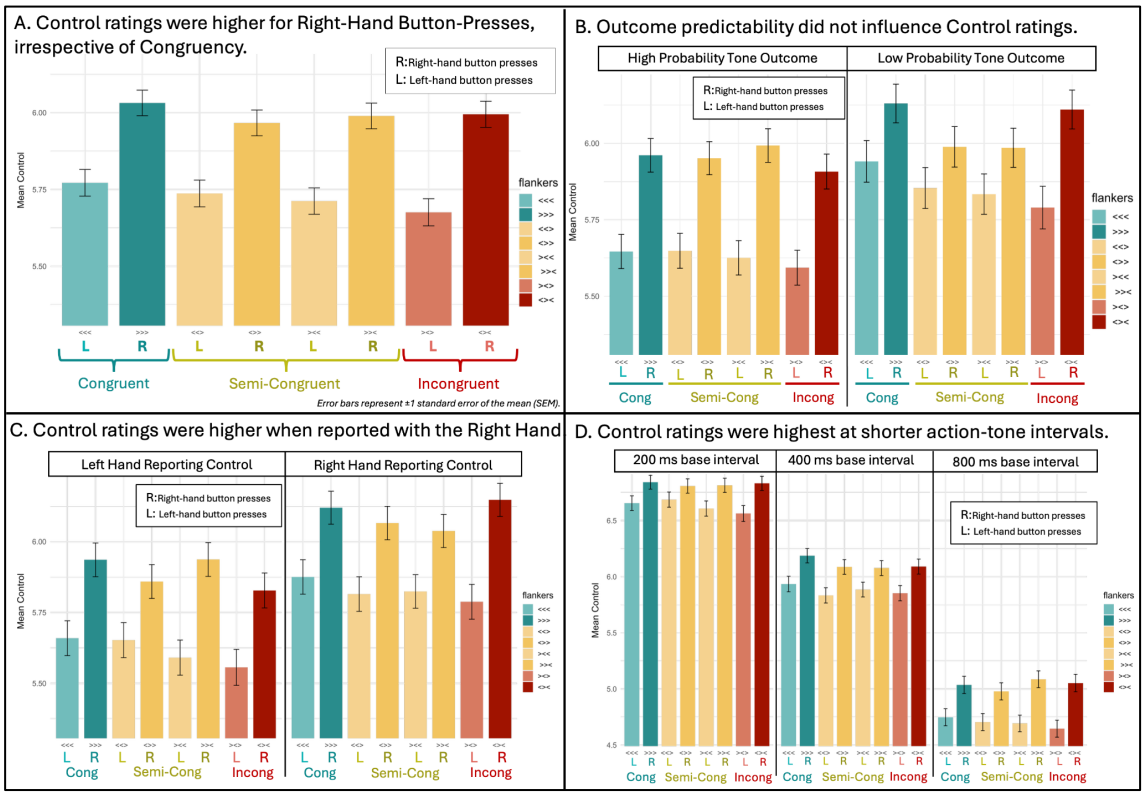


Figure 4A-4. Explicit SoA (Cognitive Control Task) Effects. ***(A)*** Mean control ratings as a function of congruency (congruent, semi-congruent, incongruent) and response hand (L: left-hand button press, R: right-hand button press). Right-hand button presses were associated with higher control ratings across all congruency conditions. Congruency did not systematically modulate control ratings, suggesting that congruency had little effect on control ratings. Error bars represent +-1 SEM. ***(B)*** Mean control ratings by high (70%) and low (30%) tone outcome probability, flanker congruency and response hand (L/R). Tone outcome predictability did not influence control-ratings. ***(C)*** Mean control ratings by the reporting hand, congruency and response hand. Control ratings were higher overall when reported with the right hand. This pattern was consistent across congruency conditions and response hands. ***(D)*** Mean control ratings by base interval between action-tone, congruency and response hand. Control ratings were highest at the shortest interval (200 ms) and declined with longer action-tone intervals. This interval effect was consistent across congruency conditions and response hands.

3. Individual stability of IB and CC effects over time

To assess test-retest stability of SoA-related effects, we tested whether individual differences (i.e., individual deviations from the group-level fixed effect estimate for that effect) were consistent per person across sessions. In other words, for example, whether a person showing a high positive random slope in Session 1 would also show a high positive random slope in Session 2.

For the IB task, despite the group-level attenuation of binding in Session 2, individual differences in binding were significantly correlated across sessions for both right-hand binding (defined as the difference between right-hand and computer-generated actions; r(25) = .53, p = .004), and left-hand binding (r(25) = .49, p = .009). Participants who showed stronger (or weaker) binding in Session 1 tended to show correspondingly stronger (or weaker) binding in Session 2, suggesting that individual differences in intentional binding effects are stable across sessions (**Fig. 4A-5A**).

For the CC task, individual differences in congruency sensitivity were not reliably correlated across sessions. This was the case for both the semi-congruent vs. congruent contrast, r(25) = .31, p = .11, and the incongruent vs. congruent contrast, r(25) = .16, p = .41 (**Fig. 4A-5B**). These null results likely reflect the weak and unreliable group-level congruency effect, which left little systematic variation across individuals to correlate across sessions.

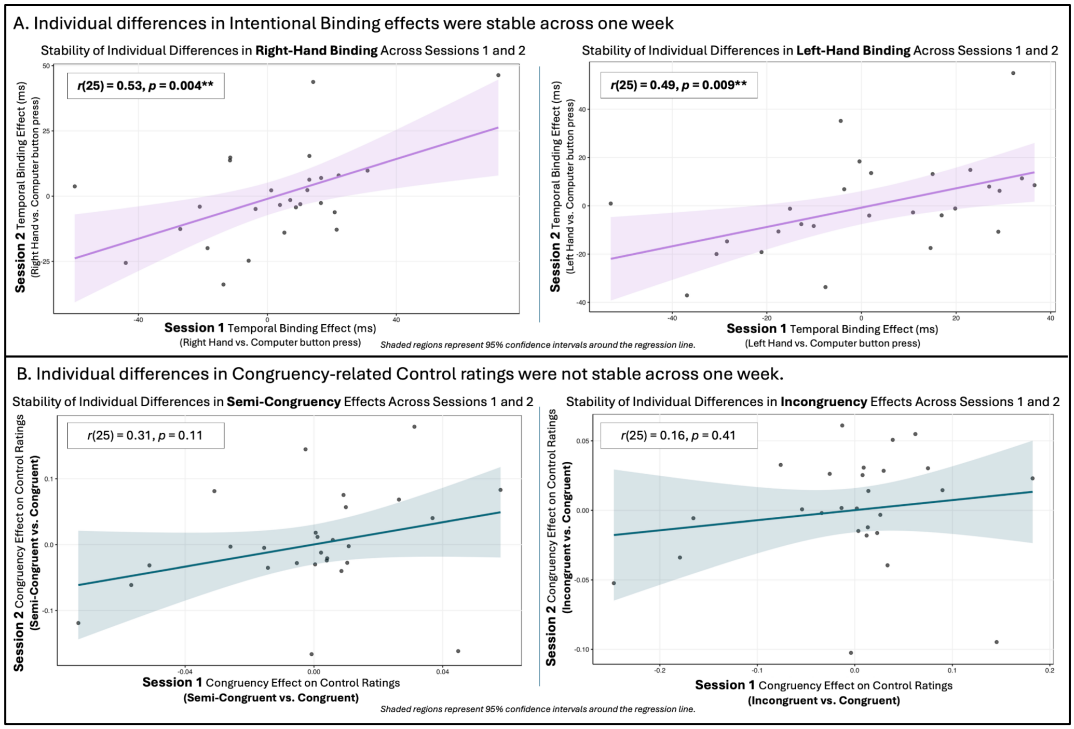


Figure 4A-5. Stability of Individual Differences in SoA-related Effects across One Week. ***(A)*** Stability of individual differences in intentional binding across Sessions 1 and 2, shown separately for right-hand and left-hand binding effects (each calculated relative to the computer button-press baseline). Both correlations were statistically significant indicating that individual differences in intentional binding were moderately stable over a one-week interval. Shaded regions represent 95% confidence intervals around the regression line. ***(B)*** Stability of individual differences in congruency-related effects on control ratings across session, shown separately for semi-congruent and incongruent flanker effects, each expressed relative to the congruent condition. Neither correlation reached

significance indicating that individual differences in how congruency influenced control ratings were not reliably stable across one week. Shaded regions represent 95% confidence intervals around the regression line.

4. Cross-Task Correlations Between IB and CC

We examined whether individual differences in SoA-related effects are related across paradigms, by testing whether participant-specific slopes from the IB and CC tasks were correlated within each session. In other words, whether individuals who showed stronger intentional binding also showed greater sensitivity to congruency manipulations in the CC task. Overall, results showed that there was no association between the SoA-related effects in IB and CC (see **Table 4A-3**).

Table 4A-3. Correlations Between Congruency Effects (CC) and Intentional Binding Effects (IB) Across Sessions

	Session 1		Session 2	
	(CC)Incongruent vs. Congruent	(CC)Semi-congruent vs. Congruent	(CC)Incongruent vs. Congruent	(CC)Semi-congruent vs. Congruent
(IB) Left hand binding (Left hand vs. Computer)	$r(25) = 0.39$, $p = 0.04$	$r(25) = 0.35$, $p = 0.07$	$r(25) = 0.04$, $p = 0.81$	$r(25) = -0.07$, $p = 0.70$
(IB) Right hand binding (Left hand vs. Computer)	$r(25) = 0.29$, $p = 0.13$	$r(25) = 0.24$, $p = 0.21$	$r(25) = -0.06$, $p = 0.74$	$r(25) = -0.14$, $p = 0.45$

* $p < .05$. IB: Intentional Binding Task, CC: Cognitive Control Task

Because congruency effects on control ratings were weak overall, whereas response hand (i.e., the hand used to press the button) showed a reliable effect where participants reported a higher sense of control following right- compared to left-hand actions), we examined whether individual differences in the response-hand effects in the CC task (right vs. left hand) were related to individual differences in left- or right-hand binding in the IB task. In other words, we tested whether participants who showed larger left–right differences in control ratings also showed stronger left- or right-hand differences in intentional binding. None of the pairs were significant in either session (all ps > .05; see **Table 4A-4**), suggesting that hand-related effects did not relate to each other across the IB and CC paradigms

Table 4A-4

Correlations of Response-Hand Effects (hand used to press the button) Across Tasks and Sessions

	Session 1	Session 2
	(CC) Left vs Right Hand	(CC) Left vs Right Hand
(IB) Left hand binding (Left hand vs. Computer)	$r(25) = 0.28, p = 0.15$	$r(25) = 0.20, p = 0.30$
(IB) Right hand binding (Left hand vs. Computer)	$r(25) = 0.22, p = 0.24$	$r(25) = -0.10, p = 0.61$

IB: Intentional Binding Task, CC: Cognitive Control Task

5. Discussion

This study presents the first investigation of lateralized implicit and explicit SoA paradigms in healthy participants, developing and evaluating tools designed for subsequent use with split-brain patients. We examined three questions: whether lateralized versions of the intentional binding (IB) and cognitive control (CC) paradigms reproduce canonical SoA effects, whether individual differences in SoA are stable over time, and whether implicit and explicit SoA measures correlate within individuals. Results were mixed. The IB paradigm partially replicated canonical effects: binding was stronger for left- than right-hand actions and was markedly attenuated in the second session. The CC paradigm showed only a minimal congruency effect, with control ratings not reliably shaped by flanker-induced response conflict. Outcome predictability did not modulate either measure. Individual differences in IB showed moderate cross-session stability, whereas CC individual differences did not. Finally, implicit and explicit measures were not correlated across individuals. We discuss the theoretical and methodological implications of these findings.

Intentional Binding is larger for left-hand actions and attenuates across sessions

The IB paradigm successfully replicated the canonical intentional binding effect in Session 1: participants underestimated action-outcome intervals more following self-generated actions than computer-generated ones. However, two patterns emerged: First, binding was stronger for left- than right-hand actions. Second, the binding effect disappeared for right-hand actions in Session 2 and was substantially attenuated for left-hand actions. These findings likely reflect the indirect nature of intentional binding as a measure of SoA. Intentional binding is fundamentally a time estimation task, and it is unclear how much of it genuinely reflects SoA versus perceptual or motor confounds. Several studies argued that the

binding effects could stem from procedural differences between active and passive conditions, rather than differences in intentionality, or sense of agency.

The hand difference observed here may relate to such procedural or motor-related confounds. The larger binding observed for left-hand actions is unlikely to reflect higher SoA when using the left-hand. Instead, it probably means that people were less accurate at estimating the interval following left-hand button presses compared to right-hand button presses. Nearly all participants in our sample were right-handed. Dominant-hand actions may be timed more accurately than non-dominant ones. This interpretation could relate to the work in embodied cognition suggesting that people perform certain perceptual estimations more accurately when using their dominant rather than their non-dominant hand.

However, because most of our participants were right-handed (all but two), any handedness-related interpretation remains speculative. Notably, the two left-handed participants did not show statistical differences between response hands—but nevertheless showed a numerically similar pattern: larger binding for left- than right-hand responses (see **Appendix Table S4A-1**). Given that we only had two left-handed participants, this observation does not provide a reliable basis for conclusions about the role of handedness.

The attenuation of binding in the second session suggests that temporal estimation improved with practice, washing out the binding effect, particularly for right-hand actions. This is a potential limitation of the paradigm: with repeated exposure, IB may lose its sensitivity as a measure of SoA. Alternatively, this may also reflect a limitation of the current study: with repetition, the task may have gradually shifted from an intentional action paradigm toward a more stimulus-response habit. Although participants were instructed to take their time and press the button "whenever they wanted," after many trials across two sessions, participants may have begun pressing the button immediately after seeing the lateralized cue, making the task more habitual stimulus-response in nature. One solution would be to introduce choice within each cued hand. Instead of mapping each cue directly to a single button press (e.g., LVF cue -> left-hand index finger; RVF cue -> right-hand index finger, see **Fig 4A-2B**), participants could be given two response options per hand and allowed to choose which button to press. This would reduce the fixed stimulus-response mapping and could help maintain an agential component throughout the task.

Explicit control ratings were not robustly modulated by congruency manipulation

Previous studies have shown that disruptions in action selection fluency (a prospective signal), induced by response conflict via incongruent vs. congruent flankers, modulate explicit SoA judgments (Wenke et al., 2010; Chambon, & Haggard, 2012). In our study, we couldn't robustly replicate this finding. The congruency effect was weak and unreliable, despite evidence that our flanker manipulation successfully induced graded levels of response conflict (as confirmed by the RT differences: incongruent > semi-congruent > congruent), yet this did not translate into control ratings.

One potential reason could be the ambiguity of the explicit SoA tasks. Explicit SoA measures have been criticized for ambiguity in what participants understand by "control". To better understand people's introspections about these SoA tasks, at the end of final session, we administered a survey with open-ended questions probing their introspections about the task, including what they based their control judgments on when moving the slider. Most reported relying primarily on timing of the tone—specifically, how quickly the tone followed their action (see **Appendix Table S4A-2** for raw responses). This is reflected in the large, robust effect of base interval on control ratings: shorter delays yielded substantially higher ratings.

One factor participants did not mention, but that strongly influenced control ratings, was the response hand. Control ratings were consistently higher for right- than left-hand button presses. One possibility is that the motoric fluency of the dominant hand could be projected onto the control ratings. However, as noted above, any handedness-related interpretation remains speculative given the limited number of left-handed participants in our sample.

Outcome predictability did not influence SoA-related measures

Prior work suggests that expected or positive outcomes are associated with greater SoA measures compared to unexpected or negative outcomes. We did not observe such effects here. One possible explanation could be a limitation of our experiments: participants may not have been sufficiently motivated to attend to the outcome tone probabilities. As a result, our "outcome predictability" manipulation may not have effectively engaged expectations about outcomes, instead functioning more as passive exposure to one tone occurring more frequently

than the other, without requiring any predictions about them. This limitation is discussed in the limitation section.

Individual Differences in Intentional Binding Are Stable Over One Week

Despite group-level attenuation of binding across sessions, individual differences in IB showed moderate stability across the sessions. Participants who showed stronger binding in Session 1 tended to maintain relatively stronger binding in Session 2. This moderate test-retest reliability is notable and practically important: it suggests that individual differences in intentional binding, even as overall levels change, are somewhat stable at the within-person level. This is particularly relevant for clinical applications where patients can be tested across multiple sessions (due to practical constraints such as patient fatigue or availability) to accumulate sufficient trial numbers.

In contrast, individual differences in CC congruency sensitivity showed no evidence of cross-session stability. This null result likely reflects the weak effect of the congruency manipulation on control ratings at the group level. In other words, there was little systematic variation in control ratings as a function of congruency to begin with, so, assessing any meaningful individual differences across sessions might be constrained by this lack of (or very weak) signal.

Implicit and Explicit SoA Measures Are Uncorrelated at the Individual Level

There were no cross-task correlations between implicit (IB) and explicit (CC) SoA tasks. This could suggest that the two SoA paradigms tap into distinct underlying processes. Alternatively, this may also reflect the limited sensitivity of our tasks, especially the CC task, where no reliable differences were observed in control ratings as a function of congruency.

Implications for Split-Brain Research

The primary motivation for this study was to develop and validate lateralized SoA paradigms for future application to split-brain patients. The lateralization manipulation—independently varying which hand generates the action, and which hand makes the SoA judgment—creates uncrossed (same hemisphere for both action and SoA judgment) and crossed conditions (different hemispheres). In healthy people, because the hemispheres are connected, uncrossed and crossed conditions should not differ. Consistent with this prediction, there was no interaction between response hand and reporting hand in either paradigm (i.e. no

crossed-uncrossed difference). In split-brain patients, this crossed vs. uncrossed manipulation becomes a powerful experimental lever.

For the IB paradigm, one can ask whether crossed trials (i.e. the hemisphere making the temporal judgment did not generate the action) produce binding comparable to uncrossed trials, or instead, whether they resemble computer-generated trials, suggesting that binding requires prospective signals from within the same hemisphere.

For the CC paradigm, crossed and uncrossed trials would allow us to ask whether control ratings differ depending on which hemisphere generates the action and makes the control judgment. Semi-congruent trials can be particularly informative here: they create situations where the acting and non-acting hemispheres simultaneously receive different congruency information, allowing us to test whether control judgments depend solely on signals available to the acting hemisphere or whether the state of the disconnected, non-acting hemisphere can still influence the control ratings. Finally, comparing uncrossed left- and uncrossed right-hemisphere trials would reveal whether the two hemispheres differ in how they weight prospective signals (action selection fluency, manipulated via flanker congruency) versus retrospective signals (outcome predictability). However, the weak and inconsistent effects of the congruency and outcome probability manipulations means that the CC paradigm requires substantial refinement before it can serve as a reliable tool in split-brain research. We discuss potential refinements for both tasks below.

Limitations and Future Directions

Several limitations of the current study may account for the unexpected findings; addressing them in future work could strengthen SoA-related effects and enhance the suitability of these paradigms for split-brain application.

1. Action-outcome interval. The range and distribution of base intervals warrant refinement in both paradigms. In the IB task, the interval distribution (200, 400, and 800 ms) did not align well with the response distribution (100-1000 ms slider), and 200 ms may be too short to meaningfully elicit binding effect. A more balanced interval and response space, for example anchoring participants to 100 ms and 900 ms as endpoints on the slider, could improve the sensitivity of binding effects. And in the CC task, the wide range of base intervals produced such a strong effect on control ratings that it can likely obscure the subtler influence

of congruency. Reducing interval variability could create more room for congruency effects to emerge.

2. Retrospective signals: outcome predictability. The tone outcome predictability manipulation may have been too passive to effectively engage participants as a retrospective SoA cue. In this study, participants had no reason to pay attention to different tone outcomes. In the future, the outcome manipulation could be strengthened by introducing incentives, or making them more behaviorally relevant, thereby encouraging participants to form and use expectations about different outcome types.

3. Prospective signals: action selection. Both paradigms could benefit from stronger manipulations of the action selection component of SoA. For the IB task, as noted above, people may have gradually shifted toward a more habitual stimulus–response mode, contributing to the attenuation of the binding effect over time. Introducing within-hand response choice (e.g., allowing participants to freely select between two buttons, after a hand is cued) could help maintain the intentional component of action selection and preserve binding effects over time. In the CC task, although flankers successfully induced response conflict—as evidenced by RT differences—this did not reliably translate into control ratings. The conflict manipulation may simply not have been strong enough to influence explicit SoA judgments. The flanker (and hence action selection fluency) manipulation can be strengthen by increasing the salience of the flankers, or alternatively using priming paradigms (e.g., Wenke et al., 2010).

4. Lateralization manipulation. Finally, an alternative lateralized design worth exploring would lateralize not the action and judgment hands, but the action and outcome hands. In other words, administering an outcome (such as a tactile stimulus) to the same or opposite hand as the one that generated the action. This 2x2 design (acting hand x outcome hand) would produce crossed and uncrossed conditions that more directly map onto prospective and retrospective contributions to SoA and may offer a cleaner window into hemispheric contributions to SoA formation.

Conclusion

This study introduces and evaluates lateralized implicit and explicit SoA paradigms in healthy participants, providing a methodological foundation for investigating hemispheric contributions SoA. The IB paradigm replicated intentional binding in Session 1, though effects

were asymmetric across hands and attenuated substantially across sessions. The CC paradigm showed only minimal sensitivity to the intended SoA manipulations in its current form. Importantly, individual differences in IB showed moderate test-retest reliability over one week, an encouraging result for multi-session patient-testing. Implicit and explicit measures were uncorrelated across individuals, though this null finding could also reflect the weak effects observed in CC. Taken together, these findings highlight both the promise and the challenges of applying lateralized SoA paradigms to split-brain patients. With targeted design improvements—particularly strengthening prospective and retrospective manipulations and refining action-outcome intervals—these paradigms can illuminate how the two hemispheres contribute to and integrate prospective and retrospective signals in the formation of SoA. Beyond split-brain research, such findings may inform our understanding of how SoA is formed in the intact brain and shed light on conditions where SoA is disrupted.

B. A DIVIDED VISUAL FIELD ADAPTATION OF THE MENTAL IMAGERY FMRI PARADIGM

Collaborators:

Tyler Santander, Emma Kates-Harbeck, Lukas J. Volz, Michael B. Miller

1. Abstract

Mental imagery tasks in fMRI, such as imagining playing tennis or navigating through one's home, have been used to detect volitional brain activity, hence of consciousness, in non-communicative patients with severe brain injury. Spatial navigation and motor imagery were shown to be the most robust paradigms for this purpose. Building on this established approach, we developed a lateralized adaptation specifically designed for future investigation of split-brain patients whose disconnected hemispheres offer a rare experimental window into the nature of consciousness. In this task, we replaced auditory cues with lateralized visual stimuli to probe the content of the imagery. A tennis racket or a house image was flashed for 150 ms to either the left or right visual field, followed by an imagery period requiring sustained motor (tennis) or spatial navigation (house) imagery. As a validation step, we scanned 24 neurologically healthy participants to determine whether this modified paradigm reliably evokes activity in expected brain regions of interest. Here we present results from this validation study in healthy controls, showing expected activation patterns within canonical regions of interest during motor and spatial imagery. However, the extent of these effects varied across participants and visual field conditions. This approach opens an exciting avenue for probing conscious awareness in the divided brain by investigating whether a lateralized cue can effectively engage the contralateral hemisphere in the mental imagery task and whether the disconnected hemispheres will correlate in their activation patterns for the same probe.

Keywords: mental imagery, split-brain, consciousness, motor imagery, lateralization

2. Introduction

How can we detect conscious awareness in the absence of any behavioral output?

Assessing consciousness in non-communicative brain-injured patients is difficult because we currently lack a full understanding of the neural correlates of consciousness. However, mental imagery fMRI paradigms have offered a powerful way to approach this problem by testing whether patients can willfully modulate their brain activity in response to task instructions. In a seminal study, Owen and colleagues showed that when non-communicative patients were asked to imagine playing tennis (motor imagery) or navigating through their homes (spatial imagery), they exhibited task-specific brain activation patterns similar to those of healthy controls: tennis imagery engaged the supplementary motor area (SMA), while house navigation imagery engaged the Parahippocampal place area (PPA) . This voluntary, task-dependent modulation of brain activity provided evidence of conscious awareness in patients who appeared entirely unresponsive . And spatial and motor imagery are shown to be the most robust paradigms for this purpose (Boly et al., 2007).

Extending this approach to split-brain patients.

We wanted to adapt this paradigm for a different population: split-brain patients. Split-brain patients are individuals whose cerebral hemispheres have been surgically disconnected to treat intractable epilepsy. An unresolved question concerns the nature of their consciousness, specifically, whether they have a unified conscious experience, two separate conscious experiences, or something in between (Bayne, 2008; de Haan et al., 2020; Schechter, 2012; Schechter & Bayne, 2021; Volz & Gazzaniga, 2017). Resolving this question has broader implications because it can inform theories of consciousness and how consciousness arises in intact brains (Ferrante et al., 2025; Koch et al., 2016; Mashour et al., 2020; Tononi et al., 2025).

Assessing consciousness in split-brain patients is, however, difficult. Behavioral studies using lateralized testing procedures have shown that each hemisphere can independently perceive, process, and respond to stimuli without the other being aware (Gazzaniga et al., 1962), suggesting a disruption of unified consciousness, or even the presence of “two minds in one skull”. Yet, other studies have failed to replicate these effects, arguing that these disruptions are not as evident (Pinto, Neville, et al., 2017; Sergent, 1986). Part of this difficulty likely stems from the compensatory mechanisms that split-brain patients

develop. Despite dramatic disconnection effects observed under well-controlled lateralized testing conditions, these patients appear largely unchanged and behaviorally "unified" in everyday life. Several mechanisms may contribute to this apparent unity. For example, cross-cueing (subtle bodily signals) can allow one hemisphere to indirectly communicate with the other; intact subcortical pathways, such as the superior colliculus, may enable one hemisphere to orient gaze in ways that provide informative cues to the other; ipsilateral control of proximal muscles allows each hemisphere to retain some influence over gross limb movements on both sides of the body, helping guide behavior (Volz et al., 2018; Volz & Gazzaniga, 2017). Together, these mechanisms may allow the hemispheres to anticipate and coordinate actions without direct callosal communication, giving rise to an "apparent motor unity."

Additionally, the left-hemisphere interpreter hypothesis may further contribute to this apparent unity. According to this hypothesis, the left hemisphere does not merely produce speech, but it actively constructs coherent, plausible narratives to account for behavior (Gazzaniga, 2000). We observed a striking example of this in our German cohort: one patient verbally offered a series of seemingly reasonable explanations, such as having visual impairments, for why she was unable to perform a task with her right hand (controlled by the speaking left hemisphere). Yet her left hand, controlled by the mute right hemisphere, completed the same task perfectly, revealing that no such visual impairment existed (Bekir et al., 2025). Her speaking left hemisphere's confabulations were so convincing that they nearly led the experimenter to terminate the task. These confabulations, generated by the speaking left hemisphere, may mask the underlying disconnections, making behavior appear more unified and intentional than it actually is. Together, these factors suggest that relying on overt behavior alone presents challenges for testing the nature of consciousness in split-brain patients.

The fMRI mental imagery paradigm can offer a way around these limitations. By providing a neural readout of volitional, task-specific brain activity in the absence of overt behavior, it can serve as a promising complementary tool for examining conscious awareness in each hemisphere independently, and for asking whether it is unified or dissociable across hemispheres.

Lateralized Mental Imagery fMRI paradigm

To make the mental imagery paradigm suitable for split-brain testing, we made three key modifications to the classic tennis/house mental imagery fMRI paradigm:

First, we replaced auditory instructions with lateralized visual cues. In the classic mental imagery paradigm, task instructions are delivered auditorily. However, this would make them available to both hemispheres, which is not suitable for split-brain testing, where the goal is to cue each hemisphere independently. We instead adapted the paradigm into a divided visual field design (Bourne, 2006), in which a tennis racket or house image was briefly flashed to either the left or right visual field to cue the imagery content. Because lateralized visual stimuli are initially processed by the contralateral hemisphere, this allows us to cue each hemisphere independently for motor or spatial imagery. Crucially, in addition to unilateral presentations, this divided visual field design also permits bilateral presentations, in which imagery cues can be delivered to both hemispheres simultaneously. These bilateral trials can either be congruent—both visual fields, hence both hemispheres, receiving the same cue—or incongruent, with one hemisphere cued to imagine playing tennis while the other is cued to imagine navigating through their house. In split-brain patients, incongruent trials can provide a critical test of whether the two hemispheres can simultaneously engage distinct, stimulus-specific activation patterns within their respective regions of interest (ROIs).

Second, we introduced explicit "no cue" ("nothing") trials to serve as baseline rest condition. The classic paradigm alternates between imagery and rest periods in a block design, where each imagery period (tennis or house) is followed by a rest period. We initially adopted this imagery-rest block design. However, piloting the task in a split-brain patient revealed a critical limitation of this design when testing the disconnected hemispheres: Following the scanning session, the patient (i.e. his speaking left hemisphere) reported that on some trials he did not see any cue and assumed he had simply missed it. As a result, he said he switched back and forth between tennis and house imagery. Given the lateralized design, this likely occurred on left visual field trials, where the cue was presented to the mute right hemisphere and was therefore not accessible to the speaking left hemisphere. As a result, the left hemisphere—unaware that the right hemisphere had received the cue—thought it had simply missed it, didn't know what to do, and switched back and forth between the two imageries. This kind of uncontrolled switching introduces a fundamental interpretational problem as the fMRI signal

would no longer reflect a stable imagery content (e.g., sustained tennis or house imagery). To prevent this, instead of using imagery-rest blocks, we used three types of cue trials: tennis, house, and—critically—explicit "no cue" ("nothing") trials. On these "nothing" trials, we instructed participants to *not* imagine tennis or house. By explicitly instructing participants that some trials would contain no cue, each hemisphere received a clear behavioral directive: if no cue is perceived—whether due to an actual "nothing" trial or (for split-brain patients) because the stimulus was presented to the opposite hemisphere—*do not* engage in any motor or spatial imagery. This way, the "nothing" trials served not only as a baseline rest condition but also as a better control over each hemisphere's imagery content.

Third, we also collected bimanual responses at the end of each imagery period. Each hand, hence, hemisphere, reported independently (via button presses) which cue they saw: tennis, house, or nothing. This addition is critical for split-brain testing, where it becomes possible to examine dissociations between brain activation patterns and reportability, for example, whether a hemisphere would show SMA activation following a tennis cue presented to the opposite visual field, yet fails to explicitly report having seen the tennis cue.

Before applying this modified paradigm to split-brain patients, we aimed to establish that the key modifications we have made to the task still reliably evoke the expected imagery-related brain activation patterns in neurologically healthy participants. Specifically, we asked whether divided visual field cues, replacing the classic auditory instructions, still reliably evoke the imagery-specific activation patterns—greater SMA activation following tennis cues and greater PPA activation following house cues—and whether the explicit "no cue" trials effectively served as a reliable baseline rest condition, replacing traditional rest blocks, such that contrasting imagery against those "no cue" trials would robustly evoke the predicted activation patterns (e.g., tennis > nothing, analogous to the classic tennis > rest, reliably engaging SMA). To this end, we scanned 24 right-handed healthy adults while they completed our modified mental imagery task. We predicted that tennis cue trials (tennis>nothing and tennis>house contrasts) would elicit greater activation in SMA, and house cue trials (house>nothing, house>tennis contrasts) would elicit greater activation in PPA, replicating the canonical imagery-specific patterns of the original paradigm. Critically, in neurologically healthy participants, we predicted no difference in activation patterns as a function of which visual field the cue was presented to. In other words, in intact brains, it should not matter

whether participants saw the tennis or house cue on the left or right of the screen, they should engage in the respective imagery regardless of where the cue was flashed.

3. Methods

Participants

Twenty-seven right-handed people participated in this study. All of them reported normal or corrected-to-normal vision and did not report neurologic conditions. Procedures were approved by the UCSB Institutional Review Board (#42-24-0824). All subjects gave written informed consent before participating and were compensated for their time ($20/h for scanning sessions, $10/h for behavioral familiarization/training). Three participants were excluded due to falling asleep or poor fixation compliance, which caused the gaze-contingent task to stall, and hence the task was aborted early. The final sample consisted of 24 participants (M_{age} = 22.7 years, SD_{age} = 8.5, 17 female).

Stimuli and Procedure

Participants completed a 15-minute training session on a separate day prior to their scanning session to ensure that their gaze could be reliably detected by the eye tracker, and to familiarize them with the task instructions and gaze-contingent procedure. In the scanning session, we scanned participants for a single 1.5-hour period that included the mental imagery task (approximately 30 minutes), as well as additional scans acquired for a separate study.

Stimuli were presented using PsychoPy, version 2022.2.5 (Peirce et al., 2019). During the fMRI session, visual stimuli were rear-projected onto a screen positioned 110 cm from the participant's eyes at the head of the scanner bore, using a contrast-linearized 32'' widescreen LCD display (1920x1080, 60 Hz refresh rate). During the training session, stimuli were presented on a Mac Mini HP 22uh 22.5'' monitor (1920x1080, 60 Hz refresh rate, WLED backlight), with participants seated 93 cm from the monitor and their heads were stabilized using a chinrest. Eye movements were recorded in both sessions using an EyeLink Plus 1000 Desktop eye tracker (SR Research Ltd, n.d.). Stimuli were presented on a neutral gray background (hex #808080) with a central fixation cross (subtending 1 x 1 visual angle degree). Target images were presented 4 visual angle degrees to the left or right of fixation (from the center of the screen to the inner edge of the tennis or house image). Both house and tennis stimuli subtended 5 x 5 visual angle degrees.

Mental Imagery task. Participants completed a mental imagery task where they were asked to imagine either playing tennis or navigating through their house. Before the task began, participants were presented with the following instructions and given time to form mental imageries for tennis and house: *"please take a moment to create mental imagery for TENNIS and HOUSE. For TENNIS: Imagine standing still on a tennis court and swing your arm to 'hit the ball' back and forth. For HOUSE: Imagine walking from room to room in your home and visualize all that you would 'see' if you were there."*. Participants were also informed that on some trials no image would be presented and were instructed as follows: *"sometimes NO IMAGE will be shown. If you see NOTHING, please just REST and DO NOT think about tennis or house"*. Following the instruction phase, participants completed the task. Each trial began with a central fixation cross presented for 1 sec, plus a randomly selected gaze-contingent period of 100-150 ms, during which participants were required to maintain central fixation before the stimulus could appear. A stimulus was then presented for 150 ms in one of three visual field conditions: left visual field (LVF), right visual field (RVF), or bilaterally (BVF). The stimulus was either a tennis racket (motor imagery cue), a house (spatial imagery cue), or no stimulus (baseline rest condition). Following stimulus offset, participants were given 12 s mental imagery period where they were asked to imagine playing tennis (if they saw the tennis image), navigating through their home (if they saw the house image), or resting without engaging in any motor or spatial imagery (if they saw nothing) (**see Fig. 4B-1**). In BVF trials, the two stimuli could be either congruent (tennis image in both visual fields) or incongruent (tennis in one visual field and house in the other, or vice versa). Only one congruent type was included (tennis-tennis rather than both tennis-tennis and house-house) to reduce the total number of trials and minimize scan duration (particularly important for future patient testing), while still permitting a congruent-versus-incongruent comparison. For incongruent BVF trials, healthy participants were instructed to select one stimulus to imagine and to alternate their choice across repetitions. The incongruent trials are of particular interest for future split-brain testing, where they would allow us to ask whether the disconnected hemispheres can simultaneously engage distinct, stimulus-specific patterns of activation within their respective ROIs. At the end of each imagery period, participants reported which image they saw (and hence what they imagined) using a two-button response: one key for tennis, one for house, and no response if no stimulus had appeared. Responses

were made bimanually to allow simultaneous and independent reporting from each hand, which is critical for future split-brain testing, where dissociations between brain activation patterns and reportability can be examined. Each condition–Tennis vs. House by VF (LVF, RVF, BVF)--was presented 5 times (5 trials per condition), along with 7 baseline ("nothing") trials, yielding a total of 42 trials. Trial order and inter-trial interval (ITI) jitters were pseudo-randomized using the easy-optimize-x MATLAB toolbox to maximize design efficiency (Spunt, n.d.).

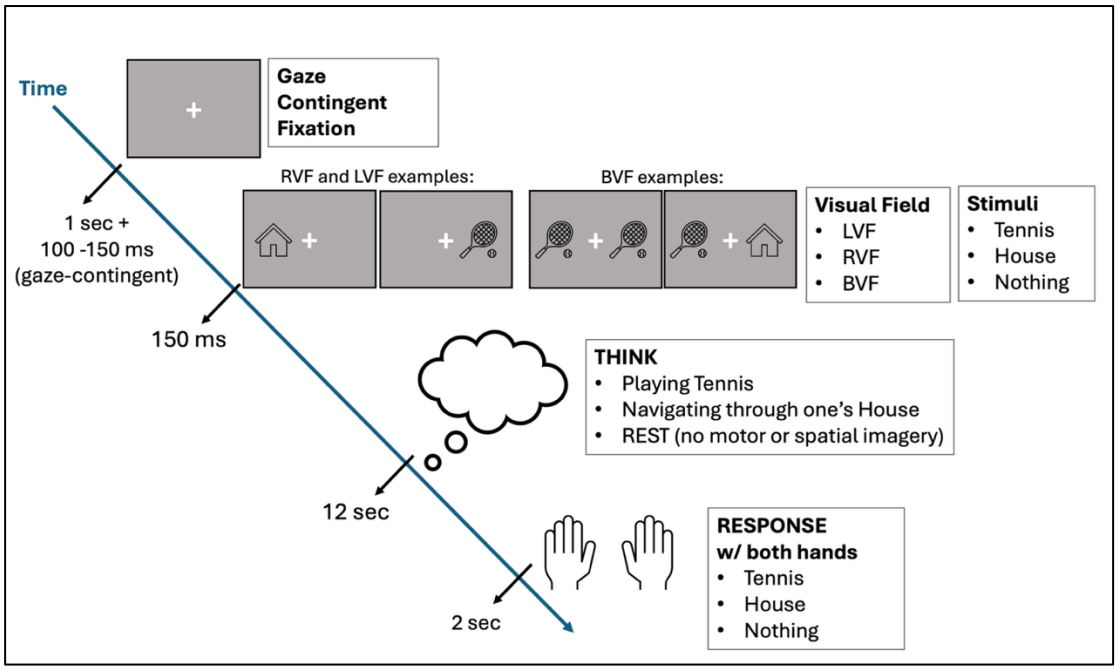


Figure 4B-1. Mental Imagery Task. Each trial began with a gaze-contingent fixation cross (1 s + 100-150 ms jitter), followed by a 150 ms stimulus presentation. Stimuli (tennis racket, house, or nothing) were presented in the left visual field (LVF), right visual field (RVF), or bilaterally (BVF). BVF trials could be congruent (tennis-tennis) or incongruent (tennis-house or house-tennis). Participants then engaged in a 12 s mental imagery period — imagining playing tennis (motor imagery), navigating through their home (spatial imagery), or resting without engaging in any imagery (baseline). At the end of each trial, participants had 2 s to report their response bimanually: one hand for tennis, the other for house, or no response for nothing trials.

MRI Acquisition

MRI data were collected on a 3T Siemens Prisma scanner using a 64-channel head coil. T1-weighted anatomical images were acquired using a 3D MPRAGE sequence (TR = 2.5 s, TE = 2.31 ms, TI = 934 ms, flip angle = 7°, FOV = 256 mm, voxel size = 0.8 mm isotropic, GRAPPA acceleration factor = 2). Functional images were acquired using a single shot echo-planar imaging (EPI) sequence (TR = 2 s; TE = 30 ms, FA = 90°, voxel size = 3 x 3 x 3.5 mm, GRAPPA acceleration factor = 2; phase encoding: anterior-posterior). And the gradient-echo

(GRE) field map was acquired with two echos (TE1 = 4.92 ms, TE2 = 7.38 ms), TR = 400 ms, flip angle = 60°, slice thickness = 3 mm, spacing between slices = 3.51 mm.

fMRI preprocessing

Preprocessing is performed using fMRIPrep 25.0.0 (Esteban et al., 2019),which is based on Nipype 1.9.2 (Gorgolewski et al., 2011).

Anatomical data preprocessing

The T1w image was corrected for intensity non-uniformity (INU) with N4BiasFieldCorrection (Tustison et al., 2010), distributed with ANTs 2.5.4 (Avants et al., 2008) (RRID:SCR_004757), and used as T1w-reference throughout the workflow. The T1w-reference was then skull-stripped with a Nipype implementation of the antsBrainExtraction.sh workflow (from ANTs), using OASIS30ANTs as target template. Brain tissue segmentation of cerebrospinal fluid (CSF), white-matter (WM) and gray-matter (GM) was performed on the brain-extracted T1w using fast (FSL (version unknown), RRID:SCR_002823, (Zhang et al., 2001). Brain surfaces were reconstructed using recon-all (FreeSurfer 7.3.2, RRID:SCR_001847) (Dale et al., 1999), and the brain mask estimated previously was refined with a custom variation of the method to reconcile ANTs-derived and FreeSurfer-derived segmentations of the cortical gray-matter of Mindboggle (RRID:SCR_002438) (Klein et al., 2017). Volume-based spatial normalization to the standard space (MNI152NLin6Asym) was performed through nonlinear registration with antsRegistration (ANTs 2.5.4), using brain-extracted versions of both T1w reference and the T1w template. The following templates were selected for spatial normalization and accessed with TemplateFlow (24.2.2), (Ciric et al., 2022): FSL's MNI ICBM 152 non-linear 6th Generation Asymmetric Average Brain Stereotaxic Registration Model (Evans et al., 2012) [RRID:SCR_002823; TemplateFlow ID: MNI152NLin6Asym]

Functional data preprocessing

First, a reference volume was generated, using a custom methodology of fMRIPrep, for use in head motion correction. Head-motion parameters with respect to the BOLD reference (transformation matrices, and six corresponding rotation and translation parameters) are estimated before any spatiotemporal filtering using mcflirt (FSL)

(Jenkinson et al., 2002). The estimated fieldmap was then aligned with rigid-registration to the target EPI (echo-planar imaging) reference run. The field coefficients were mapped on to the reference EPI using the transform. The BOLD reference was then co-registered to the T1w reference using bbregister (FreeSurfer) which implements boundary-based registration (Greve & Fischl, 2009). Co-registration was configured with six degrees of freedom. Several confounding time-series were calculated based on the preprocessed BOLD: framewise displacement (FD), DVARS and three region-wise global signals. FD was computed using two formulations following Power (absolute sum of relative motions) (Power et al., 2014) and Jenkinson (relative root mean square displacement between affines) (Jenkinson et al., 2002). FD and DVARS are calculated for each functional run, both using their implementations in Nipype, following the definitions by Power et al. (Power et al., 2014). The three global signals are extracted within the CSF, the WM, and the whole-brain masks. Additionally, a set of physiological regressors were extracted to allow for component-based noise correction (CompCor) (Behzadi et al., 2007). Principal components are estimated after high-pass filtering the preprocessed BOLD time-series (using a discrete cosine filter with 128s cut-off) for the two CompCor variants: temporal (tCompCor) and anatomical (aCompCor). tCompCor components are then calculated from the top 2% variable voxels within the brain mask. For aCompCor, three probabilistic masks (CSF, WM and combined CSF+WM) are generated in anatomical space. The implementation differs from that of Behzadi et al. in that instead of eroding the masks by 2 pixels on BOLD space, a mask of pixels that likely contain a volume fraction of GM is subtracted from the aCompCor masks. This mask is obtained by dilating a GM mask extracted from the FreeSurfer's aseg segmentation, and it ensures components are not extracted from voxels containing a minimal fraction of GM. Finally, these masks are resampled into BOLD space and binarized by thresholding at 0.99 (as in the original implementation). Components are also calculated separately within the WM and CSF masks. For each CompCor decomposition, the k components with the largest singular values are retained, such that the retained components' time series are sufficient to explain 50 percent of variance across the nuisance mask (CSF, WM, combined, or temporal). The remaining

components are dropped from consideration. The head-motion estimates calculated in the correction step were also placed within the corresponding confounds file. The confound time series derived from head motion estimates and global signals were expanded with the inclusion of temporal derivatives and quadratic terms for each (Satterthwaite et al., 2013). Frames that exceeded a threshold of 0.5 mm FD or 1.5 standardized DVARS were annotated as motion outliers. Additional nuisance timeseries are calculated by means of principal components analysis of the signal found within a thin band (crown) of voxels around the edge of the brain, as proposed by (Patriat et al., 2017). All resamplings can be performed with a single interpolation step by composing all the pertinent transformations (i.e. head-motion transform matrices, susceptibility distortion correction when available, and co-registrations to anatomical and output spaces). Gridded (volumetric) resamplings were performed using nitransforms, configured with cubic B-spline interpolation. Many internal operations of fMRIPrep use Nilearn 0.11.1 (Abraham et al., 2014) (RRID:SCR_001362), mostly within the functional processing workflow.

fMRI First-level modeling and ROI analysis

First level modeling. First level GLM analyses were conducted in SPM25 (Tierney et al., 2025). Functional images were spatially smoothed using a 6 mm FWHM Gaussian kernel prior to model estimation. Each condition was modeled as a separate regressor: BVF-tennis (congruent), BVF-tennis(LVF)/house(RVF) (incongruent), BVF-house(LVF)/tennis(RVF) (incongruent), LVF-house, LVF-tennis, RVF-house, RVF-tennis, and Nothing (baseline), convolved with the canonical hemodynamic response function (HRF) without temporal or dispersion derivatives. A high-pass filter of 128 s was applied, and temporal autocorrelation was modeled using the FAST method. Nuisance regressors included the six rigid-body motion parameters (three translations, three rotations), mean white matter signal, mean CSF signal, non-steady-state volumes, and motion spike regressors identified during fMRIPrep preprocessing. The GLM was estimated using SPM's Restricted Maximum Likelihood (ReML) estimation procedure. A quantitative summary of participant head motion is provided in **Appendix Table 4B-1.**

ROI Definition and Signal Extraction. Regions of interest (ROIs), including the supplementary motor area (SMA) and parahippocampal place area (PPA), which are

classically implicated in motor and spatial imagery (Owen et al., 2006), respectively, were defined using two complementary approaches.

First, anatomical ROIs for both SMA and PPA were derived from the Harvard-Oxford Cortical Probabilistic Atlas (Lateralized) (HOCPAL) (RRID: SCR_001476, n.d.). However, because the HOCPAL SMA parcel was relatively large and likely encompassed regions beyond the SMA (**Fig. 4B-2A**), we additionally defined a more focal, functionally derived SMA ROI using Neurosynth's (Yarkoni et al., 2011) meta-analytic map for the term "motor-imagery" (https://neurosynth.org/analyses/terms/motor%20imagery/). The peak activation coordinate from this map was identified, and a 5 mm radius spherical ROI was constructed around it. As this peak fell in the left hemisphere, a right SMA ROI was obtained by mirror-imaging the coordinate across the midline (see **Fig. 4B-2A**). The HOCPAL SMA did not reliably distinguish tennis from house contrasts and exhibited substantial house-related activation, likely due to its broader spatial extent (see **Fig. 4B-2B**). Therefore, all subsequent statistical analyses focus on the Neurosynth-defined SMA. For all ROIs, mean parameter estimates were extracted per contrast per participant using FSL's fslstats (Jenkinson et al., 2012).

In a complementary approach we charactered each individuals' SMA peak activation location during tennis imagery. A 7 mm spherical ROI, providing a broader region constraint, centered on the same Neurosynth-derived peak coordinate was used. Then, similarly, a mirror-imaged counterpart was created for the right SMA. Because these two 7 mm spherical ROIs overlapped near the midline, hemispheric masks were applied to restrict each ROI to its respective hemisphere, yielding non-overlapping left and right SMA ROIs. Peak coordinates from these ROI masks were then extracted in MNI space and shown for each participant (see **Table 4B-2**).

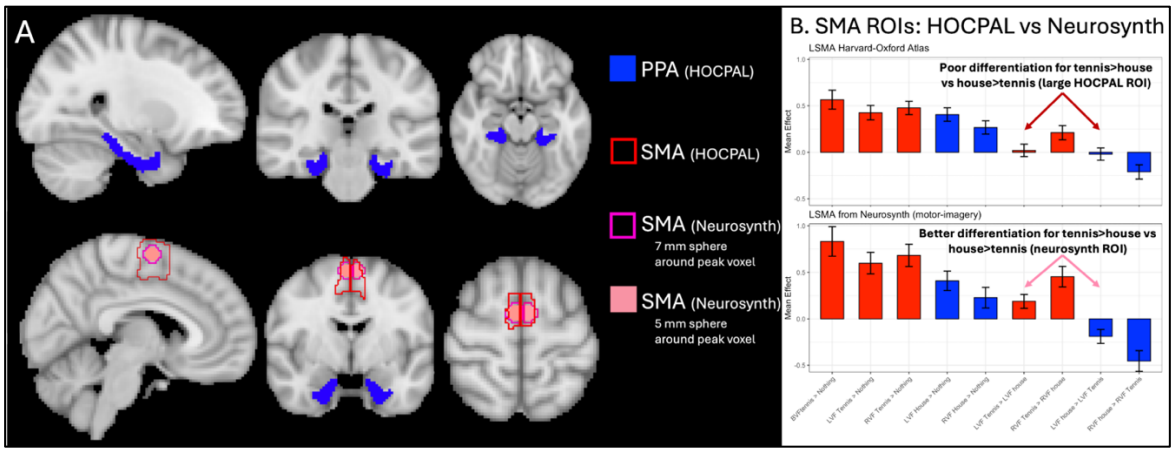


Figure 4B-2. Region of Interest (ROI) Definitions and Comparison of SMA ROIs. ***(A).*** Locations of ROIs are shown on a standard MNI brain. The Parahippocampal place area (PPA; blue) was defined using the Harvard-Oxford Cortical Probabilistic Atlas (Lateralized) (HOCPAL). The supplementary motor area (SMA) was defined using three approaches: using HOCPAL (red outline), a 7 mm sphere centered on the Neurosynth-derived peak motor-imagery coordinate (magenta outline), and a 5 mm sphere centered on the same coordinate (pink fill). The larger 7 mm Neurosynth sphere was used to identify each participant's individual peak SMA activation voxel during tennis imagery; the MNI peak coordinates from this boundary is shown in **Table 4B-2**. ***(B).*** Mean effects across Tennis and House contrasts for the left SMA (LSMA), separately for the HOCPAL-derived ROI (top) and the Neurosynth-derived ROI (bottom). Red bars indicate tennis imagery conditions; blue bars indicate house imagery conditions. The larger HOCPAL anatomical ROI showed poor differentiation between tennis > house contrasts (top, red arrows). In contrast, the functionally defined motor-imagery Neurosynth ROI (5 mm sphere around the peak voxel) showed better separation between these conditions (bottom, pink arrows) and was therefore used in all subsequent analyses.

ROI Analysis

In this study, we aimed to determine whether this lateralized version of the tennis/house mental imagery fMRI task elicited the expected patterns of activation in SMA and PPA ROIs in healthy participants. To this end, incongruent conditions were not included in the analyses. Instead, we focused on contrasts comparing tennis and house imagery conditions to rest (tennis > nothing(rest); house > nothing(rest)) and to each other (tennis > house; house > tennis), computed separately for each visual field presentation condition (e.g., RVF tennis > nothing; RVF tennis > RVF house). ROI-level parameter estimates were analyzed in R (R Core Team, 2021) to validate that this modified and lateralized version of the task engaged expected imagery-related regions. One-sample t-tests (against zero) were conducted on mean parameter estimates within each ROI for the key contrasts of interest (Tennis> contrasts for SMA and House> contrasts for PPA), to confirm above-baseline activation during imagery. A double dissociation between ROI and imagery type (greater tennis-related activation in SMA; greater house-related activation in PPA) would provide validation that the task successfully

recruited canonical motor and spatial imagery network. We report both uncorrected *p*-values ($p < .05$) and false discovery rate (FDR)-adjusted *p*-values, along with effect sizes (Cohen's d) (**Table 4B-1; Fig. 4B-3**).

Next, given the intended application of this paradigm in split-brain patients–where single-subject interpretability is critical–we assessed how many participants exhibited the expected activation patterns. For each participant, we examined whether the expected pattern of task-specific activation was present in each ROI and visual field (VF) condition. Specifically, for motor imagery we tested whether the tennis > house contrast produced activation above zero (>0) in left and right SMA (LSMA, RSMA), separately for each VF presentation (e.g., LVF tennis > LVF house, RVF tennis > RVF house). For spatial imagery, we tested whether the house > tennis contrasts produced activation above zero in left and right PPA (LPPA, RPPA), again for each VF. Each cell was coded 1 if the expected activation pattern was observed, and 0 if not. To summarize individual differences in these activation patterns, we categorized each participant based on how many 0s (failure to show the expected activation pattern) they had across the eight ROI x VF combinations. Participants who showed fully expected activation patterns (all 1s) were labeled as "fully expected". Those with only one zero were labeled as "mostly expected," indicating that the majority of contrast-ROI pairings showed the expected activation patterns. When only one visual field condition showed the expected activation pattern while the other did not, participants were labeled as showing a "VF difference" (e.g., LVF tennis engaging both L-SMA and R-SMA, while RVF tennis did not). A "modality difference" was assigned when one imagery type recruited its ROI regardless of VF condition (e.g., tennis contrasts engaging SMAs, while house contrasts did not engage PPAs). Participants who did not fit any of these categories and were labeled "mixed". The individual activation patterns are summarized in **Fig 4B-4**.

Finally, we report each participant's peak activation (MNI coordinates) for tennis>rest contrasts within a 7 mm Neurosynth SMA ROI (**Table 4B-2**).

4. Results

Activation patterns show imagery-specific engagement of SMA and PPA

One-sample t-tests were conducted on mean parameter estimates within each ROI to confirm that the lateralized mental imagery task engaged the expected canonical regions. Full results are reported in **Table 4B-1**. Overall, tennis imagery produced greater activation than house

imagery in SMA; whereas house imagery produced greater activation than tennis in PPA, confirming the predicted double dissociation between imagery type and region of interest (**Fig. 4B-3**).

For SMA ROIs, tennis imagery (cued with a LVF, RVF or BVF prompt) produced above-baseline activations in both the left and right SMA (all FDR-adjusted *p*s ≤ .006; Cohen's ds = 0.66-1.17). In contrast, house imagery generally did not engage SMA (except for the LVF House > Rest contrast in the left SMA, $t(23) = 3.93$, $p < .001$ (FDR-adjusted $p = .002$); all other house contrasts were insignificant (all *p*s ≥ .050)). Notably, Left SMA exhibited larger effect sizes for tennis imagery than Right SMA (Cohen's ds: 1.05-1.17 vs. 0.66-0.79). This hemispheric asymmetry may reflect the right-handedness of the sample and the lateralized motor demands of the imagery task where participants were asked to imagine hitting a ball with a racket (using their dominant hands). This is addressed in the Discussion.

In the PPA, the opposite pattern was observed. House imagery (cued via LVF or RVF house image) produced significant above-baseline activation in both left and right PPA (all FDR-adjusted *p*s ≤ .020), whereas tennis imagery did not elicit significant activation (all *p*s ≥ .453).

Taken together, these results suggest that briefly presenting a lateralized tennis or house cue (150 ms) effectively elicits motor or spatial imagery and engage the SMA and PPA, respectively, consistent with findings from classical paradigms using auditory instructions (Boly et al., 2007; Monti et al., 2010; Owen et al., 2006).

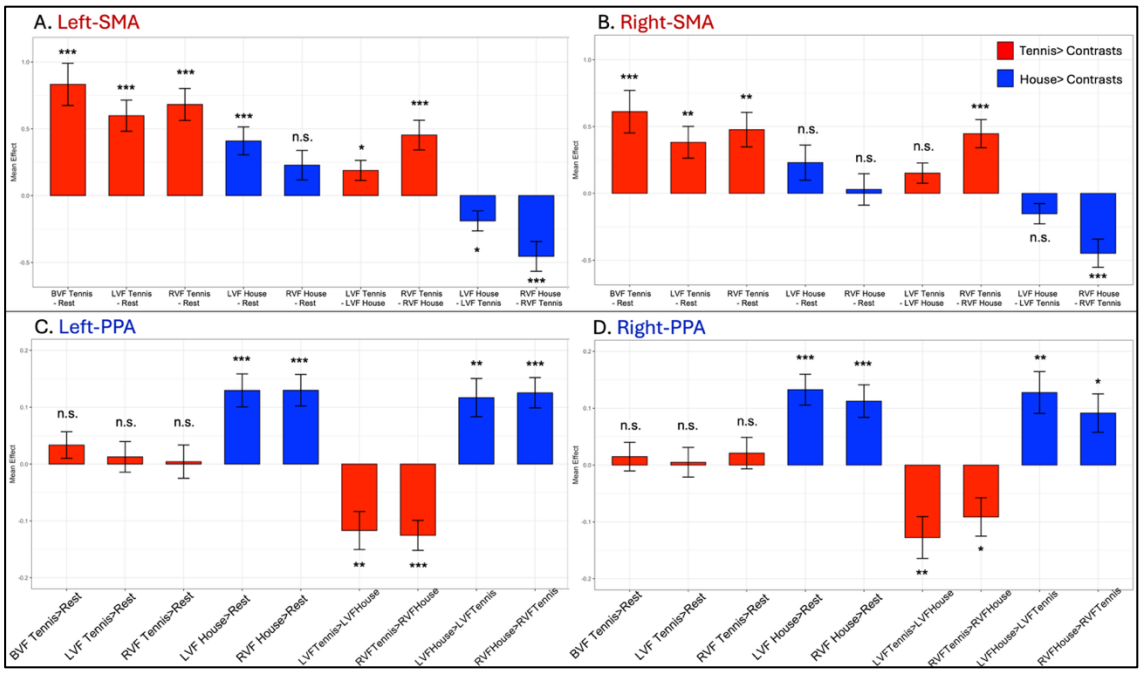


Figure 4B-3. Region of Interest (ROI) activation patterns for lateralized mental imagery task. Mean effect sizes (beta weights) are shown for four ROIs: (A) Left Supplementary Motor Area (Left-SMA), (B) Right Supplementary Motor Area (Right-SMA), (C) Left Parahippocampal Place Area (Left-PPA), and (D) Right Parahippocampal Place Area (Right-PPA). Red bars represent motor imagery contrasts (e.g., Tennis>Rest, Tennis>House) and blue bars represent spatial imagery contrasts (e.g., House>Rest, House>Tennis). Contrasts are displayed separately for each visual field condition (LVF, RVF, BVF) and include comparisons against baseline (e.g., Tennis > Rest, House > Rest) as well as direct contrasts between imagery conditions (e.g., Tennis > House, House > Tennis). BVF = Bilateral Visual Field; LVF = Left Visual Field; RVF = Right Visual Field. Error bars represent standard error of the mean. Significance markers indicate one-sample t-tests against zero (* $p < .05$, ** $p < .01$, *** $p < .001$, uncorrected; n.s. = not significant). SMA showed greater activation for tennis (motor imagery) than house conditions, whereas PPA showed greater activation for house (spatial imagery) than tennis conditions, demonstrating a double dissociation between ROI and imagery type. The final four contrasts in each panel (i.e., Tennis > House and House > Tennis) are redundant—each pair reflects the same comparison with reversed sign— but are plotted separately for completeness and to facilitate visual interpretation in both directions.

Table 4B-1

One-sample t-tests of mean ROI effects against zero

Contrast	*M*	*SD*	*t*	*p*	*p adjusted*	*Cohen's d*
Right SMA						
BVF Tennis > Rest	0.612	0.779	3.85	**< .001** ***	.002	0.79
LVF Tennis > Rest	0.383	0.580	3.23	**.004** **	.006	0.66
RVF Tennis > Rest	0.477	0.632	3.70	**.001** **	.003	0.76
LVF House > Rest	0.231	0.645	1.75	.093	.116	0.36
RVF House > Rest	0.030	0.577	0.25	.802	.849	0.05
LVF Tennis > LVF house	0.152	0.369	2.02	.055	.071	0.41

RVF Tennis > RVF house	0.447	0.514	4.26	< **.001** ***	.001	0.87
Left SMA						
BVF Tennis > Rest	0.833	0.774	5.27	**< .001** ***	< .001	1.08
LVF Tennis > Rest	0.599	0.568	5.16	**< .001** ***	< .001	1.05
RVF Tennis > Rest	0.683	0.586	5.71	**< .001** ***	< .001	1.17
LVF House > Rest	0.410	0.512	3.93	**< .001** ***	.002	0.80
RVF House > Rest	0.229	0.542	2.07	.050	.070	0.42
LVF Tennis > LVF House	0.189	0.366	2.53	**.019** *	.027	0.52
RVF Tennis > RVF House	0.454	0.542	4.10	**< .001** ***	.001	0.84
Right PPA						
BVF Tennis > Rest	0.015	0.123	0.59	.558	.628	0.12
LVF Tennis > Rest	0.005	0.128	0.19	.851	.875	0.04
RVF Tennis > Rest	0.021	0.136	0.76	.453	.526	0.16
LVF House > Rest	0.133	0.133	4.88	**< .001** ***	< .001	1.00
RVF House > Rest	0.113	0.140	3.94	**< .001** ***	.002	0.80
LVF House > LVF Tennis	0.128	0.180	3.47	**.002** **	.004	0.71
RVF House > RVF Tennis	0.091	0.165	2.71	**.012** *	.020	0.55
Left PPA						
BVF Tennis > Rest	0.034	0.115	1.43	.165	.198	0.29
LVF Tennis > Rest	0.013	0.132	0.47	.640	.698	0.10
RVF Tennis > Rest	0.004	0.143	0.15	.880	.880	0.03
LVF House > Rest	0.130	0.142	4.46	**< .001** ***	< .001	0.91
RVF House > Rest	0.130	0.136	4.67	**< .001** ***	< .001	0.95
LVF House > LVF Tennis	0.117	0.164	3.49	**.002** **	.004	0.71
RVF House > RVF Tennis	0.125	0.130	4.73	**< .001** ***	< .001	0.97

Note. *M* = mean effect size; *SD* = standard deviation; *p* = uncorrected two-tailed *p*-value; *p adjusted* = FDR-adjusted *p*-value; Cohen's *d* = mean/SD. All tests are one-sample *t*-tests against zero (df = 23, n = 24). BVF = bilateral visual field; LVF = left visual field; RVF = right visual field. SMA = Supplementary Motor Area; PPA = Parahippocampal Place Area; *$p < .05$. **$p < .01$. ***$p < .001$. For cross-category contrasts, only one direction is reported per ROI: Tennis > House for SMA and House > Tennis for PPA regions, as the opposing contrasts are sign-reversed equivalents conveying no additional information.

Individual differences in activation patterns

At the single-subject level, we observed some variability in the extent to which participants exhibited the expected task-specific activation patterns across ROIs and visual field (VF)

conditions (**Fig. 4B-4**). Of the 24 participants, 7 (29.1%) exhibited fully expected activation patterns across all ROI x VF combinations, showing reliable tennis > house activation in both Left SMA and Right SMA, and house > tennis activation in both Left PPA and Right PPA for both LVF and RVF presentations. Three participants (12.5%) showed mostly expected patterns, with only a single ROI x VF combination failing to show the expected activation. 9 participants (37.5%) showed a VF difference, in which the expected contrast was present for one VF presentation but not the other—either the LVF or RVF condition failing to engage the relevant ROIs. This pattern was observed both for motor imagery (SMA) and spatial imagery (PPA). 4 participants (16.6%) showed a modality difference, where one imagery type reliably recruited its ROI across VF conditions while the other did not; notably, three of these participants showed expected SMA activation for motor imagery but no PPA activation for spatial imagery, while one participant showed the opposite pattern. Finally, 1 participant did not fit any of these categories and was labeled as mixed, reflecting an inconsistent pattern of activation across both VFs and modalities. Together, these results indicate that while the expected double dissociation between motor imagery–SMA and spatial imagery–PPA can be observed at the group level, its expression at the individual level is variable, with participants showing selective deviations driven by visual field presentation condition or imagery modality. When considering each imagery modality-ROI independently (i.e. considering SMA-tennis and PPA-house separately), 14 of 24 participants (58.3%) showed the expected tennis > house activation across all SMA x VF combinations, and 13 of 24 (54.2%) showed the expected house > tennis activation across all PPA x VF combinations. These findings suggest that, at the individual level, the lateralized imagery paradigm engaged canonical motor and spatial imagery networks in over half of participants.

	Left-SMA		Right-SMA		Left-PPA		Right-PPA	
	tennis > house		tennis > house		house>tennis		house>tennis	
sub	LVF	RVF	LVF	RVF	LVF	RVF	LVF	RVF
	Fully expected patterns of activation across all VF and ROIs, n = 7, 29.1% of participants							
1	1	1	1	1	1	1	1	1
9	1	1	1	1	1	1	1	1
11	1	1	1	1	1	1	1	1
16	1	1	1	1	1	1	1	1
21	1	1	1	1	1	1	1	1
27	1	1	1	1	1	1	1	1
29	1	1	1	1	1	1	1	1
	Mostly expected patterns (all but one specific VF-ROI), n = 3, 12.5% of participants							
4	1	1	0	1	1	1	1	1
15	0	1	1	1	1	1	1	1
20	1	1	1	1	1	1	1	0
	VF difference (one VF condition not engaging either the left or right ROI), n = 9, 37.5%							
2	0	1	0	1	1	1	1	1
8	0	1	0	1	1	1	1	1
10	0	1	0	1	1	1	1	0
25	0	1	0	1	1	0	1	1
12	1	0	1	0	1	1	1	1
30	1	0	1	0	1	1	1	1
18	1	1	1	1	0	1	0	1
22	1	1	1	1	0	1	0	1
28	1	1	1	1	0	1	0	1
	Modality difference (one imagery type not recruiting its ROI, while the other did), n = 4, 16.6%							
3	1	1	1	1	0	1	0	0
7	1	1	1	1	0	1	0	0
24	1	1	1	1	0	0	0	0
19	0	0	0	0	1	1	0	1
	Mixed (does not clearly fit into one category), n = 1, 4%							
13	0	1	1	0	1	0	1	0

Figure 4B-4. Figure 4B-4. Individual activation patterns across regions of interest (ROIs) and visual field (VF) conditions. Each row represents a single participant (sub), and each column represents one of eight ROI x VF combinations: left and right Supplementary Motor Area (LSMA, RSMA) for the motor imagery contrasts (tennis > house), and left and right Parahippocampal Place Area (LPPA, RPPA) for the spatial imagery contrasts (house > tennis), separately for left (LVF) and right (RVF) visual field presentations. Cells are coded green (1) if the expected activation pattern was observed (contrast > 0) and red (0) if not. Participants are grouped into five categories based on their overall pattern of results: fully expected (all 1s; n = 7, 29.1%), mostly expected (one deviation; n = 3, 12.5%), VF difference (one VF condition failing to engage either ROI; n = 9, 37.5%), modality difference (one imagery type failing to recruit its ROI regardless of VF; n = 4, 16.6%), and mixed (n = 1, 4%). Finally, when considered independently by ROI (examining 1s and 0s within SMA and PPA columns separately), 14 of 24 participants (58.3%) showed the expected tennis > house activation across all four SMA x VF combinations (i.e., all 1s in the Left-SMA and Right-SMA columns), and 13 of 24 (54.2%) showed the expected house > tennis activation across all four PPA × VF combinations (i.e., all 1s in the Left-PPA and Right-PPA columns).

Individual peak SMA activation during tennis imagery in MNI space

Finally, we extracted each participant's peak activation coordinate, in MNI space, within left and right SMA ROIs for the tennis > rest contrast across all three VF conditions (BVF, LVF,

RVF; **Table 4B-2**). We hypothesized that, in healthy controls, the spatial location of the briefly presented tennis cue (150 ms; LVF, RVF, or BVF) should not influence the content of the motor imagery. Hence, peak SMA activation locations were expected to be spatially consistent across BVF, LVF, and RVF conditions. Consistent with this, we observed that mean peak coordinates were highly similar across BVF (-5, -4, 63), LVF (-5.5, -4.8, 63), and RVF (-5, -4, 64) in LSMA and in RSMA: BVF (4, -4, 65), LVF (5, -4, 65), and RVF (4, -3, 66).

Table 4B-2

Individual and Mean Peak SMA Activation Coordinates (MNI) for Tennis > Nothing Contrast

Participant	**L-SMA**			**R-SMA**		
	x	*y*	*z*	*x*	*y*	*z*
BVF Tennis > Rest						
sub-01	-10	-2	66	2	0	66
sub-02	-2	-6	58	6	2	62
sub-03	-6	-6	58	6	0	68
sub-04	-4	-2	60	2	-2	64
sub-07	-2	-4	62	8	-8	68
sub-08	-6	-4	64	8	-2	68
sub-09	-10	-6	66	6	-2	68
sub-10	-6	-4	70	6	-4	62
sub-11	-2	0	60	8	-8	64
sub-12	-2	0	60	2	2	66
sub-13	-2	0	60	2	-8	64
sub-15	-2	-8	62	2	-6	60
sub-16	-6	-8	60	2	-8	62
sub-18	-8	-8	68	8	-8	68
sub-19	-6	-2	58	2	-2	58
sub-20	-4	-6	66	2	-8	68
sub-21	-2	0	60	2	0	60
sub-22	-6	-10	66	2	-6	66
sub-24	-4	-10	66	2	-10	64
sub-25	-4	2	62	2	2	62
sub-27	-2	-2	58	6	-8	66
sub-28	-8	-6	68	2	-2	60
sub-29	-10	-2	66	2	-2	66
sub-30	-6	-2	70	8	0	68
M	**-5.00**	**-4.00**	**63.08**	**4.08**	**-3.67**	**64.50**

SD	**2.77**	**3.39**	**3.96**	**2.60**	**3.90**	**3.13**
LVF Tennis > Rest						
sub-01	-2	-4	70	2	-2	70
sub-02	-2	-6	58	6	2	62
sub-03	-4	-8	60	6	-2	66
sub-04	-4	-2	60	2	-2	68
sub-07	-4	-4	58	8	-8	68
sub-08	-6	-6	68	8	-6	68
sub-09	-10	-6	66	10	-6	66
sub-10	-2	-6	60	4	-6	62
sub-11	-2	-6	68	8	-8	64
sub-12	-4	-2	64	2	-6	60
sub-13	-6	-8	60	8	-8	64
sub-15	-6	-2	58	2	-8	62
sub-16	-4	-8	60	2	-10	64
sub-18	-8	-8	68	6	-6	70
sub-19	-2	-2	58	2	-2	58
sub-20	-10	-6	64	2	2	66
sub-21	-6	-2	58	2	0	60
sub-22	-6	-10	66	2	-6	66
sub-24	-8	-8	66	4	-10	64
sub-25	-8	0	68	8	0	68
sub-27	-10	-6	66	6	-10	62
sub-28	-2	-2	58	2	-2	60
sub-29	-10	-2	66	2	0	66
sub-30	-6	-2	70	8	0	68
M	**-5.50**	**-4.83**	**63.25**	**4.67**	**-4.33**	**64.67**
SD	**2.84**	**2.76**	**4.37**	**2.81**	**3.90**	**3.37**
RVF Tennis > Rest						
sub-01	-10	-2	66	2	-2	70
sub-02	-2	-6	58	6	2	62
sub-03	-4	-8	60	4	-2	66
sub-04	-4	-2	60	2	-2	68
sub-07	-2	-6	58	2	-4	60
sub-08	-6	-8	68	8	-6	68
sub-09	-10	-6	66	8	-8	68
sub-10	-4	-6	70	4	-4	62
sub-11	-2	-6	68	2	-4	68
sub-12	-2	0	60	2	2	66

sub-13	-4	-8	68	6	-6	70
sub-15	-6	-2	58	2	-2	58
sub-16	-6	-8	68	10	-6	66
sub-18	-8	-8	68	2	-4	60
sub-19	-2	-2	58	2	-2	58
sub-20	-6	2	64	2	-8	68
sub-21	-2	0	60	4	-2	70
sub-22	-4	-10	66	2	-6	66
sub-24	-8	-6	68	4	-2	68
sub-25	-4	2	62	6	2	66
sub-27	-10	-6	66	8	-6	68
sub-28	-2	0	60	6	0	62
sub-29	-10	-4	66	6	-4	70
sub-30	-6	-2	70	6	-2	70
M	**-5.17**	**-4.25**	**64.00**	**4.42**	**-3.17**	**65.75**
SD	**2.88**	**3.50**	**4.25**	**2.50**	**2.88**	**3.93**

Note. Coordinates are peak MNI voxel locations within the left and right supplementary motor area (L-SMA and R-SMA) for each participant for the Tennis > Rest contrasts. The L-SMA ROI was defined as a 7 mm sphere centered on the Neurosynth motor imagery meta-analytic peak voxel; the R-SMA ROI was its mirror image across the midline. *M* = mean. *SD* = standard deviation. BVF = bilateral visual field; LVF = left visual field; RVF = right visual field.

5. Discussion

In this study, we aimed to develop and validate a lateralized adaptation of the classic tennis/house mental imagery fMRI paradigm, building on the seminal work of Owen and colleagues (Owen et al., 2006), with the goal of applying it to split-brain patients. We introduced three key modifications to the original design. First, we replaced auditory instructions with brief lateralized visual cues, consistent with divided visual field paradigms (Bourne, 2006). Second, we replaced the "rest" periods from the classic imagery–rest block structure with explicit "no cue" ("nothing") trials that served as a baseline rest condition. Third, we collected bimanual responses at the end of each trial, allowing us to obtain reports from both hemispheres independently. This makes it possible to dissociate brain activity from reportability in disconnected brains, something that will be critical for split-brain testing, but is not the primary focus in this healthy control validation.

At the group level, we observed the expected pattern of imagery-specific activation: motor (tennis) imagery preferentially engaged the SMA while spatial (house) imagery preferentially engaged the PPA, replicating the canonical double dissociation established in

the original paradigm (Owen et al., 2006). One exception was the absence of a significant LVF tennis > LVF house effect in the right SMA. This likely reflects the overall weaker activation profile of the right SMA compared to the left SMA, potentially due to the motor lateralization of the tennis imagery, as participants imagined hitting the racket with their dominant (right) hand, which could engage the left SMA more than the right SMA. This point is further discussed in the limitation section. Overall, these results provide encouraging evidence that our modified mental imagery paradigm largely replicates the predicted effects.

At the individual level, however, the expression of these effects varied. The most unexpected finding was that nine participants showed visual field (VF) differences, where the expected activation was observed for one visual field condition but not the other. These differences are difficult to interpret. In intact brains, the content of the imagery should not depend on whether the cue was briefly presented to the left or right visual field. That is, a participant should engage in the same imagery—e.g., imagining hitting the ball with the racket in the same way—regardless of where the tennis cue appears on the screen. Thus, it is hard to interpret these differences. They likely reflect variability in the reliability of the fMRI signal at the single-subject level. The mental imagery paradigm is not a one-to-one measure of volitional cognition. Prior work has shown that even among patients who can clearly follow verbal instructions, only a subset exhibit the expected imagery-related activation patterns (Bodien et al., 2024). Therefore, individual variability and false negatives are expected. While the variability at the individual level places important constraints on single-subject interpretation, the paradigm reliably captured the expected effects at the group level and in a substantial proportion of individuals, suggesting that it can still be an informative tool to probe conscious awareness in split-brain patients.

Limitations

One limitation of the study concerns the weaker and less consistent activation observed in the right SMA relative to the left. Across all tennis imagery contrasts, the left SMA showed larger effect sizes (Cohen's d = 1.05-1.17) than the right SMA (d = 0.66-0.79), and the right SMA was the only region to produce a non-significant result where significance was predicted (the LVF tennis > LVF house contrast not reaching significance for RSMA). This asymmetry can be related to the inherently lateralized nature of the tennis imagery task. Participants were asked to imagine swinging their arm to hit a ball with a racket: a motor act that evokes imagery

of a right-hand swing and hence likely engaging the contralateral left SMA. Importantly, using the tennis imagery choice was intentional, as we aimed to closely match and extend the original tennis/house mental imagery paradigm . However, for future applications—especially in split-brain research, where hemispheric differences is critical—it may be advantageous to use motor imagery tasks that allow for more controlled and symmetric engagement of the two hemispheres. For example, instructing participants to imagine left- versus right-hand movements (e.g., finger tapping) would provide a more balanced way to selectively engage each hemisphere and help dissociate task-induced lateralization from hemispheric disconnection-related effects.

Conclusion

In sum, we developed and validated a lateralized adaptation of the classic tennis/house mental imagery fMRI paradigm, designed for future application in split-brain research. Our findings show that this modified paradigm replicates the expected SMA–motor and PPA–spatial activation patterns at the group level, with some variability in their expression across individuals, visual field conditions, and imagery type. Despite this variability, the paradigm captured the expected task-specific brain activity in many individuals, providing encouraging support for its use as a tool for assessing conscious awareness. This approach offers a promising way to probe whether conscious awareness remains unified or becomes dissociable across the two hemispheres of the divided brain. Determining whether each disconnected hemisphere can independently sustain volitional, stimulus-specific neural activity—and whether the two hemispheres show convergent or divergent activation patterns in response to the same probe—can inform current theories of consciousness and provide insight into neural correlates of consciousness in the intact brain.

CHAPTER 5.
CONCLUSION

1. Thesis Summary

In this thesis, I investigated the behavioral and neural consequences of callosotomy using bedside testing, computerized behavioral experiments, and resting-state fMRI. Chapter 2 replicated classic behavioral disconnection effects in a new cohort, while Chapter 3 provided novel fMRI evidence of disrupted interhemispheric functional network organization in complete split-brain patients—and remarkably intact organization in a partial case with a small splenial remnant with also no evidence of behavioral disconnection. Chapter 4 developed and validated lateralized paradigms for assessing sense of agency and conscious awareness for future use in split-brain patients.

2. Implications

There are several implications of this work.

Bridging the Gap Between Clinical and Experimental Approaches to Callosotomy

This work helps bridge clinical neuropsychology and experimental cognitive neuroscience by introducing a standardized lateralized assessment battery that can be implemented easily in clinical settings. The bedside battery and the disconnection score make it possible to systematically and longitudinally characterize each patient's disconnection profile across pre- and post-surgical timepoints—an approach not previously implemented in this population.

Replicating Classic Split-Brain Effects in a New Cohort

The classic split-brain findings have been recently questioned, suggesting that the disconnection syndrome does not clearly hold (Pinto et al., 2017). This work provides timely evidence that could inform the contemporary debates about unity in split-brain patients (de Haan et al., 2020). Here we showed that, although some patients can appear behaviorally unified under certain testing conditions, changing task demands, response modalities, and stimulus complexity can reveal classic disconnection effects. These findings reinforce the importance of careful experimental design when testing split-brain patients.

Structure-Function Relationships in the Human Brain

The resting-state fMRI findings in Chapter 3 provide supporting evidence for the relationship between structural and functional connectivity in the human brain. If structural and functional connectivity are related, then severing the largest inter-hemispheric structural link should disrupt inter-hemispheric functional connectivity. Consistent with this prediction, complete callosotomy patients showed markedly reduced inter-hemispheric functional connectivity.

***Nonlinear* Structure-Function Relationships in the Human Brain**

At the same time, the findings from the partial split-brain patient BT demonstrate that structure-function relationships can be drastically nonlinear. Despite extensive callosal section, even a small splenial remnant was sufficient to preserve remarkably intact whole-brain inter-hemispheric functional connectivity. This finding was unexpected and highlights how limited residual anatomical connectivity can support substantial large-scale functional connectivity.

Convergent Evidence for Neural and Behavioral Disconnection

Importantly, the resting-state findings in Chapter 3 mirrored the behavioral findings in Chapter 2. Patients who showed behavioral disconnections also showed markedly disrupted inter-hemispheric functional connectivity; and BT—who showed no behavioral disconnections—also showed preserved inter-hemispheric functional connectivity. This convergence suggests that resting-state connectivity measures capture behaviorally meaningful aspects of inter-hemispheric information integration, providing supporting evidence for broader brain-behavior relationships.

New Paradigm for Probing Neural Correlates of Conscious Awareness across Hemispheres The mental imagery fMRI paradigm developed in Chapter 4 offers a new method for testing the neural correlates of conscious awareness across hemispheres by examining whether a lateralized cue presented to one hemisphere can engage the opposite hemisphere, and whether dissociations emerge between subjective reportability and the neural activation patterns associated with mental imagery. The results can inform theories of consciousness.

Hemispheric Asymmetries in Sense of Agency

The lateralized sense of agency paradigms developed in Chapter 4 allow principled investigation of whether the hemispheres differentially weight prospective and retrospective cues when forming a sense of agency, which could inform our understanding of psychiatric conditions associated with disruptions in sense of agency formation, such as Schizophrenia, where these disturbances may partly reflect hemispheric imbalances.

3. Conscious Unity Hanging by a Thread?

Perhaps the most unexpected finding of this thesis was the behavioral and neural results of partial split-brain patient BT. Across both behavioral experiments and resting-state fMRI analyses, BT appeared remarkably intact, despite having a near-complete callosotomy. How was this possible?

Why Posterior Preservation May Be Uniquely Enabling

We argue that the posterior location of the preserved callosal remnant can be critical in BT's largely intact behavioral and neural results. Humans rely heavily on sensorimotor processes to interact with the world. Thus, posterior inter-hemispheric integration might better preserve system integrity and might allow more effective compensation than the other way around. Moreover, the multisensory integration zones in the parietal cortex may serve as inter-hemispheric hubs. By taking advantage of spared posterior callosal pathways connecting these regions, the processing of various intra-hemispheric brain regions can still be integrated and exchanged along polysynaptic routes running between hemispheres. Moreover, although the splenium is typically implicated in visual interhemispheric transfer, tractography studies suggest that its fibers may project to posterior parietal regions as well, and critically, there is individual variability in the precise cortical endpoints of these projections (Doron & Gazzaniga, 2008; Putnam et al., 2010). Future studies examining the cortical endpoints of BT's preserved splenial remnant may therefore be particularly informative for understanding how such limited anatomical link between the hemispheres could preserve large-scale functional and behavioral integration.

Implications for Neural Correlates of Consciousness and the Importance of Partial Cases

The findings from BT may inform the current theories of consciousness. The two most widely discussed theories are the Global Neuronal Workspace Theory (GWT) (Dehaene et al., 1998; Dehaene & Naccache, 2001) and Integrated Information Theory (IIT) (Tononi, 2004, 2005). IIT proposes that consciousness corresponds to the amount of maximally irreducible integrated information ("phi") generated by a network in a given state; and that the highest levels of integrated information are likely supported by a temporo-parietal-occipital "hot zone" within the posterior cerebral cortex. GWT proposes that consciousness arises from global broadcasting (or "ignition") of information higher-order areas and especially prefrontal cortex. Typically, IIT and GWT are contrasted in terms their distinct predictions about the neural correlates of consciousness: posterior cortical regions are for IIT, and prefrontal cortex is for GWT (Ferrante et al., 2025).

BT's findings do not directly evaluate or endorse any specific theory, but they nevertheless provide insights into their distinct predictions. First, BT clearly demonstrates the importance of posterior regions in keeping the system integrated, consistent with IIT's emphasis on posterior cortical "hot zones". Moreover, other partial split-brain patients with preserved anterior—but not posterior—callosal remnants do show disconnections, in contrast to posteriorly preserved cases, like BT, who remain largely integrated (Funnell et al., 2000). Together, these findings are consistent with IIT's proposal that the highest levels of integrated information are primarily supported by a temporo-parietal-occipital "hot zone". On the other hand, BT also showed relatively preserved functional integration involving prefrontal regions, which may also be relevant from the perspective of GWT. If consciousness arises from the global broadcasting of information across higher-order, frontal cortical regions, then preserved integration for those frontal regions may contribute to BT's unified behavior. Thus, BT's findings may be broadly compatible with aspects of both IIT and GWT, while also suggesting that preserved ***posterior*** connectivity is especially important for maintaining large-scale integration across hemispheres.

Complete split-brain cases typically attracted greater attention across fields and have therefore dominated discussions. Partial cases, however, have received relatively little attention. As this thesis has shown, partial split-brain patients may provide unique and critical insights. Despite having a near-complete callosal severance, with only a small callosal

remnant remaining at the posterior end of the corpus callosum, BT showed remarkably preserved behavioral and neural integration. His case suggests that conscious unity may, in some cases, be hanging by a thread.

References

Aboitiz, F., & Montiel, J. (2003). One hundred million years of interhemispheric communication: The history of the corpus callosum. *Brazilian Journal of Medical and Biological Research*, *36*(4), 409–420. https://doi.org/10.1590/S0100-879X2003000400002

Abraham, A., Pedregosa, F., Eickenberg, M., Gervais, P., Mueller, A., Kossaifi, J., Gramfort, A., Thirion, B., & Varoquaux, G. (2014). Machine learning for neuroimaging with scikit-learn. *Frontiers in Neuroinformatics*, *8*. https://doi.org/10.3389/fninf.2014.00014

Akelaitis, A. J. (1945). Studies on the corpus callosum. *American Journal of Psychiatry*, *101*, 594–599. https://doi.org/10.1176/ajp.101.5.594

Avants, B., Epstein, C., Grossman, M., & Gee, J. (2008). Symmetric diffeomorphic image registration with cross-correlation: Evaluating automated labeling of elderly and neurodegenerative brain. *Medical Image Analysis*, *12*(1), 26–41. https://doi.org/10.1016/j.media.2007.06.004

Barlas, Z., & Kopp, S. (2018). Action Choice and Outcome Congruency Independently Affect Intentional Binding and Feeling of Control Judgments. *Frontiers in Human Neuroscience*, *12*, 137. https://doi.org/10.3389/fnhum.2018.00137

Bassett, D. S., & Sporns, O. (2017). Network neuroscience. *Nature Neuroscience*, *20*(3), 353–364. https://doi.org/10.1038/nn.4502

Basso, M. A., Bickford, M. E., & Cang, J. (2021). Unraveling circuits of visual perception and cognition through the superior colliculus. *Neuron*, *109*(6), 918–937. https://doi.org/10.1016/j.neuron.2021.01.013

Bayne, T. (2008). The unity of consciousness and the split-brain syndrome. *The Journal of Philosophy*, *105*(6), 277–300.

Bayne, T., & Chalmers, D. (2003). What Is the Unity of Consciousness? In A. Cleeremans (Ed.), *The Unity of Consciousness* (pp. 23–58). Oxford University Press.

Behzadi, Y., Restom, K., Liau, J., & Liu, T. T. (2007). A component based noise correction method (CompCor) for BOLD and perfusion based fMRI. *NeuroImage*, *37*(1), 90–101. https://doi.org/10.1016/j.neuroimage.2007.04.042

Bekir, S., Hopf, J. L., Paul, T., Wiemer, V. M., Santander, T., Skinner, H. E., Rada, A., Woermann, F. G., Kalbhenn, T., Giesbrecht, B., Bien, C. G., Sporns, O., Gazzaniga, M. S., Volz, L. J., & Miller, M. B. (2025). No disconnection syndrome after near-complete callosotomy. *Communications Psychology*, *4*(1), 9. https://doi.org/10.1038/s44271-025-00377-5

Bishop, D. V. M. (2013). Cerebral asymmetry and language development: Cause, correlate or consequence? *Science (New York, N.Y.)*, *340*(6138), 1230531. https://doi.org/10.1126/science.1230531

Bodien, Y. G., Allanson, J., Cardone, P., Bonhomme, A., Carmona, J., Chatelle, C., Chennu, S., Conte, M., Dehaene, S., Finoia, P., Heinonen, G., Hersh, J. E., Kamau, E., Lawrence, P. K., Lupson, V. C., Meydan, A., Rohaut, B., Sanders, W. R., Sitt, J. D., … Schiff, N. D. (2024). Cognitive Motor Dissociation in Disorders of Consciousness. *New England Journal of Medicine*, *391*(7), 598–608. https://doi.org/10.1056/NEJMoa2400645

Boly, M., Coleman, M. R., Davis, M. H., Hampshire, A., Bor, D., Moonen, G., Maquet, P. A., Pickard, J. D., Laureys, S., & Owen, A. M. (2007). When thoughts become action: An

fMRI paradigm to study volitional brain activity in non-communicative brain injured patients. *NeuroImage*, *36*(3), 979–992. https://doi.org/10.1016/j.neuroimage.2007.02.047

Bourne, V. J. (2006). The divided visual field paradigm: Methodological considerations. *Laterality*, *11*(4), 373–393. https://doi.org/10.1080/13576500600633982

Boveroux, P., Vanhaudenhuyse, A., Bruno, M.-A., Noirhomme, Q., Lauwick, S., Luxen, A., Degueldre, C., Plenevaux, A., Schnakers, C., Phillips, C., Brichant, J.-F., Bonhomme, V., Maquet, P., Greicius, M. D., Laureys, S., & Boly, M. (2010). Breakdown of within- and between-network Resting State Functional Magnetic Resonance Imaging Connectivity during Propofol-induced Loss of Consciousness. *Anesthesiology*, *113*(5), 1038. https://doi.org/10.1097/ALN.0b013e3181f697f5

Caillé, S., Sauerwein, H. C., Schiavetto, A., Villemure, J.-G., & Lassonde, M. (2005). Sensory and Motor Interhemispheric Integration after Section of Different Portions of the Anterior Corpus Callosum in Nonepileptic Patients. *Neurosurgery*, *57*(1), 50–59. https://doi.org/10.1227/01.NEU.0000163089.31657.08

Catani, M., & Schotten, M. T. de. (2012). *Atlas of Human Brain Connections*. OUP Oxford.

Chambon, V., & Haggard, P. (2012). Sense of control depends on fluency of action selection, not motor performance. *Cognition*, *125*(3), 441–451. https://doi.org/10.1016/j.cognition.2012.07.011

Ciric, R., Thompson, W. H., Lorenz, R., Goncalves, M., MacNicol, E. E., Markiewicz, C. J., Halchenko, Y. O., Ghosh, S. S., Gorgolewski, K. J., Poldrack, R. A., & Esteban, O. (2022). TemplateFlow: FAIR-sharing of multi-scale, multi-species brain models. *Nature Methods*, *19*(12), 1568–1571. https://doi.org/10.1038/s41592-022-01681-2

Corballis, M. (1995). Visual integration in the split brain. *Neuropsychologia*, *33*(8), 937–959. https://doi.org/10.1016/0028-3932(95)00032-X

Dale, A. M., Fischl, B., & Sereno, M. I. (1999). Cortical Surface-Based Analysis. *NeuroImage*, *9*(2), 179–194. https://doi.org/10.1006/nimg.1998.0395

de Haan, E. H. F., Corballis, P. M., Hillyard, S. A., Marzi, C. A., Seth, A., Lamme, V. A. F., Volz, L., Fabri, M., Schechter, E., Bayne, T., Corballis, M., & Pinto, Y. (2020). Split-Brain: What We Know Now and Why This is Important for Understanding Consciousness. *Neuropsychology Review*, *30*(2), 224–233. https://doi.org/10.1007/s11065-020-09439-3

Dehaene, S., Kerszberg, M., & Changeux, J. P. (1998). A neuronal model of a global workspace in effortful cognitive tasks. *Proceedings of the National Academy of Sciences of the United States of America*, *95*(24), 14529–14534. https://doi.org/10.1073/pnas.95.24.14529

Dehaene, S., & Naccache, L. (2001). Towards a cognitive neuroscience of consciousness: Basic evidence and a workspace framework. *Cognition*, *79*(1–2), 1–37. https://doi.org/10.1016/s0010-0277(00)00123-2

Dennet, D. (1992). The Self as a Center of Narrative Gravity. In F. Kessel, P. Cole, & D. Johnson (Eds.), *Self and Consciousness: Multiple Perspectives*. Erlbaum.

Di Virgilio, G., Clarke, S., Pizzolato, G., & Schaffner, T. (1999). Cortical regions contributing to the anterior commissure in man. *Experimental Brain Research*, *124*(1), 1–7. https://doi.org/10.1007/s002210050593

Doron, K., & Gazzaniga, M. (2008). Neuroimaging techniques offer new perspectives on callosal transfer and interhemispheric communication. *Cortex*, *44*(8), 1023–1029. https://doi.org/10.1016/j.cortex.2008.03.007

Doron, K. W., Bassett, D. S., & Gazzaniga, M. S. (2012). Dynamic network structure of interhemispheric coordination. *Proceedings of the National Academy of Sciences*, *109*(46), 18661–18668. https://doi.org/10.1073/pnas.1216402109

Esteban, O., Markiewicz, C. J., Blair, R. W., Moodie, C. A., Isik, A. I., Erramuzpe, A., Kent, J. D., Goncalves, M., DuPre, E., Snyder, M., Oya, H., Ghosh, S. S., Wright, J., Durnez, J., Poldrack, R. A., & Gorgolewski, K. J. (2019). fMRIPrep: A robust preprocessing pipeline for functional MRI. *Nature Methods*, *16*(1), 111–116. https://doi.org/10.1038/s41592-018-0235-4

Evans, A. C., Janke, A. L., Collins, D. L., & Baillet, S. (2012). Brain templates and atlases. *NeuroImage*, *62*(2), 911–922. https://doi.org/10.1016/j.neuroimage.2012.01.024

Fabri, M., Del Pesce, M., Paggi, A., Polonara, G., Bartolini, M., Salvolini, U., & Manzoni, T. (2005). Contribution of posterior corpus callosum to the interhemispheric transfer of tactile information. *Cognitive Brain Research*, *24*(1), 73–80. https://doi.org/10.1016/j.cogbrainres.2004.12.003

Fabri, M., & Polonara, G. (2013). Functional Topography of Human Corpus Callosum: An fMRI Mapping Study. *Neural Plasticity*, *2013*, 1–15. https://doi.org/10.1155/2013/251308

Fabri, M., & Polonara, G. (2023). Functional topography of the corpus callosum as revealed by fMRI and behavioural studies of control subjects and patients with callosal

resection. *Neuropsychologia*, *183*, 108533. https://doi.org/10.1016/j.neuropsychologia.2023.108533

Fabri, M., Polonara, G., Pesce, M. D., Quattrini, A., Salvolini, U., & Manzoni, T. (2001). Posterior Corpus Callosum and Interhemispheric Transfer of Somatosensory Information: An fMRI and Neuropsychological Study of a Partially Callosotomized Patient. *Journal of Cognitive Neuroscience*, *13*(8), 1071–1079. https://doi.org/10.1162/089892901753294365

Fabri, M., Polonara, G., Quattrini, A., Salvolini, U., Del Pesce, M., & Manzoni, T. (1999). Role of the corpus callosum in the somatosensory activation of the ipsilateral cerebral cortex: An fMRI study of callosotomized patients. *European Journal of Neuroscience*, *11*(11), 3983–3994. https://doi.org/10.1046/j.1460-9568.1999.00829.x

Ferrand-Sorbets, S., Fohlen, M., Bourdillon, P., Chipaux, M., Bulteau, C., Goetz, L., Delalande, O., Taussig, D., & Dorfmuller, G. (2022). Complete callosotomy in children with drop attacks; A retrospective monocentric study of 50 patients. *Seizure*, *96*, 34–42. https://doi.org/10.1016/j.seizure.2022.01.008

Ferrante, O., Gorska-Klimowska, U., Henin, S., Hirschhorn, R., Khalaf, A., Lepauvre, A., Liu, L., Richter, D., Vidal, Y., Bonacchi, N., Brown, T., Sripad, P., Armendariz, M., Bendtz, K., Ghafari, T., Hetenyi, D., Jeschke, J., Kozma, C., Mazumder, D. R., … Melloni, L. (2025). Adversarial testing of global neuronal workspace and integrated information theories of consciousness. *Nature*, *642*(8066), 133–142. https://doi.org/10.1038/s41586-025-08888-1

Fortunato, S., & Barthélemy, M. (2007). Resolution limit in community detection. *Proceedings of the National Academy of Sciences of the United States of America*, *104*(1), 36–41. https://doi.org/10.1073/pnas.0605965104

Friedrich, P., Forkela, S. J., & Thiebaut de Schotten, M. (2020). Mapping the principal gradient onto the corpus callosum. *NeuroImage*, *223*, 117317. https://doi.org/10.1016/j.neuroimage.2020.117317

Frith, C. D., Blakemore, S. J., & Wolpert, D. M. (2000). Abnormalities in the awareness and control of action. *Philosophical Transactions of the Royal Society B: Biological Sciences*, *355*(1404), 1771–1788. https://doi.org/10.1098/rstb.2000.0734

Funnell, M. G., Corballis, P. M., & Gazzaniga, M. S. (2000). Cortical and subcortical interhemispheric interactions following partial and complete callosotomy. *Archives of Neurology*, *57*(2), 185–189. https://doi.org/10.1001/archneur.57.2.185

Gazzaniga, M. S. (1988). Interhemispheric Integration. *Neurobiology of Neocortex*, 385–405.

Gazzaniga, M. S. (2000). Cerebral specialization and interhemispheric communication: Does the corpus callosum enable the human condition? *Brain: A Journal of Neurology*, *123 (Pt 7)*, 1293–1326. https://doi.org/10.1093/brain/123.7.1293

Gazzaniga, M. S., Bogen, J. E., & Sperry, R. W. (1962). Some functional effects of sectioning the cerebral commissures in man*. *Proceedings of the National Academy of Sciences*, *48*(10), 1765–1769. https://doi.org/10.1073/pnas.48.10.1765

Gazzaniga, M. S., Holtzman, J. D., Deck, M. D., & Lee, B. C. (1985). MRI assessment of human callosal surgery with neuropsychological correlates. *Neurology*, *35*(12), 1763–1766. https://doi.org/10.1212/wnl.35.12.1763

Gazzaniga, M. S., Holtzman, J. D., & Smylie, C. S. (1987). Speech without conscious awareness. *Neurology*, *37*(4), 682–685. https://doi.org/10.1212/wnl.37.4.682

Gazzaniga, M. S., & LeDoux, J. E. (1978). *The Integrated Mind*. New York: Plenum Press.

Geffen, G., Nilsson, J., Quinn, K., & Teng, E. L. (1985). The effect of lesions of the corpus callosum on finger localization. *Neuropsychologia*, *23*(4), 497–514. https://doi.org/10.1016/0028-3932(85)90004-1

Glickstein, M., & Sperry, R. W. (1960). Intermanual somesthetic transfer in split-brain rhesus monkeys. *Journal of Comparative and Physiological Psychology*, *53*(4), 322–327. https://doi.org/10.1037/h0046386

Gordon, H. W., Bogen, J. E., & Sperry, R. W. (1971). Absence of deconnexion syndrome in two patients with partial section of the neocommissures. *Brain: A Journal of Neurology*, *94*(2), 327–336. https://doi.org/10.1093/brain/94.2.327

Gorgolewski, K., Burns, C. D., Madison, C., Clark, D., Halchenko, Y. O., Waskom, M. L., & Ghosh, S. S. (2011). Nipype: A Flexible, Lightweight and Extensible Neuroimaging Data Processing Framework in Python. *Frontiers in Neuroinformatics*, *5*. https://doi.org/10.3389/fninf.2011.00013

Greve, D. N., & Fischl, B. (2009). Accurate and robust brain image alignment using boundary-based registration. *NeuroImage*, *48*(1), 63–72. https://doi.org/10.1016/j.neuroimage.2009.06.060

Güntürkün, O., Ströckens, F., & Ocklenburg, S. (2020). Brain Lateralization: A Comparative Perspective. *Physiological Reviews*, *100*(3), 1019–1063. https://doi.org/10.1152/physrev.00006.2019

Haggard, P. (2017). Sense of agency in the human brain. *Nature Reviews Neuroscience*, *18*(4), 196–207. https://doi.org/10.1038/nrn.2017.14

Haggard, P., Clark, S., & Kalogeras, J. (2002). Voluntary action and conscious awareness. *Nature Neuroscience*, *5*(4), 382–385. https://doi.org/10.1038/nn827

Hansen, M. J. (2024). Modelling developments in consciousness within a multidimensional framework. *Neuroscience of Consciousness*, *2024*(1), niae026. https://doi.org/10.1093/nc/niae026

Hofer, S., & Frahm, J. (2006). Topography of the human corpus callosum revisited—Comprehensive fiber tractography using diffusion tensor magnetic resonance imaging. *NeuroImage*, *32*(3), 989–994. https://doi.org/10.1016/j.neuroimage.2006.05.044

Holtzman, J. D., & Gazzaniga, M. S. (1982). Dual task interactions due exclusively to limits in processing resources. *Science*, *218*(4579), 1325–1327. https://doi.org/10.1126/science.7146915

Holtzman, J. D., Sidtis, J. J., Volpe, B. T., Wilson, D. H., & Gazzaniga, M. S. (1981). DISSOCIATION OF SPATIAL INFORMATION FOR STIMULUS LOCALIZATION AND THE CONTROL OF ATTENTION. *Brain*, *104*(4), 861–872. https://doi.org/10.1093/brain/104.4.861

Honey, C. J., Sporns, O., Cammoun, L., Gigandet, X., Thiran, J. P., Meuli, R., & Hagmann, P. (2009). Predicting human resting-state functional connectivity from structural connectivity. *Proceedings of the National Academy of Sciences*, *106*(6), 2035–2040. https://doi.org/10.1073/pnas.0811168106

Hua, K., Zhang, J., Wakana, S., Jiang, H., Li, X., Reich, D. S., Calabresi, P. A., Pekar, J. J., van Zijl, P. C. M., & Mori, S. (2008). Tract probability maps in stereotaxic spaces:

Analyses of white matter anatomy and tract-specific quantification. *NeuroImage*, *39*(1), 336–347. https://doi.org/10.1016/j.neuroimage.2007.07.053

Hung, S.-C., Lee, C.-C., Chen, H.-H., Chen, C., Wu, H.-M., Lin, C.-P., & Peng, S.-J. (2019). Early recovery of interhemispheric functional connectivity after corpus callosotomy. *Epilepsia*, *60*(6), 1126–1136. https://doi.org/10.1111/epi.14933

Jenkinson, M., Bannister, P., Brady, M., & Smith, S. (2002). Improved Optimization for the Robust and Accurate Linear Registration and Motion Correction of Brain Images. *NeuroImage*, *17*(2), 825–841. https://doi.org/10.1006/nimg.2002.1132

Jenkinson, M., Beckmann, C. F., Behrens, T. E. J., Woolrich, M. W., & Smith, S. M. (2012). FSL. *NeuroImage, 20 YEARS OF fMRI*, *62*(2), 782–790. https://doi.org/10.1016/j.neuroimage.2011.09.015

Johnston, J. M., Vaishnavi, S. N., Smyth, M. D., Zhang, D., He, B. J., Zempel, J. M., Shimony, J. S., Snyder, A. Z., & Raichle, M. E. (2008). Loss of resting interhemispheric functional connectivity after complete section of the corpus callosum. *The Journal of Neuroscience: The Official Journal of the Society for Neuroscience*, *28*(25), 6453–6458. https://doi.org/10.1523/JNEUROSCI.0573-08.2008

Kaufman, A. S. (2009). *IQ Testing 101*. Springer Publishing.

Kingstone, A., & Gazzaniga, M. S. (1995). Subcortical transfer of higher order information: More illusory than real? *Neuropsychology*, *9*(3), 321–328. https://doi.org/10.1037/0894-4105.9.3.321

Klein, A., Ghosh, S. S., Bao, F. S., Giard, J., Häme, Y., Stavsky, E., Lee, N., Rossa, B., Reuter, M., Chaibub Neto, E., & Keshavan, A. (2017). Mindboggling morphometry of human

brains. *PLOS Computational Biology*, *13*(2), e1005350. https://doi.org/10.1371/journal.pcbi.1005350

Koch, C., Massimini, M., Boly, M., & Tononi, G. (2016). Neural correlates of consciousness: Progress and problems. *Nature Reviews Neuroscience*, *17*(5), 307–321. https://doi.org/10.1038/nrn.2016.22

LeDoux, J. E., Wilson, D. H., & Gazzaniga, M. S. (1977). Manipulo-spatial aspects of cerebral lateralization: Clues to the origin of lateralization. *Neuropsychologia*, *15*(6), 743–750. https://doi.org/10.1016/0028-3932(77)90004-5

Lipkin, B., Tuckute, G., Affourtit, J., Small, H., Mineroff, Z., Kean, H., Jouravlev, O., Rakocevic, L., Pritchett, B., Siegelman, M., Hoeflin, C., Pongos, A., Blank, I. A., Struhl, M. K., Ivanova, A., Shannon, S., Sathe, A., Hoffmann, M., Nieto-Castañón, A., & Fedorenko, E. (2022). Probabilistic atlas for the language network based on precision fMRI data from >800 individuals. *Scientific Data*, *9*(1), 529. https://doi.org/10.1038/s41597-022-01645-3

Liu, Y., Hsu, C.-C. H., Huang, C.-C., Zhang, Y., Zhao, J., Tsai, S.-J., Chen, L.-K., Lin, C.-P., & Lo, C.-Y. Z. (2021). Connectivity-Based Topographical Changes of the Corpus Callosum During Aging. *Frontiers in Aging Neuroscience*, *13*, 753236. https://doi.org/10.3389/fnagi.2021.753236

Luck, S. J., Hillyard, S. A., Mangun, G. R., & Gazzaniga, M. S. (1989). Independent hemispheric attentional systems mediate visual search in split-brain patients. *Nature*, *342*(6249), 543–545. https://doi.org/10.1038/342543a0

Mashour, G. A., Roelfsema, P., Changeux, J.-P., & Dehaene, S. (2020). Conscious Processing and the Global Neuronal Workspace Hypothesis. *Neuron*, *105*(5), 776–798. https://doi.org/10.1016/j.neuron.2020.01.026

Miller, M. B., & Kingstone, A. (2005). Taking the high road on subcortical transfer. *Brain and Cognition*, *57*(2), 162–164. https://doi.org/10.1016/j.bandc.2004.08.037

Mitchell, M. (2011). *Complexity: A Guided Tour*. Oxford University Press.

Monti, M. M., Vanhaudenhuyse, A., Coleman, M. R., Boly, M., Pickard, J. D., Tshibanda, L., Owen, A. M., & Laureys, S. (2010). Willful modulation of brain activity in disorders of consciousness. *The New England Journal of Medicine*, *362*(7), 579–589. https://doi.org/10.1056/NEJMoa0905370

Myers, R. E., & Sperry, R. W. (1958). Interhemispheric Communication Through the Corpus Callosum: Mnemonic Carry-Over Between the Hemispheres. *A.M.A. Archives of Neurology & Psychiatry*, *80*(3), 298–303. https://doi.org/10.1001/archneurpsyc.1958.02340090034004

Nagel, T. (1971). Brain Bisection and the Unity of Consciousness. *Synthese*.

Oishi, H., Tanaka, K., & Watanabe, K. (2018). Feedback of action outcome retrospectively influences sense of agency in a continuous action task. *PloS One*, *13*(8), e0202690. https://doi.org/10.1371/journal.pone.0202690

Owen, A. M., Coleman, M. R., Boly, M., Davis, M. H., Laureys, S., & Pickard, J. D. (2006). Detecting awareness in the vegetative state. *Science (New York, N.Y.)*, *313*(5792), 1402. https://doi.org/10.1126/science.1130197

Parkes, L., Fulcher, B., Yücel, M., & Fornito, A. (2018). An evaluation of the efficacy, reliability, and sensitivity of motion correction strategies for resting-state functional MRI. *NeuroImage*, *171*, 415–436. https://doi.org/10.1016/j.neuroimage.2017.12.073

Patriat, R., Reynolds, R. C., & Birn, R. M. (2017). An improved model of motion-related signal changes in fMRI. *NeuroImage*, *144*, 74–82. https://doi.org/10.1016/j.neuroimage.2016.08.051

Paul, L. K., Brown, W. S., Adolphs, R., Tyszka, J. M., Richards, L. J., Mukherjee, P., & Sherr, E. H. (2007). Agenesis of the corpus callosum: Genetic, developmental and functional aspects of connectivity. *Nature Reviews. Neuroscience*, *8*(4), 287–299. https://doi.org/10.1038/nrn2107

Peirce, J., Gray, J. R., Simpson, S., MacAskill, M., Höchenberger, R., Sogo, H., Kastman, E., & Lindeløv, J. K. (2019). PsychoPy2: Experiments in behavior made easy. *Behavior Research Methods*, *51*(1), 195–203. https://doi.org/10.3758/s13428-018-01193-y

Pinto, Y., De Haan, E. H. F., & Lamme, V. A. F. (2017). The Split-Brain Phenomenon Revisited: A Single Conscious Agent with Split Perception. *Trends in Cognitive Sciences*, *21*(11), 835–851. https://doi.org/10.1016/j.tics.2017.09.003

Pinto, Y., Lamme, V. A. F., & de Haan, E. H. F. (2017). Cross-cueing cannot explain unified control in split-brain patients. *Brain*, *140*(11), e68. https://doi.org/10.1093/brain/awx235

Pinto, Y., Neville, D. A., Otten, M., Corballis, P. M., Lamme, V. A. F., de Haan, E. H. F., Foschi, N., & Fabri, M. (2017). Split brain: Divided perception but undivided consciousness. *Brain: A Journal of Neurology*, *140*(5), 1231–1237. https://doi.org/10.1093/brain/aww358

Pinto, Y., Villa, M.-C., Siliquini, S., Polonara, G., Passamonti, C., Lattanzi, S., Foschi, N., Fabri, M., & De Haan, E. H. F. (2023). Visual integration across fixation: Automatic processes are split but conscious processes remain unified in the split-brain. *Frontiers in Human Neuroscience*, *17*, 1278025. https://doi.org/10.3389/fnhum.2023.1278025

Pizoli, C. E., Shah, M. N., Snyder, A. Z., Shimony, J. S., Limbrick, D. D., Raichle, M. E., Schlaggar, B. L., & Smyth, M. D. (2011). Resting-state activity in development and maintenance of normal brain function. *Proceedings of the National Academy of Sciences of the United States of America*, *108*(28), 11638–11643. https://doi.org/10.1073/pnas.1109144108

Polonara, G., Mascioli, G., Foschi, N., Salvolini, U., Pierpaoli, C., Manzoni, T., Fabri, M., & Barbaresi, P. (2015). Further Evidence for the Topography and Connectivity of the Corpus Callosum: An fMRI Study of Patients with Partial Callosal Resection. *Journal of Neuroimaging*, *25*(3), 465–473. https://doi.org/10.1111/jon.12136

Power, J. D., Mitra, A., Laumann, T. O., Snyder, A. Z., Schlaggar, B. L., & Petersen, S. E. (2014). Methods to detect, characterize, and remove motion artifact in resting state fMRI. *NeuroImage*, *84*, 320–341. https://doi.org/10.1016/j.neuroimage.2013.08.048

Pryke, A., Jayachandran, K., & Martin, A. K. (2025). The causal neural substrates underpinning prospective and retrospective sense of agency. *Cortex; a Journal Devoted to the Study of the Nervous System and Behavior*, *188*, 53–67. https://doi.org/10.1016/j.cortex.2025.04.014

Putnam, M. C., Steven, M. S., Doron, K. W., Riggall, A. C., & Gazzaniga, M. S. (2010). Cortical Projection Topography of the Human Splenium: Hemispheric Asymmetry and

Individual Differences. *Journal of Cognitive Neuroscience*, *22*(8), 1662–1669. https://doi.org/10.1162/jocn.2009.21290

R Core Team. (2021). *R: A Language and Environment for Statistical Computing* [Computer software]. R Foundation for Statistical Computing. https://www.R-project.org/

Risse, G. L., Gates, J., Lund, G., Maxwell, R., & Rubens, A. (1989). Interhemispheric transfer in patients with incomplete section of the corpus callosum. Anatomic verification with magnetic resonance imaging. *Archives of Neurology*, *46*(4), 437–443. https://doi.org/10.1001/archneur.1989.00520400097026

Risse, G. L., LeDoux, J., Springer, S. P., Wilson, D. H., & Gazzaniga, M. S. (1978). The anterior commissure in man: Functional variation in a multisensory system. *Neuropsychologia*, *16*(1), 23–31. https://doi.org/10.1016/0028-3932(78)90039-8

Roland, J. L., Snyder, A. Z., Hacker, C. D., Mitra, A., Shimony, J. S., Limbrick, D. D., Raichle, M. E., Smyth, M. D., & Leuthardt, E. C. (2017). On the role of the corpus callosum in interhemispheric functional connectivity in humans. *Proceedings of the National Academy of Sciences of the United States of America*, *114*(50), 13278–13283. https://doi.org/10.1073/pnas.1707050114

RRID: SCR_001476. (n.d.). *Harvard-Oxford Cortical Structural Atlas (Lateralized)*.

Rubinov, M., & Sporns, O. (2011). Weight-conserving characterization of complex functional brain networks. *NeuroImage*, *56*(4), 2068–2079. https://doi.org/10.1016/j.neuroimage.2011.03.069

Saenz, M., & Fine, I. (2010). Topographic organization of V1 projections through the corpus callosum in humans. *NeuroImage*, *52*(4), 1224–1229. https://doi.org/10.1016/j.neuroimage.2010.05.060

Salmaso, D., & Longoni, A. M. (1985). Problems in the assessment of hand preference. *Cortex; a Journal Devoted to the Study of the Nervous System and Behavior*, *21*(4), 533–549. https://doi.org/10.1016/s0010-9452(58)80003-9

Santander, T., Bekir, S., Paul, T., Simonson, J. M., Wiemer, V. M., Skinner, H. E., Hopf, J. L., Rada, A., Woermann, F. G., Kalbhenn, T., Giesbrecht, B., Bien, C. G., Sporns, O., Gazzaniga, M. S., Volz, L. J., & Miller, M. B. (2025). *Full inter-hemispheric integration sustained by a fraction of posterior callosal fibers*. https://doi.org/10.1101/2025.02.14.638327

Satterthwaite, T. D., Elliott, M. A., Gerraty, R. T., Ruparel, K., Loughead, J., Calkins, M. E., Eickhoff, S. B., Hakonarson, H., Gur, R. C., Gur, R. E., & Wolf, D. H. (2013). An improved framework for confound regression and filtering for control of motion artifact in the preprocessing of resting-state functional connectivity data. *NeuroImage*, *64*, 240–256. https://doi.org/10.1016/j.neuroimage.2012.08.052

Sattler, J. M. (2008). *Assessment of children: Cognitive foundations* (5th ed.). San Diego : J.M. Sattler.

Schaefer, A., Kong, R., Gordon, E. M., Laumann, T. O., Zuo, X.-N., Holmes, A. J., Eickhoff, S. B., & Yeo, B. T. T. (2018). Local-Global Parcellation of the Human Cerebral Cortex from Intrinsic Functional Connectivity MRI. *Cerebral Cortex*, *28*(9), 3095–3114. https://doi.org/10.1093/cercor/bhx179

Schechter, E. (2012). Intentions and Unified Agency: Insights from the Split-brain Phenomenon. *Mind & Language*, *27*(5), 570–594. https://doi.org/10.1111/mila.12003

Schechter, E., & Bayne, T. (2021). Consciousness after split-brain surgery: The recent challenge to the classical picture. *Neuropsychologia*, *160*, 107987. https://doi.org/10.1016/j.neuropsychologia.2021.107987

Sergent, J. (1983). Unified response to bilateral hemispheric stimulation by a split-brain patient. *Nature*, *305*(5937), 800–802. https://doi.org/10.1038/305800a0

Sergent, J. (1986). SUBCORTICAL COORDINATION OF HEMISPHERE ACTIVITY IN COMMISSUROTOMIZED PATIENTS. *Brain*, *109*(2), 357–369. https://doi.org/10.1093/brain/109.2.357

Sporns, O., & Betzel, R. F. (2016). Modular Brain Networks. *Annual Review of Psychology*, *67*, 613–640. https://doi.org/10.1146/annurev-psych-122414-033634

Spunt, B. (n.d.). *Easy-optimize-x* [Computer software]. Retrieved https://www.bobspunt.com/easy-optimize-x/

SR Research Ltd. (n.d.). *EyeLink 1000 Plus* [Computer software]. Retrieved https://www.sr-research.com

Szaflarski, J. P., Holland, S. K., Schmithorst, V. J., & Byars, A. W. (2006). fMRI study of language lateralization in children and adults. *Human Brain Mapping*, *27*(3), 202–212. https://doi.org/10.1002/hbm.20177

Tazoe, T., & Perez, M. A. (2014). Selective Activation of Ipsilateral Motor Pathways in Intact Humans. *The Journal of Neuroscience*, *34*(42), 13924–13934. https://doi.org/10.1523/JNEUROSCI.1648-14.2014

Tian, Y., Margulies, D. S., Breakspear, M., & Zalesky, A. (2020). Topographic organization of the human subcortex unveiled with functional connectivity gradients. *Nature Neuroscience*, *23*(11), 1421–1432. https://doi.org/10.1038/s41593-020-00711-6

Tierney, T. M., Alexander, N. A., Ashburner, J., Avila, N. L., Balbastre, Y., Barnes, G., Bezsudnova, Y., Brudfors, M., Eckstein, K., Flandin, G., Friston, K., Jafarian, A., Kowalczyk, O. S., Litvak, V., Medrano, J., Mellor, S., O'Neill, G., Parr, T., Razi, A., … Zeidman, P. (2025). SPM 25: Open source neuroimaging analysis software. *Journal of Open Source Software*, *10*(110), 8103. https://doi.org/10.21105/joss.08103

Tobii AB. (n.d.). *Tobii Pro Fusion* [Computer software]. Retrieved https://www.tobii.com/products/eye-trackers/screen-based/tobii-pro-fusion

Tononi, G. (2004). An information integration theory of consciousness. *BMC Neuroscience*, *5*, 42. https://doi.org/10.1186/1471-2202-5-42

Tononi, G. (2005). Consciousness, information integration, and the brain. *Progress in Brain Research*, *150*, 109–126. https://doi.org/10.1016/S0079-6123(05)50009-8

Tononi, G., Albantakis, L., Barbosa, L., Boly, M., Cirelli, C., Comolatti, R., Ellia, F., Findlay, G., Casali, A. G., Grasso, M., Haun, A. M., Hendren, J., Hoel, E., Koch, C., Maier, A., Marshall, W., Massimini, M., Mayner, W. G., Oizumi, M., … Zaeemzadeh, A. (2025). Consciousness or pseudo-consciousness? A clash of two paradigms. *Nature Neuroscience*, 1–9. https://doi.org/10.1038/s41593-025-01880-y

Tustison, N. J., Avants, B. B., Cook, P. A., Yuanjie Zheng, Egan, A., Yushkevich, P. A., & Gee, J. C. (2010). N4ITK: Improved N3 Bias Correction. *IEEE Transactions on Medical Imaging*, *29*(6), 1310–1320. https://doi.org/10.1109/TMI.2010.2046908

Tustison, N. J., Cook, P. A., Holbrook, A. J., Johnson, H. J., Muschelli, J., Devenyi, G. A., Duda, J. T., Das, S. R., Cullen, N. C., Gillen, D. L., Yassa, M. A., Stone, J. R., Gee, J. C., & Avants, B. B. (2021). The ANTsX ecosystem for quantitative biological and

medical imaging. *Scientific Reports*, *11*(1), 9068. https://doi.org/10.1038/s41598-021-87564-6

Tustison, N. J., Cook, P. A., Klein, A., Song, G., Das, S. R., Duda, J. T., Kandel, B. M., van Strien, N., Stone, J. R., Gee, J. C., & Avants, B. B. (2014). Large-scale evaluation of ANTs and FreeSurfer cortical thickness measurements. *NeuroImage*, *99*, 166–179. https://doi.org/10.1016/j.neuroimage.2014.05.044

Uddin, L. Q., Mooshagian, E., Zaidel, E., Scheres, A., Margulies, D. S., Kelly, A. M. C., Shehzad, Z., Adelstein, J. S., Castellanos, F. X., Biswal, B. B., & Milham, M. P. (2008). Residual functional connectivity in the split-brain revealed with resting-state functional MRI. *NeuroReport*, *19*(7), 703–709. https://doi.org/10.1097/WNR.0b013e3282fb8203

Vaddiparti, A., Huang, R., Blihar, D., Du Plessis, M., Montalbano, M. J., Tubbs, R. S., & Loukas, M. (2021). The Evolution of Corpus Callosotomy for Epilepsy Management. *World Neurosurgery*, *145*, 455–461. https://doi.org/10.1016/j.wneu.2020.08.178

van den Heuvel, M. P., & Sporns, O. (2011). Rich-club organization of the human connectome. *The Journal of Neuroscience: The Official Journal of the Society for Neuroscience*, *31*(44), 15775–15786. https://doi.org/10.1523/JNEUROSCI.3539-11.2011

Van Waganen, W. P., & Herren, R. Y. (1940). SURGICAL DIVISION OF COMMISSURAL PATHWAYS IN THE CORPUS CALLOSUM: RELATION TO SPREAD OF AN EPILEPTIC ATTACK. *Archives of Neurology & Psychiatry*, *44*(4), 740–759. https://doi.org/10.1001/archneurpsyc.1940.02280100042004

Vanbellingen, T., Kersten, B., Van de Winckel, A., Bellion, M., Baronti, F., Müri, R., & Bohlhalter, S. (2011). A new bedside test of gestures in stroke: The apraxia screen of

TULIA (AST). *Journal of Neurology, Neurosurgery, and Psychiatry*, *82*(4), 389–392. https://doi.org/10.1136/jnnp.2010.213371

Volz, L. J., & Gazzaniga, M. S. (2017). Interaction in isolation: 50 years of insights from split-brain research. *Brain: A Journal of Neurology*, *140*(7), 2051–2060. https://doi.org/10.1093/brain/awx139

Volz, L. J., Hillyard, S. A., Miller, M. B., & Gazzaniga, M. S. (2018). Unifying control over the body: Consciousness and cross-cueing in split-brain patients. *Brain: A Journal of Neurology*, *141*(3), e15. https://doi.org/10.1093/brain/awx359

Voss, M., Moore, J., Hauser, M., Gallinat, J., Heinz, A., & Haggard, P. (2010). Altered awareness of action in schizophrenia: A specific deficit in predicting action consequences. *Brain: A Journal of Neurology*, *133*(10), 3104–3112. https://doi.org/10.1093/brain/awq152

Wada, J., & Rasmussen, T. (2007). Intracarotid injection of sodium amytal for the lateralization of cerebral speech dominance. 1960. *Journal of Neurosurgery*, *106*(6), 1117–1133. https://doi.org/10.3171/jns.2007.106.6.1117

Wakana, S., Caprihan, A., Panzenboeck, M. M., Fallon, J. H., Perry, M., Gollub, R. L., Hua, K., Zhang, J., Jiang, H., Dubey, P., Blitz, A., van Zijl, P., & Mori, S. (2007). Reproducibility of quantitative tractography methods applied to cerebral white matter. *NeuroImage*, *36*(3), 630–644. https://doi.org/10.1016/j.neuroimage.2007.02.049

Wang, Z., Chen, L. M., Négyessy, L., Friedman, R. M., Mishra, A., Gore, J. C., & Roe, A. W. (2013). The relationship of anatomical and functional connectivity to resting state connectivity in primate somatosensory cortex. *Neuron*, *78*(6), 1116–1126. https://doi.org/10.1016/j.neuron.2013.04.023

Wechsler, D. (2012). *Wechsler Adult Intelligence Scale—Fourth Edition* [Dataset]. https://doi.org/10.1037/t15169-000

Wegner, D. M. (2003). *The Illusion of Conscious Will*. MIT Press.

Wenke, D., Fleming, S. M., & Haggard, P. (2010). Subliminal priming of actions influences sense of control over effects of action. *Cognition*, *115*(1), 26–38. https://doi.org/10.1016/j.cognition.2009.10.016

Yarkoni, T., Poldrack, R. A., Nichols, T. E., Van Essen, D. C., & Wager, T. D. (2011). Large-scale automated synthesis of human functional neuroimaging data. *Nature Methods*, *8*(8), 665–670. https://doi.org/10.1038/nmeth.1635

Yeh, F.-C. (2025). DSI Studio: An Integrated Tractography Platform and Fiber Data Hub for Accelerating Brain Research. *Nature Methods*, *22*(8), 1617–1619. https://doi.org/10.1038/s41592-025-02762-8

Yeh, F.-C., Verstynen, T. D., Wang, Y., Fernández-Miranda, J. C., & Tseng, W.-Y. I. (2013). Deterministic diffusion fiber tracking improved by quantitative anisotropy. *PloS One*, *8*(11), e80713. https://doi.org/10.1371/journal.pone.0080713

Yeh, F.-C., Wedeen, V. J., & Tseng, W.-Y. I. (2010). Generalized q-sampling imaging. *IEEE Transactions on Medical Imaging*, *29*(9), 1626–1635. https://doi.org/10.1109/TMI.2010.2045126

Yeo, B. T. T., Krienen, F. M., Sepulcre, J., Sabuncu, M. R., Lashkari, D., Hollinshead, M., Roffman, J. L., Smoller, J. W., Zöllei, L., Polimeni, J. R., Fischl, B., Liu, H., & Buckner, R. L. (2011). The organization of the human cerebral cortex estimated by intrinsic functional connectivity. *Journal of Neurophysiology*, *106*(3), 1125–1165. https://doi.org/10.1152/jn.00338.2011

Zamani Esfahlani, F., Jo, Y., Puxeddu, M. G., Merritt, H., Tanner, J. C., Greenwell, S., Patel, R., Faskowitz, J., & Betzel, R. F. (2021). Modularity maximization as a flexible and generic framework for brain network exploratory analysis. *NeuroImage*, *244*, 118607. https://doi.org/10.1016/j.neuroimage.2021.118607

Zhang, Y., Brady, M., & Smith, S. (2001). Segmentation of brain MR images through a hidden Markov random field model and the expectation-maximization algorithm. *IEEE Transactions on Medical Imaging*, *20*(1), 45–57. https://doi.org/10.1109/42.906424

Appendix

Appendix Table S3-1.
Scan Duration and Head Motion Estimates by Patient and Scan Number

Patient	Scan num.	Scan duration		Head motion estimates					
		Minutes	Frames	Min FWD	Max FWD	Med FWD	MAD FWD	Num spikes	Spike %
EM	1	8	240	0.03	2.44	0.13	0.05	9	3.75
BT	1	7	210	0.04	1.09	0.19	0.07	11	5.24
BT	2	7	210	0.05	1.34	0.25*	0.08	9	4.29
HY	1	12	360	0.02	0.44	0.14	0.05	0	0.00
DT	1	12	360	0.02	10.74*	0.15	0.05	31	8.61*
TJ	1	7	210	0.02	0.59	0.13	0.04	2	0.95
TJ	2	7	210	0.03	0.38	0.11	0.04	0	0.00
LJ	1	7	210	0.06	0.55	0.20	0.04	2	0.95
LJ	2	7	210	0.04	0.38	0.18	0.04	0	0.00
LJ	3	7	210	0.06	0.56	0.20	0.05	3	1.43

* Denotes head motion estimate exceeding normal range, see corresponding figure(s) below.

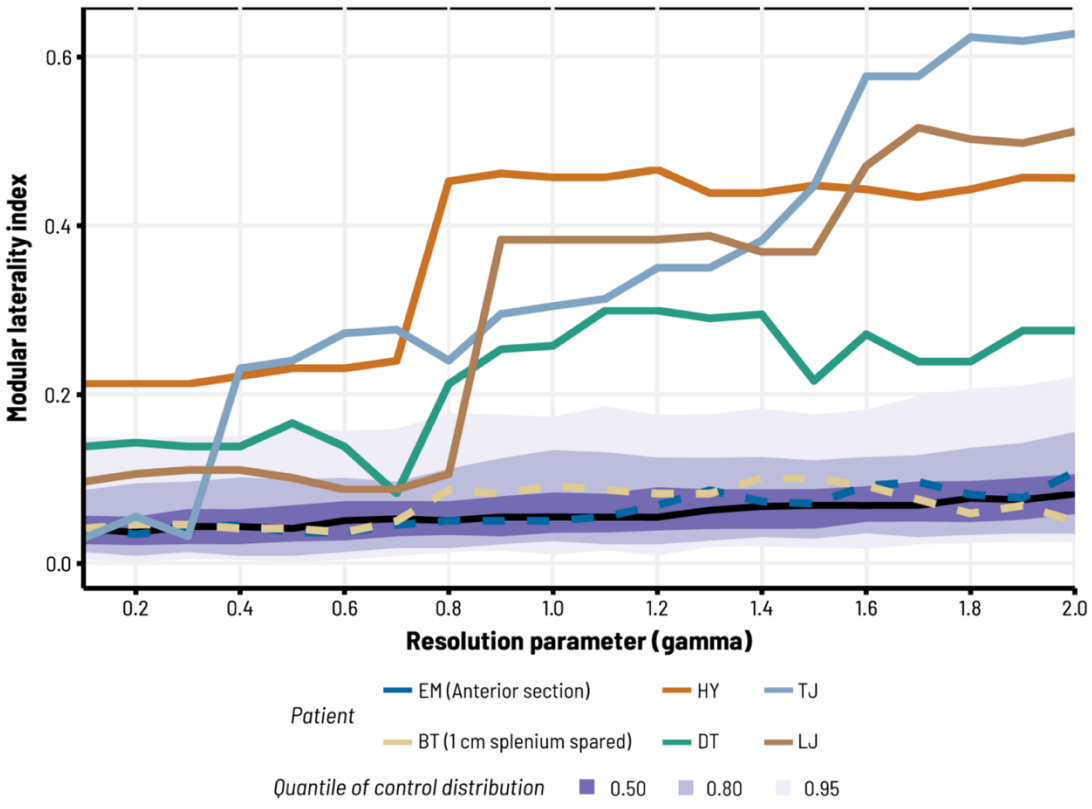


Figure S3-1. Lateralization of functional modules by different resolution (γ) parameter. Modularity maximization algorithms are sensitive to a spatial resolution parameter, γ. A value of $\gamma = 1$ is often treated as a 'default' level of resolution, whereas values of $\gamma < 1$ or $\gamma > 1$ produce progressively more coarse or fine-grained solutions, respectively. Here we show that differences in modular laterality between patients and healthy adult controls are not dependent upon the chosen value of γ. We performed 1000 iterations of modularity maximization at each of 20 levels of γ (ranging from [0.10, 2] in steps of 0.10), derived an optimal consensus partition at each level, and estimated a laterality index for the resulting partitions (such that values closer to 1 indicate more lateralized network topologies). Complete callosotomy patients (solid-colored lines) rapidly diverged from the distribution of healthy controls (quantile intervals shown in gradations of purple, with the solid black line representing the median) demonstrating more lateralized organization of functional modules, even at coarse levels of $\gamma < 1$. Partial patients (dashed colored lines), by contrast, consistently remained within the control distribution.

Table 4A-1

Fixed Effects of the Linear Mixed Model for Judgement Errors Left-Handed Participants Only

Effect	*Contrast*	*b*	*95% CI*	*p*
Intercept		-55.83	[-73.91, -37.76]	<.001
Response hand	Left hand vs. Computer	-19.34	[-25.06, -13.63]	<.001
	Right hand vs. Computer	-5.46	[-11.17, 0.25]	.061
Outcome	High vs. Low	2.89	[-1.75, 7.53]	.222
Session	1 vs. 2	-26.63	[-31.42, -21.85]	<.001
Report hand	Left vs. Right	0.34	[-4.32, 4.99]	.887
Base interval	400 vs. 200	-76.24	[-81.93, -70.55]	<.001
	800 vs. 200	-261.85	[-267.57, -256.14]	<.001
Response hand × Outcome	Left hand vs. Computer × High vs. Low	2.15	[-9.29, 13.58]	.713
	Right hand vs. Computer × High vs. Low	-4.95	[-16.37, 6.46]	.395
Session × Response hand	1 vs. 2 × Left hand vs. Computer	-18.79	[-30.22, -7.35]	.001
	1 vs. 2 × Right hand vs. Computer	-14.26	[-25.68, -2.85]	.014
Session × Outcome	1 vs. 2 × High vs. Low	9.28	[0.00, 18.56]	.050

Base interval × Response hand	400 vs. 200 × Left hand vs. Computer	-4.15	[-18.17, 9.87]	.562
	400 vs. 200 × Right hand vs. Computer	-5.24	[-19.25, 8.76]	.463
	800 vs. 200 × Left hand vs. Computer	-16.26	[-30.33, -2.18]	.024
	800 vs. 200 × Right hand vs. Computer	-15.13	[-29.16, -1.10]	.035
Session × Response hand × Outcome	1 vs. 2 × Left hand vs. Computer × High vs. Low	3.29	[-19.58, 26.15]	.778
	1 vs. 2 × Right hand vs. Computer × High vs. Low	1.39	[-21.44, 24.22]	.905

Note. b = regression coefficient (estimate), CI = confidence interval.

Appendix Table S4A-2
Participant Responses to Open-Ended Question on Control Slider Adjustment Criteria

Response
If I heard the sound right when I clicked a button I would slide the dot to total control. If the sound played after I had clicked the button I would slide it towards the no control part.
I adjusted it based on whether there was a pattern between the high tone and the low tone. Usually my rule of thumb was if the high tone corresponded with one arrow and the low tone corresponded with the other one then I would assume I had some control. If the same pattern would keep going on for 5 or 6 or more times then I kept increasing the amount of control I had on the slider.
Based on how well I was able to slide the mouse with my right hand or left hand.
I adjusted to more control if there were similar tones in a row and if the tones are consistently different then I moved the slider to less control.
The time interval between the pressing and the tone.
How immediately I heard the sound after pressing the button, although the first couple times I ever did it was somewhat ambiguous. I wasn't sure exactly what the instructions meant.
The way I heard the noise. I was trying to compare the sound I hear with my breath.
Whether the tone was caused by me pushing the button.
When the period between my click and the sound is short I select total control; when it is long I select the opposite.

I adjusted it on the basis that I could correctly guess the arrow and the tone of the sound was connected to what arrow was pointing what way.
Based on how quick the noise was following the click. If it was too slow or too fast I felt like I had less control.
I adjusted based on the timing between the press and the sound.
Sometimes it was just a gut feeling, but mostly it was how quickly the tone responded to my click.
How much I felt like when I pressed the button affected when the sound played.
I try to feel the relation between the two sounds and how that impacts my action.
I adjusted it based on how much the timing corresponded with when I pressed the button. If the sound played almost at the same time as my button press it was more in control and vice versa.
WITH AS MUCH ACCURACY AS I COULD.
I understood that the slider was moved when the sign was exposed.
I based my adjustments on the proximity of the sound to my button presses, with a more immediate sound meaning having more control and vice versa.
How much control I felt I had over when and whether the beep happened and which sound it was.
I observe the overall pattern like which sound is matched to the left hand and which sound is to the right hand, and then judge the control level based on how much they match.
Time.
Based on the variation in sound with respect to less than or greater than.
I did so based on feeling and timing from the click to hearing the sound.
Based on how much the sound lagged or the different pitches I associated with the right and left.
How long after it clicked.
I adjusted it based on whether the sound followed immediately after pressing the button or if there was a noticeable delay.
If the sound came right after my press I felt in control; if it seemed random I moved the slider down.
I matched the pitch of the tone to the direction of the arrow I pressed, and judged control by how consistent that mapping was.

Appendix Table S4B-1
Motion Quality Summary by Subject in Mental Imagery Task

	Min FWD	Max FWD	Median FWD	Mean FWD	No. Spikes	% Spikes
Sub						
1	0.02	0.37	0.09	0.09	25	5.72
2	0.02	0.37	0.08	0.09	8	1.81
3	0.04	3.87	0.13	0.26	53	12.21
4	0.01	1.93	0.07	0.12	36	8.28
7	0.01	0.51	0.08	0.10	17	3.86
8	0.01	1.26	0.08	0.14	51	11.46
9	0.01	1.06	0.07	0.12	76	16.81
10	0.01	2.29	0.08	0.13	25	5.76
11	0.03	7.62	0.15	0.26	64	14.65
12	0.01	0.68	0.10	0.12	68	13.26
13	0.02	1.27	0.07	0.09	34	7.76
15	0.01	0.25	0.09	0.09	198	45.73
16	0.01	0.49	0.07	0.08	34	7.62
18	0.01	0.64	0.11	0.14	25	5.57
19	0.02	4.04	0.08	0.09	73	16.55
20	0.00	0.88	0.07	0.09	116	26.54
21	0.01	0.24	0.06	0.07	120	27.71
22	0.02	0.42	0.10	0.10	18	3.79
24	0.01	0.59	0.06	0.08	27	6.15
25	0.02	0.20	0.06	0.07	64	14.13
27	0.01	0.53	0.05	0.06	54	10.23
28	0.02	1.35	0.12	0.15	4	0.86
29	0.01	2.28	0.15	0.22	134	28.94
30	0.02	0.59	0.09	0.10	17	3.65

Note. FWD = framewise displacement. Spikes = motion outlier volumes identified by fMRIPrep. % Spikes = number of spikes divided by total TRs.